Sede Amministrativa: Università degli Studi di Padova

Dipartimento di Ingegneria Civile, Edile ed Ambientale (ICEA)

CORSO DI DOTTORATO DI RICERCA IN:
SCIENZE DELL'INGEGNERIA CIVILE ED AMBIENTALE

CICLO XXXII

BOND AND ANCHORAGE OF PRESTRESSING TENDONS IN PRESTRESSED-CONCRETE MEMBERS

Coordinatore: Ch.mo Prof. Marco Marani

Supervisore: Ch.mo Prof. Carlo Pellegrino

Co-Supervisore: Eng. Flora Faleschini

Dottorando: Nicola Fabris

Abstract

Over the last few decades, pretensioned Prestressed-Concrete (PC) has become very common in structural applications. Its extensive use, however, requires adequate knowledge of bond development between prestressing tendons and surrounding concrete. Bond is of paramount importance both for prestress transfer at release and anchorage capacity under flexural loading. Current design codes for concrete structures provide simplified formulations to describe the force transfer mechanisms from steel to concrete, and seem to be not always conservative when compared to experimental evidences. More refined models are actually needed to reasonably consider the effect of the main parameters affecting bond properties, thus resulting in a sound design of PC members.

The first part of this contribution presents a broad review of the literature on various aspects of pre-tensioning anchorage. The bond mechanisms governing the transmission of the prestressing-force to the concrete and the subsequent behaviour of PC members are illustrated. The common experimental methods to investigate both transmission length and anchorage capacity of prestressing tendons are described and discussed. Then, the existing provisions from the main design codes are analysed and compared.

The second part of the work is focused on the general assessment of the principal design formulations on pre-tensioning reinforcement. Big differences in the evaluation of the transmission length and anchorage length are highlighted when the different provisions are applied to the same structural configuration, due to discrepancies in the considered influencing factors. Thus, the accuracy of the suggested relationships is assessed in detail by applying them to a comprehensive experimental database of transmission length and anchorage length values, collected from the literature. It is shown that the performances of the various design concepts are not always acceptable, since the theoretical predictions do not always fit well the experimental results. Lastly, the role of some key variables affecting bond, such as strand diameter, strand surface condition and concrete strength, is studied based on the analysis of the collected dataset.

In the third part of the contribution, the analytical modelling of the transmission length in PC members is carried out. For practical purpose, simplified bond stress distributions along the beam are assumed by all the common design codes, even though they do not reflect the real properties at the interface steel-concrete. A more accurate representation of the internal behaviour of PC members can be achieved by means of physically-based

models, rationally incorporating the effect of several influencing parameters. A first bond model is presented based on the radial expansion of the tendon at the release operation, considering anisotropic characteristics of the concrete around the tendon. Then, a second theoretical investigation is developed by appropriately describing the bond stress-slip relationship. In both cases, the bond stresses between the materials after release appear to describe a non-linear distribution along the transmission zone. The global results show the capability of the developed analytical models to simulate the bond behaviour during transmission of the prestressing-force to the concrete.

Sommario

Negli ultimi decenni il calcestruzzo armato precompresso a cavi pre-tesi ha assunto una crescente rilevanza nelle applicazioni strutturali. Il suo ampio utilizzo richiede comunque un'adeguata conoscenza in merito allo sviluppo dell'aderenza tra i trefoli e il calcestruzzo circostante. L'aderenza è un fenomeno di importanza fondamentale, sia per il trasferimento della forza di precompressione al rilascio dei trefoli che per la capacità di ancoraggio del cavo in seguito a carichi flessionali. Gli attuali codici normativi per strutture in calcestruzzo forniscono formulazioni semplificate per descrivere i meccanismi di trasferimento delle forze da acciaio a calcestruzzo, e sembrano essere talvolta non conservativi quando comparati a evidenze sperimentali. Per considerare in maniera ragionevole l'effetto dei principali parametri che influenzano le proprietà di aderenza sono in realtà necessari modelli più raffinati, in grado di indirizzare verso una più corretta progettazione degli elementi precompressi.

La prima parte di questo contributo presenta un'ampia revisione della letteratura riguardo vari aspetti delle armature da precompressione. Vengono illustrati in particolare i meccanismi di aderenza che governano la trasmissione della forza di precompressione al calcestruzzo e il successivo comportamento della membratura. Vengono inoltre descritti e commentati i comuni metodi sperimentali che permettono di indagare la lunghezza di trasmissione e la capacità di ancoraggio di trefoli da precompressione. Infine, vengono presentate e comparate le principali disposizioni normative in vigore.

La seconda parte del lavoro di tesi è focalizzata sulla valutazione generale delle principali formulazioni normative in merito alle armature di precompressione. Si riscontrano grandi differenze nella valutazione delle lunghezze di trasmissione e di ancoraggio quando le diverse prescrizioni vengono applicate alla medesima configurazione strutturale, in seguito a discrepanze sulle variabili di influenza considerate. Viene pertanto studiata nel dettaglio l'accuratezza delle formule proposte, andandole ad applicare ad un ampio database di prove sperimentali sulle lunghezze di trasmissione e di ancoraggio, raccolto dalla letteratura disponibile. Si vedrà che le performance dei vari codici normativi non sono sempre accettabili, poiché le predizioni teoriche non si adattano sempre bene ai risultati sperimentali. Infine, viene studiato il ruolo di alcuni parametri fondamentali (per es. il diametro del trefolo, le condizioni

superficiali dello stesso e la resistenza del calcestruzzo) nei confronti dell'aderenza, sulla base dell'analisi dello stesso database.

Nella terza parte del contributo si affronta la modellazione analitica della lunghezza di trasmissione in travi precompresse. Per questioni di praticità, tutte le principali normative assumono una distribuzione semplificata delle tensioni di aderenza lungo la trave, anche se tale situazione non riflette le reali proprietà all'interfaccia trefolo-calcestruzzo. Una rappresentazione più accurata del comportamento interno di membrature precompresse può essere ottenuta tramite modelli fisicamente basati, in grado di incorporare in maniera razionale l'effetto di molti parametri di influenza. A tale scopo, un primo modello di aderenza viene presentato sulla base dell'espansione radiale del trefolo che si verifica al rilascio dei cavi, considerando le caratteristiche anelastiche del calcestruzzo attorno al trefolo. In seguito, un secondo approccio teorico viene sviluppato andando a descrivere in maniera appropriata la relazione aderenza-scorrimento. In entrambi i casi, le tensioni di aderenza tra i due materiali al rilascio dei trefoli sembrano descrivere distribuzioni non lineari lungo la zona di trasmissione. I risultati globali mostrano l'effettiva capacità dei modelli analitici sviluppati di simulare il comportamento dell'aderenza durante la trasmissione della forza di precompressione al calcestruzzo.

Acknowledgements

I would like to express my deep gratitude to my supervisor, Prof. Carlo Pellegrino, for giving me the opportunity to work with him on such an interesting research topic. His support and willingness in every situation have been very much appreciated.

I am very grateful to Eng. Flora Faleschini, my co-supervisor, for her patient guidance and constructive suggestions throughout my PhD studies, as well as for revision of this thesis. Her constant support was essential for carrying out the entire work.

I gratefully acknowledge Prof. Marco Marani and all the Board of Professors of the PhD Course, especially Prof. Luca Bergamaschi for his valuable advice on the development of the numerical part of the work.

Finally, I wish to thank my parents and colleagues for their encouragement and patience during the last years.

Table of Contents

List of Figures

List of Tables

Nomenclature

Upper case letters

A_c	Cross-sectional area of concrete
A_{sp}	Cross-sectional area of prestressing tendon
$A_{sp,eq}$	Cross-sectional area of the equivalent prestressing tendon in the bond stress-slip model
C_{sp}	External circumference of prestressing tendon
$C_{sp,eq}$	External circumference of the equivalent prestressing tendon in the bond stress-slip model
E_c	Elastic modulus of concrete
E_{ci}	Elastic modulus of concrete at the time of prestressing-force release
E_{ps}	Elastic modulus of prestressing steel
J	Broyden's matrix approximating the Jacobian matrix
J_x	Moment of inertia of the concrete section
$L_{\Delta\sigma}$	Flexural bond length of the prestressing tendon
L_b	Anchorage length of the prestressing tendon
L_t	Transmission length of the prestressing tendon
$L_{t\ exp}$	Experimental transmission length
$L_{t\ theor}$	Theoretical transmission length
$L_{t\ ACI}$	Transmission length predicted by ACI 318-14
$L_{t\ EC2}$	Transmission length predicted by Eurocode 2 (l_{pt})
$L_{t\ MC10}$	Transmission length predicted by *fib* MC2010 (with $\alpha_{p2} = 0.75$)
$L_{t\ TWC}$	Transmission length predicted by the TWC model (with $\mu = 0.6$)
M_c	Bending moment in the concrete section
N_s	Axial force in the tendon
P	Initial prestressing-force in the tendon

Lower case letters

b	Width of the concrete section
c	Concrete cover thickness
c_1	Coefficient of the bond stress-slip model
c_2	Coefficient of the bond stress-slip model
c_3	Coefficient of the bond stress-slip model
c_4	Coefficient of the bond stress-slip model
c_5	Coefficient of the bond stress-slip model
e	Vertical eccentricity of the considered tendon with respect to the centre of gravity of the concrete section

f	Performance function of the bond stress-slip model
f_{bpd}	Flexural bond at the interface surface between tendon and concrete
f_{bpt}	Prestress transfer bond at the interface between tendon and concrete
f_c,	Concrete compressive strength at 28 days
f_{ci},	Concrete compressive strength at the time of prestressing-force release
f_{cd}	Design concrete compressive strength
f_{ct}	Tensile strength of concrete
f_{ctd}	Design tensile strength of concrete
f_{ctk}	Characteristic tensile strength of concrete
f_{ctm}	Average tensile strength of concrete
f_{ps}	Tendon stress at the nominal strength
f_{ptd}	Design tensile strength of the prestressing steel
f_{ptk}	Characteristic tensile strength of the prestressing steel
f_s	Tendon stress at the considered point along the length of the member
f_{se}	Tendon stress after allowance of all prestress losses
f_{si}	Jacking stress of the tendon at prestressing-force release
f_{su}	Ultimate tensile strength of the tendon
h	Height of the concrete section
k	Coefficient taking into account the member depth in AASHTO
l_{bp}	Basic anchorage length according to *fib* MC2010
l_{pt}	Basic value of the transmission length according to Eurocode 2
l_{pt1}	Lower value of the transmission length according to Eurocode 2
l_{pt2}	Upper value of the transmission length according to Eurocode 2
n_{sp}	Number of prestressing tendons with identical diameter
Δr	Increment in tendon radius at prestressing-force release
r	Radial distance from the tendon centroid
r_{jack}	Radius of the tendon after release
r_{ps}	Radius of the unstressed tendon
r_{tip}	Distance from the tendon centroid to the crack tip
s	Tendon clear spacing
u	Radial displacement
u_c	Radial displacement of the concrete
u_{ps}	Radial displacement of the tendon outer surface
y	Vertical distance from the centre of gravity of the concrete section
y_G	Distance from centre of gravity of the concrete section to bottom fiber
y_{tot}	Distance from the tendon centroid to the concrete bottom fiber
Δz	Length of the single finite element in which the prestressing tendon is subdivided
z	Longitudinal distance from the free-end of the PC member

Greek letters

α	Shape coefficient describing the functional form of the bond stress distribution
α_3	Coefficient taking into account the effect of fatigue on the anchorage length, according to the proposal by RWTH Aachen University
α_{ct}	Coefficient for long-term effects
α_{p1}	Coefficient which takes into account the prestress release method, according to *fib* MC2010
α_{p2}	Coefficient which takes into account the action effect to be verified, according to *fib* MC2010
α_{p3}	Coefficient which takes into account the influence of bond situation, according to *fib* MC2010
α_{rel}	Coefficient which takes into account the prestress release method, according to the findings proposed by the author
β_{cc}	Coefficient taking into account the age of concrete
γ_c	Partial safety coefficient for concrete
γ_s	Partial safety coefficient for prestressing steel
δ	Longitudinal slip of the tendon to the concrete at prestress release
ε_1	Concrete strain (assumed as 0.0003) corresponding to concrete tensile stress equal to 0.15 f_t, according to Han's softening model
$\varepsilon_{c,ck}$	Cracking strain of concrete
$\varepsilon_{c,r}$	Concrete strain in the radial direction
$\varepsilon_{c,\theta}$	Concrete strain in the circumferential direction
$\varepsilon_{c,z}$	Concrete axial strain at the level of the tendon centroid
$\Delta\varepsilon_{s,z}$	Change in tendon strain after prestressing-force release
ε_{si}	Initial strain of the tendon
ε_u	Ultimate concrete strain (assumed as 0.002) corresponding to concrete tensile stress equal to zero, according to Han's softening model
η_1	Coefficient taking into account bond condition, according to Eurocode 2
η_{p1}	Coefficient which takes into account the type of tendon, according to *fib* MC2010 or Eurocode 2
η_{p2}	Coefficient which takes into account the position of the tendon, according to *fib* MC2010, or the type of tendon according to Eurocode 2
η_{p3}	Coefficient which takes into account the action effect to be verified, according to the proposal of modification by University of Padova
μ	Overall friction coefficient between the tendon and the surrounding concrete, combining actual frictional and mechanical bond
υ_c	Poisson's ratio of the concrete
υ_{ps}	Poisson's ratio of the prestressing steel
$\sigma_{c,r}$	Concrete radial stress

$\sigma_{c,\theta}$	Concrete circumferential stress
$\sigma_{c,z}$	Concrete axial stress
σ_r	Tendon radial stress
$\sigma_r(r_{jack})$	Radial compressive stress at the interface between steel and concrete, arising from the Hoyer effect
$\Delta\sigma_s$	Increment in tendon stress resulting from the development of bond stress along the finite element
σ_s	Tendon stress at the considered point along the length of the member
$\sigma_{s,max}$	Effective tendon stress after prestressing-force release
σ_{si}	Jacking stress of the tendon at prestressing-force release
ϕ	Nominal tendon diameter
χ	Influence function of the bond stress-slip model

Acronyms

3PBT	3-point bending test
4PBT	4-point bending test
AASHTO	American Association of State Highway and Transportation Officials
ACI	American Concrete Institute
AMS	Average Maximum Strain
AVE	Average ratio between theoretical and experimental values
COV	Coefficient of variation
DEMEC	Detachable Mechanical Strain gauges
EC2	Eurocode 2
ECADA	Ensayo para Caracterizar la Adherencia mediante Destesado y Arrancamiento
ERSG	Electrical Resistance Strain Gauge
fib	International Federation for Concrete
LVDT	Linear Variable Displacement Transducer
MC2010	Model Code 2010
NC%	Percentage of not conservative results
PC	Prestressed-Concrete
PCA	Portland Cement Association
RMSE	Root mean square error
TWC	Thick-wall cylinders
ULS	Ultimate Limit State

Unit of measurements conversion

1 MPa = 145.038 psi = 0.145 ksi
1 mm = 0.039 in

1. INTRODUCTION

Prestressed-concrete (PC) is a widely diffused material in the modern engineering practise, allowing long-span and high load-carrying capacity of the structural members. Such important advantages connected to its use, especially in the field of bridge superstructures, arise from overcoming the problem of low tensile strength and premature cracking of the conventional concrete. Indeed, the basic concept of prestressed-concrete consists in the introduction of an initial compressive force in the member during production, so as to counteract the tensile stresses caused by the subsequent external loading. Particularly, prestressed-concrete structures can be classified into pre-tensioned and post-tensioned applications, depending on the technique employed to achieve the prestress.

In a pre-tensioning process, the tendons are firstly tensioned between temporary anchorages on the prestressing bed. Then, concrete is cast inside formworks and steam-cured in order to reach the desired compressive strength. Finally, once the formworks are removed, the tendons are released to introduce the prestressing-force to the concrete. In this phase, a crucial issue is represented by bond development at the interface between the materials. Bond is responsible for the correct transmission of the prestressing-force from steel to concrete within the so-called “transmission length”, and contributes to the general integrity of the PC member. Additionally, bond also plays a significant role during the service life of the beam, when it is loaded to flexure. In this situation, the tendon stress at the nominal flexural strength is assumed to be anchored to the concrete within the “anchorage length”. The transmission of the prestressing-force from steel to concrete at a predictable length and the development of the nominal flexural capacity over an adequate anchorage length are key points for achieving a good PC member detailing. However, bond mechanisms governing the force transmission between steel and concrete are quite complex and depend on several influencing parameters, including quantitative and qualitative factors. Despite many studies have been proposed on this research area, the problem still seems to be open and critical for a number of applications. The topic is under discussion within the *fib* Task Group 2.5 “Bond and Material Models”, in which the author is involved.

In this context, the first objective of this thesis is to investigate the real performances of the current codes for concrete structures when considering the design recommendations on the pre-tensioning anchorage. For practical purpose, the existing formulations are

based on simplified models, often derived from empirical evidences. Among the different code provisions, big discrepancies are found with respect to the influencing parameters considered in the calculation, thus reflecting in disagreeing predictions of the transmission length and anchorage capacity. As an example, ACI 318-14 adopted in the north-American practice considers only the tendon diameter and the initial prestress level as primary factors. No mention of concrete properties is present, despite a number of studies carried out in the literature seems to confirm it to be one of the factors having a major role on bond characteristics. In this work, the main design formulations on pre-tensioning anchorage are assessed in detail by applying them to a comprehensive dataset of experimental results, gathered from the literature. The general result is that the existing recommendations are not always conservative in predicting the transmission length and anchorage length of prestressing tendons. Particularly, the assumption of uniform bond strength at the steel-concrete interface after release seems not to adequately represent the internal behavior of PC members.

The bond mechanisms controlling the introduction of the prestressing-force to the concrete can be described more reliably by means of analytical models, involving physically-based approaches. In principle, numerical investigations are able to capture the actual bond stress distribution along the transmission zone, introducing the effect of many crucial variables such as tendon diameter, tendon spacing, concrete strength and concrete cover. Thus, in the second part of the contribution, the analytical modeling of the transmission length in PC members is addressed, on the basis of some pioneering works carried out on this topic. A first theoretical model is developed according to the so-called Thick-Walled Cylinders (TWC) theory. Here, the bond stress can be derived as a function of the radial pressure arising at the interface as a result of the expansion of the tendon after release, through the use of a proper friction coefficient. However, with materials commonly used in the prefabrication practice, concrete tensile strength is easily exceeded. Therefore, in order to incorporate possible radial cracking of the concrete, an appropriate softening model is needed to represent the behavior of concrete in tension. Then, the nature of bond between prestressing steel and concrete is analysed through a second bond stress-slip model. In this case, the bond development along the PC member is studied by describing the dependence of the bond stress upon the longitudinal slip of tendon on concrete. For this purpose, a generic power function is introduced and calibrated based on a collected experimental database of transmission length values. The major advantage of this generalized approach is that the bond stress-slip relationship is derived incorporating the effect of as many influencing parameters as

wanted. Both models appear to describe non-linear distributions of the interface bond stresses along the transmission length, different from the constant values suggested by all current design codes. The comparison with the experimental results shows the capability of the developed analytical models to accurately simulate the bond behaviour during transmission of the prestressing-force to the concrete. It is thought that consideration of such models can provide a sound and better design of PC members detailing. Moreover, they can be seen as useful support tools in view of a possible revision of the existing design formulations.

This dissertation is organized into five main chapters. Following Chapter 1, Chapter 2 presents the state of the art about bond in PC members, including the description of the experimental methods commonly used to investigate the pre-tensioning anchorage. Chapter 3 deals with the evaluation of the principal design code formulations on the transmission length and anchorage length of prestressing tendons. In Chapter 4, the analytical modeling of the transmission length in PC members is investigated. General conclusions of the work are drawn in Chapter 5. The list of references cited along the contribution is provided at the end of each chapter.

2. STATE OF THE ART

2.1. Bond of prestressing tendons: terminology

In a prestressed-concrete (PC) member, when the tendon is released from the temporary anchorage on the prestressing bed, the jacking force is transferred to the concrete entirely by bond, arising at the interface between the materials. The bond which accomplishes this function is commonly defined as *"prestress transfer bond"* and it develops from the free-end of the member to the beginning of a central region where the steel stress reaches a constant value. An idealisation of steel stress development along the length of a PC member after the release operation is shown in Figure 2-1. The stress in the tendon starts from zero at the free-end and increases until reaching the effective stress (i.e. a maximum value) after a certain distance, because of the bond strength that restrains, or hold back, the strand. At full transfer of the prestressing force, steel stresses remain constant (as depicted by the flat branch of the curve in the figure). The distance from the free-end of the member necessary to transmit the fully effective prestressing force to the concrete is called *transmission length* (according to *fib* Model Code 2010 [2-1]) or *transfer length* (in accordance with ACI 318-14 [2-2]). This bond situation is often referred to as "push-in", identifying the behaviour of the member where the tendon is shortened in the longitudinal direction and expanded in the transverse direction due to the release of the jacking force.

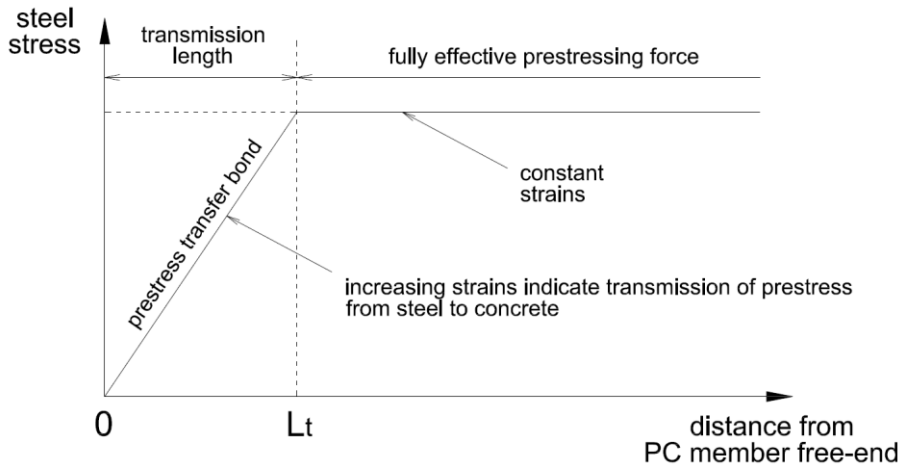

Figure 2-1: Idealised steel stress development in a prestressed-concrete member after release.

Prestressing tendons in PC members have a dual function. Firstly, part of the available tensile strength of the steel, as reported, is used to establish a compressive stress in the concrete. The jacking stress usually involve about 75-80% of the ultimate tensile

strength of the strand. Secondly, when the element is loaded to flexure beyond cracking, all or part of the tendon tensile strength can be exploited to assist the concrete in resisting the externally-applied bending moment, similarly to ordinary reinforcement in concrete structures. The increase in strand stress resulting from flexure is relatively low under service (i.e. uncracked) conditions. However, when cracking occurs for higher bending moments, bond stresses develop at the interface between tendon and concrete as a direct consequence of the shear action, governing the overall behaviour of the member. Bond arising as a result of flexure is different from that necessary to establish the prestress, and is commonly known as *"flexural bond"*.

The *flexural bond length* is defined as the additional embedment length required by a strand to increase the stress level due to external loads from the effective prestress to the stress at the nominal flexural strength of the member (Figure 2-2). Moreover, the *anchorage length* of the tendon is the sum of the transmission length and the flexural bond length, which is also referred to as *development length* in US [2-2]. The bond situation occurring in the flexural bond length, i.e. when the tendon is pulled and contracted due to the increasing stress in the bending crack, is often identified as *"pull-out"*.

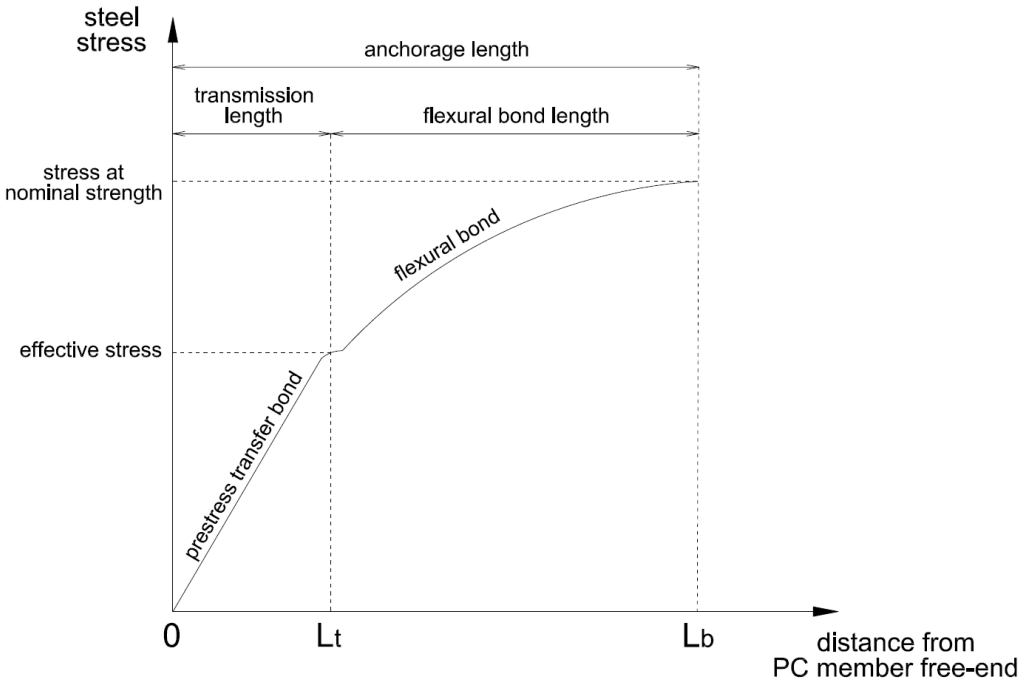

Figure 2-2: Steel stress levels near the free-end of a PC member at ultimate load conditions.

It should be noted that the term *development length* as defined per *fib* Model Code 2010 refers instead to the distance from the end face of the member beyond which the

longitudinal stresses can be considered linearly distributed along the concrete cross-section. For straight tendons arranged in a concrete rectangular cross-section, an empirical formulation is also provided in *fib* MC2010 (alternatively, it can be calculated similarly as in force spreading zones in post-tensioned beams).

Finally, it is worth recalling that a good estimation of the transmission length of prestressing strands is of primary importance in two different stages of the PC member design process [2-3]. Firstly, it is commonly used for checking allowable stresses near the free-ends of the member, immediately after the release of the prestressing force. Such calculation is typically more critical for shorter transmission length values, where a poor shear resistance of the element can result [2-4]. Secondly, the transmission length is also involved in the Ultimate Limit State (ULS) verification of flexural and shear strength, being necessary for determining the anchorage length of the tendon (in this case, load-carrying capacity depends on the development of stresses in the strand). With respect to this situation, it is more critical when longer transmission length values are considered because they reduce the available member length to resist flexure and shear.

2.2. Bond mechanisms

In structural applications, bond can be defined as the fundamental property which allows hardened concrete to hold back an embedded steel bar, so as to prevent sliding of the reinforcement longitudinally through the concrete, due to external forces. However, two different bond situations should be analysed when considering pre-tensioning anchorage. In fact, the nature of bond arising as a result of the transmission of the prestressing force to the concrete (i.e. "*push-in*" situation) may present differences with respect to that required to anchor the tendon tensile force when the member is subject to flexure, at ULS (i.e. "*pull-out*" situation) [2-5].

2.2.1. Bond nature in the transmission length

In the push-in condition, i.e. when the tendon is shortened in the longitudinal direction at prestress release, three main mechanisms are commonly recognised as contributing to bond development between the strand and the concrete, within the transmission length: *adhesion*, *mechanical interlocking* and *friction*.

The first, adhesion, refers to the elastic deformation of the cementitious layer surrounding the tendon due to its chemical and physical properties, as well as interlocking between cement-matrix particles and microscopically roughness of the steel

external surface. Hence, adhesion can be present only if no relative slips (or very small) take place between steel and concrete. Such condition is usually satisfied just in the central portion of the PC member, where the prestressing force is almost fully transmitted to the concrete and the strand stress is practically constant. However, in the regions near the free-ends of the element (i.e. along the transmission length), in which a steel stress gradient is present, the reduction in tensile strain of the tendon is greater than the corresponding compressive strain in the concrete. This strain difference becomes larger as the free-end is approached: there, the limit case is represented being maximum the reduction in steel strain and minimum the corresponding concrete strain (which is zero at the free-end). Consequently, relative displacements between the two materials break the adhesive effect, which may actually be discounted as a major factor contributing to prestress transfer bond [2-6; 2-7].

The second contribution, the so-called mechanical interlocking (or "mechanical anchorage"), depends on shape, indentation and surface characteristics of the bar, and therefore should be discussed in relation to the different types of tendon. In fact, the interlocking effect arises from the axial component of bearing stress due to contact between the tendon rib and the surrounding concrete, which restricts relative displacements at the interface. In the case of individual clean wires, it is reasonable to assume that mechanical anchorage plays a minimal role in governing the whole bond behaviour, because of the smooth texture of the outer surface of the wire. Conversely, seven-wire strands exhibit helical patterns of the individual wires that are expected to offer significantly higher mechanical resistance and bond capacity, unavailable to straight wires.

The third mechanism is represented by friction, which is considered to be the principal responsible for the transmission of the prestressing force from the tendon to the concrete, at the release operation. The term "friction" is generally referred to the resistance against a parallel displacement between two surfaces that are kept in contact by a compressive force, perpendicular to the contact plane. Thus, in order to activate frictional bond stresses at the interface between strand outer surface and the concrete, radial compressive forces are required. However, in addition to frictional contribution offered similarly to that in conventional ribbed bars [2-8], in a PC member the strand diameter tends to increase when the force is released from the temporary anchorage on the prestressing bed, as a result of the recovery of the lateral contraction (Poisson's effect). As long as the surrounding concrete remains intact and uncracked, such radial expansion of the strand results in a wedging action between the two materials, leading

to an enhanced frictional bond capacity in the transmission zone (Figure 2-3). This phenomenon was first analysed by Hoyer and Friedrich, and is commonly known as the "*Hoyer effect*" [2-9].

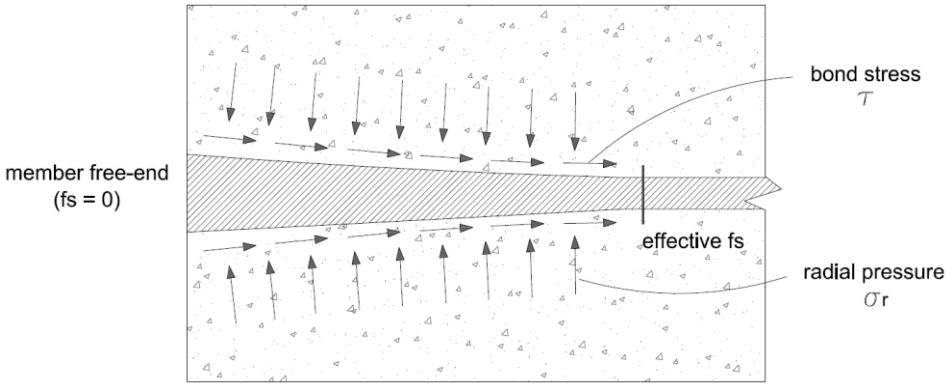

Figure 2-3: "Hoyer effect" due to recovery of lateral contraction of the strand, at release.

2.2.2. Bond nature in the flexural bond length

In general, the bond mechanisms which are activated at ULS in the flexural bond length to anchor the tensile force of the tendon due to flexure (i.e. in the pull-out condition) are similar to those described for the transmission of the prestressing force within the transmission length. However, a significantly reduced bond strength is present in the flexural bond length because of the different behaviour of the tendon. When the PC member is subject to flexure due to external loads, the additional tensile stress in the strand tends to reduce the cross-sectional area of the prestressing steel, resulting in a reverse Poisson effect which relieves the lateral pressure at the interface. Consequently, the magnitude of the flexural bond is also lower than the prestress transfer bond.

The increase in strand stress is usually negligible under service uncracked conditions, where flexural bond stresses are relatively low (Figure 2-4a). Nevertheless, for higher loads, cracking can occur in the vicinity of the point of application of the external load (for example the mid-span of a simply-supported PC member), and in this case flexural bond stresses play a key role in governing the whole performance of the member. Flexural bond stresses rise rapidly over the cracked region, and when a limiting value is reached some slip takes place between the tendon and the concrete at the interface surface in that zone (Figure 2-4b). This situation suddenly reduces the bond stress near the cracked section and increases the bond stress in the adjacent regions of the member, until the limiting value of flexural bond stress is reached again (Figure 2-4c). Therefore, as external loads are incremented, the concentration of high strand stresses and flexural bond stresses spreads outward from the initial cracked area and moves towards the free-

ends of the member, until bond failure (Figure 2-4d). However, the slip between the tendon and the concrete does not take place in stages, but progresses gradually as the wave of flexural bond concentration moves smoothly to the free-ends of the member.

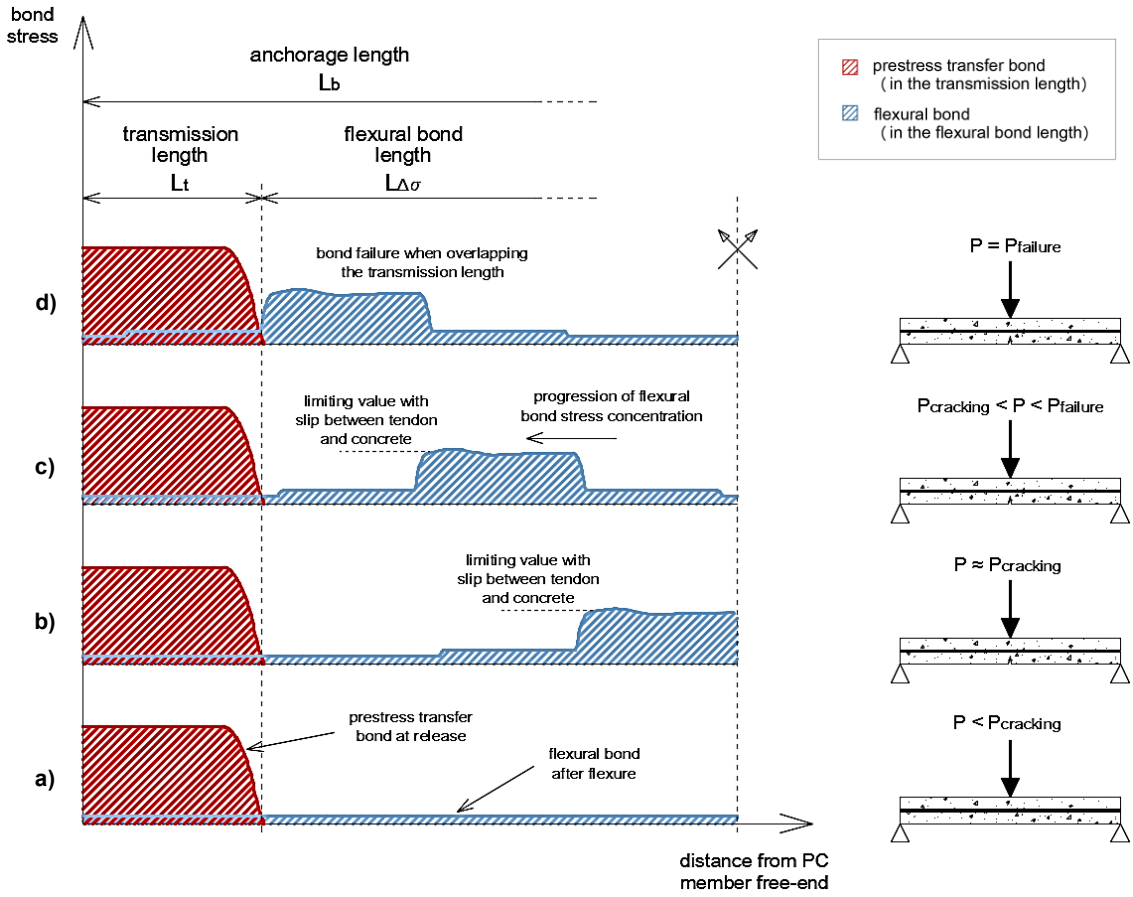

Figure 2-4: Qualitative progression of flexural bond stresses until bond failure.

Janney [2-6] sustained that the effective length of the tendon available for developing flexural bond stresses is approximately equal to the difference between its entire length and the length required to establish the prestressing force to the concrete (i.e. the transmission length). Indeed, in the end regions of the PC member the concrete surrounding the strand is stressed highly at the release of the prestressing force (in most cases beyond the elastic domain, see also chapter 4 of the document), and probably does not recover completely so that the bonding quality is not comparable to that in the central portion of the element. Accordingly, the bond failure of the member is expected to occur when the progression of the wave of flexural bond stress concentration overlaps the transmission length.

2.3. Test methods for investigation of pre-tensioning anchorage

In this section, the most common experimental methods to evaluate both transmission length and anchorage capacity of pre-tensioning steel are presented and discussed. Particularly, the *95% Average Maximum Strain* method (95% AMS, described at point 2.3.1.2.) and the *ECADA* method (illustrated at point 2.3.1.3.) are investigated as techniques widely used to determine the transmission length of small-scale PC specimens or real scale PC bridge girders. Then, a description of the common trial-and-error test to evaluate the anchorage capacity of PC beams is provided, based on *three-point bending* (3PB) or *four-point bending* (4PB) setup.

2.3.1. Experimental methods to evaluate the transmission length

2.3.1.1. Use of Electrical Resistance Strain Gauges (ERSGs)

In the first pioneering studies investigating bond properties of pre-tensioning anchorage within PC elements [2-6; 2-7; 2-10], the most common technique adopted to experimentally evaluate the transmission length involved the use of *Electrical Resistance Strain Gauges (ERSGs)*. ERSGs were fixed directly on the pretensioned strand before concrete placement, enabling to monitor the variation in strand strain along the PC member as a consequence of the release of the prestressing force. These strain readings, ideally, allow to measure the transmission length of the tendon. However, such testing setup based on the use of ERSGs proved to be unreliable for a number of reasons [2-11]. First, the presence of strain gauges onto the strand surface might significantly interfere with the normal bond development at the interface, especially when the devices are too close together [2-10], reducing the available bonded area (at least locally). Secondly, a large percentage of the strain gauges could be damaged whether during concrete placement or at release of prestress. In the first case, this situation can happen because of the difficulty in protecting ERGs from vibration and moisture; in the second case, the problem can be caused by the relative displacement occurring between the strand and the concrete in the transmission zone (i.e. near the free-end of the member). Lastly, it should be noted that when testing strands as pre-tensioning anchorage, ERSGs are mounted along a helix of a single wire, but each wire of the seven-wire strand could experience a slightly different strain condition. As the prestressing force is released from the temporary anchorages and some displacements between strand and concrete take place, relative movements between wires are also possible [2-12].

All these adverse effects contribute to make ERSGs quite ineffective in measuring transmission length of pre-tensioning strands. Consequently, alternative test methods were conceived in most recent investigations, aimed at preserving the integrity of bond at the interface between the strand and the concrete. In particular, the transmission length of prestressing tendons can be experimentally estimated in a more reliable way by measuring either the progression of strain on the concrete surface along the length of the member, or the strand end-slip. Nevertheless, it is still considered desirable to use a small number of ERSGs on the strand surface, as a control of the concrete strain or strand end-slip measurements.

2.3.1.2. 95% Average Maximum Strain (95% AMS) test method

The transmission length in a PC member can be determined through strain measurement on the concrete surface along its longitudinal axis. Particularly, concrete strains can be monitored by *Detachable Mechanical Strain Gauges (DEMEC gauges)*, used in conjunction with *DEMEC target points* which are fixed on the concrete external surface. Essentially, these gauges measure the change in the distance between target points before and after releasing the prestressing force in the tendons. After stressing the strands, concrete is placed inside formworks in the prestressing bed and moist-cured in a high-humidity environment - or steam-cured - in order to reach the desired compressive strength. Once the formworks are removed, mechanical target points are externally attached on both sides of the concrete specimen, using rapid adhesive glue. Starting from each free-end, these control points are set along the length of the member at the level of the strands, or along the centre of gravity of the steel if strands are arranged in different levels. They are easily identified being equally-spaced, generally at 50-100 mm intervals (see Figure 2-5).

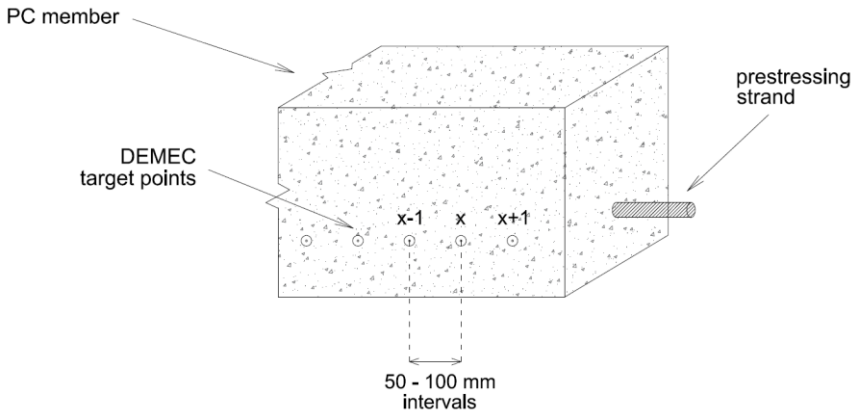

Figure 2-5: DEMEC target points on the concrete surface to obtain its strain profile.

Basically, mechanical target points are stainless steel discs with a small hole in the centre, designed to fit the DEMEC gauge, which registers the change in length between two successive holes. In this way, two sets of strain readings are taken both before and after transmission of the prestressing force to the concrete, i.e. one per each side of the PC element. However, it is recommended that two different operators are involved in the strain measurements, sequentially, to avoid (or limit) human errors during the operation.

The total shortening on the concrete external surface over a gauge length is simply the algebraic difference between readings taken before and after release. Such shortening, divided by the gauge length, gives the average longitudinal strain which is assumed to occur at the middle point between the two considered target points. Thus, the measured concrete strains can be plotted over the length of the specimen, obtaining the so-called "*concrete raw strain profile*" due to the transmission of the prestressing force [2-13]. The concrete raw strain profile is derived from the average readings of four sets of strain measurements: two operators by two sides of the member (strains are registered on both sides to take into account possible non-uniform prestress between the strands). Typically, concrete strain values are zero at the free-ends of the element, and increase along the transmission length until they remain almost constant, demonstrating the full transmission of the prestressing force.

In the test procedure, the raw strain profile of the concrete should be smoothed in order to reduce anomalies in data recording and obtain a more realistic strain distribution, as illustrated in Figure 2-6. The most commonly used smoothing technique consists in taking the average of strain data over three consecutive gauge lengths (see Figure 2-5). This approach, applied in an overlapping manner, can be summarised with the following *three-point moving equation* [2-13]:

$$(\varepsilon_c)_x = \frac{(\varepsilon_c)_{x-1} + (\varepsilon_c)_x + (\varepsilon_c)_{x+1}}{3} \tag{2-1}$$

where $(\varepsilon_c)_x$ is the strain on the concrete surface associated to the middle point x, while $(\varepsilon_c)_{x-1}$ and $(\varepsilon_c)_{x+1}$ represent the concrete surface strains associated to the previous and subsequent position, respectively. From the smoothed strain profile of the concrete surface, the *Average Maximum Strain (AMS)* can be determined by computing the numerical average of all strain values within the horizontal branch of the diagram, identifying the full transmission of prestress. However, the test procedure described herein is referred to the *95% Average Maximum Strain (95% AMS)* since, once the 95% of the AMS is computed, the transmission length (L_t) of the PC member is identified by

the intersection of the horizontal 95% AMS line with the smoothed strain diagram (Figure 2-6):

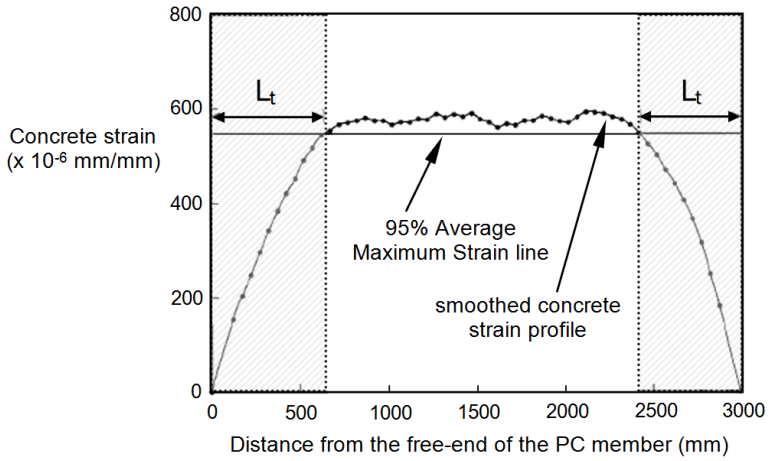

Figure 2-6: Typical smoothed concrete strain profile obtained from experimental tests by [2-14] and implementation of the 95% AMS method.

The use of the 95% AMS method has been employed in many experimental studies [2-11; 2-14; 2-15; 2-16; 2-17] and is thought to provide reliable results when assessing the transmission length of prestressing strands, since it does not depend on arbitrary interpretation of test data. The major advantage of adopting this technique is that final results (i.e. the calculation of the transmission length) do not change significantly if a little number of test data is either included or excluded from the average. It should be noted that the 95% AMS method identifies the transmission length as the distance from the free-end of the PC member to the location at which 95% of the prestressing force is transferred to the concrete. Instead, when the fully effective concrete strain (100% of the AMS) is employed in the computation, it might be difficult to determine the exact intersection between the 100% AMS line and the strain buildup curve, which could approach the plateau asymptotically. The transmission length resulting from applying the 95% of the AMS could be a bit shorter than the real value. However, it should be recognised that the use of mechanical strain gauges combined with the described smoothing technique of recorded data can artificially increase the measured transmission length [2-11].

2.3.1.3. ECADA test method

A second experimental method for the assessment of the transmission length in PC specimens is the so-called *ECADA*, which is the acronym for “Ensayo para Caracterizar la Adherencia mediante Destesado y Arrancamiento” (in English: “Test to Characterise the bond by release and pull-out”). The test setup was developed at the Polytechnic

University of Valencia (Spain) by Martì-Vargas et al. [2-18]. It is based on the measurement and analysis of the force supported by the strand in a series of identical PC specimens with different embedment lengths. One end of the test frame, named *"stressed-end"*, is arranged with an anchorage-measurement-access (AMA) system, equipped with two plates in series (Figure 2-7). The first plate supports the specimen throughout the test, while the second plate holds the strand fix anchorage device and may be separated from the other by pulling out the strand. Sequentially, the strand is placed in the frame, fixed at the stressed-end, tensioned by means of a hydraulic jack and anchored to the other end of the test frame, named *"transmission end"*, through an adjustable strand anchorage. Then, concrete is cast and cured so that, after the required maturation, the adjustable strand anchorage can be relieved using the hydraulic jack. The release operation is accomplished at a controlled speed rate. Once the prestressing force is transferred to the concrete, strand force loss at the stressed-end can be measured in the AMA system by a force transducer, which is placed between the fix anchorage device and the plate supporting the specimen. However, the force in the strand at the stressed-end requires a stabilisation period of a few hours to be read correctly, because it depends on strain compatibility with the concrete.

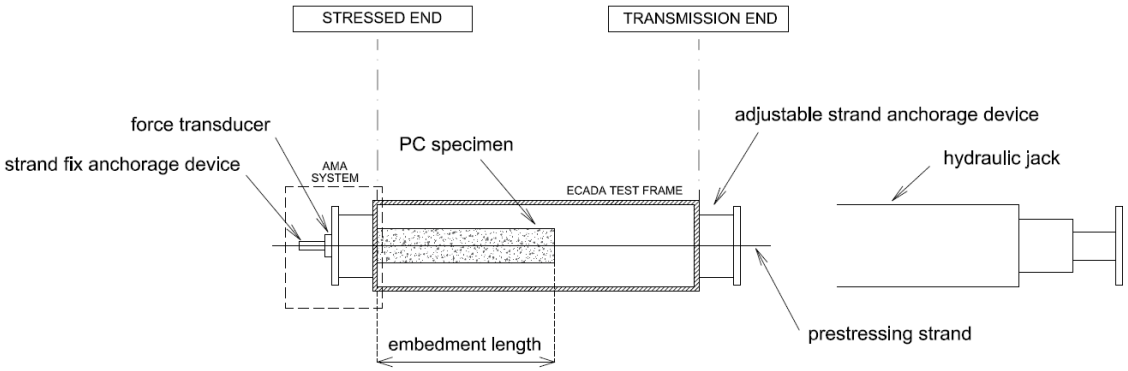

Figure 2-7: Scheme of the ECADA test setup.

The transmission length of the PC small-scale member can be determined with the ECADA test method after testing (following the abovementioned procedure) a set of identical specimens, but with different embedment lengths. For each specimen, the loss in strand force at the stressed-end is measured after the stabilisation period, enabling the force loss vs embedment length diagram to be constructed (Figure 2-8). This curve typically shows a bilinear tendency, with an initial descendant branch characterised by steep slopes and a subsequent almost horizontal branch, starting from a certain value of the embedment length. Such particular value marking the beginning of the horizontal segment in the graph is defined as the transmission length of the strand. The accuracy in

the assessment of the transmission length value depends on the series of selected embedment lengths of the tested specimens, where an embedment length sequence of 50 mm is suggested to obtain reliable results.

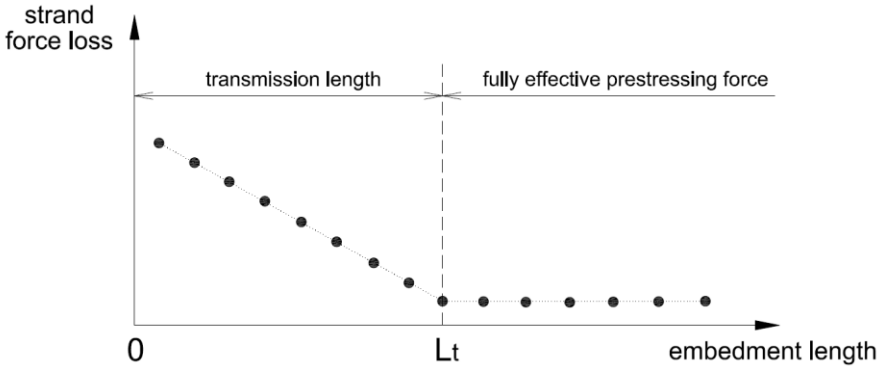

Figure 2-8: Typical strand force loss vs specimen embedment length diagram to derive the transmission length according to the ECADA test method.

The AMA system should be designed in order to simulate the behaviour of the remaining part of the PC member that is actually replaced. Therefore, it should have the same sectional stiffness as the replaced part of the element [2-19]. Such stiffness depends on the cross-section and concrete properties of the specimen (including the age at the time of testing). However, it will not be feasible to design a proper device for each specific test condition. Consequently, a section of discontinuity is generated at the interface between the PC specimen and the AMA system, being the stiffness of the latter device either smaller or greater than the sectional stiffness of the member. Therefore, the strand force loss measured at the stressed-end after release could be slightly different than that in the real situation, resulting in a small over- or under-estimation of the transmission length.

In any case, many tests must be performed to obtain a single value of the transmission length, making the entire test procedure long and sometimes difficult to be applied in a simplified manner. Conversely, one of the advantages of the ECADA method is that it also allows to measure the anchorage length of a prestressing strand on the same specimens previously used for assessing the transmission length. In fact, after measuring the force loss in the strand, the investigation can continue with a pull-out test by positioning the hydraulic jack at the stressed-end of the frame, and increasing the applied force in the strand until its slippage (or until concrete fails by splitting). In this way, a series of PC specimens with different embedment lengths is tested, and the force in the strand is measured at the stressed-end. Thus, the anchorage length of the strand

can be defined as the lowest embedment length of the specimen for which the ultimate stress in the strand is reached during the test.

2.3.2. Experimental methods to evaluate the anchorage length

2.3.2.1. Flexural beam tests

The most common experimental test to evaluate the anchorage capacity in a PC member consists in a simple flexural test where the beam is loaded to failure with either a single-point load (i.e. *three-point bending* setup - 3PB) or a two-point load (i.e. *four-point bending* setup - 4PB). The deflections of the specimen at the loading points and at the lateral supports are measured continuously during loading by Linear Variable Displacement Transducers (LVDTs), which are also used to indirectly control the applied load. In addition, dial gauges are mounted on the strands at each end of the beam to detect any strand-end slippage during testing.

In contrast to the transmission length, the anchorage length of the PC member can not be measured directly [2-20; 2-21], but is determined iteratively using a *trial-and-error* procedure. Initially, the load - or the loads in the case of 4PB test - is applied on the beam at a distance from the free-end equal to the estimated anchorage length for the adopted type of strands, and is increased until the failure of the element. The initial choice of load-point distance from the element free-end should be made in accordance with the provisions by current design codes [2-1; 2-2; 2-22]. After testing, the global failure mode of the specimen is investigated. In particular, four main failure configurations can be detected for PC flexural elements [2-23]: flexural failure (F), shear failure (S), bond failure (B) and combined failures (C). Within the last category, a combination of bond and flexural failure (B/F), a combination of bond and shear failure (B/S) or a combination of flexural and shear failure (F/S) are possible. However, special care should be taken in the end regions of the member in order to avoid any premature shear failure [2-24]. If considerable end slip of any of the strands occurs before reaching the ultimate flexural capacity of the element (i.e. bond failure or another mixed mechanism involving bond), then a subsequent test of another PC beam with the same characteristics is carried out, moving the applied load at a longer distance from the free-end. Conversely, if flexural failure of the specimen occurs without any consistent strand slippage, then the next test is conducted by shifting the applied load at a shorter distance from the element free-end. In this way, after some flexural tests of identical PC specimens, the anchorage length can be accurately estimated.

During testing, the increments of strand stress beyond the effective prestress are relatively small up to cracking of the section, representing typical service conditions. However, as the initial flexural cracks occur in the zone near the applied load, the stress in the strand increases dramatically. As the external force is incremented further, strand stress increases again, and flexural bond stress profile moves from the central portion towards the transmission length zone of the beam, accompanied by small slips between the strand and the concrete (see section 2.2.2.). Such wave of flexural bond stresses can develop along the strand until it reaches the transmission zone at the free-ends of the member, necessary to transmit the prestress from the tendon to the concrete [2-6]. In fact, when the prestressing force is initially released, the strand surface in the transmission length is bonded by radial pressures resulting from the Hoyer effect (i.e. the increase in strand diameter), and the surrounding concrete is usually cracked being stressed beyond the elastic limit. On the other hand, the increase in strand stress due to flexure reduces the diameter again, relieving such radial pressures. As a result, a general bond slip is likely to happen once the flexural bond stress concentration overlaps the transmission end-zone of the member, characterised by poor bonding capacity.

The anchorage of prestressing tendons can be investigated comprehensively with flexural beam tests, where the same specimens can be used in sequence for determining both the transmission length and the anchorage length. However, flexural beam tests similar to those described in the present paragraph are rather elaborate and time-consuming, since the procedure to determine the anchorage length requires several tests with identical specimens. Moreover, the method may not give reliable and accurate results for the anchorage length, as the scatter of the resulting values is usually high.

2.4. Design rules for transmission and anchorage length

In the current design codes for concrete structures, a variety of rules on transmission length and anchorage capacity of pre-tensioning tendons can be found. The existing formulations can be ideally divided in two main groups, i.e. those based on empirical evidences (for example *ACI 318-14* [2-2] and *AASHTO* [2-25]) and those which directly refer to a physically-based model (for instance *fib Model Code 2010* [2-1] and *Eurocode 2* [2-22]). Among the models of the first group, the mechanical basic part is not evident since they arise from factors empirically determined, and in most cases the formulation is not unit-conforming. Instead, in the models of the second group, transmission length and flexural bond length are calculated from the equilibrium of forces in the

longitudinal direction of the tendon, involving strand axial stress and bond strength at the interface (see Figure 2-9).

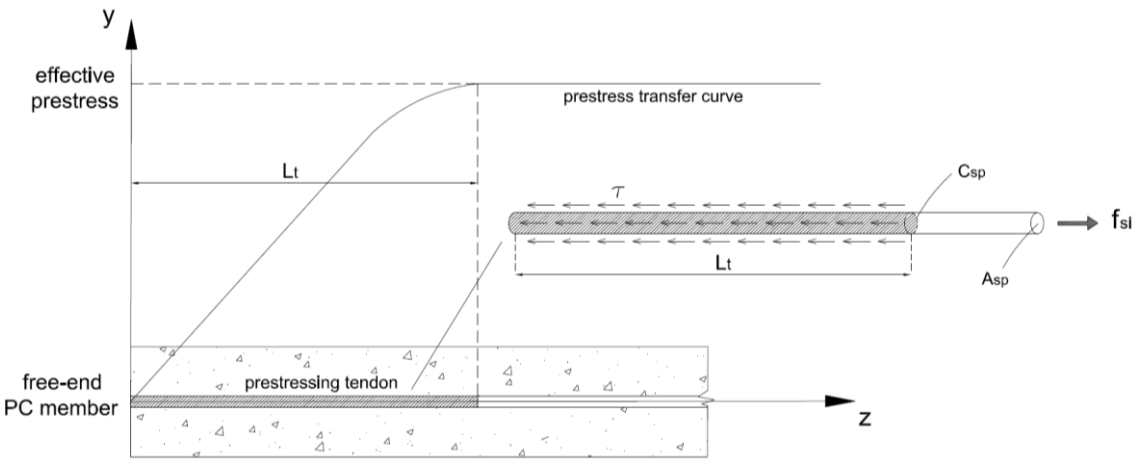

Figure 2-9: Equilibrium of forces along the tendon.

However, a simplified uniform distribution of bond strength along the transmission length and flexural bond length is assumed by all codes for practical use, even though it does not completely represent the real behaviour at the interface between strand and concrete. In particular, the idealised tri-linear curve depicted in Figure 2-10 is considered for the development of tendon stresses along the length of a PC member (curve "1" refers to the situation at the release of the tendons, while curve "2" should be considered at the Ultimate Limit State). It should be noted that the bond stress at any point of the curve is proportional to the corresponding slope. Therefore, it is evident that the bond stress in the transmission length is higher than the bond stress in the flexural bond length.

In the following sections of the chapter, an overview of the principal code provisions for a reasonable determination of the transmission length and anchorage length of PC members is presented. However, among the different formulations, big differences can be found with respect to the considered influencing parameters. For instance, only some design models (*fib* Model Code 2010 and Eurocode 2) include the dependence of the transmission and anchorage length upon the concrete strength, even though many studies in the literature confirm it to be one of the most important factors affecting the bond properties at the interface surface between steel and concrete. Moreover, the adoption of additional quantitative and qualitative parameters such as concrete cover, tendon spacing and tendon surface condition could improve the accuracy of the design. A comprehensive assessment of the role of the major influencing parameters on the anchorage of pre-tensioning tendons will be addressed in sections 3.4 and 4.3.5. In order

to avoid ambiguity, and to easily compare different formulations, a harmonized nomenclature will be adopted in the following for all the design codes.

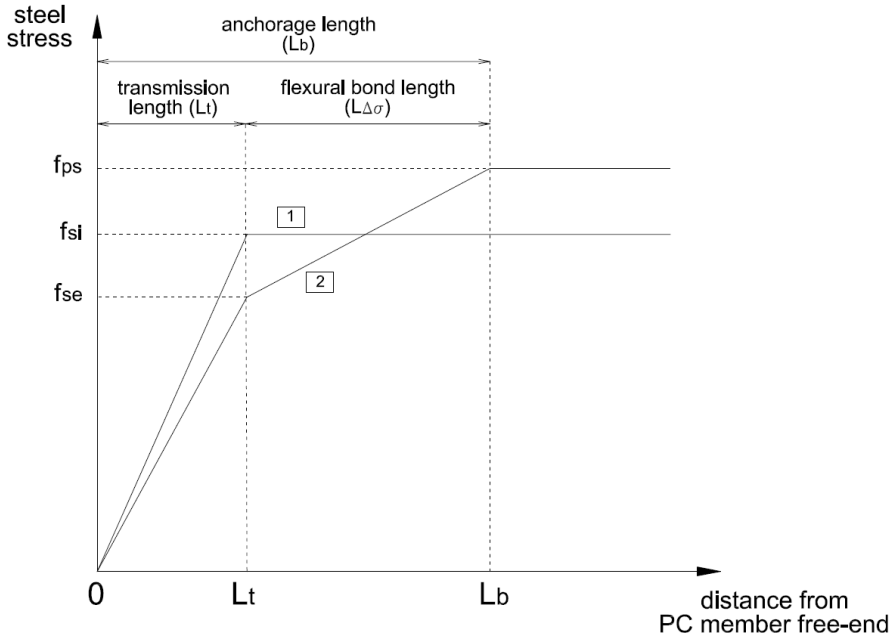

Figure 2-10: Idealised stress transfer curve adopted by the main design codes.

2.4.1. ACI 318-14

ACI Committee 318-14 guidelines are typically adopted in the North American practise, providing very simple formulations for the assessment of the transmission length and anchorage length of PC members. The qualitative tri-linear curve of Figure 2-10 is also taken into account by ACI 318-14, highlighting how prestress transfer bond is much higher than flexural bond.

The transmission length of prestressing tendons is calculated as reported in Eq. 2-2, considering a constant bond strength equal to 2.76 MPa (400 psi) at the interface between steel and concrete. The expression has been adapted with respect to the original formulation, in order to incorporate the unit conversion into the metric system (stresses in MPa and lengths in mm). It can be noted that only the nominal strand diameter (ϕ) and the effective strand stress after allowance for all prestress losses (f_{se}) are considered as influencing parameters.

$$L_t = \frac{f_{se}\ \phi}{20.7} \tag{2-2}$$

However, many authors suggest the use of the strand stress at release (f_{si}) in place of f_{se}, since the transmission length is actually established at the release of the prestressing force [2-3; 2-23]. Moreover, as reported by many experimental campaigns conducted in

the literature, other important factors such as concrete strength, concrete cover, strand spacing and release type actually seem to affect the transmission length of prestressing strands. Nevertheless, they are not taken into consideration in ACI-318-14. It is worth recalling that current ACI 318-14 provisions first appeared in 1963 (ACI 318-63) [2-26], and have not changed to the present day despite several proposed modifications. The design formula is based on the experimental tests carried out by Hanson and Kaar [2-7] and Kaar et al. [2-27] on 7-wire strands embedded in concrete with compressive strength of 20.7 MPa [2-28]. Therefore, for concretes of new conception with higher strengths, ACI 318-14 equation may result in overestimations of the transmission length. For shear design specifications, ACI 318-14 also provides the simplified calculation of the transmission length based on 50 times the tendon diameter (Eq. 2-3):

$$L_t = 50\,\phi \tag{2-3}$$

For the determination of the anchorage length, the flexural bond length is added to the transmission length as reported in Eq. 2-4. Particularly, the flexural bond length is identified by the product between the additional tendon stress (f_{ps} - f_{se}) and strand diameter (ϕ), divided by the factor 6.9 representing the reduced flexural bond strength.

$$L_b = L_t + \frac{(f_{ps} - f_{se})\ \phi}{6.9} \tag{2-4}$$

By comparing Eq. 2-2 and Eq. 2-4, it emerges that the bond strength in the transmission length is three times higher than the bond strength in the flexural bond length.

2.4.2. AASHTO

In the LFRD bridge design specifications of the American Association of State Highway and Transportation (AASHTO), the recommended value of the transmission length only depends on the tendon diameter (Eq. 2-5), similarly to the simplified ACI 318-14 formula for shear-based design:

$$L_t = 60\,\phi \tag{2-5}$$

Moreover, prestressing tendons shall be bonded beyond the section required to develop the stress at nominal resistance (f_{ps}) for an anchorage length expressed as in Eq. 2-6 (stresses in MPa and diameter in mm). It can be seen that such calculation incorporates a coefficient “k”, which takes into account the depth of the pretensioned member as resulting from Buckner, 1995 [2-29] and Lane and Rekenthaler, 1998 [2-30].

$$L_b = 0.145\,k\left(f_{ps} - \frac{2}{3}f_{se}\right)\phi \tag{2-6}$$

where: k 1.0 for pretensioned panels, piling, and other pretensioned members with a depth of less than or equal to 24 in. (609.6 mm);

k 1.6 for pretensioned members with a depth greater than 24 in. (609.6 mm);

However, the different magnitude of the bond strength in the transmission length and flexural bond length (i.e. prestress transfer bond and flexural bond) can not be identified within AASHTO formulation, despite a tri-linear bond curve similar to that of Figure 2-10 is considered.

2.4.3. *fib* Model Code 2010

The approach of *fib* Model Code 2010 for concrete structures (*fib* MC2010 in the following) for the calculation of the transmission length and anchorage length of PC members is worth to be mentioned, having a wide diffusion in Europe. *fib* MC2010 provisions, inspired by *fib* Model Code 1990 [2-31], are more refined if compared with ACI 318-14 or AASHTO, but are also based on a constant bond stress (f_{bpd}) developing at the interface steel-concrete during and after the release of the prestressing tendons. In particular, the design value of the bond stress is prescribed to be as in Eq. 2-7.

$$f_{bpd} = \eta_{p1}\,\eta_{p2}\,f_{ctd}(t) \tag{2-7}$$

being η_{p1} a coefficient that depends on the type of prestressing tendon, η_{p2} a coefficient that considers the position of the tendon during concreting and $f_{ctd}(t)$ the lower value of the design concrete tensile strength (which should be considered at the time of prestressing force release for transmission length calculation, and at 28 days for anchorage length calculation):

η_{p1} 1.20 for 7-wire strands;

1.40 for indented or crimped wires.

η_{p2} 1.00 for all tendons with an inclination of 45-90° with respect to the horizontal during concreting, and for all horizontal tendons which are up to 250 mm from the bottom or at least 300 mm below the top of the concrete section during casting (see Figure 2-11);

0.70 for all other cases.

$f_{ctd}(t) = f_{ctk,min}(t) / \gamma_c$

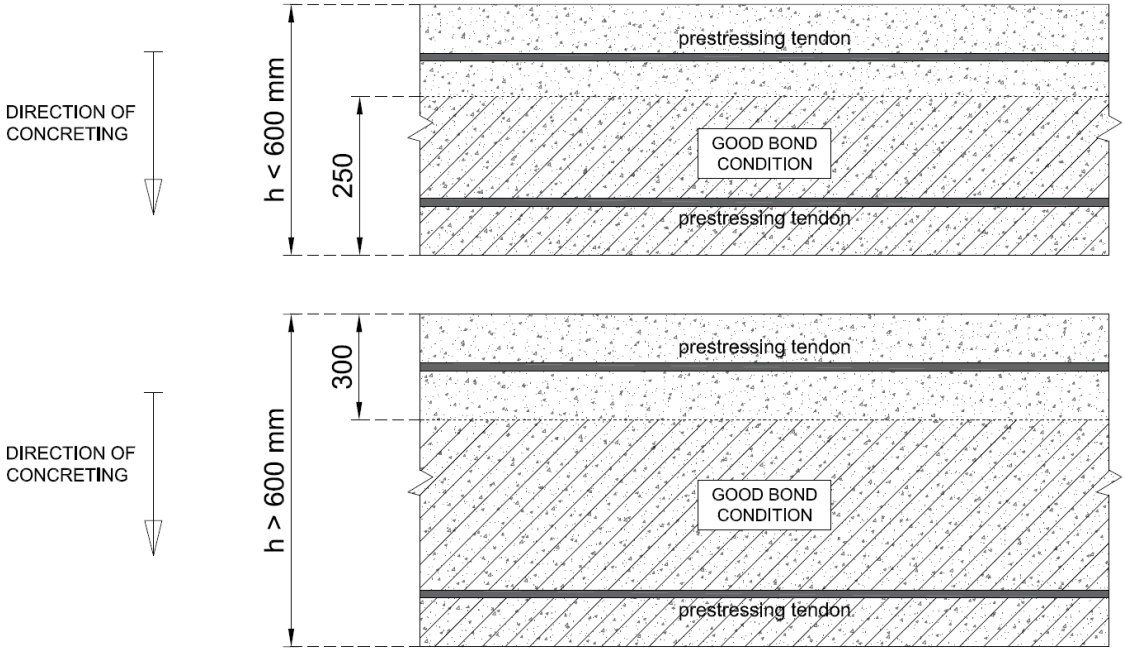

Figure 2-11: Description of good bond conditions according to fib MC2010.

The calculation of the transmission length is based on the basic anchorage length, representing the length required to anchor an individual untensioned tendon (l_{bp}), as expressed by Eq. 2-8:

$$l_{bp} = \frac{A_{sp}}{\phi\,\pi}\,\frac{f_{ptd}}{f_{bpd}} \tag{2-8}$$

where ϕ is the nominal tendon diameter, A_{sp} is the cross-sectional area of the tendon, f_{bpd} is the design value of the bond stress (as calculated in Eq. 2-7) and $f_{ptd} = f_{ptk} / \gamma_s$ is the design tensile strength of the prestressing steel. The above equation, Eq. 2-8, is the result of a simple equilibrium between the force in the prestressing tendon and the forces due to bond strength developing at the interface between steel and concrete. Thus, the transmission length of the tendon (l_{bpt}) is derived as a portion of the basic anchorage length (Eq. 2-9), being proportional to the ratio between the strand stress just after release (f_{si}) and the design tensile strength of the prestressing steel (f_{ptd}). Some empirical coefficients are also used.

$$L_t = l_{bpt} = \alpha_{p1}\,\alpha_{p2}\,\alpha_{p3}\,\frac{f_{si}}{f_{ptd}}\,l_{bp} \tag{2-9}$$

in which α_{p1} is a coefficient that considers the type of release, α_{p2} is a coefficient taking into account the action effect to be verified and α_{p3} is a factor that accounts for the influence of bond situation:

α_{p1}	1.00	for gradual release;
	1.25	for sudden release.
α_{p2}	0.50	for verification of the transverse stress at release due to development and distribution of prestress in the anchorage zone;
	1.00	for calculation of the anchorage length at ULS when moment and shear capacity is considered.
α_{p3}	0.50	for strands;
	0.70	for indented or crimped wires.

It can be noted that the coefficient α_{p2} allows to compute a lower and upper bound of the transmission length value, with a dual purpose (see paragraph 2.1). In particular, short transmission length values are important when checking allowable stresses near the member free-end at the release of the tendons, whereas long transmission length values might be critical when evaluating the anchorage capacity of the PC member at Ultimate Limit State. Once the transmission length is calculated, the design anchorage length of a prestressing tendon according to *fib* MC2010 can be determined as in Eq. 2-10, by adding the flexural bond length (similarly to ACI 318-14 recommendations):

$$L_b = l_{bpd} = L_t + l_{bp} \frac{f_{ps} - f_{se}}{f_{ptd}} \tag{2-10}$$

where f_{ps} is the tendon stress under design load and f_{se} is the tendon stress due to prestress including all losses.

fib MC2010 apparently suggests the use of the same bond strength at the interface between tendon and concrete to determine both the transmission length and the flexural bond length. However, different values of the concrete tensile strength should be used in the calculation in order to take into account the different age of the concrete in the two design situations (Eq. 2-11):

$$f_{ctd}(t) = f_{ctk,min}(t) / \gamma_c = \alpha_{ct}\ 0.7\ [\beta_{cc}(t)]^{\alpha}\ f_{ctm} / \gamma_c \tag{2-11}$$

where:

α_{ct}	coefficient for long-term effects on the concrete tensile strength;
$[\beta_{cc}(t)]^{\alpha}$	coefficient depending on the age of the concrete;
f_{ctm}	mean value of the tensile strength of concrete;
γ_c	partial safety factor for concrete applications.

2.4.4. Eurocode 2

The design process of Eurocode 2 (EC2 hereafter) for the anchorage of prestressing tendons in PC members is similar to that of *fib* MC2010. The magnitude of the bond strength at the interface between steel and concrete, as in *fib* MC2010, is determined through the tensile strength of the concrete, even though two different values are considered for the transmission length and flexural bond length calculation.

The prestressing force is assumed to be transferred to the concrete by a constant bond stress in the transmission length (f_{bpt}) which is based on the concrete properties at the time of release (Eq. 2-12):

$$f_{bpt} = \eta_{p1}\,\eta_1\,f_{ctd}(t) \tag{2-12}$$

where η_{p1} is a coefficient that considers the type of tendon and the bond situation at the release, η_1 is a parameter taking into account the bond condition and $f_{ctd}(t)$ is the design tensile value of concrete strength at time of release:

η_{p1}	2.70	for indented wires;
	3.20	for 3- and 7-wires strands.
η_1	1.00	for good bond conditions;
	0.70	otherwise.

$f_{ctd}(t) = \alpha_{ct}\ 0.7\ [\beta_{cc}(t)]^{\alpha}\ f_{ctm}\ /\ \gamma_c$ with same meaning of Eq. 2-11

Differently from *fib* MC2010, the basic value of the transmission length (l_{pt}) is directly given by EC2 as in Eq. 2-13, without computing the basic anchorage length:

$$l_{pt} = \alpha_1\,\alpha_2\,\phi\,f_{si}\,/\,f_{bpt} \tag{2-13}$$

in which α_1 considers the type of prestressing-force release, α_2 takes into account the type of tendon, ϕ is the tendon diameter and f_{si} is the tendon stress just after release:

α_1	1.00	for gradual release;
	1.25	for sudden release.
α_2	0.19	for 3- and 7-wire strands;
	0.25	for tendons with circular cross-section.

Thus, the design value of the transmission length can be taken as the less favourable of the following two values, depending on the design situation:

$$l_{pt1} = 0.8\,l_{pt} \tag{2-14 a}$$

$$l_{pt2} = 1.2\,l_{pt} \tag{2-14 b}$$

where the shorter and the larger transmission length values should be selected for local stress verification after release and for calculation of shear and anchorage capacity at ULS, respectively, in order to take into account the variations in the bond strength.

According to EC2, no anchorage check of tendons at ULS is necessary when the concrete is uncracked along the anchorage length, with tensile stress less than $f_{ctk,0.05}$. Instead, if concrete tensile stress exceeds $f_{ctk,0.05}$ and flexural cracks occur along the PC member, the anchorage of tendons should be checked with a reduced bond strength in the flexural bond length (f_{bpd}), as reported in Eq. 2-15. By comparing the two bond situations in the transmission length and in the flexural bond length (Eqs. 2-12 and 2-15, respectively), it is noted that the flexural bond is greatly reduced compared to the value of the prestress transfer bond:

$$f_{bpd} = \eta_{p2}\, \eta_1\, f_{ctd} \tag{2-15}$$

η_{p2} 1.20 for 7-wires strands;
1.40 for indented wires.

η_1 as defined for prestress transfer bond in Eq. 2-12.

The additional flexural bond length required for anchoring a tendon stress f_{ps} in the concrete is calculated to be proportional to the difference between such maximum tendon stress under design load (f_{ps}) and the tendon stress after all prestress losses (f_{se}). Therefore, the total anchorage length l_{bpd} can be expressed as in Eq. 2-16.

$$L_b = l_{bpd} = l_{pt2} + \alpha_2\, \phi\, \frac{f_{ps} - f_{se}}{f_{bpd}} \tag{2-16}$$

where l_{pt2} is the upper design value of the transmission length (Eq. 2-14 b) and α_2 is the coefficient depending on the type of tendon, as already explained in Eq. 2-13.

References

[2-1] *fib* Model Code 2010 (2013). "*fib* Model Code for concrete structures". International Federation for Structural Concrete (*fib*), Lausanne, Switzerland.

[2-2] ACI Committee 318 (2014). "Building Code requirements for structural concrete (ACI 318-14) and Commentary (ACI 318R-14)". American Concrete Institute, Farmington Hills, MI, USA.

[2-3] Mitchell, D., Cook, W.D., Kahn, A.A. and Tham, T. (1993). "Influence of High-Strength concrete on transfer and development length of pretensioning strand". *PCI Journal*, vol. 38(3), 52-66.

[2-4] Mohandoss, P., Pillai, R.G. and Sengupta, A.K. (2018). "Transmission length of pretensioned concrete systems - comparison of codes and test data". *Magazine of Concrete Research*, vol. 71(17), 1-13.

[2-5] den Uijl, J. (1992). "Background of the CEB-FIP Model Code 90 clauses on anchorage and transverse tensile actions in the anchorage zone of prestressed concrete members". *Comitè Euro-International du Beton (CEB): Bulletin d'Information*, vol. 212, 71-94.

[2-6] Janney, J.R. (1954). "Nature of bond in pretensioned prestressed concrete". *ACI Journal*, vol. 50(9), 717-736.

[2-7] Hanson, N.W. and Kaar, P.H. (1959). "Flexural bond of pretensioned prestressed beams". *ACI Journal*, vol. 55(7), 783-802.

[2-8] Metelli, G. and Plizzari, G.A. (2014). "Influence of the relative rib area on bond behaviour". *Magazine of Concrete Research*, vol. 66(6), 277-294.

[2-9] Hoyer, E. and Friedrich, E. (1939). "Beitrag zur frage der hafspaannung in eisenbeton-bauteilen". *Beton und Eisen*, vol. 30(6), 107-110.

[2-10] Over, S. and Au, T. (1965). "Prestress transfer bond of pretensioned strands in concrete". *ACI Journal*, vol. 62(11), 1451-1459.

[2-11] Russell, B.W. and Burns, N.H. (1996). "Measured transfer lengths of 0.5 and 0.6 in. Strands in pretensioned concrete". *Journal of Structural Engineering*, vol. 123(5), 44-65.

[2-12] Castrodale, R.W., Kreger, M.E. and Burns, N.H. (1988). "A study of pretensioned high strength concrete girders in composite highway bridges - Laboratory tests". Research report 381-3, *Center for Transportation Research*, University of Texas at Austin, Austin, TX, USA.

[2-13] Russell, B.W. and Burns, N.H. (1993). “Design guidelines for transfer, development and debonding of large diameter seven wire strands in pretensioned concrete girders”. Research report 1210-5F, *Center for Transportation Research*, University of Texas at Austin, Austin, TX, USA.

[2-14] Oh, B.H. and Kim, E.S. (2000). “Realistic evaluation of transfer lengths in pretensioned prestressed concrete members”. *ACI Structural Journal*, vol. 97(6), 821-830.

[2-15] Kahn, L.F., Dill, J.C. and Reutlinger, C.G. (2002). “Transfer and development length of 15-mm strand in High-Performance concrete girders”. *Journal of Structural Engineering*, vol. 128(7), 913-921.

[2-16] Barnes, R.W., Groove, J.W. and Burns, N.H. (2003). “Experimental assessment of factors affecting transfer length”. *ACI Structural Journal*, vol. 100(6), 740-748.

[2-17] Kose, M.M. and Burkett, W.R. (2005). “Evaluation of Code requirement for 0.6 in. (15 mm) prestressing strand”. *ACI Structural Journal*, vol. 102(3), 422-428.

[2-18] Martì-Vargas, J.R., Serna-Ros, P., Fernández-Prada, M.A., Miguel-Sosa, P.F. and Arbeláez, C.A. (2006). “Test method for determination of the transmission and anchorage lengths in prestressed reinforcement”. *Magazine of Concrete Research,* vol. 58(1), 21-29.

[2-19] Martì-Vargas, J.R., Arbeláez, C.A., Serna-Ros, P. and Castro-Bugallo, C. (2007). “Reliability of transfer length estimation from strand end slip”. *ACI Structural Journal,* vol. 104(4), 487-494.

[2-20] Ramirez, J.A. and Russell, B.W. (2008). “Transfer, development, and splice length for strand/reinforcement in High-Strength concrete”. NCHRP report 603, *Transportation Research Board*.

[2-21] Floyd, R.W., Ruiz, E.D., Do, N.H., Staton, B.W. and Hale, W.M. (2011). “Development lengths of High-Strengths self-consolidating concrete beams”. *PCI Journal,* vol. 56(1), 36-53.

[2-22] Eurocode 2 (2004). “Design of concrete structures - Part 1-1: General rules and rules for buildings”. Comitè Europèen de Normalisation, Brussels, Belgium.

[2-23] Deatherage, J.H., Burdette, E.G. and Chew, C.K. (1994). “Development length and lateral spacing requirements of prestressing strand for prestress concrete bridge girders”. *PCI Journal,* vol. 39(1), 70-83.

[2-24] Elliott, K.S. (2014). "Transmission length and shear capacity in prestressed concrete hollow core slabs". *Magazine of Concrete Research,* vol. 66(12), 585-602.

[2-25] AASHTO (2012). "LFRD bridge design specifications - 6th edition". American Association of State Highway and Transportation, Washington, DC, USA.

[2-26] ACI Committee 318 (1963). "Building Code requirements for structural concrete (ACI 318-63) and Commentary (ACI 318R-63)". American Concrete Institute, Detroit, MI, USA.

[2-27] Kaar, P.H., LaFraugh, R.W. and Mass, M.A. (1963). "Influence of concrete strength on strand transfer length". *Journal of Prestressed Concrete Institute*, vol. 8(5), 47-67.

[2-28] Tabatabai, H. and Dickson, T. (1993). "The history of the prestressing strand development length equation". *PCI Journal,* vol. 38(6), 64-75.

[2-29] Buckner, C.D. (1995). "A review of strand development length for pretensioned concrete members". *PCI Journal,* vol. 40(2), 84-105.

[2-30] Lane, S. and Rekenthaler, D.Jr. (1998). "The ties that bind: the 10-year fight for 0.6-inch diameter strand". *Public Roads,* vol. 31(5), 27-29.

[2-31] *fib* Model Code 1990 (1990). "*fib* Model Code for concrete structures". International Federation for Structural Concrete (*fib*), Lausanne, Switzerland.

3. ASSESSMENT OF EXISTING DESIGN FORMULATIONS ON PRESTRESSING TENDONS

3.1. Preface

Many formulations about transmission length and anchorage length of prestressing tendons, as illustrated in the previous section of this contribution, are provided by existing design codes for concrete structures. Furthermore, as bond characteristics in PC members have been increasingly investigated by researchers in the last decades, a number of proposed empirical equations, based on the results of experimental campaigns, is also available in the literature. A summary of the most relevant formulations and practical relationships on transmission length and anchorage length of PC members is reported in Table 3-1 and Table 3-2, respectively.

It has already been highlighted that the commonly used design specifications differ with respect to the influencing parameters which are included in the calculation. For example, although several studies [3-1; 3-2; 3-3; 3-4] carried out in the literature have shown that concrete compressive strength plays a key role on bond development at the interface between the tendon and the concrete, only some practical provisions actually take into account it as a primary variable. However, this heterogeneity on the considered influencing factors could lead to big differences when evaluating the transmission length and anchorage capacity of PC members. For this reason, a detailed assessment of the main design recommendations on pre-tensioning anchorage is worth addressing, to understand the real accuracy within real structural applications.

The key point for a correct dimensioning of pre-tensioning anchorage on PC members is related to the calculation of the transmission length and anchorage length. In this chapter, a general assessment of the principal formulations on prestressing tendons is carried out. Initially, the evaluation of the main provisions on the transmission length and anchorage length is analysed by applying them to commonly used PC member configurations. However, many experimental studies on this research area can be found in the literature, even though they were focused on different objectives and purposes. Thus, in the second part of the section, the accuracy of the available relationships is discussed when comparing them to a comprehensive dataset of transmission length and anchorage length values. Data will be analysed through common statistical indicators and main findings will be reported separately for each formulation.

Table 3-1: Main provisions on transmission length - design codes and researchers' proposals.

Reference	Equation	Notes
ACI 318 (2014) [3-5]	$L_t = \frac{f_{se}\ \phi}{20.7}$	Lengths in mm. Stresses in MPa.
ACI 318 simplified (2014) [3-5]	$L_t = 50\ \phi$	Lengths in mm.
fib Model Code 2010 (2013) [3-6]	$L_t = \alpha_{p1}\ \alpha_{p2}\ \alpha_{p3}\ \frac{f_{si}}{f_{ptd}}\ l_{bp}$	α_{p2} set to 0.5 when checking transverse stresses at release.
AASHTO (2012) [3-7]	$L_t = 60\ \phi$	Lengths in mm.
Eurocode 2 (2004) [3-8]	$L_t = c\ \alpha_1\ \alpha_2\ \phi\ \frac{f_{si}}{f_{bpt}}$	c set to 0.8 when checking transverse stresses at release.
Pellegrino et al. (2015) [3-9]	$L_t = exp(\alpha + \beta\phi + \gamma f_{si} + \delta f_{ci}')$	α = 1.34; β = 0.03967; γ = 0.00358; δ = -0.00815.
Buckner (1995) [3-10]	$L_t = \frac{1250\ f_{si}\ \phi}{E_{ci}}$	E_{ci} is concrete elastic modulus at release.
Russell and Burns (1993) [3-11]	$L_t = \frac{f_{se}\ \phi}{13.8}$	It provides an "upper limit" for Lt. Lengths in mm. Stresses in MPa.
Mitchell et al. (1993) [3-2]	$L_t = \frac{0.33}{6.9}\ f_{si}\phi\ \sqrt{\frac{20.7}{f_{ci}'}}$	f_{ci}' is concrete compressive strength at release.
Shahawy et al. (1992) [3-12]	$L_t = \frac{f_{si}\ \phi}{20.7}$	Lengths in mm. Stresses in MPa.
Lane (1990) [3-13]	$L_t = 4\ \frac{f_{si}\ \phi}{f_c'}$ - 127	It provides a design value for Lt. f_c' is concrete compressive strength limited to 69 MPa.
Cousins et al. (1990) [3-14]	$L_t = 0.5\left(\frac{U_t'\sqrt{f_{ci}'}}{B}\right) + \frac{f_{se}\ A_{ps}}{\pi\ \phi\ U_t'\ \sqrt{f_{ci}'}}$	U_t' = constant bond stress along the plastic zone. B = slope of bond stress curve along the elastic zone. Lengths in inches. Stresses in psi.
Zia and Mostafa (1977) [3-1]	$L_t = 1.5\ \frac{f_{si}}{f_{ci}'}\ \phi$ - 117	f_{ci}' is concrete compressive strength at release limited to 55.2 MPa. Lengths in mm. Stresses in MPa.
Martin and Scott (1976) [3-15]	$L_t = 80\ \phi$	Lengths in mm.

Table 3-2: Main provisions on anchorage length - design codes and researchers' proposals.

Reference	Equation	Notes
ACI 318 (2014) [3-5]	$L_b = \frac{f_{se}\ \phi}{20.7} + \frac{1}{6.9}(f_{ps} - f_{se})\ \phi$	Lengths in mm. Stresses in MPa.
fib Model Code 2010 (2013) [3-6]	$L_b = \alpha_{p1}\ \alpha_{p2}\ \alpha_{p3}\ \frac{f_{si}}{f_{ptd}}\ l_{bp} + l_{bp}\ \frac{f_{ps} - f_{se}}{f_{ptd}}$	α_{p2} set to 1.0 when calculating anchorage capacity at ULS.
AASHTO (2012) [3-7]	$L_b = 0.145\ k\ (f_{ps} - \frac{2}{3} f_{se})\ \phi$	k considers the depth of the PC member.
Eurocode 2 (2004) [3-8]	$L_b = c\ \alpha_1\ \alpha_2\ \phi\ \frac{f_{si}}{f_{bpt}} + \alpha_2\ \phi\ \frac{f_{ps} - f_{se}}{f_{bpd}}$	c set to 1.2 when calculating anchorage capacity at ULS.
Shahawy (2001) [3-16]	$L_b = \frac{f_{si}}{20.7}\ \phi + \frac{1}{6.9}\ \frac{f_{ps} - f_{se}}{1.2}\ \phi$	For member depth less than 610 mm. Lengths in mm, stresses in MPa.
Buckner (1994) [3-17]	$L_b = \frac{f_{si}}{20.7}\ \phi + \frac{\lambda}{6.9}(f_{ps} - f_{se})\ \phi$	$1 \leq \lambda = (0.6 + 40\varepsilon_{ps}) \leq 2$ ε_{ps} is strand strain at the nominal strength.
Deatherage et al. (1994) [3-18]	$L_b = \frac{f_{si}}{20.7}\ \phi + \frac{1.5}{6.9}(f_{ps} - f_{se})\ \phi$	Lengths in mm. Stresses in MPa.
Mitchell et al. (1993) [3-2]	$L_b = \frac{0.33}{6.9} f_{si}\ \phi \sqrt{\frac{20.7}{f_{ci}'}} + \frac{f_{ps} - f_{se}}{6.9}\ \phi \sqrt{\frac{31.05}{f_{c}'}}$	f_{ci}' is concrete compressive strength at release. f_c' is concrete compressive strength.
Lane (1990) [3-13]	$L_b = 4\ \frac{f_{si}\ \phi}{f_{c}'} - 127 + \frac{6.4\ (f_{ps} - f_{se})}{f_{c}'}\ \phi + 381$	It provides a design value for Lb. f_c' is concrete compressive strength limited to 69 MPa.
Cousins et al. (1990) [3-14]	$L_b = 0.5 \left(\frac{U_t' \sqrt{f_{ci}'}}{B}\right) + \frac{f_{se}\ A_{ps}}{\pi\ \phi\ U_t' \sqrt{f_{ci}'}} + (f_{ps} - f_{se})\ \frac{A_{ps} / (\pi\ \phi)}{U_d'\ \sqrt{f_c'}}$	U_d' is the constant bond stress along the plastic zone. Lengths in inches. Stresses in psi.
Zia and Mostafa (1977) [3-1]	$L_b = 1.5\ \frac{f_{si}}{f_{ci}'}\ \phi - 117 + \frac{1.25}{6.9}(f_{ps} - f_{se})\ \phi$	f_{ci}' is concrete compressive strength at release limited to 55.2 MPa. Lengths in mm. Stresses in MPa.

3.2. Comparison of existing design concepts

A first simple investigation to emphasise the differences between the aforementioned design specifications when evaluating the transmission length or anchorage capacity of prestressing tendons can be performed by applying them to specific structural configurations involving commonly used materials. In particular, a rectangular PC test member (b = 100 mm; h = 120 mm) equipped with one 7-wire strand of diameter $Ø$ = 12.7 mm, embedded in concrete with a compressive strength at release f_{ci}' of 30 and 45 MPa, respectively, is considered for a comparison of the existing formulations. The concrete strength at 28 days (f_c') is taken to be equal to 41 MPa, i.e. approximately 1.37 times the concrete compressive strength at release. The beam setup also consists in a jacking stress equal to f_{si} 1400 MPa (prestress losses are usually estimated as 15% of the strand stress at release, so that f_{se} = 1190 MPa) and a sudden release of the strand from the temporary anchorages. Moreover, the uncoated prestressing strand is characterised by a tensile strength f_{su} equal to 1862 MPa, whereas a strand stress f_{ps} at the ultimate nominal strength equal to 1650 MPa is considered for the application. Such configuration, involving materials and conditions which are commonly employed in pretensioning applications, is summarised in Figure 3-1.

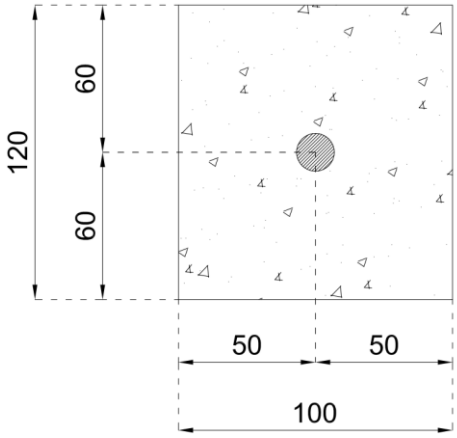

Strand diameter	$Ø$ = 12.7 mm
Concrete strength at release	f_{ci}' = 30-45 MPa
Concrete strength at 28 days	f_c' = 41-62 MPa
Jacking stress	f_{si} = 1400 MPa
Strand stress after losses	f_{se} = 1190 MPa
Strand tensile strength	f_{pt} = 1862 MPa
Strand stress at nominal strength	f_{ps} = 1650 MPa
Release type	sudden

Figure 3-1: PC beam configuration for comparison of design specifications.

3.2.1. Comparison of the transmission length formulations

Table 3-3 shows the numerical values of the transmission length when referring to the described PC member (illustrated in Figure 3-1), calculated for f_{ci}' = 30 MPa and f_{ci}' = 45 MPa by the existing formulations (both design code provisions and researchers' empirical proposals), where design values are considered. It can be noted that a relatively large scatter exists among the different analytical models. In particular, the

minimum values of L_t are provided by the simplified formula of ACI 318-14 (equal to 635.0 mm) and the expression proposed by Zia and Mostafa (equal to 475.7 mm) for concrete compressive strength equal to 30 and 45 MPa, respectively. Instead, the maximum values of L_t (equal to 1603.6 mm and 1126.7 mm for f_{ci}' = 30 MPa and f_{ci}' = 45 MPa, respectively) both correspond to the Lane's formula, which proves to be far from the other recommendations in determining the transmission length of the selected beam (especially for lower concrete compressive strengths).

Table 3-3: Calculated transmission length values for the described PC member configuration.

Formulation	f_{ci}' = 30 MPa	f_{ci}' = 45 MPa
	Transmission length [mm] (diff. with *fib* MC2010)	Transmission length [mm] (diff. with *fib* MC2010)
ACI 318 (2014)	730.1 (-10.9 %)	730.1 (+26.1 %)
ACI 318 simplified (2014)	635.0 (-22.5 %)	635.0 (+9.6 %)
fib Model Code 2010 (2013)	819.1	579.2
AASHTO (2012)	762.0 (-7.0 %)	762.0 (+31.6 %)
Eurocode 2 (2004)	960.4 (+17.3 %)	679.1 (+17.3 %)
Pellegrino et al. (2015)	743.5 (-9.2 %)	657.9 (+13.6 %)
Buckner (1995)	726.6 (-11.3 %)	643.4 (+11.1 %)
Russell and Burns (1993)	1095.1 (+33.7 %)	1095.1 (+89.1 %)
Mitchell et al. (1993)	706.4 (-13.8 %)	576.7 (-0.4 %)
Shahawy et al. (1992)	858.9 (+4.9 %)	858.9 (+48.3 %)
Lane (1990)	1603.6 (+95.8 %)	1126.7 (+94.4 %)
Cousins et al. (1990)	983.1 (+20.0 %)	810.3 (+39.9 %)
Zia and Mostafa (1977)	772.0 (-5.7 %)	475.7 (-17.9 %)
Martin and Scott (1976)	1016.0 (+24.0 %)	1016.0 (+75.4 %)

It should be noted that the lower value of the transmission length is taken both for the expressions of *fib* MC2010 and Eurocode 2, by using the coefficients α_{p2} = 0.5 (for *fib* MC2010) and c = 0.8 (for Eurocode 2), respectively. Considering the design code provisions, the formulations of *fib* MC2010 and Eurocode 2, which are based on a physically-based and more refined calculation (see sections 2.4.3 and 2.4.4), exhibit a different behaviour if compared to ACI 318-14 or AASHTO. In fact, they result in larger transmission lengths for the lower concrete compressive strength (i.e. 30 MPa), while they provide smaller transmission length values for the higher concrete compressive strength (i.e. 45 MPa). This is mainly due to the fact that concrete

compressive strength, which actually plays an important role on the transmission length calculation, is not taken into account as a primary variable in ACI 318-14 and AASHTO, thus resulting in the same value of L_t for the two different concrete types. Particularly, for the described configuration of the PC member, it can be easily derived that the transmission length estimated by ACI 318-14 is comparable with those evaluated by *fib* MC2010 and Eurocode 2 when the concrete compressive strength reaches the values of about 34 and 41 MPa, respectively.

The divergence of the existing formulations when evaluating the transmission length of the considered PC member is also depicted in Figure 3-2 for both the selected concrete compressive strength. However, for practical comparison, the equation of Lane is not represented in the graph as the transmission lengths which arise from its application are much different from the other models, particularly for $f_{ci}' = 30$ MPa.

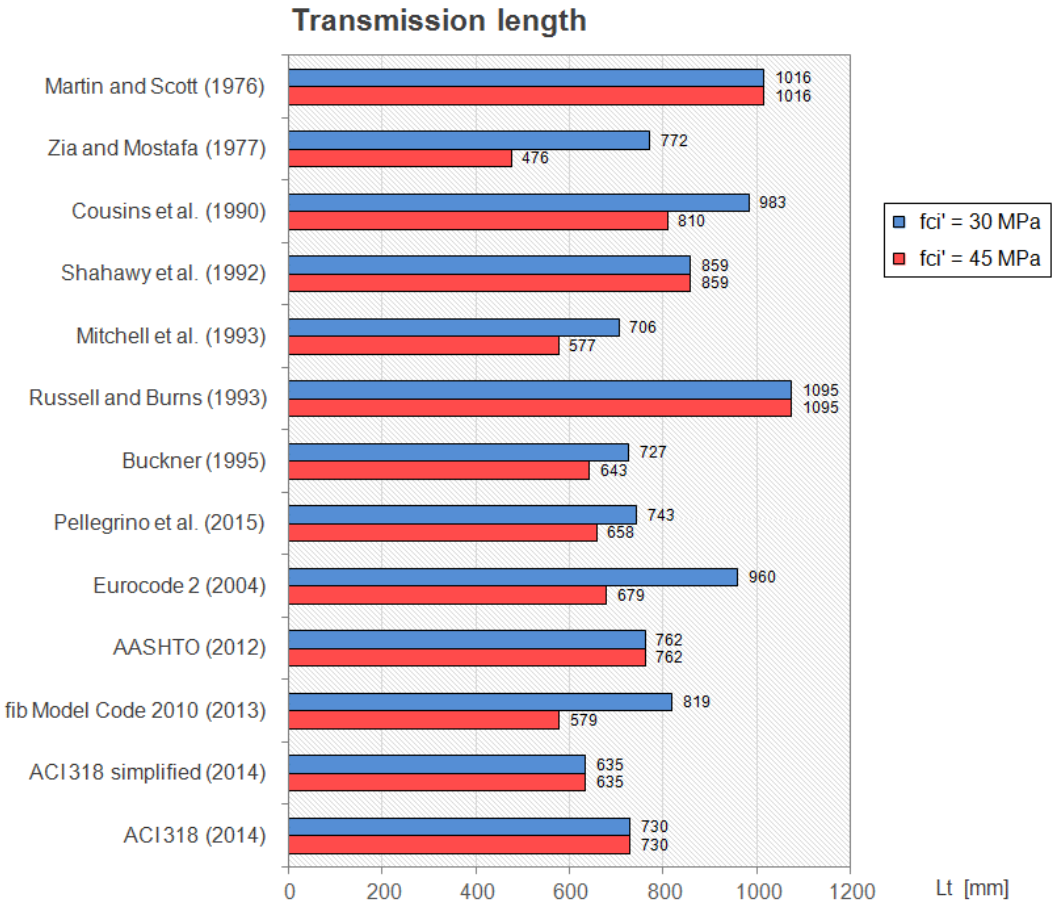

Figure 3-2: Comparison of the calculated transmission lengths for the described PC member.

In Table 3-3 and Figure 3-3, the percentage difference with respect to the equation of *fib* MC2010 is also reported for each formulation. Within this document, *fib* MC2010 is taken as a reference code for concrete structures, since it seems to provide the best

performances in the evaluation of the transmission length and anchorage capacity of prestressing strands (this matter will be addressed and commented in the next section of the chapter). It can be noted that the percentage difference with *fib* MC2010 generally increases as concrete compressive strength becomes higher (the only exception is the equation of Zia and Mostafa). Moreover, the comparison between *fib* MC2010 and Eurocode 2 gives the same deviation (+17.3%) for both values of the concrete compressive strength (30 and 45 MPa), demonstrating that such parameter is considered identically within the respective formulations. The proposals by Mitchell et al., Pellegrino et al. and Buckner are those which better replicate the transmission lengths obtained with *fib* MC2010 for both values of the concrete compressive strength, presenting a discrepancy of -13.8%, -9.2% and -11.3% when considering $f_{ci}^{'}$ = 30 MPa, and a difference of -0.4%, +13.6% and +11.1% for $f_{ci}^{'}$ = 45 MPa, respectively.

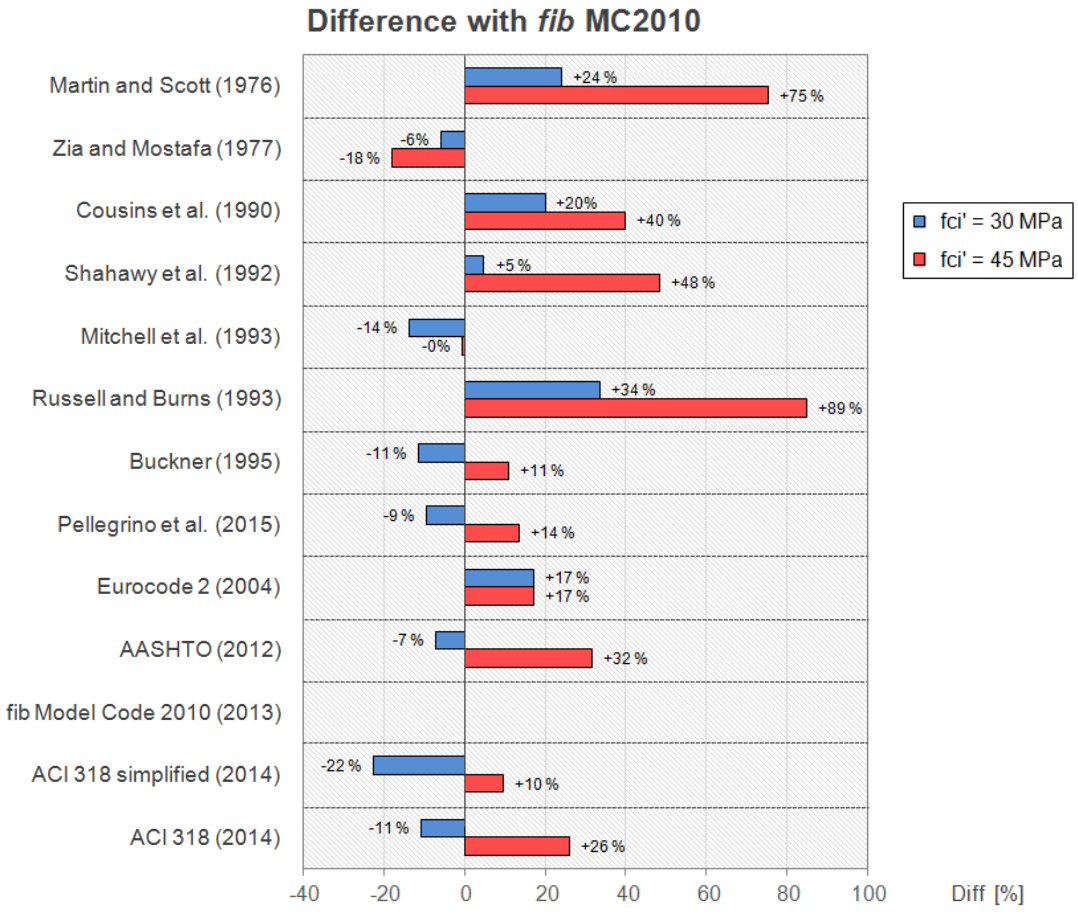

Figure 3-3: Percentage difference of the transmission lengths calculated by the existing formulations when compared to fib MC2010.

3.2.2. Comparison of the anchorage length formulations

The comparison of the anchorage length values arising from applying the available models to the PC member setup described in Figure 3-1 is shown in the following Table 3-4 for the selected concrete compressive strengths of f_{ci}' = 30 MPa and f_{ci}' = 45 MPa (design values of the anchorage length are considered, too). Similarly to what presented above for the transmission length, a certain variability of the results is also revealed for the anchorage length calculation of the tendon. In this case, the minimum values of the anchorage length are those evaluated by the formula of Mitchell et al. (L_b = 1422.3 mm for f_{ci}' of 30 MPa, and L_b = 1177.6 mm for f_{ci}' of 45 MPa, respectively). The maximum values of the anchorage length are again reached when considering the Lane's expression (L_b = 2894.4 mm for f_{ci}' of 30 MPa, and L_b = 2164.3 mm for f_{ci}' of 45 MPa, respectively), which uses the concrete compressive strength at 28 days for determining both the transmission length and the flexural bond length contribution. The recommended values by Cousins et al., which incorporate the effect of the strand surface condition (uncoated or coated tendon with different levels of grit), are also close to the prediction of Lane. However, only few formulations are able to capture the effect of the concrete compressive strength on the anchorage capacity of the tendon: the formulas of ACI 318, AASHTO, Shahawy, Buckner and Deatherage do not cause any variation on L_b between the cases of f_{ci}' equal to 30 and 45 MPa.

Table 3-4: Calculated anchorage length values for the described PC member configuration.

Formulation	f_{ci}' = 30 MPa	f_{ci}' = 45 MPa
	Anchorage length [mm] (diff. with *fib* MC2010)	Anchorage length [mm] (diff. with *fib* MC2010)
ACI 318 (2014)	1576.8 (-36.9 %)	1576.8 (-10.8 %)
fib Model Code 2010 (2013)	2499.3	1767.3
AASHTO (2012)	1577.6 (-36.9 %)	1577.6 (-10.8 %)
Eurocode 2 (2004)	2282.1 (-8.7 %)	1613.7 (-8.7 %)
Shahawy (2001)	1564.5 (-37.4 %)	1564.5 (-11.5 %)
Buckner (1994)	1705.6 (-31.8 %)	1705.6 (-3.5 %)
Deatherage et al. (1994)	2128.9 (-14.8 %)	2128.9 (+20.5 %)
Mitchell et al. (1993)	1422.3 (-42.3 %)	1177.6 (-33.4 %)
Lane (1990)	2894.4 (+15.8 %)	2164.3 (+22.4 %)
Cousins et al. (1990)	2599.8 (+4.0 %)	2130.3 (+20.5 %)
Zia and Mostafa (1977)	1830.3 (-26.8 %)	1534.0 (-13.2 %)

In this case, i.e. when evaluating the anchorage capacity of the member at ULS, the upper values of the transmission length are considered for *fib* MC2010 and Eurocode 2, through α_{p2} set to 1.0 (for *fib* MC2010) and c set to 1.2 (for Eurocode 2). The calculation of the design anchorage length by using the specification of *fib* MC2010 and Eurocode 2 is much higher than that of ACI 318-14 or AASHTO (which are based on the same formulation) for lower values of concrete compressive strength (i.e. 30 MPa), but is very similar when considering higher values of concrete compressive strength (i.e. 45 MPa). It is noted that *fib* MC2010 and Eurocode 2 result in the higher reduction of the anchorage length when increasing f_{ci}' from 30 to 45 MPa. The general scatter of the existing formulations in the evaluation of the anchorage capacity of the selected PC beam is illustrated in Figure 3-4, where the Lane's proposal is also excluded from the comparison due to important deviation from all the other provisions (especially for f_{ci}' = 30 MPa).

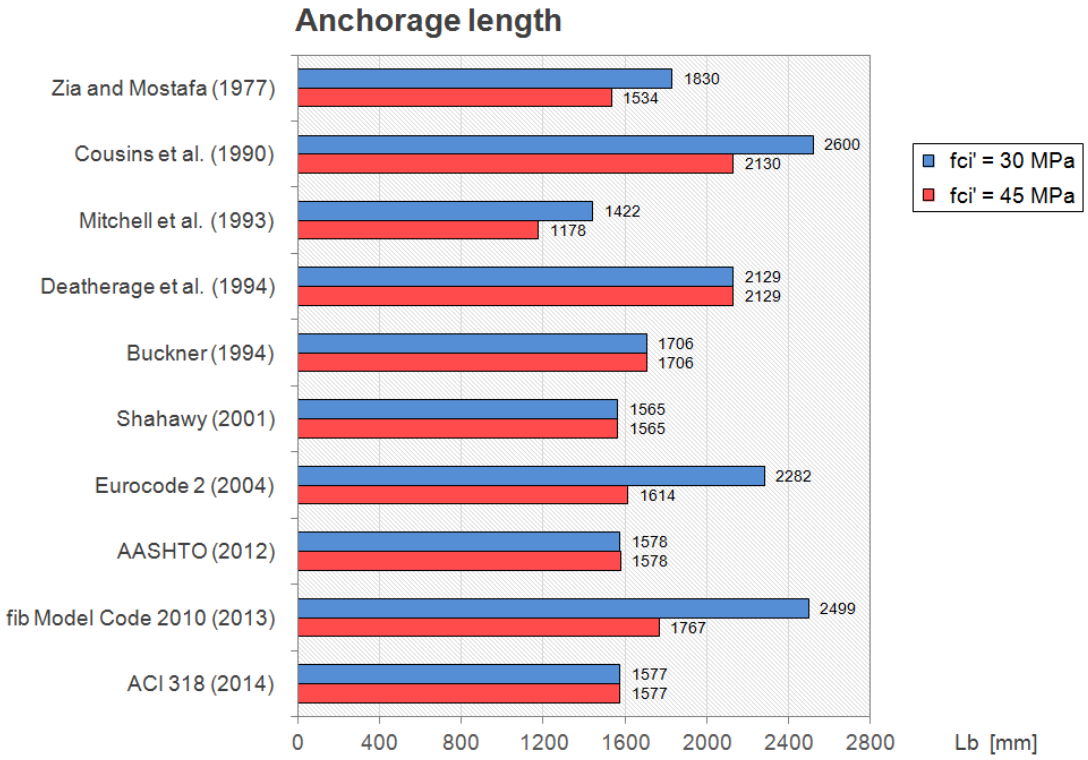

Figure 3-4: Comparison of the calculated anchorage lengths for the described PC member.

In Table 3-4 and Figure 3-5, the difference (in percentage) of each formulation is also shown in respect of *fib* MC2010. In particular, the evaluation by *fib* MC2010 gives anchorage lengths which are much larger than all the other recommendations for f_{ci}' = 30 MPa (apart from the Lane's formula the only exception is the relationship of Cousins et al.). However, Eurocode 2 only registers -9% with respect to *fib* MC2010. Instead, for

the higher concrete compressive strength of f_{ci}' = 45 MPa, it is highlighted that all the formulations get closer to *fib* MC2010, except for the expressions suggested by Deatherage et al. and Cousins et al., which provide the same higher result in terms of L_b (other than Lane's formula). Despite the anchorage lengths calculated by the formulation of Deatherage et al. are those which are closer to the results of *fib* MC2010 and Eurocode 2 for both values of concrete compressive strength, it can be noted that they are lower than *fib* MC2010 and Eurocode 2 for f_{ci}' = 30 MPa and larger than them for f_{ci}' = 45 MPa. This behaviour arises from the fact that the formulation of Deatherage et al. does not take into account the effect of concrete compressive strength when calculating the anchorage length of prestressing tendons.

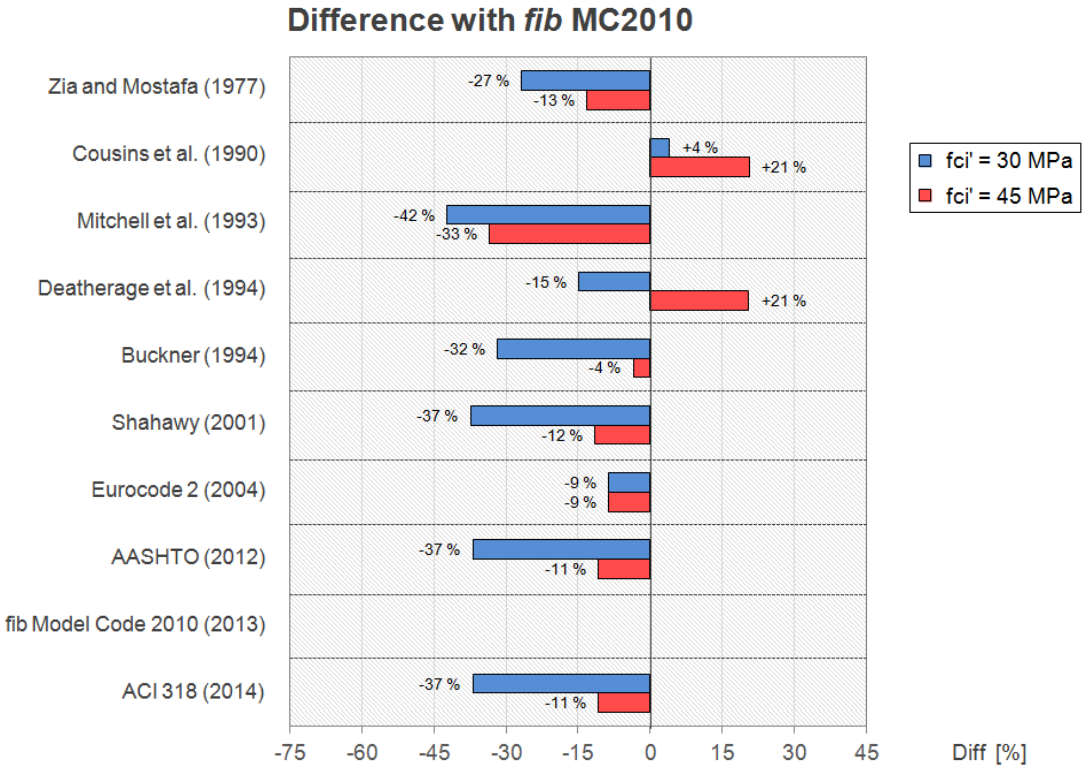

Figure 3-5: Percentage difference of the anchorage lengths calculated by the existing formulations when compared to fib MC2010.

3.2.3. Considerations on the flexural bond length

Some considerations can be drawn as regards the flexural bond length, which represents the embedment length required by a strand to increase the stress level due to external loads from the effective prestress to the stress at the nominal flexural strength of the member (see section 2-1). Basically, it can be seen as the difference between the entire anchorage length and the transmission length of the strand. With respect to the analysed configuration of the PC member, most of the existing formulations taken into

consideration in the previous paragraphs provide transmission length values which are approximately half of the total anchorage length. This means that the flexural bond length is comparable to the value of the transmission length. However, two exceptions can be found in the expressions of Cousins et al. and Zia and Mostafa. In both cases, the proposed formulation results in a very large flexural bond length if compared to the magnitude of the transmission length, regardless of the concrete compressive strength. Specifically, the transmission lengths provided by Cousins et al. are equal to 983 mm and 810 mm (for f_{ci}' of 30 and 45 MPa, respectively), while the corresponding anchorage lengths are equal to 2600 mm and 2130 mm, with a considerable increment, especially for f_{ci}' of 30 MPa. Also, the prediction by Zia and Mostafa provides anchorage length values which are much more than twice the corresponding transmission lengths (L_t = 772 mm and L_b = 1830 mm for f_{ci}' = 30 MPa; L_t = 476 mm and L_b = 1534 mm for f_{ci}' = 45 MPa). Anyway, such comparison is not possible for *fib* MC2010 and Eurocode 2 since the calculation of the transmission length is based on α_{p2} = 0.5 (*fib* MC2010) and c = 0.8 (Eurocode 2), providing a lower value for L_t, while the anchorage length is calculated based on an upper value of L_t (i.e. α_{p2} = 1.0 and c = 1.2, see Tables 3-1 and 3-2).

3.3. Evaluation of current provisions based on experimental evidences

In this section, the accuracy of the existing design provisions on the transmission length and anchorage length of prestressing tendons is assessed in detail by applying them to experimental databases of measured values of transmission and anchorage length, collected from an extensive review of the literature. The final datasets are those also considered within the *fib* Task Group 2.5 "Bond and Material Models", in which the author is involved, and they will be comprehensively presented in the forthcoming *fib* Bulletin, along with a broad review of test methods and theoretical models commonly used to evaluate the transmission length and anchorage length in PC members. The complete databases on the transmission length and anchorage length, encompassing a total number of 742 data points, have been collected as exhaustively as possible with respect to the following principal variables:

- Tendon characteristics (tendon type, nominal diameter, tensile strength);
- Tendon surface conditions (smooth or rusted tendon, tendon coating);
- Tendon stresses (at release, after allowance for all prestress losses and at the nominal strength);

- Concrete characteristics (compressive strength at release and after 28 days);
- Cross-section detailing (number and positions of tendons, concrete cover thickness and tendon spacing);
- PC member geometry (type of sample, width and height of the cross-section, total span);
- Type of prestressing release (sudden or gradual);
- Presence of debonded tendons;
- Test method for evaluating the transmission length;
- Failure mode of the sample (for the anchorage length evaluation);
- Measured values of transmission length and anchorage length.

However, incomplete data have sometimes been experienced in publications while compiling the databases. In order to avoid non-uniform collection of test results, only the literature studies with variables of interest fully known have been taken into account for evaluation purposes. Nevertheless, incomplete data points have been included in the investigation too when the missing parameters could be deducted with reasonable assurance, without manipulating the database itself. Some experimental campaigns - or part of them - are thus excluded from the present assessment. For practical reasons, not all the above mentioned influencing factors can be considered in the evaluation of the databases. Typically, the experimental setup and the method of analysis of pre-tensioning anchorage can influence significantly the obtained transmission length or anchorage length values [3-19; 3-20], where some test results could not be representative for concrete structures in the current engineering practice.

Another issue to be taken into account in the investigation is the possible presence of debonded tendons in PC members. In fact, it is known that debonded tendons, which can be used to prevent large stresses at the free-end after release, have a different behaviour if compared to the conventional fully-bonded tendons. Several studies [3-21; 3-22] have found that the presence of debonded tendons within PC members enlarges the measured transmission length. In addition, Burgueño et al. [3-23] suggest that the debonding material itself can be a further influencing variable. Among the existing design codes, the potential influence of debonded tendons on the transmission length is not considered by *fib* MC2010 and Eurocode 2, whereas ACI 318-14 and AASHTO provide simplified recommendations. On one hand, ACI 318-14 suggests a doubled transmission length when considering debonded tendons in PC members. On the other hand, AASHTO, which admits a maximum number of debonded tendons equal to 25%

of the total prestressing steel, recommends a modification of the parameter *k* in Eq. 2-6, to be increased to k = 2. In this way, the anchorage length of a PC member is increased by 100% for elements with a depth of less than or equal to 24 in. (609.6 mm) and by 25% for bigger elements (on the contrary, the transmission length is not modified, see Table 3-1).

The assessment of the databases on transmission length and anchorage length presented in the following sections of the document will not consider the particular experimental setup, the method of analysis and the effect of debonded tendons in the concrete cross-section. The relevant information on such aspects are reported in the extended version of the databases (Annex A for the transmission length database and Annex B for the anchorage length database), but not accounted for in the investigation Thus, the considered serviceable dataset is actually made of 661 data points in place of the total number of 742 mentioned above.

3.3.1. Assessment of the transmission length of PC members

The serviceable experimental database of measured transmission lengths comprises a total number of 482 test samples, both PC small-scale specimens and PC real-scale bridge girders, spanning over a great variety of influencing parameters related to geometrical features, material properties and prestressing-force release method. Data have been gathered from experimental campaigns available in the literature performed since 1965, and specifically from the 15 studies reported in Table 3-5.

In particular, eight different strand diameters from 6.4 to 18.0 mm, strand stress at release ranging from 871.0 to 1436.2 MPa, concrete compressive strength at release covering a range from 19.2 to 76.1 MPa, concrete cover from 36.4 to 76.2 mm and strand clear spacing up to 60.8 mm are considered as quantitative parameters. The rectangular - or square - small-scale specimens are reinforced with up to 5 strands (even though the majority of them are equipped with a single or couple of tendons) , while the maximum number of tendons for the I-shaped real-scale bridge girders is 9. In the tests, the considered 7-wire strands were mainly 1860 grade and low-relaxation type.

Moreover, the dataset includes a number of qualitative features such as the type of prestressing-force release (which can involve sudden flame-cutting or gradual release of the tendons), strand surface conditions (tendons can be rusted, i.e. subject to some pre-weathering processes, or with a smooth external surface) and bond conditions (good or

not good, according to Figure 2-11). Additionally, some tendons were also epoxy-coated and impregnated with different level of grit to improve the bond with concrete.

Table 3-5: Detail of the experimental database of measured transmission lengths - test samples and authors.

PC Small-scale specimens		
Reference citation	No. of experimental tests	Test method
Over and Au (1965) [3-24]	4	ERSGs
Cousins et al. (1990) [3-25]	102	100% AMS
Mitchell et al. (1993) [3-2]	40	Slope-intercept
Russell and Burns (1996) [3-26]	40	95% AMS
Russell and Burns (1997) [3-27]	21	95% AMS
Oh and Kim (2000) [3-3]	72	95% AMS
Oh et al. (2006) [3-28]	48	95% AMS
Martì-Vargas et al. (2007) [3-29]	12	ECADA
Dang et al. (2017) [3-30]	24	95% AMS
PC Real-scale bridge girders		
Reference citation	No. of experimental tests	Test method
Cousins et al. (1994) [3-31]	23	100% AMS
Deatherage et al. (1994) [3-18]	40	Slope-intercept
Russell and Burns (1996) [3-26]	20	95% AMS
Kahn et al. (2002) [3-32]	8	95% AMS
Barnes et al. (2003) [3-33]	24	95% AMS
Kose and Burkett (2005) [3-34]	4	95% AMS

ERSGs = Electrical Resistance Strain Gauges; 95% AMS = 95% Average Maximum Strain; 100% AMS = 100% Average Maximum Strain.

As mentioned, two different release methods were used in the collected experimental investigations: a sudden prestress release or a gradual cutting process for each strand. However, the distinction between sudden and gradual release depends on various aspects such as the distance from the location where cutting takes place to the active end or dead end of the PC member, and whether it is a single beam or a series of beams placed in a row on the prestressing bed (this matter will be detailed in section 4.3.4.). Particularly, it should be noted that two distinct transmission length values are usually derived from the same PC sample, when using test methods that involve strain measurement on the concrete surface, depending on the considered free-end. One is named "*cut end*", representing the free-end subject to direct flame-cutting of the strands, while the other is the "*dead end*", which is at the opposite side of the member.

Nevertheless, the subdivision in the two categories of prestressing-force release (i.e. sudden or gradual) is adopted according to the description of the test setup provided by the single authors.

Geometrical characteristics of the samples are also characterised by a relevant variability within the dataset. Among the collected investigations, the values of the transmission length were experimentally determined principally through the 95% Average Maximum Strain method (95% AMS method, see section 2.3.1.2.) or the 100% AMS method. However, Martì-Vargas et al. considered the ECADA test method (see section 2.3.1.3.), while Mitchell et al. and Deatherage et al. used the slope-intercept method. The slope-intercept method enables to determine the transmission length as the distance from the free-end of the PC member to the point of intersection of a line fitting the strain values in the transfer region with a horizontal line representative of the strain values beyond this region [3-2]. Instead, the early study by Over and Au (1965) involved the use of Electrical Resistance Strain Gauges (ERSGs, see section 2.3.1.1.), which represented the most common technique to experimentally evaluate the transmission length at that time. The whole transmission length database is reported in table form in Annex A of the thesis.

3.3.1.1. Performance of design codes and researchers' proposals

Current design code provisions for the transmission length evaluation have been compared to the results collected in the experimental dataset, to find out if the effects of the major variables affecting the transmission length of PC members are reasonably included. In order to visualise the whole dataset, the measured values of the transmission length are plotted against the corresponding theoretical values, calculated with respect to the considered test setup. Each collected data point is used to calculate the transmission length individually with different design expressions. In particular, the recommendations by ACI 318-14, *fib* MC2010 and Eurocode 2 are hereunder analysed, where the study of small-scale specimens and real-scale girders is treated separately. Additionally, a third category of data points identified by experimental tests on specimens equipped with coated tendons is also shown in the following for completeness and comparison purposes. In this respect, the results of the comparison are graphically presented with different colours for beam specimens (labelled as specimens), full-scale girders (labelled as beams) and specimens adopting coated tendons (labelled as specimens coated).

3.3.1.2. ACI 318-14

Figure 3-6 illustrates the performance of ACI 318-14, i.e. the formulation in Eq. 2-2, when compared to the collected experimental values. As ACI 318-14 relationship provides average values of the transmission length, data points in the picture should stay above the "experimental vs predicted" L_t line (the dotted line in the graph) in the case of transverse stress verification after release, and below that line when evaluating the anchorage capacity of the PC member at ULS. However, it can be seen that many observations are very far from this ideal line, identifying an overall poor performance of ACI 318-14. Such a large scatter is due to the fact that ACI 318-14 considers only the nominal strand diameter and the effective strand stress after allowance for all prestress losses as influencing parameters, although it is commonly recognised that many other factors contribute to the phenomenon, such as the effect of the concrete properties (as shown in section 3.4.).

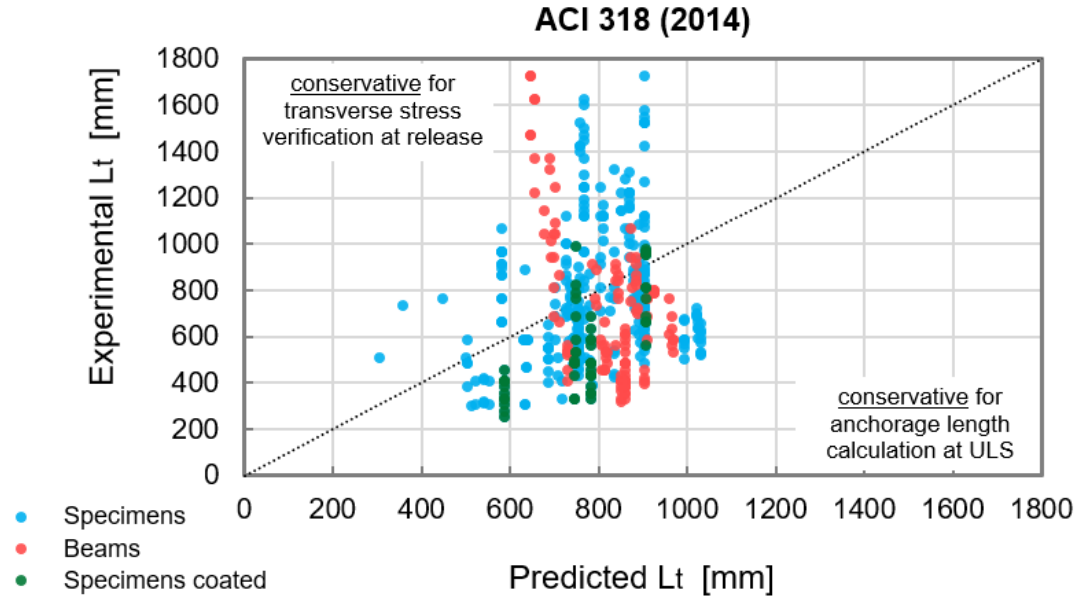

Figure 3-6: Performance of ACI 318-14 provisions on the transmission length when compared to the collected experimental database.

3.3.1.3. *fib* Model Code 2010

In Figures 3-7 and 3-8, the comparison between experimental and theoretical values of the transmission length according to *fib* Model Code 2010 is shown separately for the verification of the transverse stress at release (involving α_{p2} = 0.5 in Eq. 2-9) and for the calculation of the anchorage length at ULS (using α_{p2} = 1.0 in Eq. 2-9), respectively. Since the collected experimental tests were carried out on PC members using the real characteristics of the concrete (the tested compressive strength), average

values of the material properties are considered within *fib* MC2010 formulation (i.e. no partial safety coefficients are applied), in order to obtain a realistic assessment of the code provision.

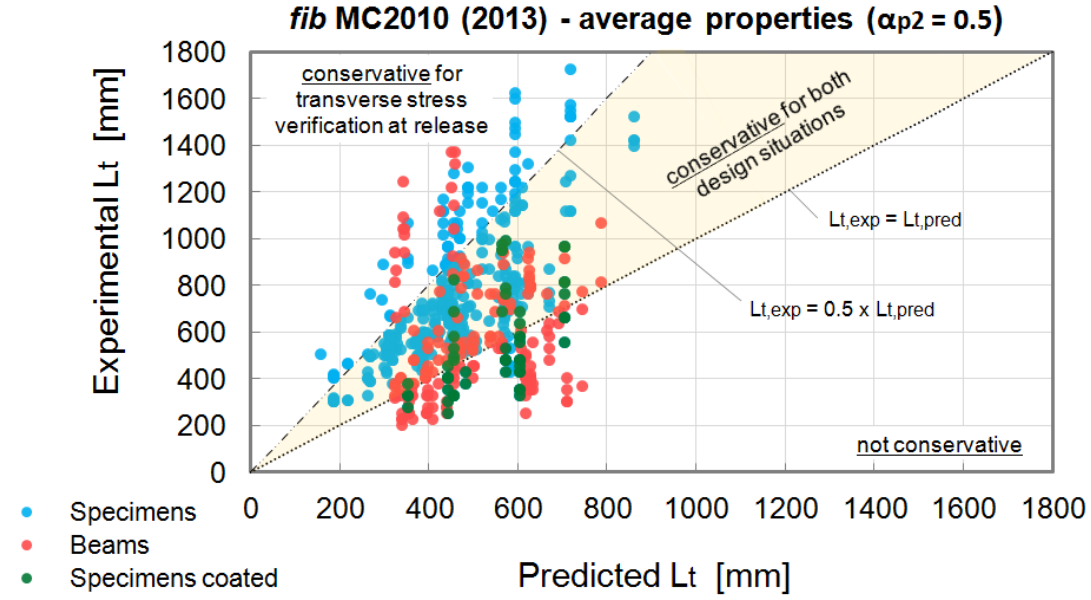

Figure 3-7: Experimental vs predicted transmission length according to fib MC2010 for verification of transverse stresses at release (lower bound), average material properties.

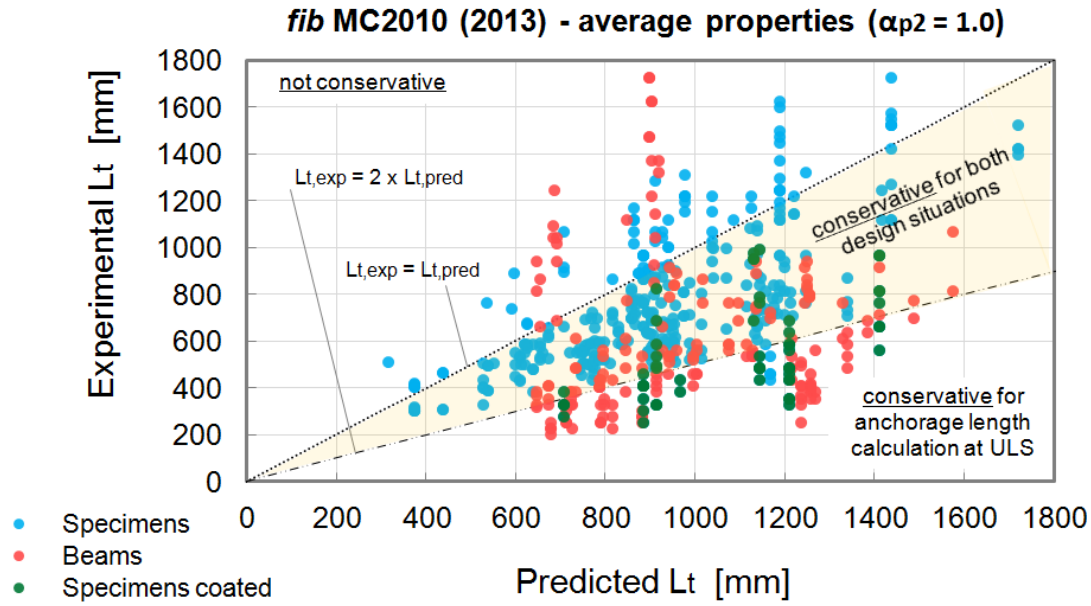

Figure 3-8: Experimental vs predicted transmission length according to fib MC2010 for calculation of the anchorage length at ULS (upper bound), average material properties.

It is recalled that shorter transmission length values are critical when checking allowable stresses near the member free-end after release, while larger transmission length values might be not conservative when evaluating the anchorage capacity of the PC member at ULS (see sections 2.1. and 2.4.3.). This means that collected data should

stay in the upper part of the diagram in Figure 3-7 (i.e. above the "$L_{t,exp} = L_{t,pred}$" line), and in the lower part of that illustrated in Figure 3-8 (i.e. below the "$L_{t,exp} = L_{t,pred}$" line). Altogether, data points should be within the ideal portion of the graphs limited by the highlighted "experimental vs predicted" L_t lines (i.e. the orange area), corresponding to the two different design situations taken into account. Specifically, the "$L_{t,exp} = 0.5 \cdot L_{t,pred}$" half-line in Figure 3-7 identifies the optimal line in the case of $\alpha_{p2} = 1.0$ (anchorage length calculation, where conservative data lie below it), while the "$L_{t,exp} = 2 \cdot L_{t,pred}$" half-line in Figure 3-8 corresponds to the optimal line in the case of $\alpha_{p2} = 0.5$ (stress check at release, where conservative data lie above it).

The formulation provided by *fib* MC2010 proves to be sufficiently accurate for both the relevant design conditions. Particularly, about 13% of the data points is not conservative when the transmission length is calculated for checking the transverse stress at release, being below the "$L_{t,exp} = L_{t,pred}$" line in Figure 3-7. Moreover, approximately 18% of the collected data is unsafe with respect to the anchorage length calculation, arranging above the dashed line depicted in Figure 3-8. Such values can be considered relatively low if considering the whole sample size, especially in the case of $\alpha_{p2} = 0.5$. Overall, about 31% of the data points falls outside the ideal graph area, being not conservative in one of the two design conditions. It can be noted that such not conservative data sets are mainly real-scale bridge girders (red points in the figures) when referring to the lower bound of the transmission length ($\alpha_{p2} = 0.5$), but are represented in the majority by small-scale specimens (blue points) when considering the upper bound ($\alpha_{p2} = 1.0$).

Compared to the performance of ACI 318-14, a relatively large scatter of the results is still evident for *fib* MC2010, even though the influence of more parameters on the transmission length is considered. Nevertheless, it should be considered that some inconsistencies might be present within the set of measured transmission lengths provided by the authors in the literature. In some cases, very different transmission length values can be found for samples with identical characteristics, probably due to the particular concrete mix design considered in the experimental tests. However, an explicit explanation for the deviating values can not be given.

3.3.1.4. Eurocode 2

The last performance evaluation of the transmission length calculation provided by existing design codes is presented with respect to Eurocode 2. Similarly to *fib* MC2010, the comparison between experimental and calculated transmission length values is

graphically illustrated for both the design phases, where average material properties are considered, too. In Figure 3-9, the assessment of Eurocode 2 formulation is shown for the transverse stress verification at release of the prestressing force. In this case, the lower bound values of the expression are considered (i.e. $l_{pt1} = 0.8\ l_{pt}$, as in Eq. 2-14a). On the other hand, in Figure 3-10, the performance of Eurocode 2 when evaluating the anchorage capacity of a PC member is depicted. In such case, the upper bound value of the transmission length is taken (i.e. $l_{pt2} = 1.2\ l_{pt}$, as in Eq. 2-14b).

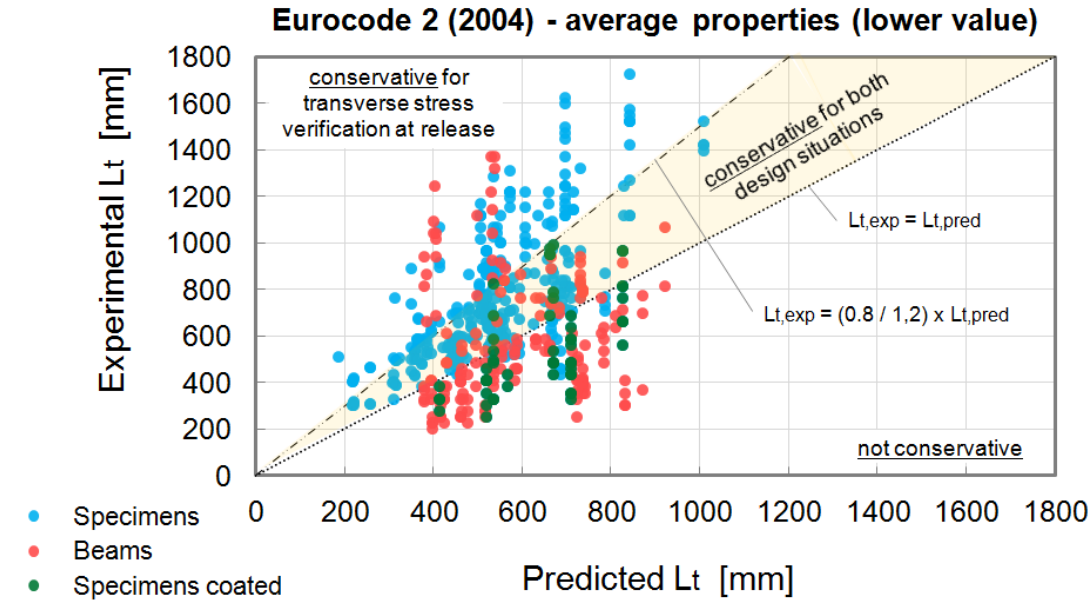

Figure 3-9: Experimental vs predicted transmission length according to Eurocode 2 for verification of transverse stresses at release (lower bound), average material properties.

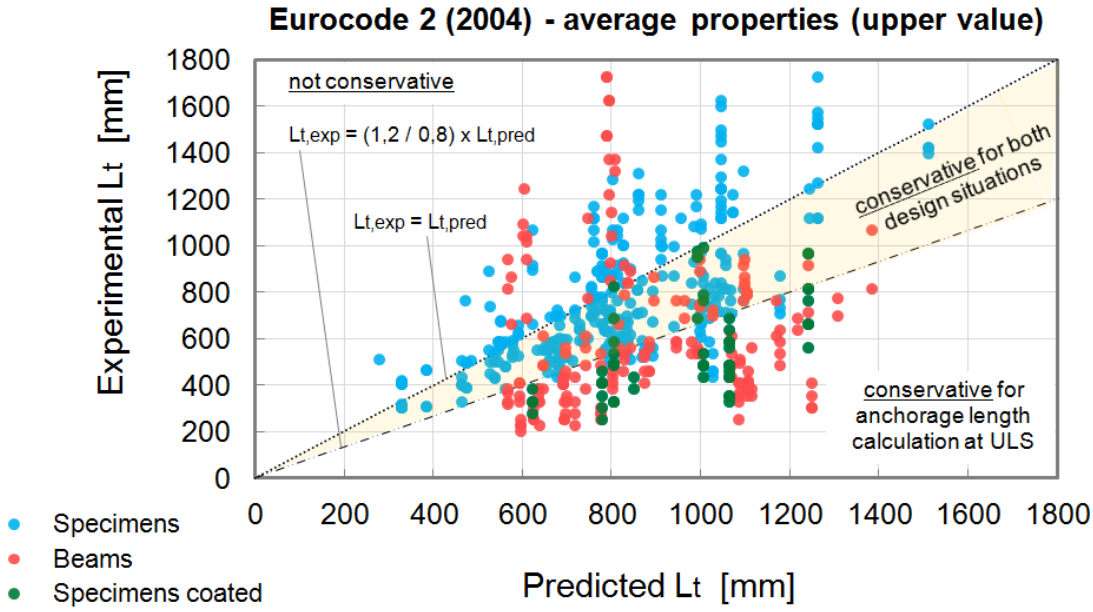

Figure 3-10: Experimental vs predicted transmission length according to Eurocode 2 for calculation of the anchorage length at ULS (upper bound), average material properties.

The same type of analysis carried out for *fib* MC2010 also applies for Eurocode 2, in that conservative data points should get the graphs area identified by the highlighted "experimental vs predicted" L_t lines (which is narrower than that described for *fib* MC2010 in the previous paragraph). However, about 24% and 30% of the data set are not conservative when checking transverse stresses and calculating flexural capacity at ULS, respectively. This globally results in a 54% of data points which are out of the ideal portion of plane. Such performance is poorer than that of *fib* MC2010.

3.3.1.5. Researchers' proposals

In addition to the evaluation of the current design codes formulations for the transmission length, the accuracy of the most recognised proposals advanced by researchers (listed in Table 3-1) is also presented. Figure 3-11 illustrates the measured transmission length values plotted against the corresponding calculated values. For all the formulations, as they provide a unique relationship to calculate the transmission length for both the transverse stress verification and the anchorage length calculation, only one diagram is shown, similarly to ACI 318-14.

It can be seen that the expressions recommended by Zia and Mostafa [3-1], Mitchell et al. [3-2], Buckner [3-10] and Pellegrino et al. [3-9] seem to better adhere to the transmission length values based on the collected experimental tests. In fact, for these formulations, approximately the same percentage of data points is arranged both above and below the "experimental vs predicted" L_t line. This means that the proposed relationships have the same performance when checking transverse stresses at release or calculating anchorage capacity at ULS. Anyway, a large scatter is also registered, being some data points particularly far from the ideal diagonal dotted line. Conversely, other design formulas such as those provided by Cousins et al. [3-14], Lane [3-13], Shahawy et al. [3-12] and Russell and Burns [3-11] result in a point cloud which is largely below the "experimental vs predicted" L_t line. This situation identifies a good performance of the cited relationships only for calculating the anchorage length of prestressing tendons, but not for checking allowable stresses at release, where the calculated transmission lengths are generally too large if compared to the experimental results. In this respect, a limit case is represented by the formula of Lane, which lead to 98% of not conservative data points when verifying transverse stresses and, on the other side, 2% (i.e. the complementary) of not conservative data points when calculating the anchorage capacity of the PC member. Lastly, it can be noted that the formulation of Martin and Scott [3-15] gives very poor performances, similar to ACI 318-14. It is remembered that

such relationships do not take into account the concrete compressive strength among the influencing parameters (it is simply L_t = 80 Ø for the expression of Martin and Scott, see Table 3-1). Generally, such conclusions are in accordance with the findings in section 3.2.1.

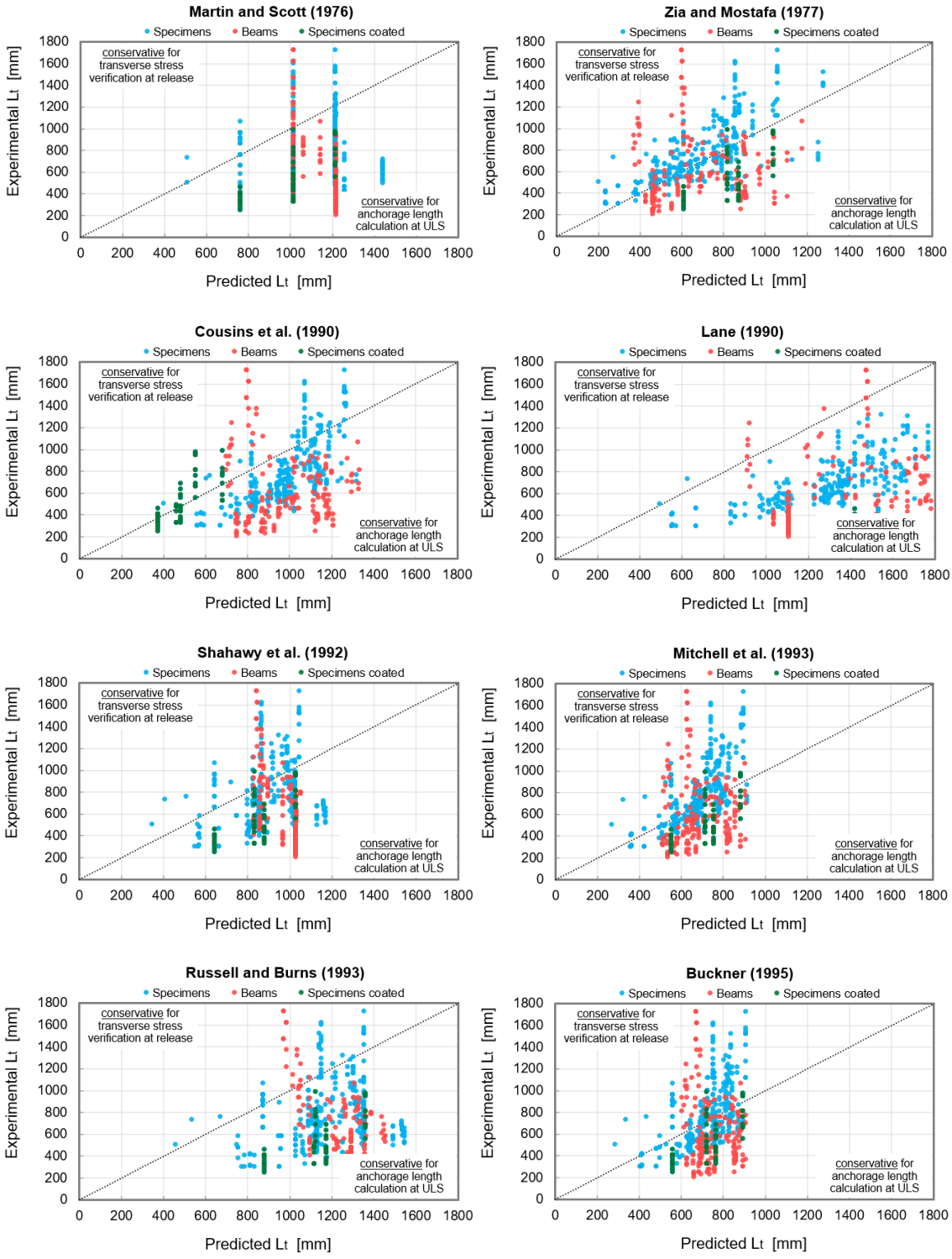

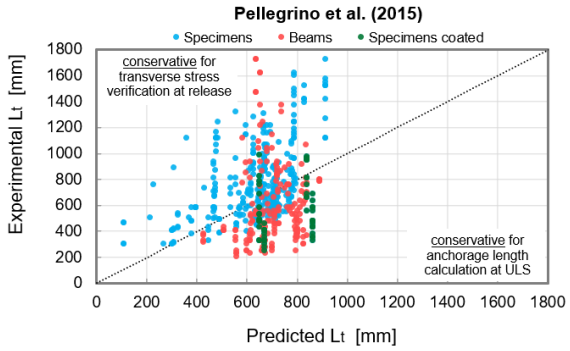

Figure 3-11: Performance of the main researchers' proposal formulations on the transmission length, when compared to the collected experimental database.

3.3.1.6. Statistical performance indicators

The accuracy of the existing design codes for concrete structures and researchers' proposal formulations in predicting the transmission length of prestressing tendons is analysed through the use of statistical performance indicators. In particular, the consistency of the suggested theoretical values with respect to the collected experimental dataset is evaluated by calculating:

- the average ratio between the theoretical and experimental values (AVE);
- the coefficient of variation of the dataset, that provides a measure of the dispersion of the values (COV);
- the root mean square error (RMSE);
- the percentage of not conservative data points (NC%).

Results are reported in the following Table 3-6 for both the typical design stages, where the label "NC% (a)" is associated with the situation involving checking the stresses near the free-end of the PC member, while the label "NC% (b)" is related to the situation involving calculating the flexural strength at ULS. Particularly, the numerical values of the performance indicators in Table 3-6 comprise the entire serviceable transmission length dataset, i.e. with no distinction between small-scale specimens and real-scale girders. Test specimens equipped with coated strands are also considered in the present evaluation (nevertheless, the scenario without considering coated tendons is also added in the table for *fib* MC2010 and Eurocode 2).

The obtained results clearly show how the less accurate formulations (i.e. characterised by the highest values of RMSE) are those providing the less conservative estimation of the transmission length with the aim of verifying transverse stresses at release. An example is given by the expressions of Russell and Burns, Lane and Martin and Scott

(for all of them a percentage of unsafe data of at least 85% is found). For these relationships, poor values of AVE and COV are also registered, indicating significant variance and weak correlation.

Table 3-6: Performance indicators of the formulations for transmission length evaluation.

Reference formulation	AVE	COV	RMSE	NC% (a)	NC% (b)
ACI 318 (2014)	1.24	0.52	319.86	67.84	32.16
ACI 318 simplified (2014)	1.07	0.42	313.89	52.49	47.51
fib MC2010 (2013); α_{p2} = 0.5	0.85	0.35	322.36	13.49	-
fib MC2010 (2013); α_{p2} = 1.0	1.27	0.55	305.33	-	18.46
fib MC2010 (2013); α_{p2} = 0.5 (excluding coated specimens)	0.80	0.34	335.79	7.28	-
fib MC2010 (2013); α_{p2} = 1.0 (excluding coated specimens)	1.19	0.45	281.83	-	20.89
AASHTO (2012)	1.28	0.57	325.20	68.67	31.33
Eurocode 2 (2004); $l_{pt1} = 0.8\ l_{pt}$	0.72	0.39	373.42	24.48	-
Eurocode 2 (2004); $l_{pt2} = 1.2\ l_{pt}$	1.45	0.70	371.70	-	30.29
Eurocode 2 (2004); $l_{pt1} = 0.8\ l_{pt}$ (excluding coated specimens)	0.68	0.40	392.31	17.37	-
Eurocode 2 (2004); $l_{pt2} = 1.2\ l_{pt}$ (excluding coated specimens)	1.36	0.58	336.86	-	34.04
Pellegrino et al. (2015)	1.02	0.40	300.75	47.30	52.70
Buckner (1995)	1.12	0.40	282.73	60.17	39.83
Russell and Burns (1993)	1.86	1.10	563.81	88.80	11.20
Mitchell et al. (1993)	1.05	0.36	279.07	53.11	46.89
Shahawy et al. (1992)	1.40	0.66	352.35	75.10	24.90
Lane (1990)	2.26	1.57	852.42	97.72	2.28
Cousins et al. (1990)	1.39	0.61	342.10	75.31	24.69
Zia and Mostafa (1977)	1.05	0.41	283.28	46.89	53.11
Martin and Scott (1976)	1.71	0.97	484.52	85.27	14.73

AVE = average ratio between theoretical and experimental values; COV = coefficient of variation; RMSE = root mean square error; NC% (a) = percentage of not conservative results when checking stresses at release; NC% (b) = percentage of not conservative results when calculating anchorage length

Conversely, a good performance of *fib* MC2010 and Eurocode 2 is obtained when applied to the large dataset of experimental tests. Such formulations, especially that of *fib* MC2010, provide sufficiently accurate results for checking the maximum transversal stress value (the percentage of not conservative data points is 13.49% for *fib* MC2010

and 24.48% for Eurocode 2, respectively). Instead, to further calculate the anchorage length they have slightly less accuracy, where 18.46% and 30.29% of unsafe evaluations is associated to *fib* MC2010 and Eurocode 2, respectively. Moreover, they provide among the best COV and RMSE, highlighting their reduced scatter if compared to the other formulations. It can also be noted that a little different scatter applies when the data set including coated tendons is considered, thus having a certain impact on the performance indicators (see Table 3-6). Among the different proposals by researchers, it is worth nothing the overall good performance of Pellegrino et al., Mitchell et al. and Zia and Mostafa. They encompass approximately the same number of unconservative data points for both the relevant design conditions.

3.3.2. Assessment of the anchorage length of PC members

An experimental database of anchorage length values measured in PC test members is collected from literature studies in the same manner as for the analysis of the transmission length. In the gathered experimental campaigns, the anchorage lengths were iteratively determined essentially through the simple flexural test described in section 2.3.2.1., i.e. the trial-and-error testing scheme. The complete anchorage length database includes 179 experimental tests, collected from 1959 until 2005, as specified in Table 2-7. It should be recalled that this is a serviceable dataset, i.e. all experimental tests experiencing premature cracking, debonded tendons and incomplete information on the setup are excluded from the analysis.

Table 3-7: Detail of the experimental database of measured anchorage lengths - test samples and authors.

PC Small-scale specimens		
Reference citation	No. of experimental tests	Test method
Hanson and Kaar (1959) [3-35]	47	3PBT - 4PBT
Cousins et al. (1990) [3-36]	37	3PBT
Mitchell et al. (1993) [3-2]	34	4PBT
PC Real-scale bridge girders		
Reference citation	No. of experimental tests	Test method
Deatherage et al. (1994) [3-18]	25	3PBT
Shahawy (2001) [3-16]	24	3PBT
Kahn et al. (2002) [3-32]	8	3PBT
Kose and Burkett (2005) [3-34]	12	4PBT

3PBT = 3-point bending test; 4PBT = 4-point bending test

It can be noted that the size of the database of anchorage lengths is lower than that of transmission lengths. Experimental tests performed on both small beam specimens and full-scale bridge girders are again considered where, in the case of specimens, coated strands were used in some cases. No results with single wires are available in the literature.

The same qualitative and quantitative parameters considered for the creation of the transmission length database are also taken into account for the analysis of the anchorage length. Particularly, some of them related to steel properties are strand diameter (from 6.4 to 15.2 mm), strand stress due to prestressing (ranging from 871.0 to 1436.2 MPa) and strand stress after allowance for all losses (from 779.1 to 1379.0 MPa). Other characteristics considered relevant for the concrete are compressive strength at 28 days (from 25.5 to 100.0 MPa) and concrete cover thickness (from 38.1 to 76.2 mm). The samples are equipped with a number of strands up to 16, with a maximum clear spacing of 48.3 mm. In addition, the strand stress at the nominal strength is also taken into account (from 1144.6 to 1931.0 MPa), being a fundamental factor in the computation of the anchorage length of a PC member. Prestressing-force release method, strand surface conditions and bond conditions are considered as qualitative features. The complete anchorage length database can be consulted in Annex B of the thesis.

In order to assess the quality of the existing anchorage length approaches, the actual theoretical values arising from the main standard code provisions and proposals by researchers are analysed in the next sections, from 3.3.2.1. to 3.3.2.4., together with the collected experimental data. Results of the comparison are graphically indicated with different colours depending on the specimen geometry (small- or full-scale in blue and red, respectively), while the presence of coated strands is highlighted with green colour. However, it should be realised that a less accurate and reliable evaluation than that carried out for the transmission length is to be expected, given the relatively limited number of anchorage length tests available in the literature.

3.3.2.1. ACI 318-14

The overall performance of ACI 318-14 on the anchorage length calculation (ref. Eq. 2-4) is illustrated in Figure 3-12. Here, it can be observed that about half of the data points are conservative when compared to the collected experimental results, being below the diagonal “experimental vs predicted” L_b line. However, the remaining part of the data falls in the upper left area of the picture, and hence it is unsafe in calculating the

anchorage length at ULS. A number of data points is relatively remote from the ideal line, even though the global scatter is less than that visualised for the calculation of the transmission length. It is noted that the majority of the conservative data is represented by small-scale specimens (in blue in the picture), while most of the unsafe values arises from full-scale beams (in red).

As stated in sections 2.4.1. and 2.4.2., the anchorage length formulation of ACI 318-14 is very similar to that of AASHTO. The only difference between the two design concepts is the coefficient "k", which enlarges the anchorage length for PC member with a depth greater than 609.6 mm (24 in.). Thus, the graph in Figure 3-12 applies also for AASHTO when considering small specimens (for which a section depth less than 609.6 mm is very likely), while for full-scale girders the point cloud can be slightly shifted toward the right part of the picture. For AASHTO, this results in a better replication of the test values for real-scale bridge girders, since the corresponding points get close to diagonal ideal line (see the summary of performance indicators in section 3.3.2.4.).

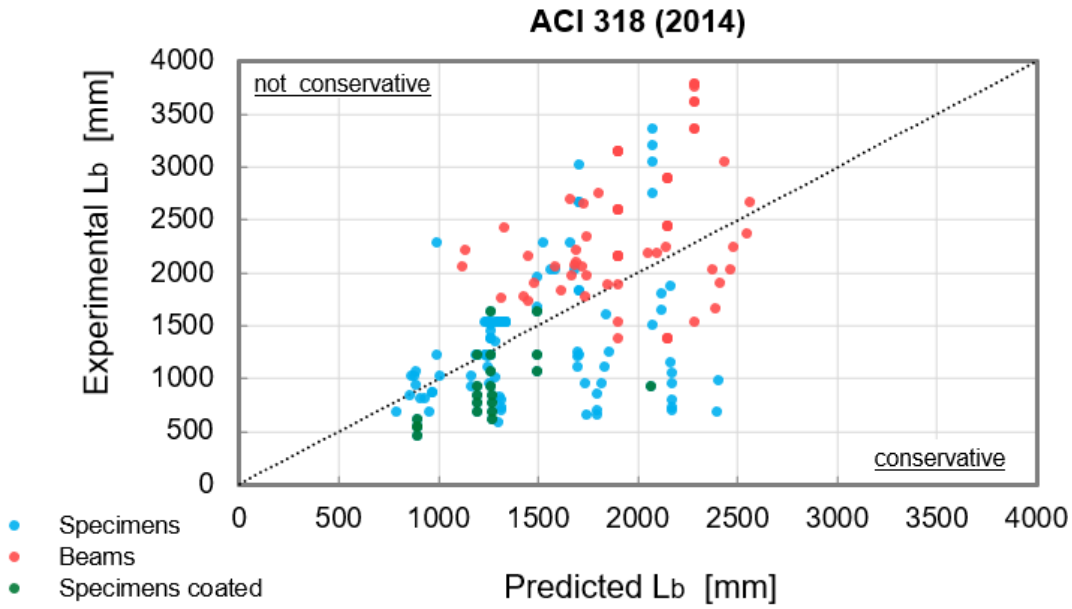

Figure 3-12: Performance of ACI 318-14 recommendation for the anchorage length calculation when compared to the collected experimental database.

3.3.2.2. *fib* Model Code 2010 and Eurocode 2

The assessment of the current *fib* MC2010 and Eurocode 2 formulations for the anchorage length is jointly presented hereafter, as they are based on similar design concepts. In Figure 3-13, the comparison between experimental and calculated values of the anchorage length obtained with *fib* MC2010 is graphically shown by taking α_{p2} =

1.0 (see Eq. 2-10), necessary for the evaluation of the flexural capacity of PC members as prescribed by the same code. In Figure 3-14, the same evaluation is depicted with respect to Eurocode 2, where the upper bound value of the transmission length (i.e. l_{pt2}) is selected according to Eq. 2-9. In both cases, average material properties with no partial safety coefficients are considered in order to better simulate the conditions of the experimental tests. The resulting data points should stay in the lower portion of the diagrams, in which predicted anchorage lengths are greater than the corresponding experimental values. However, less than 44% (for *fib* MC2010) and 27% (for Eurocode 2) of the analysed data are actually on the safe side. The other 56% (*fib* MC2010) and 73% (Eurocode 2) of the total values are in the upper part of the graph, characterised by a predicted anchorage length value less than the experimental one found by authors. Thus, the formulation of *fib* MC2010 best suits the collected database if compared to Eurocode 2, for which it can be noted that the point cloud is slightly shifted to the left, i.e. more results fall outside the conservative area of the graph. Though, a high number of unsafe results is still present. Nevertheless, the general scatter of the data points is comparable for the two considered standard codes. Moreover, similarly to the evidences from ACI 318-14, very few conservative data about full-scale girders can be found for both *fib* MC2010 and Eurocode 2. This highlights a general deficiency of the main design codes in predicting the anchorage length of full-scale PC girders with I-shaped cross-section, characterised by medium-to-high depth (if compared with small-scale specimens, i.e. for section depths greater than 400-450 mm).

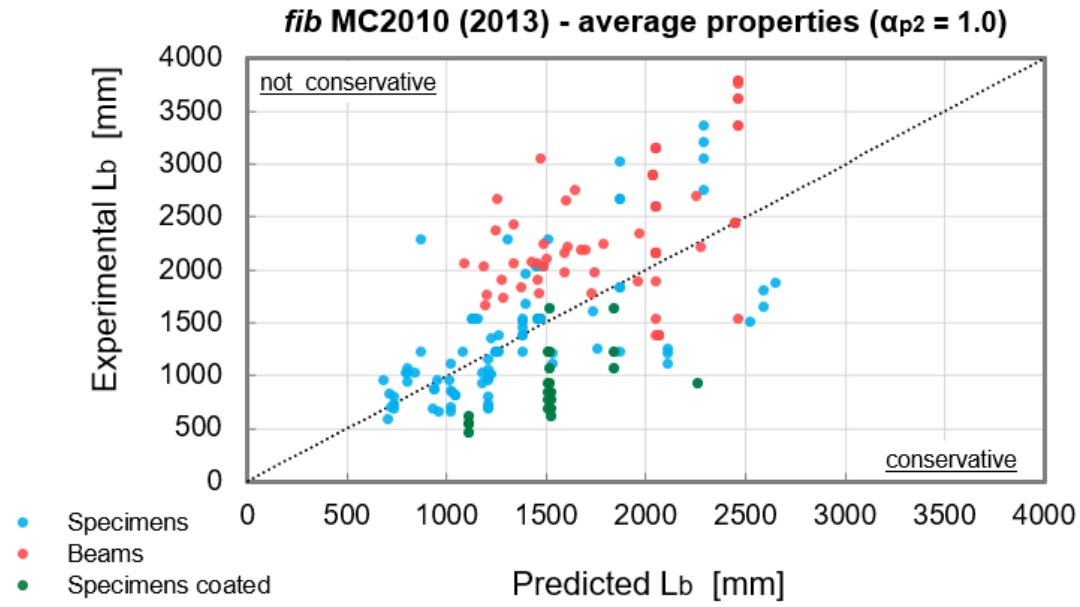

Figure 3-13: Experimental vs predicted values according to fib MC2010 for the calculation of the anchorage length, average material properties.

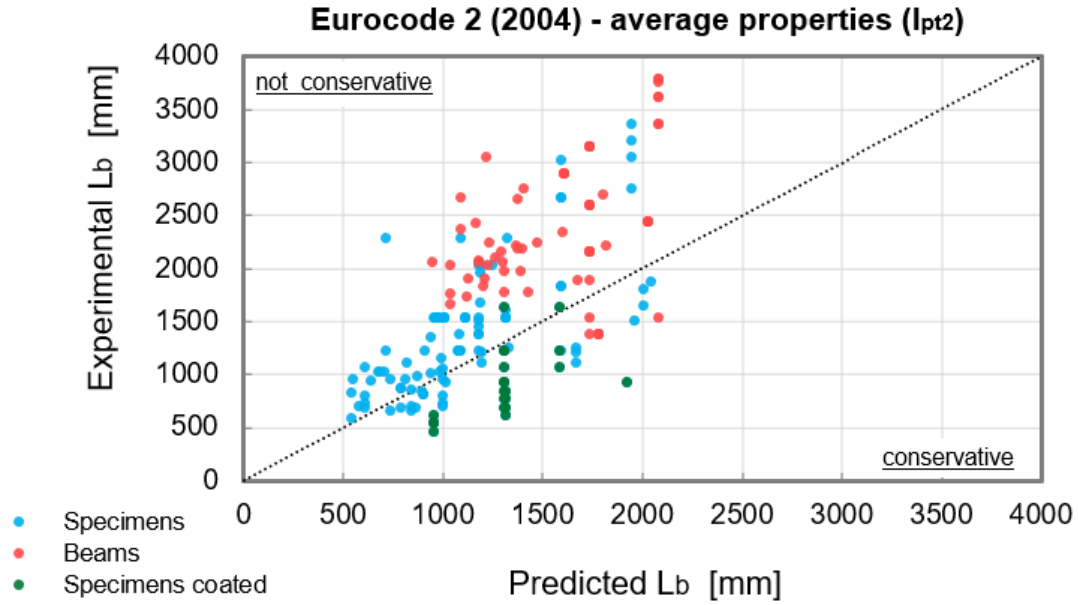

Figure 3-14: Experimental vs predicted values according to Eurocode 2 for the calculation of the anchorage length, average material properties.

The evaluation of *fib* MC2010 and Eurocode 2 for calculating the anchorage length was also carried out with respect to design values of material properties. For this purpose, the conversion factor from average to characteristic values of the concrete strength is 0.7. Then, a partial safety factor γ_c equal to 1.5 is used for the material. In this way, the bond strength is reduced, resulting in longer transmission and anchorage lengths.

Particularly, the consideration of design values of the anchorage length results in a considerable improvement of the prediction, since the percentage of not conservative values reduces to 12.30% and 37.97% for *fib* MC2010 and Eurocode 2, respectively. This finding can be considered good for *fib* MC2010, but not yet acceptable for Eurocode 2, for which many unsafe values are still registered (see Figures 3-15 and 3-16). In any case, the reasons of such poor accuracy depend on many causes. Among them, it might be recalled: the insufficient number of test samples included in the dataset; different test methods and specimens type used; the complexity of the problem itself, that includes some variables that are not even covered by the existing models; the quality of the experimental data, that sometimes are contrasting among different experimental campaigns.

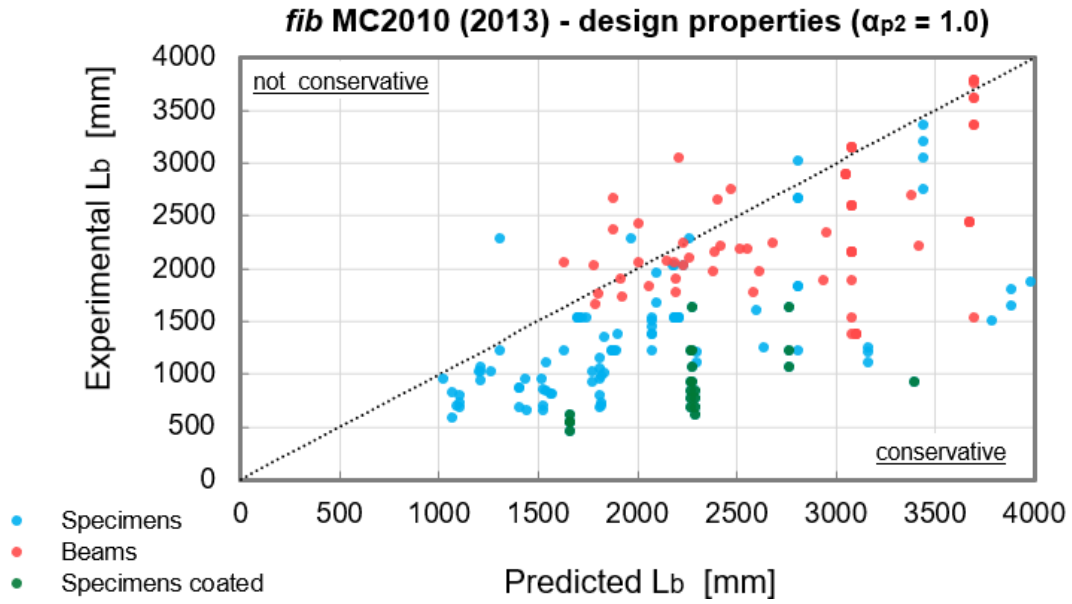

Figure 3-15: Experimental vs predicted values according to fib MC2010 for the calculation of the anchorage length, design material properties.

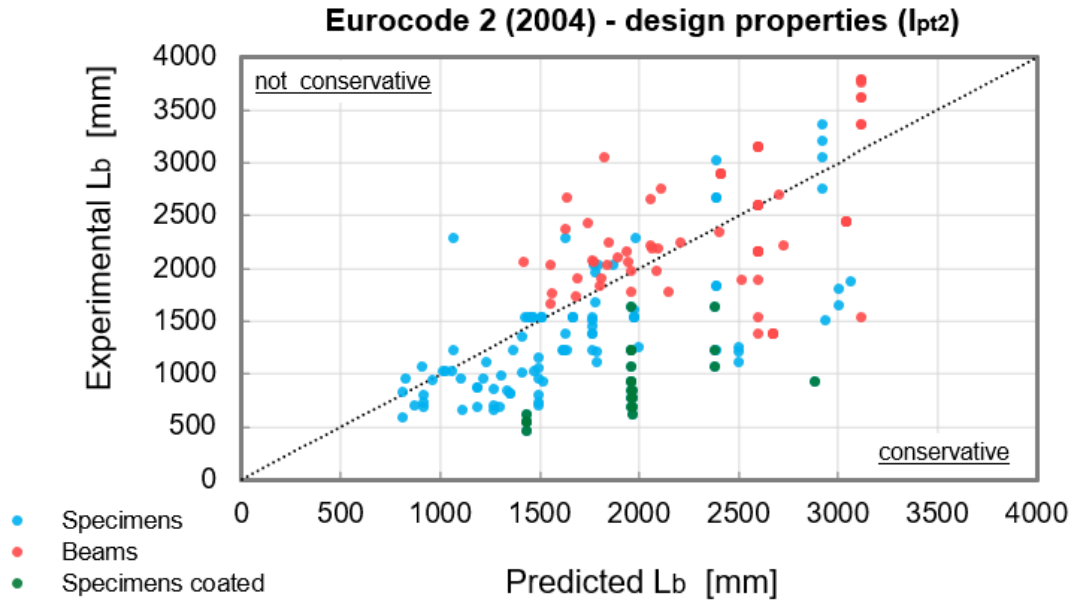

Figure 3-16: Experimental vs predicted values according to Eurocode 2 for the calculation of the anchorage length, design material properties.

3.3.2.3. Researchers' proposals

As for the analysis of the transmission length, the available researchers' proposal formulations on the anchorage length (reported in Table 3-2) are illustrated and discussed. The overview in Figure 3-17 depicts the performance of the various relationships when compared to the collected experimental values.

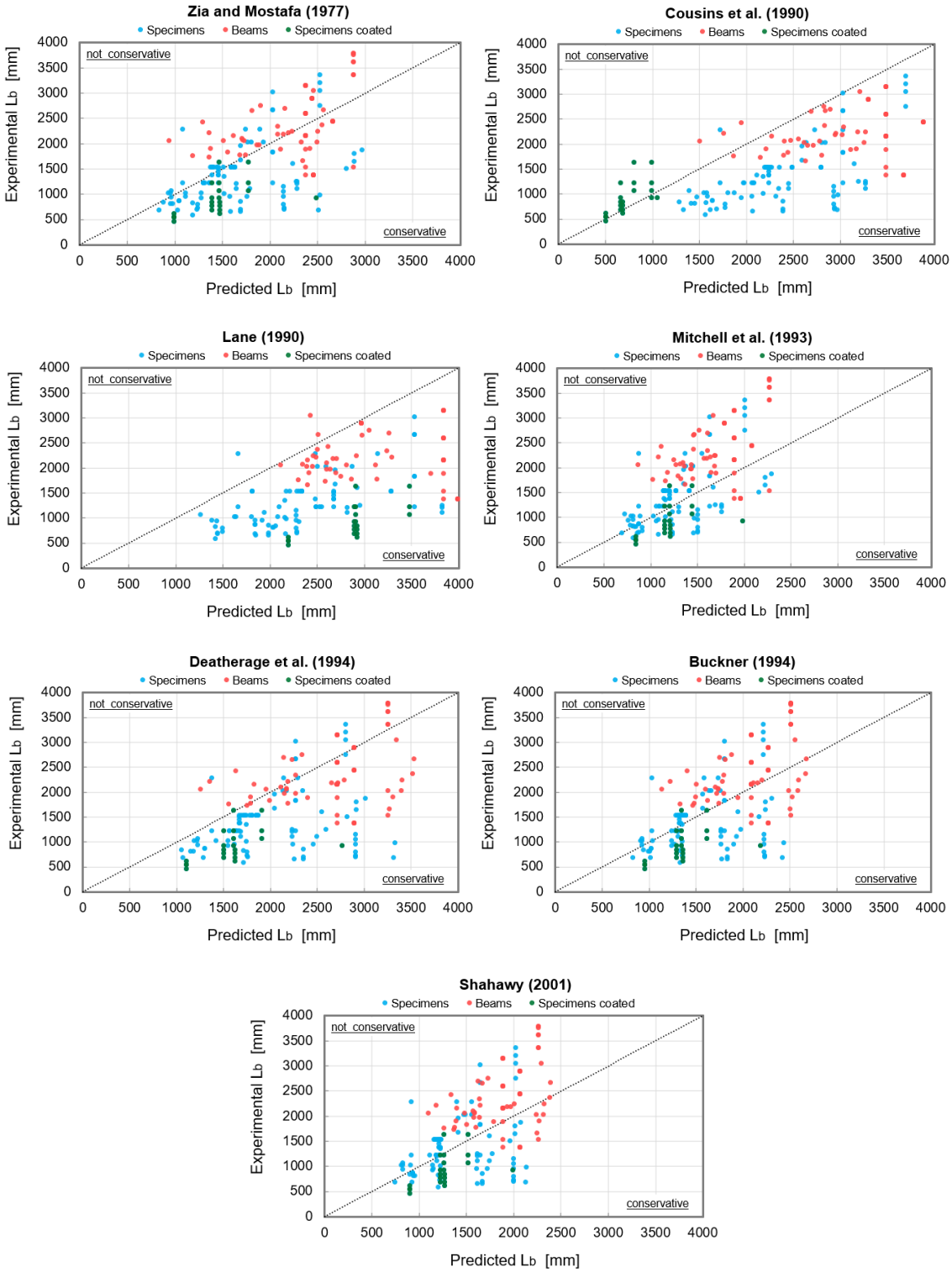

Figure 3-17: Performance of the main researchers' proposal formulations on the anchorage length, when compared to the collected experimental database.

Here, it can be easily seen that the expressions by Cousins et al. [3-14], Lane [3-13] and Deatherage et al. [3-18] are by far the most conservative with respect to the anchorage length evaluation. In fact, they present very few values above the ideal dotted line (i.e.

the unsafe area of the graph). Particularly, in the case of Cousins et al., the unconservative data are almost exclusively small-scale specimens with coated tendons. The limit case of Lane is worth mentioning, encompassing only 5 out of 179 not conservative data points. However, such results are a direct consequence of the critical performance of the mentioned formulations when calculating the transmission length. Indeed, it is recalled that the expressions of Cousins et al. and Lane for the evaluation of the transmission length are those less conservative when verifying transverse stresses at release but, conversely, they are the most conservative for calculating the anchorage capacity of a PC beam (see sections 3.3.1.5. and 3.3.1.6.). The large transmission length values generally predicted by these formulations (if compared to the experimental results) are unfavourable when the member is subject to flexure, since the length of the tendon available for developing flexural bond stresses is reduced (see section 2.2.2.). This situation results in large anchorage length values. On the other hand, the proposals by Zia and Mostafa [3-1], Mitchell et al. [3-2], Buckner [3-17] and Shahawy [3-16] for the anchorage length calculation show approximately half of the total data points both above and below the optimal line. Such finding is a consequence of a better balancing of the transmission length formulas towards the two fundamental design stages.

3.3.2.4. Statistical performance indicators

For a quantitative analysis, the principal performance indicators (AVE, COV, RMSE, NC%) associated with the current design formulations for anchorage length calculation are summarised in Table 3-8. For *fib* MC2010 and Eurocode 2, both average and design material properties are considered, whereas the upper bound for the transmission length (i.e. α_{p2} = 1.0 and l_{pt2} = 1.2 l_{pt}) is taken into account to reflect the design case of anchorage length evaluation when moment and shear capacity are considered. Furthermore, statistical indicators are also calculated excluding the results obtained from specimens with coated strands. In this case, the performance of the formulations is slightly worse in terms of unconservative values.

By looking at the results, it is possible to observe that the general accuracy of the proposed formulations (in terms of RMSE) is remarkably low, even if compared to the ones for predicting the transmission length. In this context, Eurocode 2 provides among the lowest values of RMSE when considering design properties of the materials, even though the percentage of not conservative data points is very high (reaching 42.77%). On the other hand, one of the best results in terms of conservative predictions is given by *fib* MC2010 (still considering design properties), but in this case the RMSE values

are not particularly good. However, both Eurocode 2 and *fib* MC2010 seem to have poor performances if average material properties are assumed. In this condition, Eurocode 2 presents the highest values of unsafe results, up to almost 82%, while *fib* MC2010 produces up to 62.65% of not conservative data.

Table 3-8: Performance indicators of the formulations for anchorage length evaluation.

Reference formulation	AVE	COV	RMSE	NC%
ACI 318 (2014)	1.12	0.56	777.83	58.29
fib MC2010 (2013) - average	1.05	0.39	742.11	56.15
fib MC2010 (2013) - design	1.57	0.63	879.57	12.30
fib MC2010 (2013) - average (excluding coated specimens)	0.95	0.34	749.84	62.65
fib MC2010 (2013) - design (excluding coated specimens)	1.42	0.43	808.47	13.86
AASHTO (2012)	1.32	0.64	895.36	34.76
Eurocode 2 (2004) - average	0.87	0.44	838.41	73.80
Eurocode 2 (2004) - design	1.31	0.87	756.08	37.97
Eurocode 2 (2004) - average (excluding coated specimens)	0.78	0.33	872.91	81.93
Eurocode 2 (2004) - design (excluding coated specimens)	1.18	0.65	700.03	42.77
Shahawy (2001)	1.07	0.51	773.97	59.89
Buckner (1994)	1.18	0.59	757.37	54.01
Deatherage et al. (1994)	1.50	0.88	914.08	18.72
Mitchell et al. (1993)	0.97	0.39	775.36	65.24
Lane (1990)	1.95	1.28	1421.41	3.21
Cousins et al. (1990)	1.62	0.95	1144.21	12.30
Zia and Mostafa (1977)	1.25	0.60	749.70	40.11

AVE = average ratio between theoretical and experimental values;
COV = coefficient of variation; RMSE = root mean square error;
NC% = percentage of not conservative results

Among the other proposed formulations, it has already been mentioned in the previous section how the performance of the expressions by Deatherage et al., Lane and Cousins et al. is very good, where their effectiveness is proven by the low number of not conservative results. Nevertheless, the main statistical indicators (AVE, COV and RMSE) are poor, globally identifying a low accuracy of the formulas in evaluating the real anchorage length value.

3.4. Role of the major parameters affecting the transmission length

The transmission of the prestressing-force from steel to concrete is commonly affected by many important variables, including tendon diameter, concrete strength, initial prestress level, tendon surface condition and type of release. However, according to the above evidences, it seems that is not completely clear how these parameters influence the transmission length of prestressing tendons. The effect of some of them on the transmission length is discussed in the present section, as arising from the analysis of the collected database (presented in section 3.3.1.). Moreover, some works carried out by other researchers are also mentioned.

3.4.1. Influence of tendon diameter

Many investigations were carried out by different authors about the role of the tendon diameter on the transmission length of PC members, with little uncertainties in it. Particularly, it is commonly accepted that the transmission length linearly increases with the nominal tendon diameter. It is known that the adhesion force, which depends on the amount of adhered surface, is directly proportional to the tendon diameter. Friction, instead, may be influenced by the tendon diameter due to the difference in the normal force from various wire sizes. Additionally, the effect of mechanical interlocking tends to increase with the tendon diameter, because of the larger grooves between the outer wires of a strand. Oh and Kim [3-3] conducted an experimental research project on PC specimens with same characteristics, but equipped with strands of two different diameter (12.7 and 15.2 mm). The comparison of the results clearly demonstrates that the measured transmission lengths of the 15.2 mm strand are longer than those of the 12.7 mm strand. The average difference in the transmission length was evaluated to be 25%, which is approximately the ratio between the strand diameters.

Figure 3-18 a) and b) shows the effect of strand diameter (12.7 and 15.2 mm) based on a set of data taken by Oh and Kim [3-3], varying concrete strength class (C30 and C50) and concrete cover (c = 30, 40, 50 mm). Further characteristics are maintained constant within the different PC specimens: f_{su} = 1862 MPa; f_{si} = 1303 MPa; section bxh = 113x200 mm; smooth surface condition and sudden release type. It is worth mentioning, as it will be better seen in the next paragraph, that an increment in the concrete strength has a great effect on the transmission length, reducing it. The confinement effect by the surrounding concrete has also a remarkable influence, lowering the transmission length value as concrete cover increases.

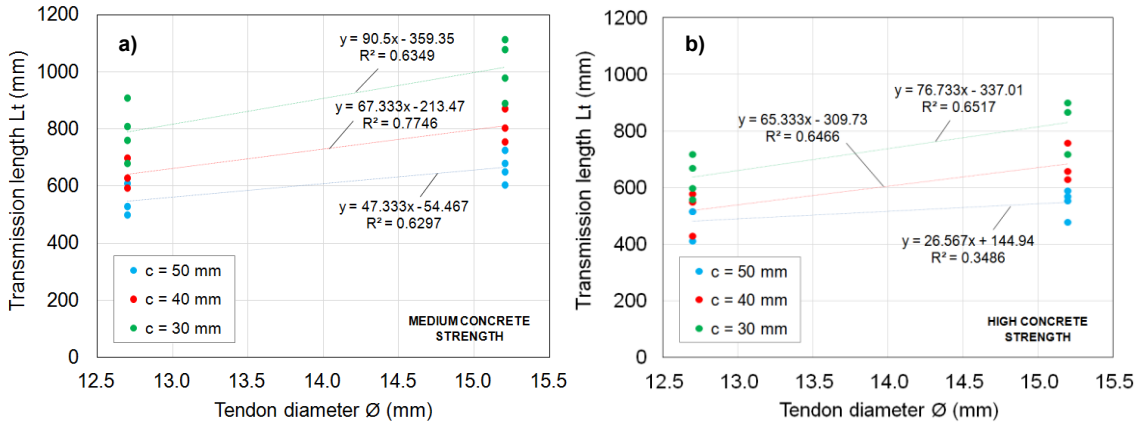

Figure 3-18: Effect of strand diameter on the transmission length in a) C30 concrete and b) C50 concrete.

3.4.2. Influence of concrete compressive strength

Despite the fact that current ACI 318-14 does not take into account the characteristics of the concrete (see Eq. 2-2), concrete compressive strength at release f_{ci}' is thought to have a primary role on the transmission length of PC members. In fact, an increase in concrete compressive strength implies - in the majority of the cases - larger modulus of elasticity, smaller shrinkage strains after release and lower creep. Such improved bond characteristics often result in smaller transmission length values. In 1963, before the advent of concrete with very high strength, Kaar et al. [3-36] performed a series of tests on PC specimens having a concrete compressive strength ranging from 11.4 to 34.5 MPa. They concluded that concrete strength has only little influence on the transmission length at release. On the same line, Stocker and Sozen [3-37] found that other factors, such as shrinkage, may have a stronger impact on bond than concrete compressive strength. Conversely, Zia et al. [3-1] derived an inverse proportional dependence between the transmission length and concrete strength (see Table 3-1).

More recently, Mitchell et al. [3-2] investigated the behaviour of 22 rectangular beams eccentrically pretensioned with one strand. The primary variables were tendon diameter (slightly rusted 9.5 mm strands, smooth 12.7 and 15.7 mm strands) and concrete compressive strength (ranging from 21 to 50 MPa at transfer). Concrete strength at the moment of prestress transfer (f_{ci}') was found to have a clear influence on the transmission length of the member. Particularly, a dependence of the transmission length upon $1/\sqrt{fci'}$ was suggested by Mitchell et al. [3-2]. Furthermore, Cousins et al. [3-31] performed several experimental tests on T-shaped beams equipped with 12.7 mm diameter strands, aimed at evaluating the role of strand spacing and concrete compressive strength. While no influence of tendon spacing was found, concrete

strength proved to have a significant impact on the transmission length. Specifically, the average transmission length for normal and high concrete strength was estimated to be 1422 mm and 944 mm, respectively. The ratio between such values is about 1.5, indicating an inverse correlation of the transmission length with respect to concrete compressive strength. Oh and Kim [3-3] compared the transmission lengths of PC specimens casted with two different concrete strengths at transfer (35 and 45 MPa). The transmission length values measured for high strength concrete were shorter than those registered for beams made with lower strength concrete, clearly showing the beneficial effect of the enhanced compressive strength in transferring the prestressing-force.

In Figure 3-19 a) and b), the influence of concrete compressive strength at release on the transmission length is shown based on the assessment of the dataset provided by Mitchell et al. [3-2]. Data are sorted according to the tendon diameter (9.5, 12.7 and 15.7 mm, respectively), to separate its effect. Both linear and power law regressions are considered in Figure 3-19 for interpolation of the data points. However, it should be noted that the presented analysis is based on small-scale specimens mainly characterised by low concrete strength values (about half of the data points presents concrete strength values at release of 21 to 27 MPa). Therefore, the proposed regression curves might not be consistent for concretes commonly used nowadays, having higher compressive strengths. Moreover, it is worth recalling that other influencing parameters vary within the selected subset of data, including PC specimens' geometry and tendon surface condition (i.e. smooth and rusted).

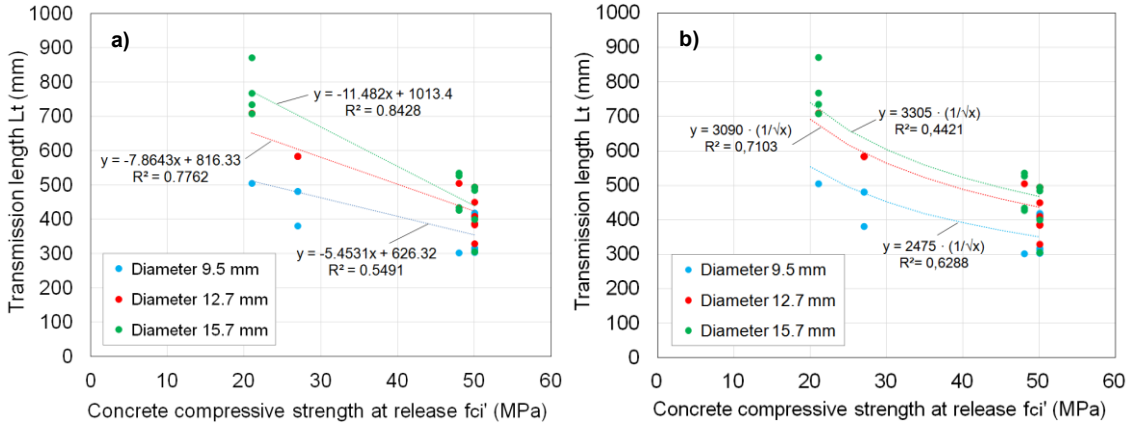

Figure 3-19: Influence of concrete compressive strength on the transmission length with a) linear regression and b) power law.

3.4.3. Influence of initial prestress level

It has already been highlighted that the design formulations provided by current standard codes are based on uniform distribution of bond stresses along the transmission

length. This assumption describes transmission lengths which are linearly proportional to the initial tendon stress, if the influence of the transverse strain of the strand on bond strength is neglected. It is thought that the practical meaning of a possible non-linear correlation between the initial prestress and the transmission length is small, because of the limited range of initial stresses used in PC applications. However, since the 1950s, changes in the manufacturing processes have improved the engineering properties of prestressing tendon materials. Until the early 1960s, the most commonly employed prestressing tendons was stress-relieved with a guaranteed tensile strength of 1720 MPa (250 ksi, or Grade 250). Then, by the late 1980s, these tendons had been largely replaced by low-relaxation strands with a guaranteed tensile strength of 1860 MPa (270 ksi, or Grade 270). In any case, prestressing tendons are usually stressed at about 80% of their ultimate strength. Consequently, there is not much uncertainty in the role of the initial prestress level on the transmission length of PC members.

3.4.4. Influence of tendon surface condition

To provide corrosion protection of prestressing tendons in PC members located in aggressive environments (for instance bridge decks in marine areas), it could be useful using an epoxy-coating as a corrosion-inhibiting barrier. In this case, the epoxy-coating should be impregnated e.g. with grit (crushed glass) to improve its bond characteristics with concrete. Cousins et al. [3-25] examined the behaviour of epoxy-coated strands compared to uncoated strands, testing square specimens equipped with one strand, concentrically placed. Primary variables were strand diameter (9.5, 12.7 and 15.2 mm) and strand surface condition, i.e. uncoated strands, strands coated without grit and strands coated with various grit densities (named as CL, CM, CH for low, medium and high density of grit, respectively). In two PC specimens equipped with epoxy-coated strands without grit, steel stress was virtually lost at prestress release, identifying little or no bond between the tendon and the surrounding concrete. On the other hand, the use of epoxy-coated strands resulted in improved bond characteristics when impregnated with grit, reducing the transmission length. Particularly, it was observed that increasing grit density results in shorter transmission length values. Nevertheless, splitting at prestress transfer occurred in some specimens with coated tendons. The authors concluded that more concrete cover is required when employing coated tendons.

Figure 3-20 shows the influence of epoxy-coating on the transmission length of PC members, as resulting from a subset of data taken from Cousins et al. [3-25]. In this case, experimental results refer to specimens with varying concrete section geometry,

tendon diameter and tendon coating (present or not), whereas concrete compressive strength and initial prestressing-force are constant. The graph clearly illustrates how the epoxy-coating of strands (with crushed glass) is effective in reducing transmission length values.

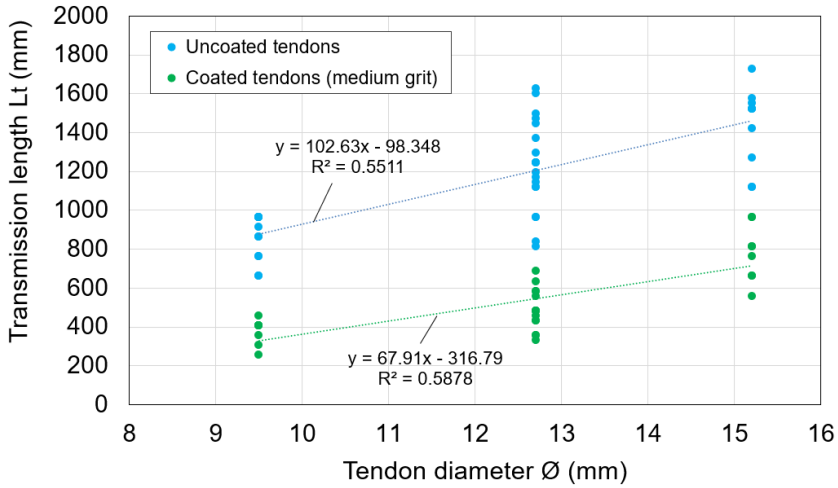

Figure 3-20: Influence of epoxy-coating on the transmission length.

Another issue related to tendon roughness is represented by the potential presence of rust, in small amount, onto the strands. It is known that slightly rusted tendons give shorter transmission lengths than smooth, untreated tendons, because of the weathering processing. However, it should be recalled that such process is usually not sufficient to create visible rust, but it causes microscopic roughness only, thus improving bond considerably [3-2; 3-18; 3-33]. In this situation, the reduction in the transmission length is mainly due to increased adhesion and friction coefficient between the tendon and the surrounding concrete.

Lastly, bond properties of wires and strands can be influenced by the presence of indentation on their surface. In the prefabrication practice, several indent shapes are used. In fact, some prestressing tendons present a surface with flat bottom and steep edges, others are characterised by a circular section with a small slope of the edge. Few information is present in the literature about the influence of the indent shape on bond strength of tendons. However, it is commonly recognised that the use of indentation reduces both transmission and anchorage length. The influence of tendon indentation on the bond strength is taken into account in *fib* MC2010 through the parameter η_{p1}, which assumes the value of 1.4 for indented or crimped wires, and 1.2 for 7-wire strands (see Eq. 2-7).

3.4.5. Influence of the type of prestress release

The method of prestressing-force release is considered as a major factor affecting the transmission length of PC members. Several studies investigating the effect of prestress release method on the nature of bond have shown that a sudden release of the tendons often results in longer transmission lengths than a gradual release process [3-38; 3-39]. This phenomenon is generally attributed to the dynamic effects associated with the transfer of energy from the tendon to the concrete. Flame-cutting is a fairly quick process during which the applied heat lowers the strength and the tendon actually breaks in tension. Russell and Burns [3-11] indicated that the influence of the release type is more evident in small-scale specimens than in full-scale girders. Kaar and Hanson [3-40] and Cousins et al. [3-25] found that sudden release by flame-cutting the tendons gives transmission lengths of 8 to 22 percent larger than those determined for similar tendons gradually released. Current *fib* MC2010 considers the type of prestress release in the coefficient α_{p1}, being 1.25 and 1.00 for sudden and gradual release, respectively (see Eq. 2-9).

However, according to experimental evidences, such values might lead to inaccurate results, as they should also take into account the "cut-end" or "dead-end" effect. In fact, two different transmission lengths can be registered on a PC member during production, depending on the considered free-end. It is recalled that the ordinary prefabrication practice usually involves simultaneous casting of two or more beams in a row, on the jacking bed. Then, the most used prestress release methods entail flame-cutting all the tendons at one location between two girders. The "cut-end" identifies the interior side between two successive beams, experiencing a higher amount of released energy. Instead, the "dead end" represents the opposite side of the member, commonly associated with shorter transmission length values. Based on the experimental campaign carried out by Oh and Kim in [3-3], it is found that the transmission length at the "cut end" is, on average, up to 16% larger than that at the "dead end", when sudden release is applied. Similar results were obtained by Russell and Burns [3-27], Barnes et al. [3-33], Oh et al. [3-28] and Dang et al. [3-30], who estimated an increase in the transmission length of 8%, 10%, 14% and 4%, respectively. Overall, the average increment of the transmission length at the "cut-end" location can be taken as 10%. Nevertheless, no direct implication of the release method on the anchorage length seems to be present in the literature.

3.5. New proposals of modification for revision of current design codes

The general evaluation of current design codes presented in the previous sections has shown that the suggested formulations on pre-tensioning anchorage are not always sufficiently accurate in predicting the real behaviour of PC members. Particularly, the effect of some influencing parameters on the transmission length and anchorage length seems not completely understood yet. The topic is still open and under discussion in the scientific world, especially within *fib* Task Group 2.5 on "Bond and Material Models". In this context, two different proposals of modification have been advanced in view of a possible revision of the existing design provisions in the 2020 version. On one side, the proposal of modification by University of Padova, in which the author has been involved, is developed based on current *fib* MC2010. On the other side, the new proposal by RWTH Aachen University is conceived adopting Eurocode 2 as a reference standard. Both proposed design models are briefly illustrated hereunder and compared in order to evaluate the different performances.

3.5.1. Proposal by University of Padova

The formulation of the transmission length proposed by University of Padova is based on current *fib* MC2010, and consists of two main amendments. A first formal modification is advanced with respect to the consideration of bond strength. In fact, it is thought that distinction between the design situations of transverse stress verification at release and anchorage length calculation at ULS should be done just within the calculation of the interface bond stress, and not only in the final value of the transmission length. In this respect, the coefficient α_{p2} accounting for the effect to be verified is suggested to be incorporated directly in the expression of the design bond strength f_{bpd}, as in the following Eq. 3-1. In this way, the constant bond stress at the interface tendon-concrete is doubled when calculating the transmission length for checking allowable stresses at release. However, in order to adopt a harmonised nomenclature, such factor is converted into coefficient η_{p3} in Eq. 3-1:

$$f_{bpd} = \frac{\eta_{p1}\,\eta_{p2}\,f_{ctd}(t)}{\eta_{p3}} \tag{3-1}$$

where η_{p1} is the coefficient that takes into account the type of prestressing tendon, η_{p2} is the coefficient that considers the position of the tendon during concreting, η_{p3} is the coefficient accounting for the action effect to be verified (the factor α_{p2} in *fib* MC2010) and $f_{ctd}(t)$ the lower value of the design concrete tensile strength. In particular:

η_{p1}	1.20	for 7-wire strands;
	1.40	for indented or crimped wires.
η_{p2}	1.00	for all tendons with an inclination of 45-90° with respect to the horizontal during concreting, and for all horizontal tendons which are up to 250 mm from the bottom or at least 300 mm below the top of the concrete section during casting;
	0.70	for all other cases.
η_{p3}	0.50	for verification of transverse stresses at release;
	1.00	for calculation of anchorage capacity at ULS.

$f_{ctd}(t) = f_{ctk,min}(t) / \gamma_c$

Then, a second adjustment is proposed with regard to the coefficient considering the type of release of the prestressing-force, i.e. α_{p1} in Eq. 2-9. Here, it is believed that the influence of the free-end location ("cut" or "dead" end, as described in section 3.4.5.) should be introduced together with the release method itself (sudden or gradual, as actually considered in *fib* MC2010). According to the findings presented in section 3.4.5., reporting an average increment of the transmission length of 10% at the "cut-end" location, the following three situations at release are incorporated in factor α_{p1}:

α_{p1}	1.00	for gradual release;
	1.25	for sudden release at the "dead-end";
	1.35	for sudden release at the "cut-end".

The latter value α_{p1} = 1.35 actually combines the increment of 25% associated to the sudden release with the further increment of 10% associated to the "cut-end" location. Thus, after calculating the basic anchorage length l_{bp} as in Eq. 3-2 (unchanged from Eq. 2-8 suggested by *fib* MC2010), the transmission length is derived as reported in Eq. 3-3.

$$l_{bp} = \frac{A_{sp}}{\phi\,\pi}\,\frac{f_{ptd}}{f_{bpd}} \tag{3-2}$$

$$L_t = \alpha_{p1}\,\alpha_{p2}\,\frac{f_{si}}{f_{ptd}}\,l_{bp} \tag{3-3}$$

being ϕ the nominal tendon diameter, A_{sp} the cross-sectional area of the tendon, f_{ptd} the design tensile strength of the prestressing steel, f_{si} the initial jacking stress and α_{p2} the

coefficient considering the type of tendon (0.50 for strands or 0.70 for indented and crimped wires). The factor α_{p2} is the original parameter α_{p3} in *fib* MC2010.

No direct modification is made in the formulation of the anchorage length (Eq. 3-4), which is expressed as indicated in *fib* MC2010, even though the amendments above illustrated indirectly affect also such length:

$$L_b = L_t + l_{bp} \frac{f_{ps} - f_{se}}{f_{ptd}} \tag{3-4}$$

in which f_{ps} is the tendon stress at the nominal strength and f_{se} is the tendon stress after allowance for all prestress losses.

3.5.2. Proposal by RWTH Aachen University

The modification proposed by RWTH Aachen University for the transmission length calculation is similar to that of current Eurocode 2, which is considered as a reference code in this case. The only substantial difference consists in the adoption of the concrete compressive strength in place of the tensile strength, although such a conversion might be not always appropriate, especially when concretes of high strength are considered. Specifically, the magnitude of the constant bond strength f_{bpt} at the interface between steel and concrete is provided as:

$$f_{bpt} = \eta_{p1}\, \eta_1\, \alpha_{ct}\, 0.7\, 0.5\, f_{cd}(t)^{1/2} \tag{3-5}$$

where η_{p1} is a coefficient that considers the type of tendon, η_1 is a parameter taking into account the bond condition during concreting, $f_{cd}(t)$ is the design concrete compressive strength at release and α_{ct} is a factor including the long-term effects and unfavourable effects resulting from the way the load is applied:

η_{p1}	2.70	for indented wires;
	3.20	for 3- and 7-wires strands.
η_1	1.00	for good bond conditions;
	0.70	otherwise.
α_{ct}	0.85	recommended value

The basic value of the transmission length l_{pt}, as in Eurocode 2, is computed as in the following Eq. 3-6:

$$l_{pt} = \alpha_1\, \alpha_2\, \phi\, f_{si} \,/\, f_{bpt} \tag{3-6}$$

being α_1 a coefficient accounting for the type of prestressing-force release, α_2 a coefficient that considers the type of tendon, ϕ the tendon diameter and f_{si} the tendon stress just after release:

α_1	1.00	for gradual release;
	1.25	for sudden release.
α_2	0.19	for 3- and 7-wire strands;
	0.25	for indented wires.

Thus, depending on the design situation, the design value of the transmission length is taken as in Eqs. 3-7 for the verification of local stresses at release and calculation of anchorage capacity at ULS, respectively:

$$l_{pt1} = (1 - \delta)\, l_{pt} \tag{3-7 a}$$

$$l_{pt2} = (1 + \delta)\, l_{pt} \tag{3-7 b}$$

Particularly, the factor δ is related to the quality control during production, being:

δ	0.1	if the execution is subject to a quality control system certified by an accredited body;
	0.2	otherwise.

It is noted that such description is equivalent to that of Eurocode 2 when δ = 0.2 (execution not subject to quality control). Nevertheless, statistical validation of the assumed values should be required.

Similarly to the formulation of Eurocode 2, the model proposed by RWTH Aachen University for the anchorage length calculation is based on a reduced bond strength f_{bpd} in the flexural bond length, where:

$$f_{bpd} = 0.5\, \eta_{p1}\, \eta_1\, \alpha_{ct}\, 0.7\, 0.5\, {f_{cd}}^{1/2} \tag{3-8}$$

Such value is approximately equal to half of the prestress transfer bond f_{bpt} described in Eq. 3-5. According to the results of experimental tests with cyclic loading reported in [3-41], the flexural bond length - and thus the anchorage length - is assumed to be affected by a new factor α_3, considering the effect of fatigue on the PC member. If concrete is uncracked all along the transmission length, the recommended expression for the anchorage length is as follows:

$$L_b = l_{pt2} + \alpha_2\, \alpha_3\, \phi\, \frac{f_{ps} - f_{se}}{f_{bpd}} \tag{3-9}$$

where f_{ps} is the tendon stress at the nominal strength calculated for a cracked section and f_{se} is the tendon stress after all prestress losses. The parameter α_3 is set to 1.5 in cases where fatigue verification is required and 1.0 in all other cases.

3.5.3. Comparison of the proposed models

The accuracy of the proposed models in predicting the transmission length of prestressing tendons is analysed in the present paragraph by considering the experimental databases collected by both the involved research groups. The dataset from University of Padova, adopted throughout the present thesis, is that reported in Annex A, while the dataset from RWTH Aachen University is courtesy of the research group by Prof. Hegger, and it can be consulted in [3-41]. Both small-scale specimens and full-scale bridge girders are included in the evaluation. Nonetheless, as in section 3.3., experimental tests encompassing debonded tendons are not taken into account.

In Figures 3-21 and 3-22, the performance of the two new proposals on the transmission length is shown when predicted values are compared to the experimental results gathered by the author. Average properties of the materials are investigated. However, in order to present the results in a compact manner, the original formulations are slightly modified to consider the average value between the transmission lengths calculated for transverse stress verification and calculation of the anchorage capacity. This means that the assessment of the proposals by University of Padova and RWTH Aachen University is carried out by adopting η_{p3} = 0.75 and δ = 0, respectively (see Eqs. 3-1 and 3-7).

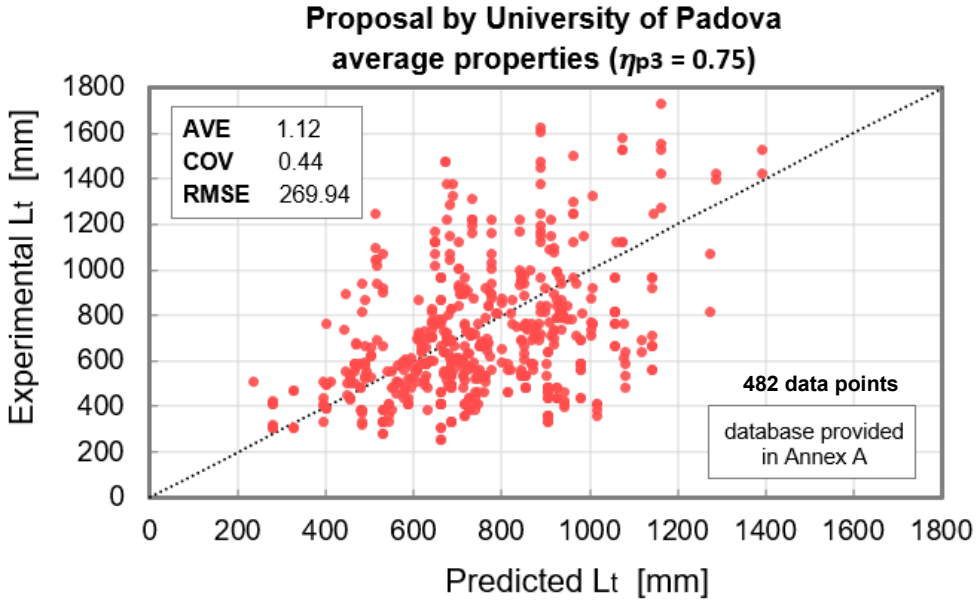

Figure 3-21: Performance of the proposal by University of Padova when applied to the database provided in Annex A.

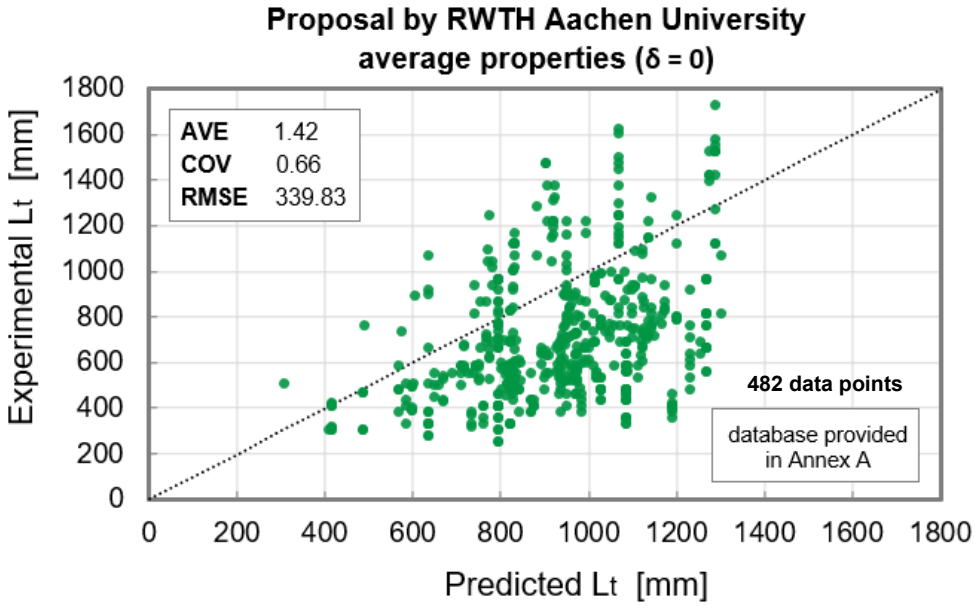

Figure 3-22: Performance of the proposal by RWTH Aachen University when applied to the database provided in Annex A.

It can be noted that the design model proposed within this work (section 3.5.1.) seems to be in better agreement with the experimental evidences. In fact, the overall point cloud is closer to the diagonal ideal line if compared to that in Figure 3-22 arising from the proposal by RWTH Aachen University. This is also confirmed by the root mean square errors (RMSEs) and average ratios between theoretical and experimental values (AVEs), as reported in the top-left area of the pictures. The coefficient of variations (COVs) associated with the two models also show a lower scatter of the data points if predicted by the proposal advanced by University of Padova.

On the other hand, Figures 3-23 and 3-24 illustrate the quality of the proposed formulation on the transmission length when considering the dataset provided by RWTH Aachen University [3-41]. The same trend depicted in the previous graphs (referring to the dataset reported in Annex A) is highlighted also in this case in that the proposal of modification based on current *fib* MC2010 seems to better adhere to the experimental results. Conversely, the proposal by RWTH Aachen University results in a point cloud which lies almost entirely below the optimal line. The values of AVE, COV and RMSE confirm the effectiveness of the model proposed in this work if compared to that based on the formulation of Eurocode 2, thus replicating the behaviour previously described (Figures 3-21 and 3-22).

The evaluation of the proposed formulations on the anchorage length is not presented here as the experimental database provided in Annex B is thought to be not sufficiently exhaustive to give an accurate judgement.

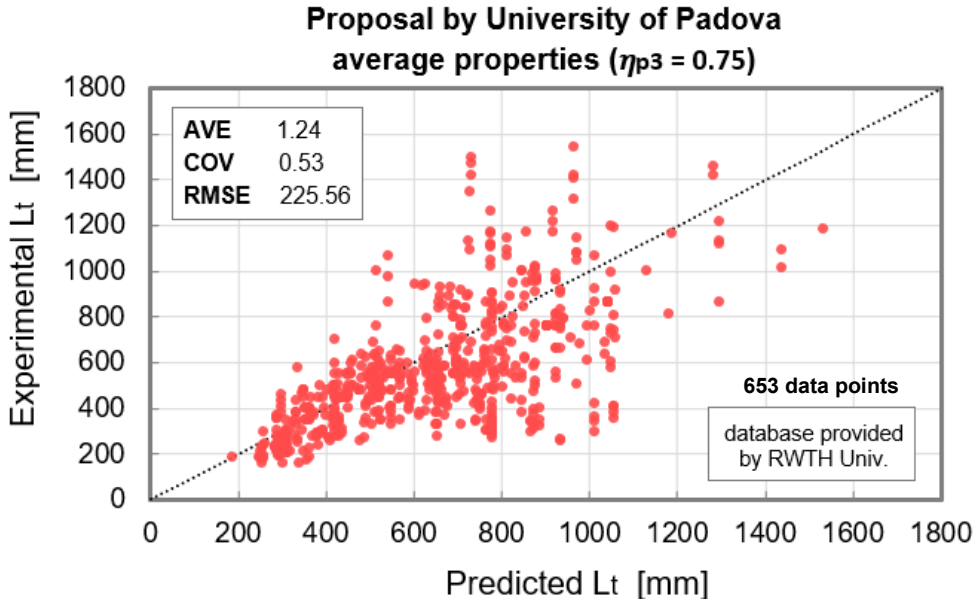

Figure 3-23: Performance of the proposal by University of Padova when applied to the database provided in [3-41].

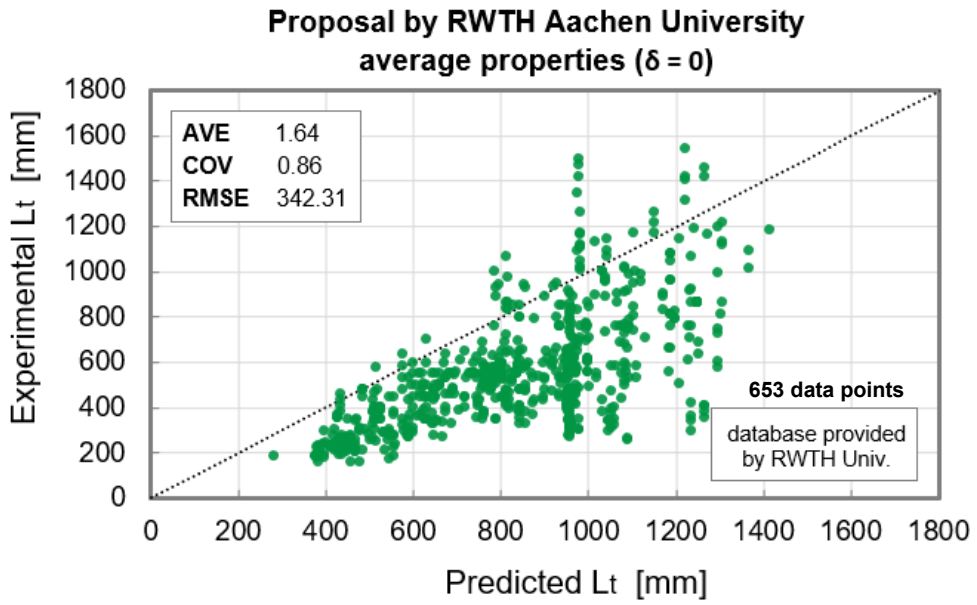

Figure 3-24: Performance of the proposal by RWTH Aachen University when applied to the database provided in [3-41].

3.6. Conclusions

In this chapter, a general assessment of the principal design codes for concrete structures when predicting the transmission length and anchorage length of PC members has been carried out. In parallel, the evaluation of the most recognised relationships proposed by researchers in the last few decades has also been considered. Many design formulations on the pre-tensioning anchorage can actually be found, even though they consider the various influencing parameters with different accuracy.

Firstly, the comparison of the existing design provisions on the transmission length and anchorage length was considered with respect to particular PC member configurations, involving commonly used techniques and materials. It was found that a relatively large scatter exists among the different formulations. Some guidelines such as ACI 318-14 and AASHTO are not able to capture the effect of the concrete compressive strength on the transmission length calculation or anchorage capacity evaluation.

In the second part of the section, the accuracy of the existing expressions was evaluated applying them to an experimental dataset of transmission and anchorage length tests performed in the literature. A total number of 742 data points from 21 studies was included, spanning over a great variety of influencing parameters. Results highlighted how an appropriate evaluation of both transmission length and, especially, anchorage length of PC members remains open and under discussion.

According to the findings on the transmission length it can be concluded that:

- The performance of ACI 318-14 (and also AASHTO, which presents similar recommendations), providing average values of the transmission length, seems to be inadequate since it considers only the nominal strand diameter and the effective strand stress after allowance for all prestress losses as influencing parameter. Many experimental values are not correctly predicted;
- The provisions by *fib* MC2010 and Eurocode 2 consider a lower bound and an upper bound value of the transmission length for checking transverse stresses at release and calculating anchorage capacity of the member at ULS, respectively. A larger number of primary factors is taken into account, resulting in a good effectiveness of the formulation, especially when verifying transverse stresses at SLS;

Furthermore, the following conclusions can be drawn with respect to the anchorage length:

- ACI 318-14 encompasses about half of conservative data points, even though the global scatter is less than that for the transmission length analysis;
- Poor performances have been found for *fib* MC2010 and, even more, for Eurocode 2 when considering average material properties, where more than half of the dataset is unsafe. The evaluation of such codes was also performed with respect to design material properties: the consideration of design values of the anchorage length results in a considerable improvement of the prediction, even though for Eurocode 2 the percentage of not conservative results was still high;

In the final part of the chapter, the role of the major parameters affecting the transmission length of PC members was studied based on the analysis of the collected database. Particularly, it was found that:

- The transmission length linearly increases with the tendon diameter and the initial prestress level, reflecting the convictions of the main design codes on the role of such parameters;
- The transmission length decreases non-linearly as concrete compressive strength increases, due to larger confining stresses on the tendon;
- The transmission length is reduced when prestressing tendons are epoxy-coated (and impregnated with grit) or slightly rusted on the external surface;
- The type of prestressing-force release greatly influences the transmission length, where a sudden release of the tendons commonly results in longer transmission lengths than a gradual release process. Moreover, the location of the free-end with respect to the flame-cutting also seems to affect the bond behaviour as it was found that the transmission length at the “cut end” is, on average, 10% larger than that at the “dead end”.

Lastly, the evaluation of two proposals of modification of current *fib* MC2010 was discussed. On one side, the model proposed by University of Padova, in which the author has been involved, was presented based on the formulation of the existing *fib* MC2010. On the other side, the new proposal by RWTH Aachen University was conceived adopting Eurocode 2 as a reference standard. Comparison of the proposed models with the collected experimental results showed the effectiveness of the formulation advanced within this work in replicating the transmission length measured in the literature.

References

[3-1] Zia, P. And Mostafa, T. (1977). "Development length of prestressing strands". *PCI Journal,* vol. 22(5), 54-65.

[3-2] Mitchell, D., Cook, W.D., Kahn, A.A. and Tham, T. (1993). "Influence of High-Strength concrete on transfer and development length of pretensioning strand". *PCI Journal*, vol. 38(3), 52-66.

[3-3] Oh, B.H. and Kim, E.S. (2000). "Realistic evaluation of transfer lengths in pretensioned prestressed concrete members". *ACI Structural Journal*, vol. 97(6), 821-830.

[3-4] Martì-Vargas, J.R., Garcìa-Taengua, E. and Serna-Ros, P. (2013). "Influence of concrete composition on anchorage bond behavior of prestressing reinforcement". *Construction Building Materials,* vol. 48, 1156-1164.

[3-5] ACI Committee 318 (2014). "Building Code requirements for structural concrete (ACI 318-14) and Commentary (ACI 318R-14)". American Concrete Institute, Farmington Hills, MI, USA.

[3-6] *fib* Model Code 2010 (2013). "*fib* Model Code for concrete structures". International Federation for Structural Concrete (*fib*), Lausanne, Switzerland.

[3-7] AASHTO (2012). "LFRD bridge design specifications - 6th edition". American Association of State Highway and Transportation, Washington, DC, USA.

[3-8] Eurocode 2 (2004). "Design of concrete structures - Part 1-1: General rules and rules for buildings". Comitè Europèen de Normalisation, Brussels, Belgium.

[3-9] Pellegrino, C., Zanini, M.A., Faleschini, F. and Corain, L. (2015). "Predicting bond formulations for prestressed concrete elements". *Engineering Structures,* vol. 97, 105-117.

[3-10] Buckner, C.D. (1995). "A review of strand development length for pretensioned concrete members". *PCI Journal,* vol. 40(2), 84-105.

[3-11] Russell, B.W. and Burns, N.A. (1993). "Design guidelines for transfer, development and bonding of large diameter seven-wire strands in pretensioned concrete girders". Research report 1210-5F, *Center for Transportation Research*, University of Texas at Austin, Austin, TX, USA.

[3-12] Shahawy, M.A., Issa, M. and Batchelor, B. (1992). "Strand transfer lengths in full-scale AASHTO prestressed concrete girders". *PCI Journal*, vol. 37(3), 84-96.

[3-13] Lane, S.N. (1990). "Development length of prestressing strand". *Public Roads,* vol. 54(2), 200-205.

[3-14] Cousins, T.E., Johnston, D.W. and Zia, P. (1990). "Transfer and development length of epoxy-coated and uncoated prestressing strand". *PCI Journal,* vol. 35(4), 92-103.

[3-15] Martin, L.D. and Scott, N.L. (1976). "Development of prestressing strand in pretensioned members". *ACI Journal*, vol. 73(8), 453-456.

[3-16] Shahawy, M. (2001). "A critical evaluation of the AASHTO provisions for strand development length of prestressed concrete members". *PCI Journal,* vol. 46(4), 94-117.

[3-17] Buckner, C.D. (1994). "An analysis of transfer and development lengths for pretensioned concrete structures". Final report FHWA-RD-94-049, *Federal Highway Administration*, Washington, D.C.

[3-18] Deatherage, J.H., Burdette, E.G. and Chew, C.K. (1994). "Development length and lateral spacing requirements of prestressing strand for prestress concrete bridge girders". *PCI Journal,* vol. 39(1), 70-83.

[3-19] Ramirez, J.A. and Russell, B.W. (2008). "Transfer, development and splice length for strand/reinforcement in High-Strength concrete". NCHRP report 603, *Transportation Research Board*.

[3-20] Caro, L.A., Martì-Vargas, J.R. and Serna, P. (2013). "Time-dependent evolution of strand transfer length in pretensioned prestressed concrete members". *Mechanics of Time-Dependent Materials,* vol. 17(4), 501-527.

[3-21] Abdalla, O.A., Ramirez, J.A. and Lee, R.H. (1993). "Strand debonding in pretensioned beams - Precast prestressed concrete bridge girders with debonded strands - Continuity issues". Final report FHWA/IN/JHRP-92/24, *Joint Highway Research Project*.

[3-22] Barnes, R.W., Burns, N.H. and Kreger, M.E. (1999). "Development length of 0.6-inch prestressing strand in standard I-shaped pretensioned concrete beams". Research report FHWA/TX-02/1388-1, Center for Transportation Research, University of Texas at Austin, Austin, TX, USA.

[3-23] Burgueño, R., Sun, Y. and Donoso, M. (2015). "Stress transfer characteristics of sheathed strand in prestressed concrete beams". *PCI Journal,* vol. 60(2), 104-120.

[3-24] Over, S. and Au, T. (1965). "Prestress transfer bond of pretensioned strands in concrete". *ACI Journal*, vol. 62(11), 1451-1459.

[3-25] Cousins, T.E., Johnston, D.W. and Zia, P. (1990). "Transfer length of epoxy-coated prestressing strand". *ACI Materials Journal,* vol. 87(3), 193-203.

[3-26] Russell, B.W. and Burns, N.H. (1996). "Measured transfer lengths of 0.5 and 0.6 in. strands in pretensioned concrete". *Journal of Structural Engineering*, vol. 123(5), 44-65.

[3-27] Russell, B.W. and Burns, N.H. (1997). "Measurement of transfer lengths on pretensioned concrete elements". *PCI Journal,* vol. 41(5), 541-549.

[3-28] Oh, B.H., Kim, E.S. and Choi, Y.C. (2006). "Theoretical analysis of transfer lengths in pretensioned prestressed concrete members". *Journal of Engineering Mechanics,* vol. 132(10), 1057-1066.

[3-29] Martì-Vargas, J.R., Arbeláez, C.A., Serna-Ros, P. And Castro-Bugallo, C. (2007). "Reliability of transfer length estimation from strand end slip". *ACI Structural Journal,* vol. 104(4), 487-494.

[3-30] Dang, C.N., Hale, W.M. and Martì-Vargas, J.R. (2017). "Assessment of transmission length of prestressing strands according to *fib* Model Code 2010". *Engineering Structures,* vol. 147, 425-433.

[3-31] Cousins, T.E., Stallings, J.M. and Simmons, M.B. (1994). "Reduced strand spacing in pretensioned, prestressed members". *ACI Structural Journal,* vol. 91(3), 277-286.

[3-32] Kahn, L.F., Dill, J.C. and Reutlinger, C.G. (2002). "Transfer and development length of 15-mm strand in High-Performance concrete girders". *Journal of Structural Engineering*, vol. 128(7), 913-921.

[3-33] Barnes, R.W., Groove, J.W. and Burns, N.H. (2003). "Experimental assessment of factors affecting transfer length". *ACI Structural Journal*, vol. 100(6), 740-748.

[3-34] Kose, M.M. and Burkett, W.R. (2005). "Evaluation of Code requirement for 0.6 in. (15 mm) prestressing strand". *ACI Structural Journal*, vol. 102(3), 422-428.

[3-35] Hanson, N.W. and Kaar, P.H. (1959). "Flexural bond of pretensioned prestressed beams". *ACI Journal*, vol. 55(7), 783-802.

[3-36] Kaar, P.H., LaFraugh, R.W. and Mass, M.A. (1963). "Influence of concrete strength on strand transfer length". *Journal of Prestressed Concrete Institute*, vol. 8(5), 47-67.

[3-37] Stocker, M.F. and Sozen, M.A. (1969). "Investigation of prestressed reinforced concrete for highway bridges". Part VI: Bond Characteristics of Prestressing Strands, Structural Research Series, University of Illinois, IL, USA.

[3-38] Base, G.D. (1958). "An investigation of transmission length in pretensioned concrete". *Proceedings of the Third Congress of FIP - Session III*, paper 9(1), 603-623.

[3-39] Holmberg, A. and Lindgren, S. (1970). "Anchorage and prestress transmission". Document D1, National Swedish Institute for Building Research, Stockholm, Sweden.

[3-40] Kaar, P.H. and Hanson, N.W. (1975). "Bond fatigue tests of beams simulating pretensioned concrete crossties". *Journal of Prestressed Concrete Institute*, vol. 20(5), 65-80.

[3-41] Geβner, S. (2017). "Bond and anchorage of pre-tensioning tendons". PhD Thesis, RWTH Aachen University, Aachen, Germany.

4. ANALYTICAL MODELLING OF THE TRANSMISSION LENGTH IN PC MEMBERS

4.1. The importance of bond modelling

An adequate knowledge of the bond development at the interface between tendon and concrete at release of the prestressing-force is a matter of paramount importance for achieving a correct prestressed-concrete member detailing. It has been discussed in the previous chapters how bond in PC elements acts fundamentally in two situations. Initially, bond anchorage enables to transfer the jacking force from steel to the concrete within the transmission length, which plays a crucial role in governing the performance of the member. Subsequently, when the external loads increase during the beam service life, flexural bond stresses develop between the two materials to anchor the ultimate tendon force to the concrete. A proper consideration of the anchorage length in this phase is necessary to guarantee the PC member to exploit its ultimate load-carrying capacity. Generally, the bond mechanisms which affect the anchorage of the pre-tensioning reinforcement are complex and depend on various influencing parameters.

However, although pre-tensioning techniques have been successfully employed worldwide in important engineering applications for over 80 years, most of the modern design codes are still not able to completely describe the transfer mechanism of the prestressing-force in a reliable manner. It has been highlighted that disagreeing predictions of the transmission length and anchorage length of prestressing tendons arise from the existing code formulations when applied to set of experimental results collected from literature [4-1; 4-2]. This is because some of them (ACI 318-14, AASHTO) introduce only few factors to evaluate the fundamental lengths. In other codes (*fib* MC2010, Eurocode 2), although a larger number of primary variables is included in the formulations, the effect of some of them may have not completely understood yet for both the relevant design situations.

Furthermore, in all the available design provisions the prestressing-force is assumed to be transferred to the concrete by a constant bond strength along the transmission length. For ACI 318-14 such value is equal to 2.76 MPa (400 psi, see section 2.4.1.). Instead, for *fib* MC2010 and Eurocode 2 the constant bond strength is calculated based on some parameters depending on the tendon type, the bond conditions and the concrete tensile strength. Eqs. 2-7 and 2-12 are used for this purpose. Obviously, such a simplified

description of the internal behaviour of the PC member does not reflect the real properties at the interface steel-concrete. Nevertheless, it should be remembered that a design model shall enable a simple and practical dimensioning of pre-tensioning anchorage. Thus, certain simplifications are somehow needed.

In any case, a more realistic representation of the mechanism controlling the transmission of the jacking force to the concrete can be achieved through the development of appropriate analytical models. In principle, the actual bond stress distribution along the transmission zone could be found by means of numerical investigations based on physically-based approaches. Moreover, the effect of a great variety of influencing parameters could also be rationally included in such models. In the present chapter of the contribution, two different modelling techniques of the transmission length in PC members will be presented. The first analytical model is developed based on the Thick-Walled Cylinders (TWC) theory, adopting an anisotropic behaviour of the concrete. On the other hand, with the second investigation, the anchorage of pre-tensioning reinforcement is analysed through a bond stress-slip model. The models will be calibrated on the basis of the experimental database presented in the previous chapter. Finally, the two approaches will be compared and discussed. It should be noted that a slightly different nomenclature will be used in the present chapter for a better clarity in that the stresses will be identified with the letter "σ" and no longer with the letter "*f*", as in the previous sections of the document.

4.2. Elastic formulation of bond behaviour

In a prestressed-concrete member, once the force is released from the bulk-heads of the prestressing bed, large radial pressures arise at the interface between steel and concrete along the transmission length, because of the increase in the tendon diameter (i.e. the Hoyer effect). Concrete surrounding the tendon near the free-ends of the beam may present circumferential stresses - or hoop stresses - far above its tensile strength, thus experiencing cracking in the radial direction. Consequently, any theoretical model aimed at evaluating the transmission length of prestressing tendons should be based on plastic analyses of the concrete.

However, an elastic description of the material can be used in the first instance, as a qualitative guide on the bonding phenomenon. In this regard, a first simplified elastic approach to study issues related to bond in PC members can be presented based on the

findings proposed by the pioneering study of Janney [4-3] on steel wires. Nevertheless, the simple model reported hereafter also applies to study bond of strands.

At the release of the prestress, the tendon stress reduces from the initial jacking stress σ_{si} to a value σ_s, specific for the considered point along the tendon. At the same time, if the tendon is free to expand, an increment Δr_1 of its radius takes place (see Figure 4-1), as described by Eq. 4-1:

$$\Delta r_1 = r_{jack}\,(\sigma_{si} - \sigma_s)\,\frac{\nu_{ps}}{E_{ps}} \tag{4-1}$$

where r_{jack} is the radius of the tendon after prestressing, σ_{si} is the initial prestress, σ_s is the tendon stress after release, ν_{ps} is the Poisson's coefficient of the prestressing steel and E_{ps} is the elastic modulus of the prestressing steel. Though, the radial stress at the interface surface is actually imposed by the presence of the surrounding concrete. Therefore, the real increase Δr_2 in tendon radius at release corresponds to the radial displacement of the concrete, as given in Eq. 4-2:

$$\Delta r_2 = r_{jack}\,\sigma_{c,r}\,\frac{1+\nu_c}{E_c} \tag{4-2}$$

being $\sigma_{c,r}$ the radial stress transmitted from the tendon to the concrete, ν_c the Poisson's coefficient of the concrete and E_c the elastic modulus of the concrete.

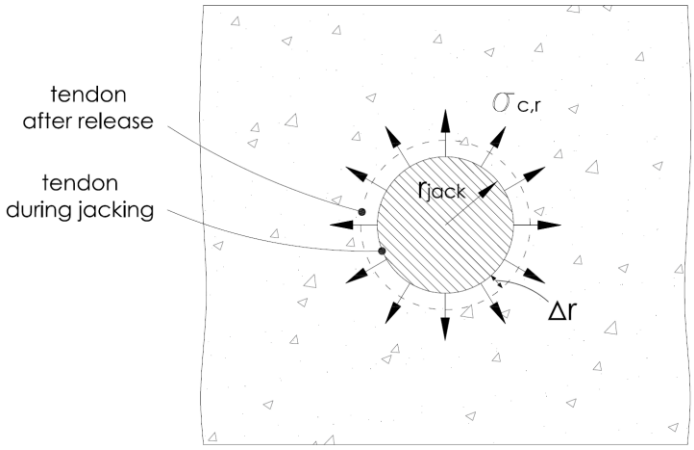

Figure 4-1: Increment of tendon radius after release of the prestressing-force.

In this way, by applying the constitutive equation 1D and considering the two reported expressions for Δr (i.e. Δr_1 from Eq. 4-1 and Δr_2 from Eq. 4-2), the extent of the radial pressure at the interface between steel and concrete can be found:

$$\sigma_{c,r} = \frac{\Delta r_1 - \Delta r_2}{r_{jack}}\,E_{ps} = (\sigma_{si} - \sigma_s)\,\nu_{ps} \;-\; \sigma_{c,r}\,(1+\nu_c)\,\frac{E_{ps}}{E_c} \tag{4-3}$$

where the tendon radius after jacking r_{jack} can be derived through consideration of the Poisson's effect on the longitudinal strain. Equivalently, Eq. 4-3 can be written as:

$$\sigma_{c,r} = \frac{(\sigma_{si} - \sigma_s)\,\nu_{ps}}{1 + (1 + \nu_c)\frac{E_{ps}}{E_c}} \tag{4-4}$$

4.2.1. Description of prestress transfer bond

The prestress transfer bond (named f_{bpt} to adopt the same nomenclature as in the European standard codes) along the transmission length of the PC member can be derived directly from the steel stress development diagram after release, typically as in Figure 4-2. In fact, the bond strength at any point along the member length is proportional to the slope of the curve represented in the diagram. Specifically, it is equal to the slope of the curve multiplied by $r_{jack}/2$ (Eq. 4-5). On the other hand, prestress transfer bond can also be obtained as a function of the radial stress developing at the interface between steel and concrete, by means of the friction coefficient (Eq. 4-6). Among the different bond mechanisms (see section 2.2), friction can be reasonably considered as the principal responsible for the transmission of prestress to the concrete.

$$f_{bpt} = \frac{d\sigma_s}{dz}\,\frac{r_{jack}}{2} \tag{4-5}$$

$$f_{bpt} = \mu\,\sigma_{c,r} \tag{4-6}$$

where z identifies the distance from the free-end of the PC member (along the longitudinal axis of the tendon) and μ the overall friction coefficient between steel and concrete, combining the actual frictional and mechanical bond.

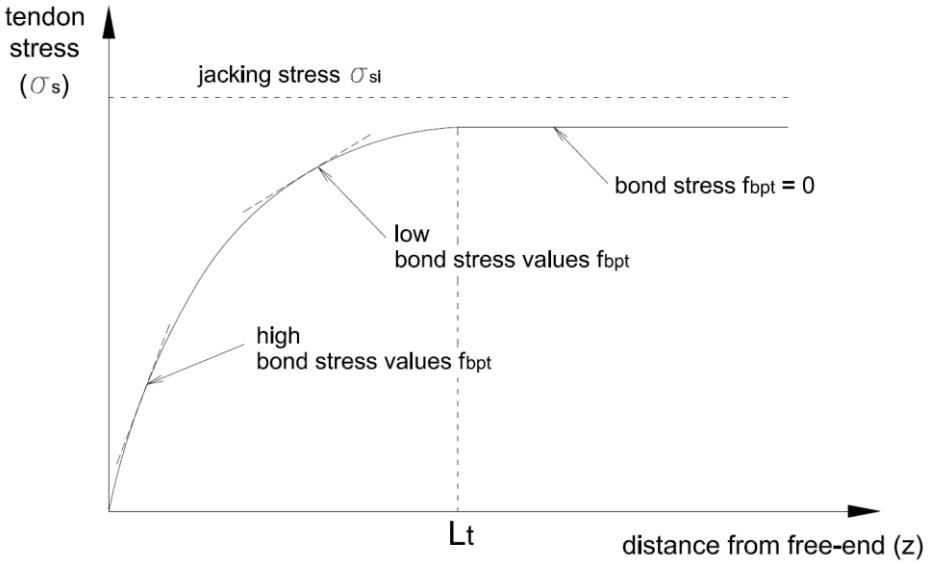

Figure 4-2: Typical steel stress development diagram near the PC member free-end at release.

By comparing Eqs. 4-5 and 4-6, and considering Eq. 4-4 for the radial stress at the interface surface, the following simple differential equation is considered:

$$dz = \frac{r_{jack}}{2\,\mu}\,\frac{1+(1+\nu_c)\,E_{ps}/E_c}{(\sigma_{si}-\sigma_s)\,\nu_{ps}}\,d\sigma_s \tag{4-7}$$

Thus, Eq. 4-7 can be integrated to evaluate the transmission length required to transmit the fully effective prestress σ_{si} to the concrete, as in Eq. 4-8. The boundary conditions are $\sigma_s = 0$ for $z = 0$ (at the free-end), and $\sigma_s = \sigma_{s,max}$ for $z = L_t$ (where the bond strength $f_{bpt} = 0$), respectively. It is recalled that L_t identifies the transmission length.

$$L_t = \frac{-r_{jack}\left[1+(1+\nu_c)\frac{E_{ps}}{E_c}\right]}{2\,\mu\,\nu_{ps}}\,ln\,\frac{\sigma_{si}-\sigma_{s,max}}{\sigma_{si}} \tag{4-8}$$

It should be noted that the global steel stress profile along the length of the PC member can be obtained from the integration of Eq. 4-7, where for the generic coordinate z from the free-end is:

$$z = \frac{-r_{jack}\left[1+(1+\nu_c)\frac{E_{ps}}{E_c}\right]}{2\,\mu\,\nu_{ps}}\,ln\,\frac{\sigma_{si}-\sigma_s}{\sigma_{si}} \tag{4-9}$$

However, as stated previously, high values of radial compressive and circumferential tensile stresses arise at the release of the prestressing-force under commonly adopted materials. In most cases, the concrete is beyond the elastic domain and such type of analysis may give only approximated results. Janney [4-3] sustained that, by using materials and technologies of that time (1954), radial and hoop stresses in the concrete at release were in the order of magnitude of 20-25 MPa. A few decades later, Oh et al. [4-4], after considerable progresses made in both concrete and prestressing steel industry during the last half of the 20th century, analysed the typical stress distribution around a tendon after the release operations. They found tensile stress values along the circumferential direction approximately 10 times larger than the actual concrete tensile strength. This means that the concrete surrounding the tendon is likely to experience cracking in the radial direction. Consequently, the resulting elastic formulations, Eqs. 4-8 and 4-9, should not be considered for design purposes.

4.3. Anisotropic model based on the thick-walled cylinders theory

In order to take into account possible cracking of the concrete around the prestressing tendon, a more refined analysis of the force transfer mechanism is worth to be developed. Among the alternative approaches, a design model based on the thick-walled cylinders (TWC) theory might be one of the most appropriate to address the problem, since the anisotropic behaviour of the concrete can be included in principle. To apply the principles of the TWC theory to such specific problem, the steel tendon can be considered as a solid internal cylinder of radius r_{ps}. Instead, the surrounding concrete section can be assimilated to an external hollow cylinder with radial thickness c (see the following Figure 4-3).

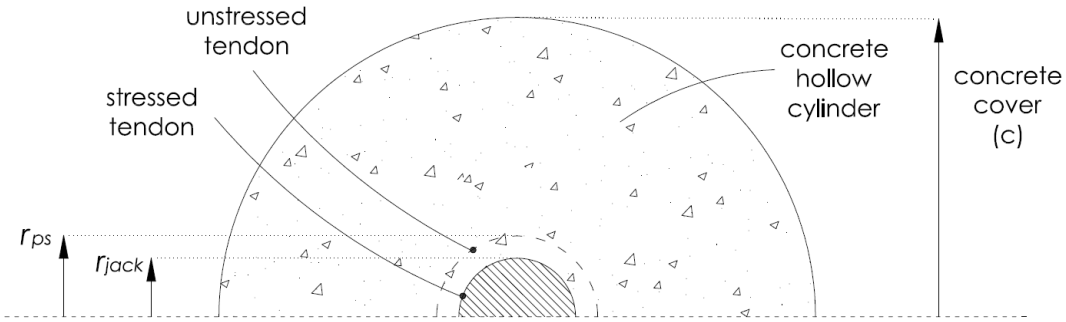

Figure 4-3: Nomenclature of the idealised steel and concrete cylinders for the application of the TWC theory.

Particularly, the radial thickness may be taken as the real concrete cover of the PC member (i.e. the minimum between the lateral and bottom cover), or the effective cover when considering multiple tendons in the same row [4-5], being limitative in the case of narrow spacing between prestressing tendons. The TWC theory, applied to this context, has allowed reaching promising results [4-4; 4-6], even though principally calibrated on a limited number of experimental evidences.

4.3.1. General calculation procedure

To obtain an accurate estimation of the transmission length, the analysed prestressing tendon can be subdivided into a number of finite elements, characterised by small finite length Δz. In particular, the element at the free-end of the PC member is certainly subject to a prestress equal to zero ($\sigma_{s,0} = 0$), as represented in the following Figure 4-4. Consequently, starting from this first element and moving towards the mid-span of the member, the increment of axial stress in the tendon $\Delta\sigma_s$ due to bond development

within the element can be subsequently calculated from the equilibrium along the tendon longitudinal axis, as in Eq. 4-10:

$$\Delta\sigma_s = \frac{\pi \ \emptyset \ \Delta z \ f_{bpt}}{A_{sp}} \tag{4-10}$$

where $\emptyset$ is the nominal tendon diameter, f_{bpt} is the bond stress along the considered element and A_{sp} is the tendon cross-sectional area. Of course, this implies that the distribution of the bond stress along the transmission zone has to be known. This matter will be addressed in the next sections.

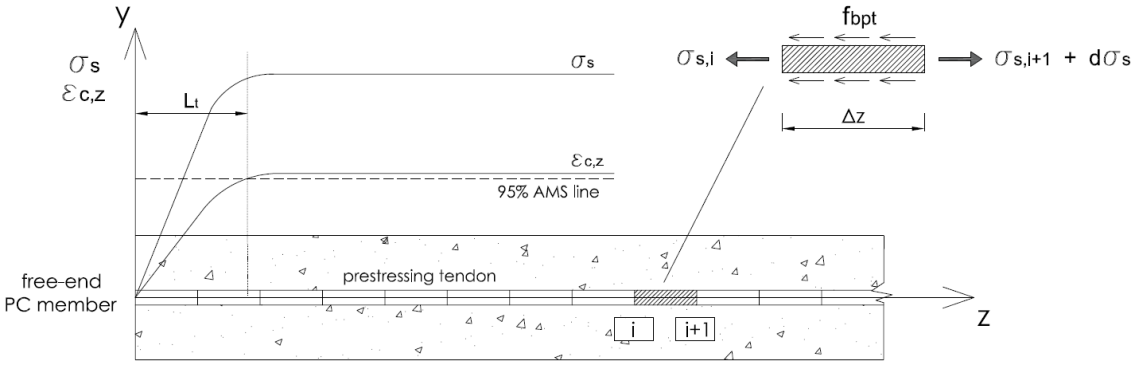

Figure 4-4: Discretization of the prestressing strand and equilibrium of forces.

The prestressing-force (P_{i+1}) and the concrete axial stress at the level of the tendon ($\sigma_{c,z,i+1}$) in the successive finite elements can be computed as in Eqs. 4-11 and 4-12, respectively.

$$P_{i+1} = \sigma_{s,i+1} A_{sp} = \sum_{n=1}^{i+1} [\Delta\sigma_{s,n} A_{sp}] \tag{4-11}$$

$$\sigma_{c,z,i+1} = P_{i+1}\left(\frac{1}{A_c} + \frac{e}{J_x}y\right) \tag{4-12}$$

where A_c and J_x are the cross-sectional area and the moment of inertia of the concrete section, respectively, while e represents the vertical eccentricity of the tendon with respect to the centroid of the concrete section and y is the vertical reference axis (see Figure 4-4). By repeating the mentioned procedure for each subsequent finite element, from the free-end to the mid-span, the transmission length of the PC member can be easily determined. Specifically, the theoretical concrete strain profile ($\varepsilon_{c,z}$) due to transmission of the prestressing-force is derived from Eq. 4-12 at any point along the length of the beam. Thus, as commonly adopted in the literature, the transmission length of the considered tendon can be obtained as the distance from the free-end to the point where concrete axial strain reaches 95% of the maximum strain (95% AMS method, as in Russell and Burns, 1996 [4-7]). However, the analytical model should also consider

the type of prestress release (i.e. sudden or gradual) and free-end location (i.e. "cut" or "dead" end), which can affect significantly the actual transmission length. This is accomplished by multiplying the obtained transmission length value by a coefficient α_{rel}, which is assumed to be 1.0 for a gradual release of the tendons or 1.3 when a sudden flame-cutting process is employed. This latter value is taken as the average between the two increasing factors associated with the "dead" and the "cut" end (i.e. α_{rel} = 1.25 and α_{rel} = 1.35, respectively, as reported in section 3.5.1. of the document), in order to achieve a better comparison with experimental data.

4.3.2. Elastic analysis based on the thick-walled cylinders theory

The distribution of the prestress transfer bond f_{bpt} along the transmission length is assumed to be constant by all the predictive formulations given in design codes. Generally, bond stress is expressed through the fundamental equation:

$$f_{bpt} = \mu\, \sigma_r(r_{jack}) \tag{4-13}$$

In this expression, μ is the overall friction coefficient between the tendon and the concrete, combining actual frictional and mechanical bond. Instead, $\sigma_r(r_{jack})$ is the radial compressive stress transmitted from the tendon to the concrete arising from the Hoyer effect, i.e. the pressure at the interface surface (r_{jack} identifies the radius of the tendon after prestressing). Typically, the coefficient of friction is assumed between 0.3 and 0.8 [4-8; 4-9; 4-10] and it is considered to be constant for a particular steel type. On the other hand, the magnitude of the interface pressure can be derived according to the TWC theory, where the whole problem is governed by three set of equations: equilibrium, compatibility and constitutive equations.

If an infinitesimal slice of the idealised concrete hollow cylinder of thickness *dz* is selected at a distance *z* from the free-end of the PC member (Figure 4-5), the three-dimensional equilibrium in the radial direction can be written as in Eq. 4-14. Particularly, $\sigma_{c,r}$ and $\sigma_{c,\theta}$ are the stresses in the radial and circumferential direction, respectively, while *r* is the radial distance. In this relationship, the stress component in the circumferential direction stems from considering its projection onto the radial plane. The expression neglects terms containing higher-order infinitesimal, and assumes all the variables to be independent of the *z* direction within the small finite length *dz*.

$$\sigma_{c,r} + \frac{d\sigma_{c,r}}{dr} r - \sigma_{c,\theta} = 0 \tag{4-14}$$

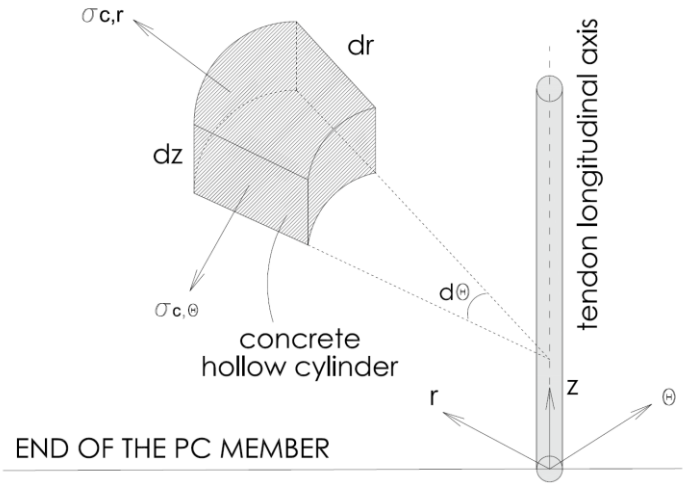

Figure 4-5: Selection of an infinitesimal element of the concrete hollow cylinder.

In addition, the displacement compatibility at the interface between strand and concrete must be satisfied also after release of the prestressing-force, and gives Eq. 4-15, where r_{ps} and r_{jack} are the tendon radius before and after prestressing, while u_{ps} and u_c represent the radial displacements of the tendon surface and the concrete, respectively. It should be noted that the radius r_{jack} also corresponds to the inner radius of the concrete hollow cylinder, since concrete is cast after the tendon is stressed. The problem is idealised as represented in Figure 4-3, where the same nomenclature is adopted.

$$r_{ps} + u_{ps} = r_{jack} + u_c \tag{4-15}$$

Finally, the radial and circumferential stresses $\sigma_{c,r}$ and $\sigma_{c,\theta}$ can be expressed according to the constitutive equations of the infinitesimal element of the concrete cylinder (Eqs. 4-16), being $\sigma_{c,z}$ the concrete axial stress, E_c and υ_c the elastic modulus and Poisson's coefficient of concrete, $\varepsilon_{c,r}$ and $\varepsilon_{c,\theta}$ the concrete strain in the radial and circumferential direction, respectively.

$$\sigma_{c,r} = \frac{E_c}{1-\upsilon_c{}^2}\left(\varepsilon_{c,r} + \upsilon_c\,\varepsilon_{c,\theta}\right) + \frac{\upsilon_c\,(1+\upsilon_c)\,\sigma_{c,z}}{1-\upsilon_c{}^2} \tag{4-16 a}$$

$$\sigma_{c,\theta} = \frac{E_c}{1-\upsilon_c{}^2}\left(\varepsilon_{c,\theta} + \upsilon_c\,\varepsilon_{c,r}\right) + \frac{\upsilon_c\,(1+\upsilon_c)\,\sigma_{c,z}}{1-\upsilon_c{}^2} \tag{4-16 b}$$

By substituting Eqs. 4-16a and 4-16b in the equilibrium equation, Eq. 4-14, it results:

$$r\,\frac{d^2u}{dr^2} + \frac{du}{dr} - \frac{u}{r} = 0 \tag{4-17}$$

whose solution, the radial displacement *u*, can be written in the following form:

$$u = c_1 r + c_2/r \tag{4-18}$$

It can be noted that, combining Eq. 4-18 and Eqs. 4-16, the radial and circumferential stresses can also be connected to the constants of integration c_1 and c_2:

$$\sigma_{c,r} = E_c \left[\frac{c_1}{1-\upsilon_c} - \frac{c_2}{r^2\,(1+\upsilon_c)} \right] + \frac{\upsilon_c\,\sigma_{c,z}}{(1-\upsilon_c)} \tag{4-19 a}$$

$$\sigma_{c,\theta} = E_c \left[\frac{c_1}{1-\upsilon_c} + \frac{c_2}{r^2\,(1+\upsilon_c)} \right] + \frac{\upsilon_c\,\sigma_{c,z}}{(1-\upsilon_c)} \tag{4-19 b}$$

Two different boundary conditions can be set separately for steel and concrete to derive the constants of integration c_1 and c_2, and thus the radial displacement *u* (Eq. 4-18) and the stresses in the radial and circumferential direction (Eqs. 4-19):

- for the steel solid cylinder, the radial displacement *u* must be zero at the tendon centroid, i.e. at *r = 0*. Therefore, being $\sigma_{c,r} = \sigma_r(r_{jack})$ at $r = r_{jack}$ (where r_{jack} is the radial distance to the outer surface of the stressed tendon and $\sigma_r(r_{jack})$ is the corresponding radial pressure at the interface), the field of the radial displacement can be expressed as in Eq. 4-20a;
- on the other hand, for concrete, the two boundary conditions are $\sigma_{c,r} = \sigma_r(r_{jack})$ at $r = r_{jack}$ and $\sigma_{c,r} = 0$ at the outer surface of the concrete hollow cylinder, i.e. at *r = c*, so that the radial displacement can be obtained as in Eq. 4-20b.

$$u(r) = \left[\frac{\sigma_r(r_{jack})\;(1-\upsilon_c) - \upsilon_c\,\sigma_{c,z}}{E_c} \right] r \tag{4-20 a}$$

$$u(r) = \frac{\sigma_r(r_{jack})\;r}{E_c\,(1/c^2 - 1/r)} \left[\frac{(1-\upsilon_c)}{c^2} + \frac{(1+\upsilon_c)}{r^2} \right] - \frac{\upsilon_c\,\sigma_{c,z}\,r}{E_c} \tag{4-20 b}$$

Particularly, the reduced tendon radius after prestressing is obtained when considering the Poisson's effect on the longitudinal strain (σ_{si} is the strand stress after release):

$$r_{jack} = (1 - \frac{\sigma_{si}}{E_{ps}}\upsilon_{ps})\,r_{ps} \tag{4-21}$$

The radial pressure at the tendon-concrete interface arising from the Hoyer effect can finally be derived from the compatibility condition (Eq. 4-15). In fact, by substituting the displacement at the tendon outer surface (u_{ps}, from Eq. 4-20a) and the displacement at the inner surface of the concrete hollow cylinder (u_c, as given by Eq. 4-20b):

$$\sigma_r(r_{jack}) = \frac{r_{ps}\,(1-\upsilon_{ps}\,\sigma_s/E_{ps}) - r_{jack}\,(1-\upsilon_c\,\sigma_{c,z}/E_c)}{(1-\upsilon_{ps})\,r_{ps}/E_{ps} + [\upsilon_c - (r_{jack}^2+c^2)/(r_{jack}^2-c^2)]\,r_{jack}/E_c} \tag{4-22}$$

being σ_s and $\sigma_{c,z}$ the axial stresses into the steel and concrete for the finite element at a generic distance *z* from the PC member free-end, respectively.

4.3.3. Anisotropic analysis for cracked concrete

The isotropic elastic analysis presented above could be accepted only in a limited number of situations, for instance when low values of the jacking force or high-strength concretes are adopted in the precast plant. However, in most cases, the actual concrete tensile strength is exceeded in the vicinity of the tendon, especially near the free-end of the PC member, where the Hoyer effect is maximum. Therefore, more refined theoretical models incorporating anisotropic concrete properties are required to better describe the bond phenomenon in presence of cracking.

Particularly, depending on the confining pressure at the interface, concrete may experience three different configurations along the transmission length when the tendon is released for transfer. It can be fully cracked near the free-end, only partially cracked at a certain distance from the free-end and it might be intact and uncracked at a further distance (where the Hoyer effect is very small or negligible). Figure 4-6 summarises such possible conditions.

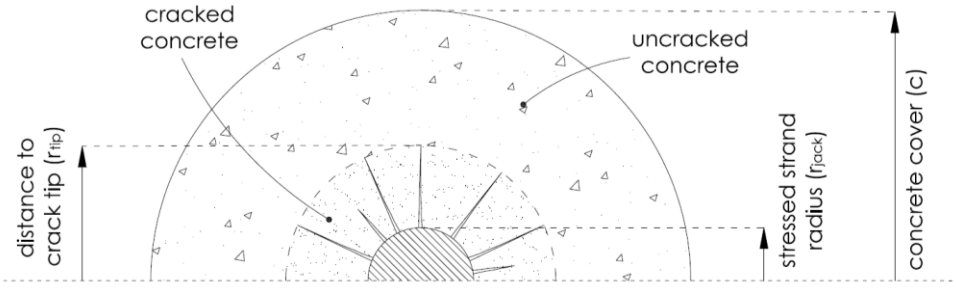

Figure 4-6: Radial cracking of the concrete around the prestressing tendon.

Similarly to Han et al., 2016 [4-6], a linear elastic field of displacement for the concrete cylinder can be assumed, resulting in the following relationship:

$$u(r) = \frac{f_{ct}}{E_c}\, r\, \frac{(c/r)^2 + 1}{(c/r_{tip})^2 + 1} \tag{4-23}$$

where f_{ct} is the tensile strength of concrete and r_{tip} is the distance from tendon centroid to the crack tip (see Figure 4-6). To determine the state of the concrete around the tendon, its circumferential strain at the interface with the strand, i.e. $\varepsilon_{c,\theta}(r_{jack})$, can be easily calculated from Eq. 4-20b, and compared with the cracking strain, $\varepsilon_{c,ck}$. The condition $\varepsilon_{c,\theta}(r_{jack}) > \varepsilon_{c,ck}$ means that concrete surrounding the tendon is cracked. In this case, the radius from the tendon centroid to the crack tip, r_{tip}, can be estimated by combining Eq. 4-20b and Eq. 4-23.

$$\frac{-\sigma_r(r_{jack})\, r_{jack}}{E_c\,(1/c^2 - 1/{r_{jack}}^2)}\left[\frac{(1-\upsilon_c)}{c^2} + \frac{(1+\upsilon_c)}{{r_{jack}}^2}\right] - \frac{\upsilon_c\, \sigma_{c,z}\, r_{jack}}{E_c} =$$

$$= \frac{f_{ct}}{E_c}\, r_{jack}\, \frac{(c/r_{jack})^2 + 1}{(c/r_{tip})^2 + 1} \qquad (4\text{-}24)$$

The influence of the potential concrete radial cracking on the magnitude of bond can be taken into account through an appropriate softening model. Among the different schematizations available in the literature, the tri-linear softening model suggested by Han et al. (2014) [4-11] can be adopted to represent the behaviour of concrete in tension, as in Figure 4-7.

Hence, from the equilibrium of the cracked concrete section (see Figure 4-8), the interface pressure $\sigma_r(r_{jack})$ can be related to the confining pressure at the crack tip $\sigma_{c,r}(r_{tip})$ and the residual circumferential stress in the cracked portion of the section $\sigma_{c,\theta}(r)$:

$$\sigma_r(r_{jack})\, r_{jack} = \sigma_{c,r}(r_{tip})\, r_{tip} + \int_{r_{jack}}^{r_{tip}} \sigma_{c,\theta}(r)\, dr \qquad (4\text{-}25)$$

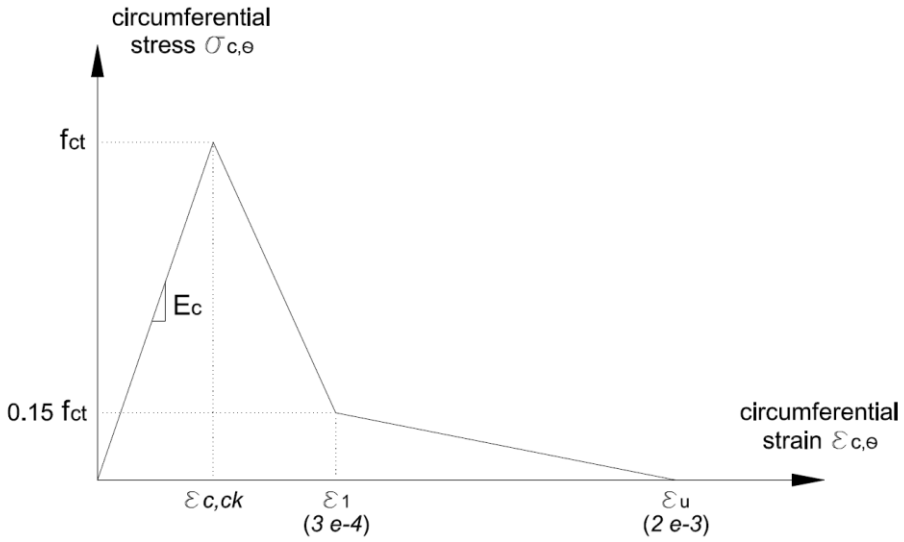

Figure 4-7: Tri-linear softening model for concrete in tension.

The confining pressure at the crack tip $\sigma_{c,r}(r_{tip})$ can be derived as in Eq. 4-26 considering that, by definition, the hoop stress at the crack tip $\sigma_{c,\theta}(r_{tip})$ is equal to the tensile strength of concrete f_{ct}. This enables the determination of the interface pressure $\sigma_r(r_{jack})$ from Eq. 4-25.

$$\sigma_{c,r}(r_{tip}) = f_{ct}\, \frac{c^2 - {r_{tip}}^2}{c^2 + {r_{tip}}^2} \qquad (4\text{-}26)$$

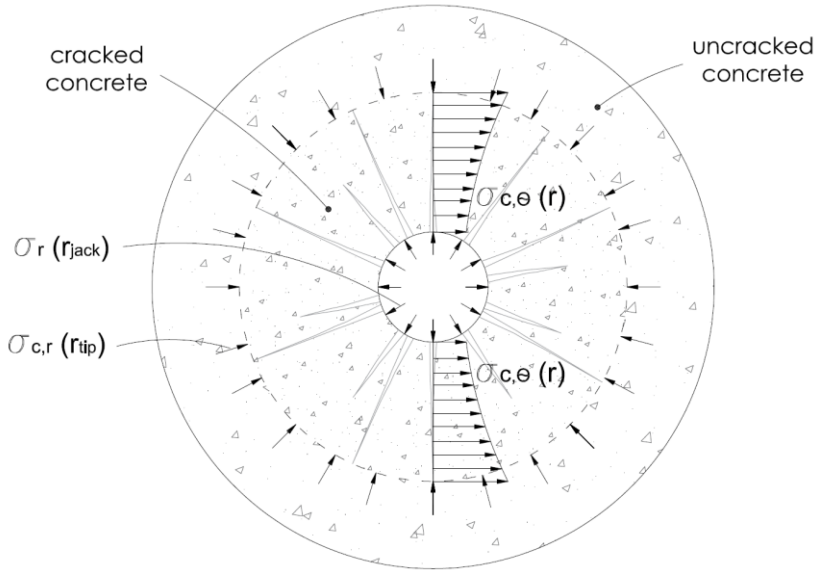

Figure 4-8: Internal equilibrium of the partially cracked concrete section.

However, in the case that the radius from tendon centroid to the crack tip (r_{tip}) is calculated to be greater than the actual concrete cover thickness *c*, i.e. for fully cracked concrete section, the field of the radial displacement results from Eq. 4-23 by taking *c* instead of r_{tip}:

$$u(r) = \varepsilon_{c,\theta}(c)\, r\, \frac{(c/r)^2 + 1}{2} \tag{4-27}$$

where the circumferential strain at the external side of concrete $\varepsilon_{c,\theta}(c)$ is derived from the following Eq. 4-28, which arises from Eqs. 4-20b and 4-27:

$$\frac{-\sigma_r(r_{jack})\; r_{jack}}{Ec\,(1/c^2 - 1/{r_{jack}}^2)}\left[\frac{(1-\upsilon_c)}{c^2} + \frac{(1+\upsilon_c)}{{r_{jack}}^2}\right] - \frac{\upsilon_c\, \sigma_{c,z}\, r_{jack}}{E_c} =$$

$$= \varepsilon_{c,\theta}(c)\, r_{jack}\, \frac{(c/r_{jack})^2 + 1}{2} \tag{4-28}$$

Therefore, for a fully cracked concrete section, the pressure at the interface between the tendon and the surrounding concrete is still calculated from Eq. 4-25, but considering that no confining stress is provided by the concrete (i.e. $\sigma_{c,r}(r_{tip})$ must be zero).

$$\sigma_r(r_{jack})\, r_{jack} = \int_{r_{jack}}^{r_{tip}} \sigma_{c,\theta}(r)\, dr \tag{4-29}$$

4.3.4. Model calibration and discussion of results

The above presented analytical model based on the TWC theory has been implemented with Matlab®, and calibrated in order to evaluate the optimal friction coefficient μ, as defined in Eq. 4-13. Then, in the following sections from 4.3.4.1. to 4.3.4.3., both the global behaviour of the model in estimating the transmission length of prestressing tendons and the local behaviour in analysing the development of radial cracking and bond stress along PC specimens are discussed.

The implementation of the model has been carried out so that the transmission length of the generic member is firstly calculated based on the elastic analysis presented in section 4.3.2. Nevertheless, if concrete in the vicinity of the tendon is found to experience cracking in the radial direction (depending on the value of the interface pressure evaluated as in Eq. 4-22), the analysis is repeated according to the anisotropic case illustrated in section 4.3.3 of the document. In this scenario, the transmission length of the PC member is recalculated on the basis of the interface pressure derived from Eq. 4-25 (partially cracked concrete section) or Eq. 4-29 (fully cracked concrete section). After implementation, the issue of the calibration of the TWC model has been addressed based on a comprehensive dataset of experimental transmission lengths derived from the literature. It is worth recalling that the global accuracy of any physically-based model is usually connected to the prior evaluation of a certain number of fundamental empirical parameters. In the case under investigation, the overall performance of the model appears to be highly dependent on the adopted coefficient of friction between the strand and the surrounding concrete.

The role of friction between the two materials was experimentally analysed in several previous studies [4-8; 4-12; 4-13; 4-14], where most of them agreed in obtaining values of the friction coefficient from 0.3 to 0.8. More recently, Arab et al. [4-15] used values of the friction coefficient up to 1.4 when modelling the transfer mechanism through a finite element software, based on AASHTO shear friction design recommendations. However, such a wide range of values might be little informative when addressing the description of bond at the release of the prestressing-force. Thus, a friction coefficient calibration is accomplished in this work by using a collected experimental database of transmission length values. The dataset is similar to that considered in chapter 3 for the general assessment of the existing formulations on the pre-tensioning anchorage. However, some filtering was necessary to avoid redundancy and ineffective data.

Firstly, the dataset incorporates test results on PC small-scale specimens only. The reason for this assumption is that most of the scientific papers concerning the investigation of real-scale bridge girders provided very few information about the exact geometrical features of the considered I-shaped beams. An assumption or reconstruction of the concrete section geometry by the author would probably have led to big distortions when calculating the cross-sectional area or the moment of inertia of the concrete mass.

Secondly, it should be noted that two different experimental transmission length values are usually derived from the same PC specimen, when using the 95% AMS method (or 100% AMS), depending on the considered free-end. In fact, the most used methods for prestress release entailed flame-cutting all the strands at one location between two beams, casted simultaneously in the prestressing bed. In this way, for a single beam, the two opposite free-ends are affected by a different amount of released energy. The interior side between two successive beams in the prestressing bed is named *"cut end"*, representing the free-end subject to direct flame-cutting of the strands and experiencing a higher amount of energy as a result of the cutting process. The other free-end is the *"dead end"*, which is at the opposite side of the member, and thus not subject to a direct flame-cutting of the tendons (a shorter transmission length is commonly registered here). In order to avoid redundant data and better compare experimental and theoretical results, the average value of the transmission length between those measured at the "cut end" and at the "dead end" is taken for each specimen, since the analytical model itself can not consider these situations at the release.

Thirdly, besides the presence of debonded tendons in PC specimens (that was excluded just for the evaluation in chapter 3), the small-scale test beams equipped with coated or rusted strands in Cousins et al. (1990) [4-16] and Mitchell et al. (1993) [4-17] have also been ignored from the present analysis. Indeed, the physically-based approach behind the developed analytical model could not be able to take into account their effect on the transmission length. Particularly, Cousins et al. studied the influence of the tendon surface conditions on pre-tensioning anchorage by examining the consequences of using corrosion protection coating - impregnated with grit - in PC members located in aggressive environments. On the other hand, in some PC specimens tested by Mitchell et al., the effect of rust presence on strands in small amounts has been analysed, promoting the roughness of the steel surface. However, the artificial weathering process which was applied to the tendons was not sufficient to create visible rust, but it caused microscopic roughness only which considerably improved bond.

The composition of the filtered dataset considered for the calibration process is reported in Table 4-1, and it comprises a total number of 130 experimental data from 7 different studies, which is also an acceptable numerousness. Such reduced database can be consulted in Annex C of the thesis, where the average values between the transmission length measured at the "cut end" and at the "dead end" are considered.

Table 4-1: Detail of the filtered dataset of experimental transmission length values for the calibration of the TWC model - test specimens and authors.

PC Small-scale specimens	
Reference citation	No. of experimental tests
Mitchell et al. (1993) [4-17]	14
Russell and Burns (1996) [4-7]	20
Russell and Burns (1997) [4-18]	12
Oh and Kim (2000) [4-19]	36
Oh et al. (2006) [4-4]	24
Martì-Vargas et al. (2007) [4-20]	12
Dang et al. (2017) [4-21]	12

Among the collected investigations, four different strand diameters (12.7, 15.2, 15.7 and 18.0 mm), strand stress at release from 871.0 to 1418.0 MPa and strand clear spacing up to 60.8 mm are considered as steel characteristics. Instead, a range of compressive strength at release from 19.2 to 68.1 MPa and cover thicknesses from 36.4 to 63.5 mm are considered as quantitative parameters for the concrete. The type of prestressing-force release method (sudden or gradual) is also included in the study as a qualitative factor.

4.3.4.1. Global behaviour: transmission length assessment

A parametric analysis has been carried out to evaluate the optimal value of the friction coefficient, i.e. the value that gives the best fit with the experimental results collected in the dataset. Table 4-2 highlights the overall performance of the analytical TWC model in predicting the transmission length of prestressing tendons when compared to the results of the experimental tests, for different values of the friction coefficient ranging from 0.3 to 0.8. It is recalled that the theoretical transmission lengths are calculated based on the interface pressure derived from the anisotropic analysis of the PC specimen, when concrete is cracked in the radial direction (Eq. 4-25 or Eq. 4-29 for the partially cracked or fully cracked concrete section, respectively).

Accordingly, it can be noted that the best accuracy, both in terms of the average ratio between theoretical and experimental values (AVE) and the root mean square error (RMSE) is provided when a coefficient of friction equal to 0.6 is selected. Instead, the lower coefficient of variation (COV) is achieved with a friction coefficient of 0.7, even though the COV for $\mu = 0.6$ is very similar. Such value is intended as the overall friction coefficient, combining actual frictional bond and mechanical bond.

Table 4-2: Performance of the analytical TWC model for different values of the friction coefficient.

Friction coefficient	AVE	COV	RMSE
$\mu = 0.3$	2.10	1.15	755.57
$\mu = 0.4$	1.62	0.67	439.31
$\mu = 0.5$	1.30	0.36	232.72
$\mu = 0.6$	1.07	0.18	139.20
$\mu = 0.7$	0.92	0.16	154.16
$\mu = 0.8$	0.81	0.23	207.22

AVE = average ratio between theoretical and experimental values; COV = coefficient of variation; RMSE = root mean square error

In Figure 4-9, the theoretical values of the transmission length obtained with the TWC model are graphically compared to the corresponding experimental results. The various pictures refer to the different values of the friction coefficient. It can be seen that for the lower friction coefficients (i.e. $\mu = 0.3$ and $\mu = 0.4$) the accuracy of the TWC prediction would be very poor, regardless of the considered statistical indicator (AVE, COV, RMSE). In these scenarios, all the data points are arranged in the lower-right part of the diagrams, providing conservative transmission lengths only when calculated for the subsequent evaluation of the flexural capacity of the PC member. In general, data are very far from the ideal line "experimental vs predicted L_t".

As the value of the friction coefficient is further increased, the point cloud progressively shifts towards the other half of the graph, characterised by transmission length values which are conservative when checking allowable transversal stresses at the release of the prestressing-force. The optimal condition is reached from adopting a friction coefficient equal to 0.6. In this case, a very good fit of the collected experimental data is provided by the TWC theory-based model, and most of the data sets are close to the diagonal line.

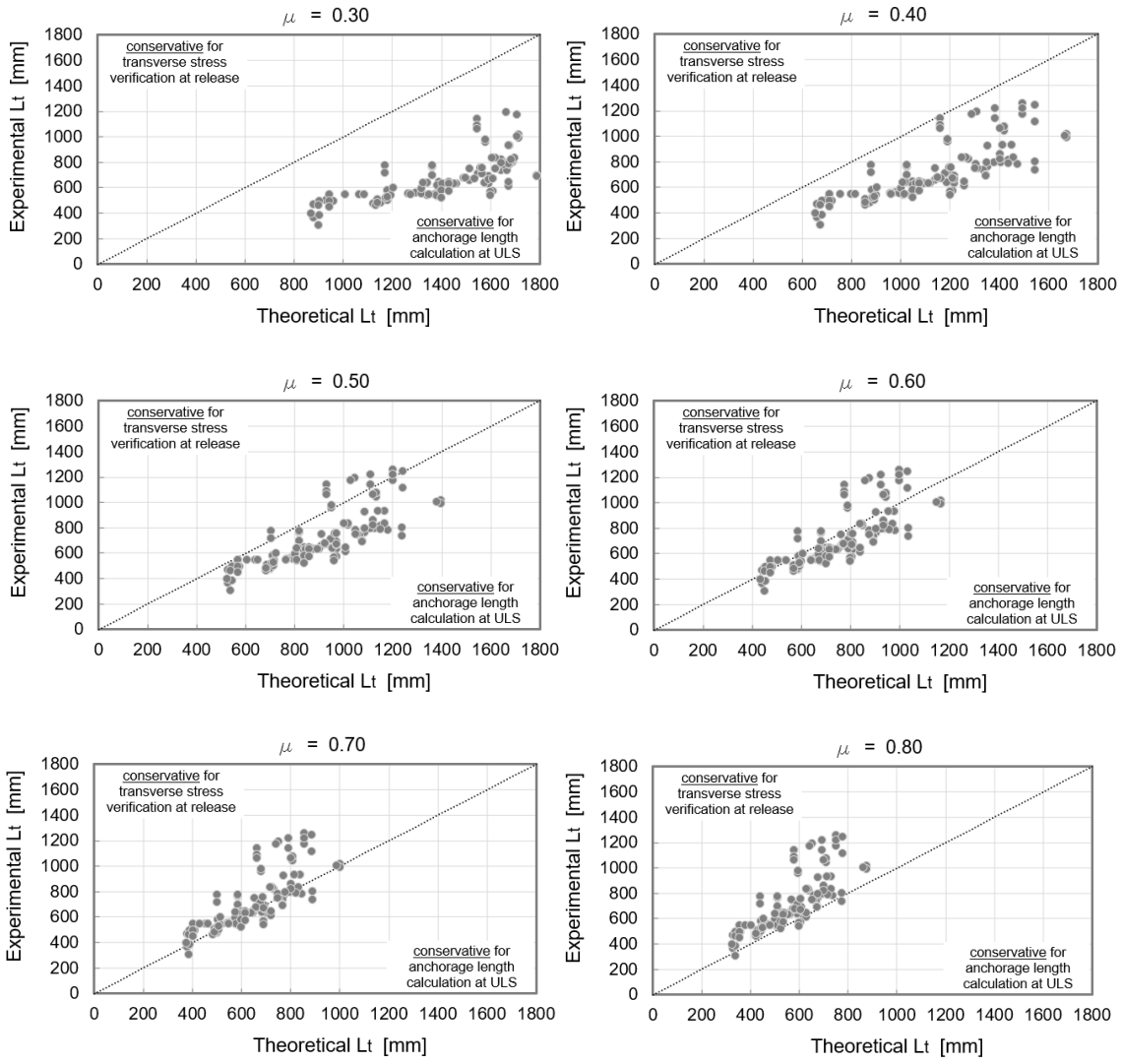

Figure 4-9: Experimental vs theoretical transmission lengths for values of the friction coefficients from 0.3 to 0.8.

As an example, the comparison between the experimental and theoretical concrete strain profile obtained with the TWC model, using a coefficient of friction of μ = 0.6, is depicted in Figure 4-10 with respect to specimen "M12-H-C4-1" tested in Oh and Kim, 2000 [4-19]. The test setup involved a 12.7 mm mono-strand rectangular specimen (b = 112.7 mm; h = 200 mm), characterised by a strand stress at release of 1396.5 MPa, a concrete compressive strength at release of 46.7 MPa and a concrete cover thickness of 46.4 mm. A sudden release of the prestressing-force has been implemented. It appears that little differences are present between concrete strain values, but the general development of the experimental curve is well captured by the theoretical one. Particularly, the transmission lengths in the two cases are very similar: the experimental reference value is equal to 502 mm, determined through the 95% AMS method as the

average between the "cut" and the "dead" end transmission length, while the analytical value is 561 mm (also derived by considering the 95% of the maximum strain).

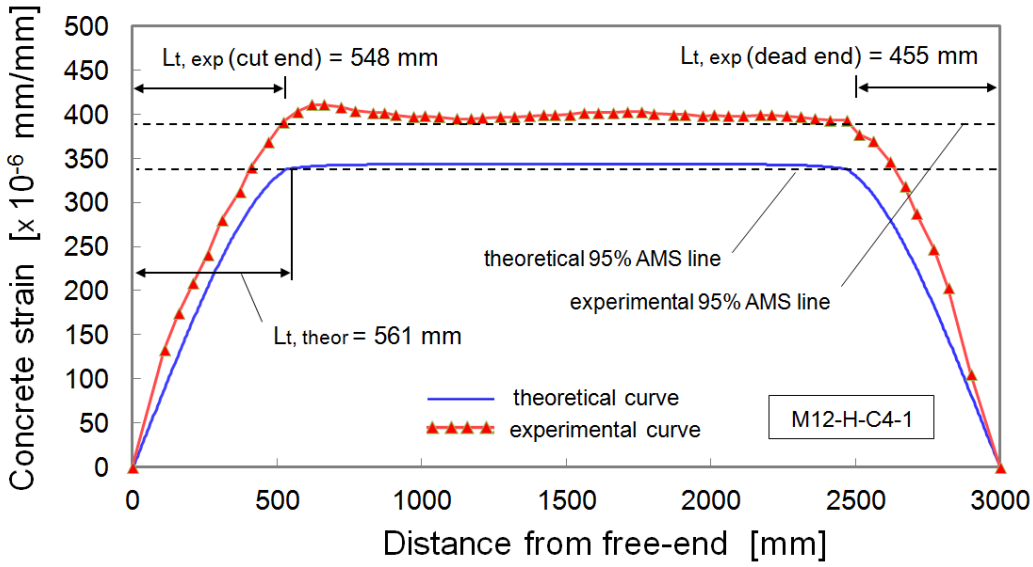

Figure 4-10: Comparison between experimental and theoretical concrete strain buildup profiles (μ = 0.6) for specimen M12-H-C4-1; experimental results are derived from [4-19].

4.3.4.2. Comparison with existing design formulations

The good accuracy of the transmission lengths calculated according to the TWC model, with anisotropic analysis of the concrete, is also demonstrated when results are compared to those arising from the formulations of the principal design codes. In Table 4-3 and Figure 4-11, the theoretical predictions obtained with the TWC model adopting a coefficient of friction μ = 0.6 are presented together with the provisions by ACI 318-14, *fib* Model Code 2010 and Eurocode 2, respectively, where the same reduced dataset of experimental transmission lengths measured on small-scale specimens is considered in place of the whole database. Average materials properties are assumed for the calculation in *fib* MC2010 and Eurocode 2.

However, in order to compare the results in a more compact way, a little modification is made in both these design formulas. Particularly, the evaluation of Eurocode 2 is accomplished without considering the shortening or enlargement of the transmission length to the lower or upper bound value. The same consideration is not possible with respect to *fib* MC2010, since the coefficient α_{p2} (representing the action effect to be verified) can not be disconnected to the whole formula. Thus, the analysis of *fib* MC2010 is carried out by considering α_{p2} = 0.75, which represent the average value

between the given bound levels for the verification of transverse stresses at release (α_{p2} = 0.5) and the calculation of anchorage length (α_{p2} = 1.0).

Table 4-3: Statistical indicators describing the performance of the TWC model and principal design codes.

Reference formulation	AVE	COV	RMSE
TWC model; μ = 0.6	1.07	0.18	139.20
ACI 318 (2014)	1.22	0.39	232.32
fib MC2010 (2013); α_{p2} = 0.75 average material properties	0.98	0.22	168.70
Eurocode 2 (2004); l_{pt} average material properties	0.95	0.22	172.75

AVE = average ratio between theoretical and experimental values; COV = coefficient of variation; RMSE = root mean square error

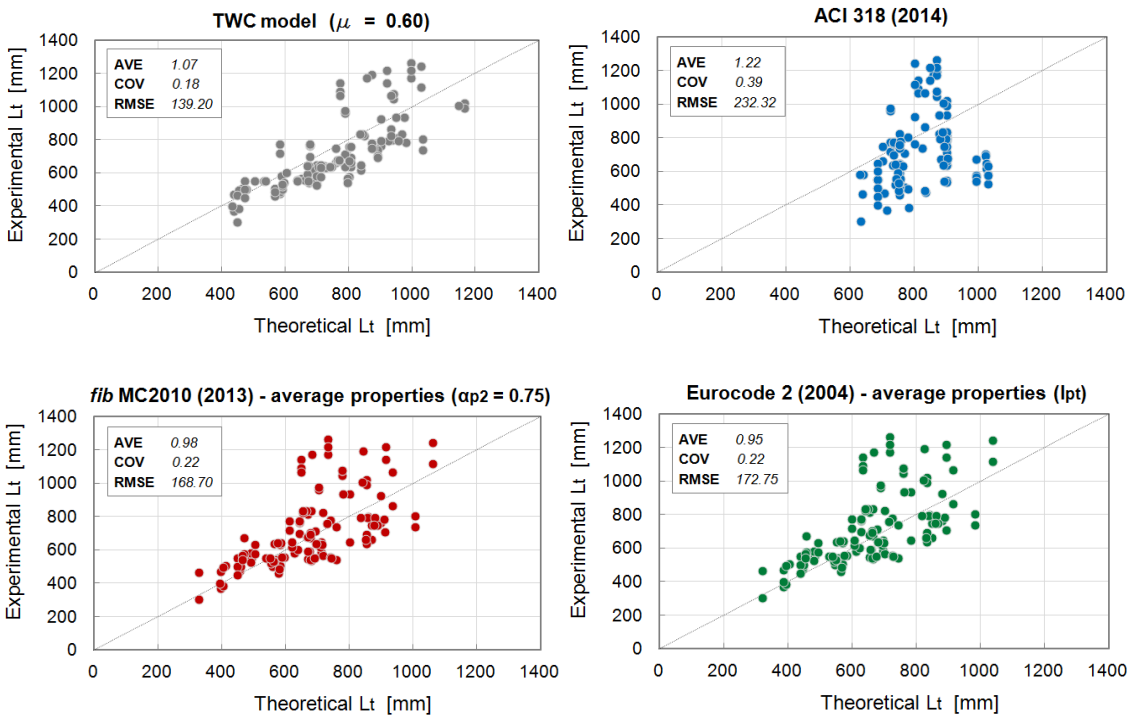

Figure 4-11: Comparison of the performance of the TWC model and main design code provisions when compared to the collected experimental results.

It can be seen that the data points exhibit the smaller scatter when described through the proposed model, with a coefficient of variation equal to 0.18. Instead, higher COVs are associated with all the other formulations, up to 0.39 in the case of ACI 318-14. Furthermore, the TWC formulation presents the lower value of root mean square error (139.20) when results are compared to the collected experimental tests, demonstrating

the overall good behaviour of the analytical model in replicating the measured transmission lengths. In this case, most of the data points are very close to the ideal dotted line. The RMSEs arising from ACI 318-14, *fib* MC2010 and Eurocode 2 are quite higher, describing weaker formulations. The average ratio between theoretical and experimental values is also very good when the TWC theory-based model is considered (AVE = 1.07), even though AVEs associated with *fib* MC2010 and Eurocode 2 are also close to 1.

4.3.4.3. Local behavior: radial cracking and bond stress development

The evolution of radial cracking along the transmission length of the same specimen M12-H-C4-1 [4-19], evaluated through the application of the TWC model, is shown in the following Figure 4-12. At the free-end section of the beam, the compressive stress $\sigma_r(r_{jack})$ at the interface between the concrete and the prestressing tendon is calculated to be around 55 MPa, when the elastic case is considered (Eq. 4-22). As a result, the circumferential tensile stress at the inner side of the concrete hollow cylinder, $\sigma_{c,\theta}(r_{jack})$, is estimated in approximately 57 MPa. For the analysed sample, such value is about 16 times larger than the concrete tensile strength at release, whose average value is equal to 3.43 MPa. Consequently, the concrete around the prestressing tendon experiences cracking in the radial direction. This means that the behaviour of the specimen must be studied according to the anisotropic model presented in section 4.3.3.

However, the magnitude of the strand expansion due to the Hoyer effect is not sufficient to allow radial cracking reaching the free outer surface of the concrete section. In fact, at the free-end of the specimen, the distance from the centroid of the tendon to the crack tip (r_{tip}, derived from Eq. 4-24) is calculated to be 35.5 mm, lower than the concrete cover thickness, equal to 46.4 mm. Then, moving towards the mid-span of the PC member, the increase in the tendon diameter due to the release of the prestressing-force becomes less significant, so that the interface pressure, the hoop stress and the extent of the radial cracking diminish progressively. At a certain distance from the free-end, i.e. just after 500 mm, the whole concrete section becomes uncracked and the transmission length is rapidly reached (561 mm) as a consequence of the larger confining stresses exerted by the surrounding concrete on the strand in the central region of the PC member.

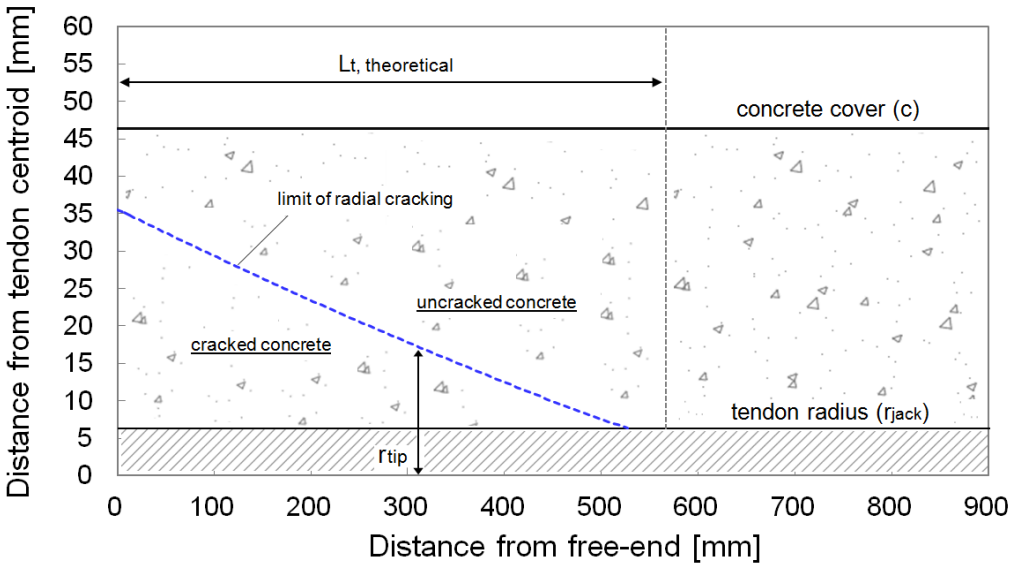

Figure 4-12: Development of the radial cracking along the length of specimen M12-H-C4-1 [4-19], evaluated with the TWC model and μ = 0.6.

In Figure 4-13, the theoretical bond stress distribution along the transmission length is also shown for the considered specimen. It can be seen that the maximum value of the bond strength developing at the interface surface between the strand and the surrounding concrete, evaluated in nearly 8 MPa, is registered in the proximity of the free-end of the member. Here, the compressive stresses on the concrete, triggered by the increase in the tendon diameter (i.e. the Hoyer effect), are relatively high. The bond stress value at any point along the tendon is proportional to the slope of the steel stress build-up curve (cfr. section 4.2.1.), depicted in red in Figure 4-13. Accordingly, bond decreases non-linearly as the transmission length of the PC specimen is approached. Then, once the transmission length is fully developed, the bond stress remains negligible.

A comparison with the bond strength values suggested by *fib* MC2010 and ACI 318-14 is worth to be mentioned. In the formulation of *fib* MC2010, the uniform bond stress f_{bp} (considering average material properties) at the interface steel-concrete after release is prescribed to be as in Eq. 4-30 (see also section 2.4.3.):

$$f_{bp} = \eta_{p1}\,\eta_{p2}\,f_{ct}(t) \tag{4-30}$$

where η_{p1} is a coefficient which takes into account the type of tendon (η_{p1} = 1.2 in the present case, i.e. for 7-wire strands) and η_{p2} is a factor considering the position of the tendon during concreting (η_{p2} = 1.0 is selected for good bond conditions). The average tensile strength of concrete at the time of the prestressing-force release $f_{ct}(t)$, as

mentioned, is equal to 3.43 MPa for specimen M12-H-C4-1. Thus, for *fib* MC2010, the prestressing-force is assumed to be transferred to the concrete by a constant bond strength equal to f_{bp} = 4.12 MPa.

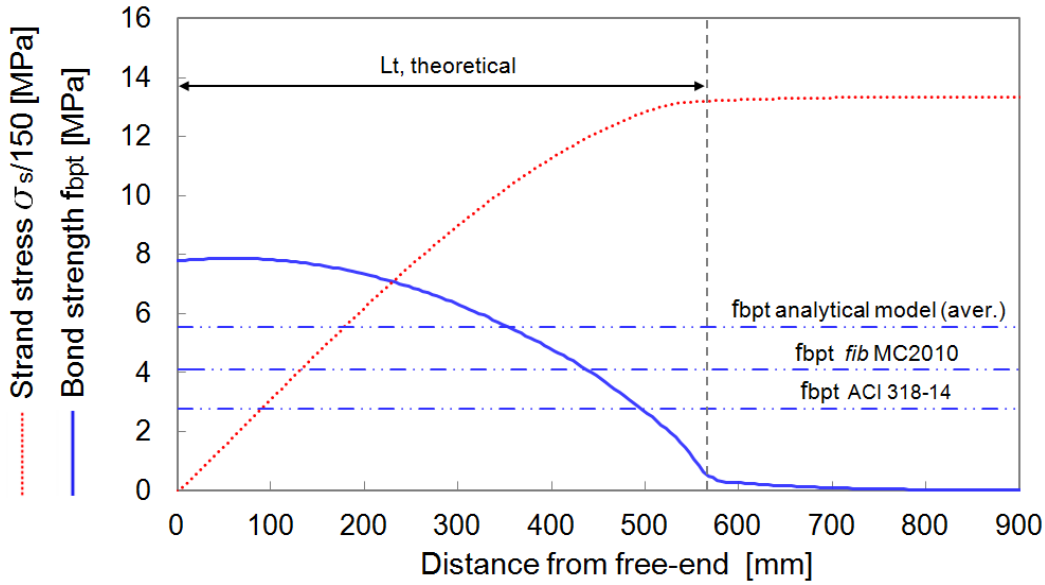

Figure 4-13: Bond stress distribution along the transmission length of specimen M12-H-C4-1 [4-19], evaluated with the TWC model (μ = 0.6) and principal design codes.

Conversely, according to the simple model of ACI 318-14, the value of the constant bond strength along the transmission length is fixed, and equal to 2.76 MPa (400 psi, see section 2.4.1.), which represents the average value obtained by Portland Cement Association (PCA), using steel Grade 250 for 7-wire strands.

On the other hand, if the area under the theoretical bond stress curve of Figure 4-13 is computed and divided by the analytical transmission length, an equivalent constant bond strength can also be obtained from the application of the TWC model. In this case, the value results to be 5.55 MPa, which is greater than the constant bond strength provided by both *fib* MC2010 and ACI 318-14. Particularly, the value recommended by ACI 318-14 is exactly twice the equivalent bond stress derived with the analytical model. It can be concluded that, for the considered PC specimen, the value of the bond strength prescribed by *fib* MC2010 or ACI 318-14 seems to under-estimate the effective bond stress that develops during prestressing-force release, thus resulting in longer transmission lengths.

4.3.5. Assessment of influencing parameters

The effect of many important parameters affecting the transmission length of prestressing tendons is explicitly taken into account by the presented analytical model. Specifically, concrete compressive strength at release, tendon diameter, concrete cover and tendon spacing greatly influence the bond characteristics at the interface between steel and concrete. In order to study the impact of such variables on the transmission length, a parametric analysis has been carried out based on the calibrated TWC model. Results are illustrated in the following paragraphs.

4.3.5.1. Effect of concrete compressive strength

Figure 4-14 presents the results of a parametric study conducted on a rectangular specimen (b=120 mm; h=170 mm) equipped with two strands of four different commonly adopted diameters (9.5, 12.7, 15.2, 18.0 mm). Strand spacing equal to 50 mm and concrete cover of 60 mm are considered, while strand stress at gradual release is set to 1400 MPa. A range of concrete compressive strength at release f_{ci}' from 20 to 120 MPa is investigated. It can be observed a dependence of the transmission length very close to $1/\sqrt{fci'}$, regardless of the strand diameter. In particular, as concrete compressive strength increases, the confining stresses on the strands get larger and the bond strength is improved, resulting in smaller transmission lengths. However, the effect of the concrete compressive strength is suggested to be very clear for concrete of low strength, becoming less pronounced for concrete of higher strength. These findings are in accordance with the evidences reported in section 3.4.2.

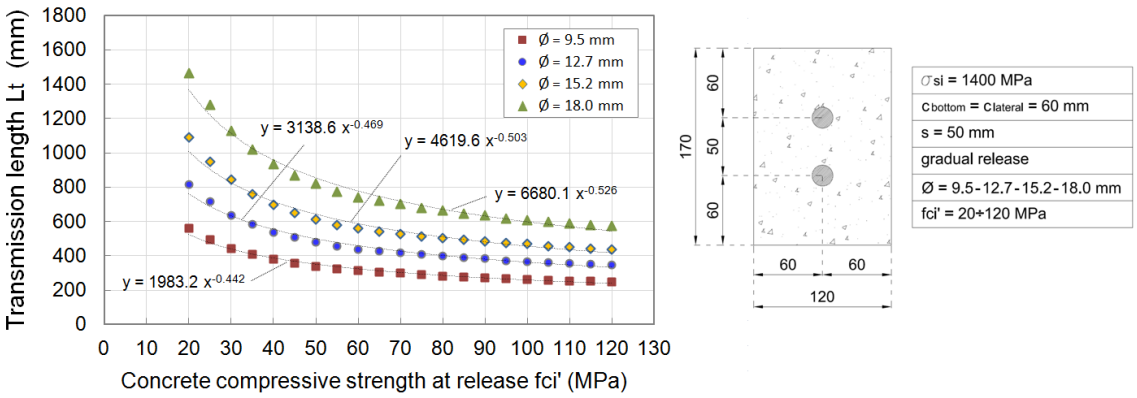

Figure 4-14: Effect of the concrete compressive strength at release on the transmission length.

4.3.5.2. Effect of tendon diameter

Little uncertainty is expressed in the principal design codes about the role of tendon diameter on the transmission length. ACI 318-14, *fib* MC2010 and Eurocode 2 are all

based on the assumption of constant bond strength along the transmission zone, regardless of the tendon size. This implies that the transmission length can be described as a linear function of the tendon diameter. Such behaviour is also confirmed by experimental campaigns conducted in the literature, which report longer transmission lengths as a result of an increase in the tendon diameter [4-19]. In Figure 4-15, the effect of tendon diameter is shown as resulting from the TWC model, considering a rectangular specimen (b=120 mm; h=170 mm) reinforced with two strands at a distance of 50 mm. Strand stress at gradual release is 1400 MPa and concrete cover is fixed to 60 mm. The parametric study is performed on four different concrete compressive strengths at release (25, 40, 55, 70 MPa), highlighting the same almost linear trend between strand diameter and transmission length.

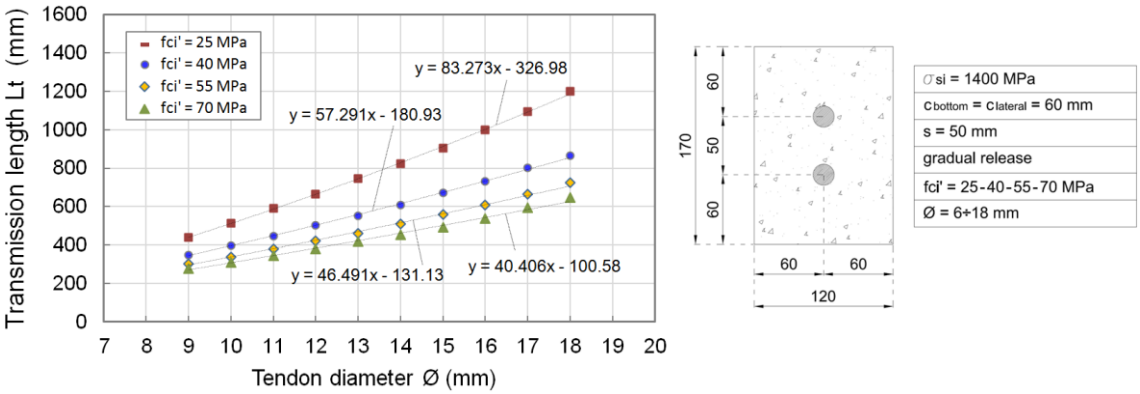

Figure 4-15: Effect of strand diameter on the transmission length.

4.3.5.3. Effect of concrete cover and tendon spacing

Appropriate detailing in the end regions of a PC member is required with regard to concrete cover and tendon spacing, which also play a remarkable role on the overall behaviour of the beam [4-5]. These variables should be such as to avoid cracking and localised bond failures at release. It is recalled that concrete cover and tendon spacing are not explicitly taken into account within current design code formulations. According to the developed TWC model, concrete cover and tendon spacing appear to have similar effects on the transmission length. Figure 4-16 shows the influence of concrete cover on the transmission length when considering different values of tendon spacing (40, 50 and 60 mm, respectively). The plot refers to a rectangular PC specimen (b=140 mm; h depending on concrete bottom cover), characterised by a concrete compressive strength at release of 35 MPa and equipped with two strands of diameter 12.7 mm. Strand stress at gradual release is 1400 MPa. An inverse correlation is highlighted, as the transmission length decreases quadratically as concrete cover increases. Nevertheless, it

can be seen that all selected strand spacing give similar transmission length values when considering large concrete cover thickness.

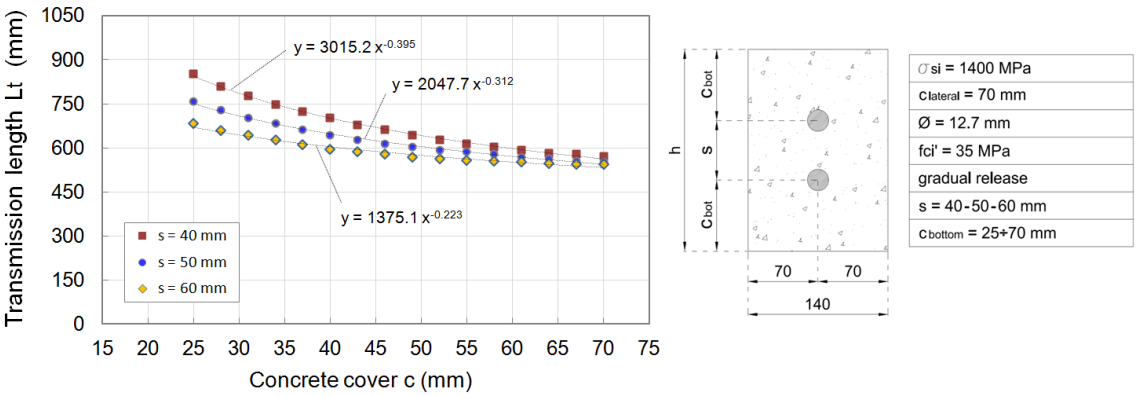

Figure 4-16: Effect of concrete cover thickness on the transmission length.

A similar trend is shown in Figure 4-17 for the dependence of the transmission length upon the strand spacing. The same twin-strand specimen, characterised by three different concrete cover values (35, 50 and 65 mm), has been analysed. However, the effect of tendon spacing on bond is found to be predominant for smaller values of concrete cover thickness, i.e. for c = 35 mm, where the increase in the distance between the strands results in a significant reduction of the transmission length. Conversely, for higher values of concrete cover, the increase in strand spacing produces only marginal variations of the transmission length, because of the development of sufficient confining stresses by the surrounding concrete (in this case the curve depicted in Figure 4-17 is almost horizontal).

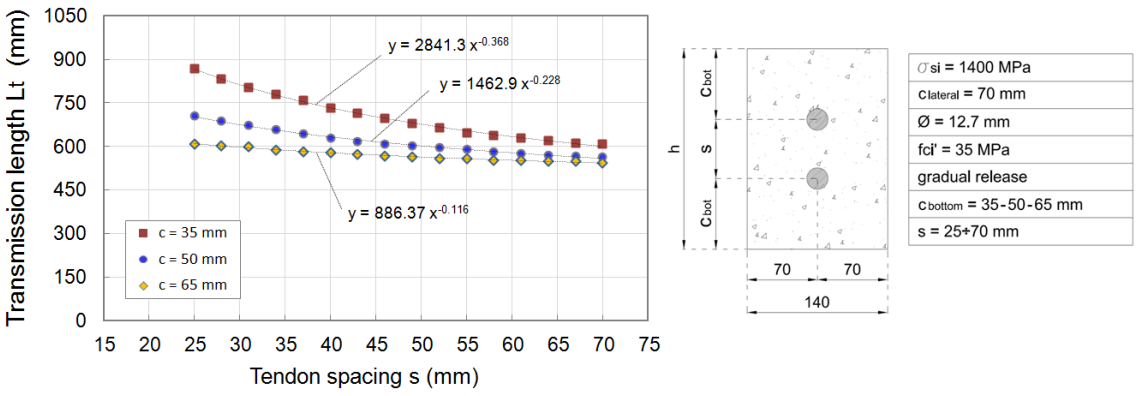

Figure 4-17: Effect of strand spacing on the transmission length.

4.4. Bond stress-slip model

The analytical model based on the theory of the thick-walled cylinders seems to provide promising results when describing the bond stress development and transmission length of PC members at the release of the prestressing-force. However, it might not be widely used for practical purposes, due to its complexity and time-consumption when applied to real cases. Thus, other types of models could actually be developed to reasonably characterise the distribution of the bond strength along the transmission length of PC members. One of the alternative theoretical approaches is represented by the bond stress-slip models, which describe the relationship of the bond stress and the slip between prestressing steel and concrete by means of appropriate functions. In fact, the variation in the tendon stress along the transmission length at release involves some slip between the strand and the concrete. The measurement of the tendon slip inside the concrete can be seen as an indirect method to determine the transmission length [4-22].

A first simple mathematical model relying on the measurement of the tendon slip is that proposed by Guyon [4-23], who described bond in the push-in situation of PC members through the expression of Eq. 4-31:

$$L_t = \alpha \frac{\delta}{\varepsilon_{si}} \tag{4-31}$$

where the transmission length L_t is determined as a function of the strand draw-in at the free-end (δ) and the initial strain of the tendon (ε_{si}). The shape coefficient α describes the functional form of the bond stress distribution along the transmission length, assuming two possible values indicating whether a constant bond stress (α = 2) or a linear descending distribution (α = 3). In the first hypothesis, the tendon stress is assumed to be linearly increasing along the transmission length, while in the second case the tendon stress is assumed to have a parabolic variation. Later, further proposals about the shape coefficient for the bond stress distribution have been suggested by other researchers, based on experimental and analytical studies. An exhaustive list of proposed values for α is present in [4-20], and it is hereunder reported in Table 4-4.

However, some problems can be encountered when determining the transmission length by means of the tendon end-slip. For instance, the difficulty in measuring small slips correctly, the excessive slips at the PC member free-end in the case of concrete with poor consolidation, or the breakage of strain gauges involved in the slip measurement [4-20].

Table 4-4: Proposed shape coefficient values (α) in the Guyon's formula.

Reference proposal	α value	Reference proposal	α value
FIP [4-24]	4.00	Logan [4-31]	2.00
FIP [4-25]	2.86	Oh and Kim [4-19]	2.00
Olesniewicz [4-26]	2.86	Rose and Russell [4-32]	2.00
Balàzs [4-27] *	2.67	Russell and Burns [4-7]	2.00
Den Uijl [4-9] **	2.60	Steinberg et al. [4-33]	2.00
Jonsson [4-28]	2.50	Wan et al. [4-34]	2.00
Balogh [4-29]	2.00	*fib* [4-35]	1.50
Brooks et al. [4-30]	2.00	Lopes and do Carmo [4-36]	1.50

* *for 12.7 mm 7-wire strands;* ** *maximum value.*

In the following of the section, the local behaviour at the interface between the tendon and surrounding concrete will be investigated according to a generalised bond stress-slip model, incorporating the effect of many important variables. Firstly, the governing equations will be presented based on common force equilibrium and strain compatibility, thus enabling the calculation of the transmission length. Secondly, the introduced bond stress-slip relationship will be calibrated through the use of collected experimental data. Finally, the model will be validated by comparing the predicted values of the transmission length to the experimental results.

4.4.1. General assumptions and governing equations

When describing the transmission of the prestressing-force to concrete through bond stress-slip models, general assumptions are usually made to express the bond stress distribution along the PC member. In the case presented in the following, as opposed to the analytical model based on the radial expansion of the tendon, an elastic behaviour of the PC member is assumed at release. This means that possible radial cracking of the concrete section in the vicinity of the tendon, due to the Hoyer effect, is actually neglected [4-37]. In addition, all the tendons in the cross-section are considered as one big tendon located in the original centroid, with equivalent characteristics (Figure 4-18).

Particularly, the equivalent external circumference ($C_{sp,eq}$) and cross-sectional area ($A_{sp,eq}$) of the prestressing steel can be computed as in Eqs. 4-32 and 4-33, respectively:

$$A_{sp,eq} = \sum_i n_{sp,i} A_{sp,i} \tag{4-32}$$

$$C_{sp,eq} = 4/3 \sum_i n_{sp,i} \pi \emptyset_i \tag{4-33}$$

where $n_{sp,i}$ identifies the number of prestressing tendons with identical diameter, while $\emptyset_i$ and $A_{sp,i}$ are the nominal diameter and cross-sectional area of the single tendon.

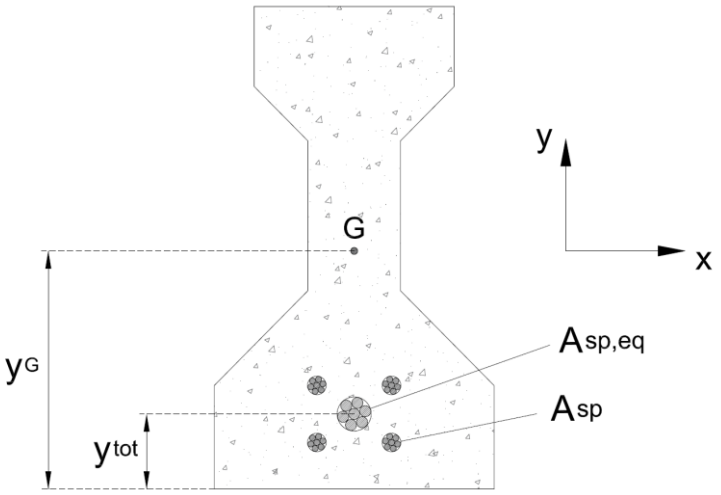

Figure 4-18: Equivalent PC member cross-section considering one big tendon.

At prestressing-force release, the bond stress distribution along the PC member can be formulated by means of the equilibrium equations and the longitudinal slip-strain compatibility. On one side, the equilibrium of moments on the concrete cross-section can be easily expressed as in Eq. 4-34:

$$M_c = N_s\,(y_G - y_{tot}) \tag{4-34}$$

being M_c the bending moment in the concrete section, N_s the axial force in the tendon (i.e. the prestressing-force), y_{tot} the distance from the tendon centroid to the concrete bottom fiber and y_G the ordinate identifying the position of the centre of gravity of the concrete section with respect to its bottom fiber (see also Figure 4-18). On the other side, selecting an infinitesimal element of the steel tendon, characterised by small length *dz* (Figure 4-19), the force equilibrium in the longitudinal direction can be written (neglecting the terms containing higher-order infinitesimal) as in Eq. 4-35, where f_{bpt} is the bond stress at the steel-concrete interface:

$$\frac{dN_s}{dz} = f_{bpt}\,C_{sp,eq} \tag{4-35}$$

Derivative of Eq. 4-34 and substitution of Eq. 4-35 produce the following expression:

$$\frac{dM_c}{dz} = f_{bpt}\,C_{sp,eq}\,(y_G - y_{tot}) \tag{4-36}$$

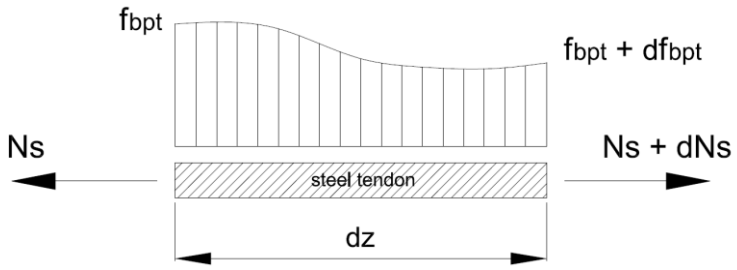

Figure 4-19: Force equilibrium of the infinitesimal element of the steel tendon.

Moreover, the strain difference between concrete and prestressing tendon can be related to the longitudinal slip between the materials, as in Eq. 4-37, representing the compatibility condition at the interface surface:

$$\varepsilon_{c,z} - \Delta\varepsilon_{s,z} = \frac{d\delta}{dz} \tag{4-37}$$

in which $\varepsilon_{c,z}$ is the concrete axial strain at the fiber in correspondence of the tendon centroid, $\Delta\varepsilon_{s,z}$ is the change in tendon strain after release and δ is the longitudinal slip of the strand to the concrete. In order to make explicit the relation in Eq. 4-37, it can be noted that the concrete strain at the level of the tendon is usually computed as:

$$\varepsilon_{c,z} = \frac{1}{E_c}\left[\frac{N_s}{A_c} + \frac{M_c\,(y_G - y_{tot})}{J_x}\right] \tag{4-38}$$

being E_c the elastic modulus of the concrete at the release, A_c the area of the concrete cross-section and J_x the moment of inertia of the concrete cross-section, respectively. Instead, the change in tendon strain after release arises from the following Eq. 4-39:

$$\Delta\varepsilon_{s,z} = \frac{1}{E_{ps}}\left(\frac{P - Ns}{A_{sp,eq}}\right) \tag{4-39}$$

where E_{ps} is the elastic modulus of the prestressing steel and P is the initial prestressing force in the tendon. Consequently, the derivative of Eq. 4-37 after substituting the expressions in Eqs. 4-38 and 4-39 gives:

$$\frac{d^2\delta}{dz^2} = \left(\frac{1}{E_c\,A_c} + \frac{1}{E_{ps}\,A_{sp,eq}}\right) f_{bpt}\,C_{sp,eq} + \\ + \frac{1}{E_c}\,\frac{(y_G - y_{tot})}{J_x}\,f_{bpt}\,C_{sp,eq}\,(y_G - y_{tot}) \tag{4-40}$$

To characterise the whole model, the relationship between the bond stress at the interface and the longitudinal slip between steel and concrete should be introduced alongside the equilibrium and compatibility equations. For this purpose, a power

function is commonly accepted in the literature [4-37; 4-38; 4-39]. Thus, the bond stress-slip relationship is formulated in the present model as reported in Eq. 4-41:

$$f_{bpt} = c_1 \chi \left(\frac{\delta}{\emptyset}\right)^{c_2} \tag{4-41}$$

Within this expression, the effect of the tendon size is explicitly taken into account by normalising the longitudinal slip δ to the strand diameter $\emptyset$, while the influence of the other fundamental parameters is contained in the so-called *influence function* χ, which will be discussed in the next section. Instead, c_1 and c_2 are model coefficients.

4.4.2. Transmission length determination

By considering the f_{bpt} - δ relationship (Eq. 4-41) in Eq. 4-40, the following second order differential equation can be found:

$$\frac{d^2\delta}{dz^2} - C_{sp,eq}\left[\left(\frac{1}{E_c A_c} + \frac{1}{E_{ps} A_{sp,eq}}\right) + \frac{1}{E_c}\frac{(y_G - y_{tot})^2}{J_x}\right]\frac{c_1 \chi}{\emptyset^{c_2}}\delta^{c_2} = 0 \tag{4-42}$$

whose solution enables the determination of the tendon slip at any point along the PC member [4-37]:

$$\delta(z) = A\,(L_t - z)^{\frac{2}{1-c_2}} \tag{4-43}$$

where z is the distance from the free-end and A is the following constant:

$$A = \left\{C_{sp,eq}\left[\left(\frac{1}{E_c A_c} + \frac{1}{E_{ps} A_{sp,eq}}\right) + \frac{1}{E_c}\frac{(y_G - y_{tot})^2}{J_x}\right]\frac{c_1 \chi}{\emptyset^{c_2}}\frac{(1-c_2)^2}{2(1+c_2)}\right\}^{\frac{1}{1-c_2}} \tag{4-44}$$

Therefore, the magnitude of the interface bond stresses along the tendon can be found directly from Eq. 4-41, considering the expression given in Eq. 4-43 for the longitudinal slip:

$$f_{bpt}(z) = \frac{c_1 \chi}{\emptyset^{c_2}} A^{c_2} (L_t - z)^{\frac{2c_2}{1-c_2}} \tag{4-45}$$

Finally, the transmission length of the (equivalent) prestressing tendon can be derived through integration of the bond stress distribution along the PC member. In fact, by integrating Eq. 4-45, the axial stress in the tendon (σ_s) is firstly evaluated as:

$$\sigma_s(z) = \sigma_{s,max} - B\,(L_t - z)^{\frac{1+c_2}{1-c_2}} \tag{4-46}$$

where $\sigma_{s,max}$ is the fully-effective strand stress (i.e. the maximum stress level after release, in correspondence of the plateau of the steel stress development curve, see Figure 2-1) and *B* represents the following constant:

$$B = \frac{1 - c_2}{1 + c_2} \frac{C_{sp,eq} \; A^{\,c_2}}{A_{sp,eq}} \frac{c_1 \, \chi}{\emptyset^{\,c_2}} \tag{4-47}$$

Then, the transmission length can be obtained noting that at the free-end of the PC member the prestress must be equal to zero, i.e. $\sigma_s(z = 0) = 0$. By setting such boundary condition in Eq. 4-46, the transmission length of the tendon is calculated as follows:

$$L_t = \alpha_{rel} \left(\frac{0.95 \, \sigma_{s,max}}{B}\right)^{\frac{1 - c_2}{1 + c_2}} \tag{4-48}$$

It should be recalled that the transmission length of a PC member is usually evaluated as the distance from the free-end to the point where concrete axial strain reaches 95% of the maximum strain (95% AMS method). Accordingly, the value of 0.95 $\sigma_{s,max}$ is actually considered in Eq. 4-48 in place of the fully-effective stress $\sigma_{s,max}$. Moreover, similarly to the bond-radial expansion model, the transmission length is assumed to be affected by a coefficient α_{rel}, taking into account the prestress release method and the free-end location. According to the evaluation in section 3.5.1., this factor can be taken as 1.0 in case of gradual release of the tendons or 1.3 when a sudden release is used (representing the average value between the factor for the "dead" end, i.e. α_{rel} = 1.25, and that for the "cut" end, i.e. α_{rel} = 1.35).

In order to derive the effective tendon stress after release ($\sigma_{s,max}$), to be considered in Eq. 4-48, it can be noted that the longitudinal slip of the tendon with respect to the concrete is accomplished within the transmission length (Figure 4-20).

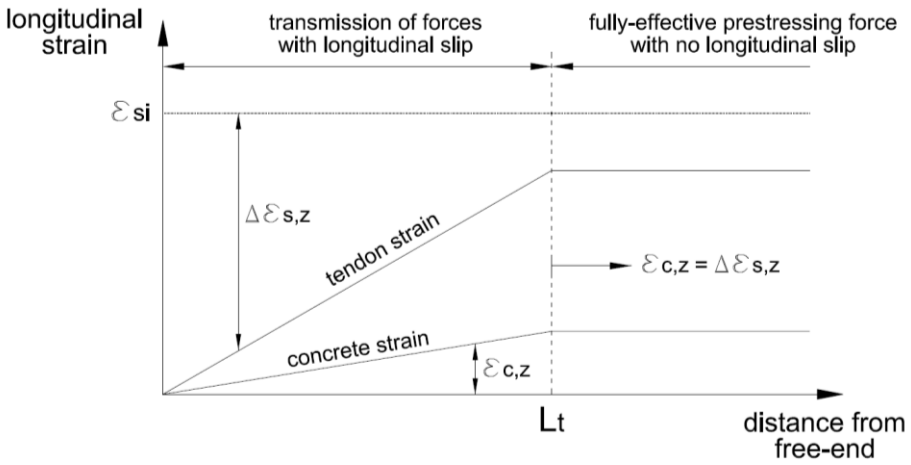

Figure 4-20: Idealised diagram of strain for steel and concrete.

Accordingly, for $z = L_t$, the change in tendon strain after prestress release should equal the overall strain in the concrete section, i.e. $\varepsilon_{c,z} = \Delta\varepsilon_{s,z}$. Such quantities are expressed by Eqs. 4-38 and 4-39, respectively. Hence, considering that $N_s = \sigma_{s,max}\, A_{sp,eq}$ once the transmission length is reached, the maximum strand stress towards the mid-span of the PC beam is found as in the following Eq. 4-49, being σ_{si} the initial jacking stress:

$$\sigma_{s,max} = \frac{(E_c\, \sigma_{si}) \,/\, (E_{ps}\, A_{sp,eq})}{1/A_c + E_c/(E_{ps}\, A_{sp,eq}) + (y_G - y_{tot})^2/J_x} \tag{4-49}$$

4.4.3. Determination of the influence function

The presented model is based on the bond stress-slip relationship formulated in Eq. 4-41, in which the effect of the primary variables affecting prestress transfer bond between the tendon and the surrounding concrete is considered within the influence function (χ). Particularly, the impact of concrete compressive strength at release, concrete cover thickness and tendon clear spacing is taken into consideration in the present case. It is recalled that the nominal tendon diameter is directly included in the f_{bpt} - δ expression, so that it will not affect the study of the influence function. The mathematical structure of the influence function can be established based on the laws of proportionality between the mentioned primary factors and the transmission length. Thus, the power function relationships highlighted for concrete strength, concrete cover and strand spacing through the parametric analysis presented in section 4.3.5. can be useful for this purpose. They can be represented in literal expressions as follows:

$$L_t \propto {f_{ci}}'^{\,-c_3} \tag{4-50 a}$$

$$L_t \propto c^{\,-c_4} \tag{4-50 b}$$

$$L_t \propto s^{\,-c_5} \tag{4-50 c}$$

where ${f_{ci}}'$ is the concrete compressive strength at the moment of prestress release, c is the concrete cover thickness and s is the clear spacing between tendons, while c_3, c_4 and c_5 are coefficients. However, it should be noted that a general relationship is also given in Eq. 4-48 between the transmission length and the influence function itself, being:

$$L_t \propto \chi^{\frac{-1}{1+c_2}} \tag{4-51}$$

Consequently, combining the dependence in Eq. 4-51 with Eqs. 4-50 and normalising concrete cover and tendon spacing to the tendon diameter, the following association can be made:

$$\chi \propto (f_{ci}')^{c_3(1+c_2)} \tag{4-52 a}$$

$$\chi \propto \left(\frac{c}{\emptyset}\right)^{c_4(1+c_2)} \tag{4-52 b}$$

$$\chi \propto \left(\frac{s}{\emptyset}\right)^{c_5(1+c_2)} \tag{4-52 c}$$

Therefore, the influence function can be developed by joining together such single relationships, as reported in Eq. 4-53. In this way, the bond stress distribution along the PC member (and thus the transmission length) is described as a function of five model coefficients (from c_1 to c_5), as in Eq. 4-54.

$$\chi = (f_{ci}')^{c_3(1+c_2)} \left(\frac{c}{\emptyset}\right)^{c_4(1+c_2)} \left(\frac{s}{\emptyset}\right)^{c_5(1+c_2)} \tag{4-53}$$

$$f_{bpt} = c_1 (f_{ci}')^{c_3(1+c_2)} \left(\frac{c}{\emptyset}\right)^{c_4(1+c_2)} \left(\frac{s}{\emptyset}\right)^{c_5(1+c_2)} \left(\frac{\delta}{\emptyset}\right)^{c_2} \tag{4-54}$$

The major advantage of such a generalised approach is that the bond stress-slip relationship can be calibrated by incorporating the effects of as many influencing parameters as wanted. In the presented case, the impact of concrete compressive strength at release, concrete cover and tendon spacing (in addition to the tendon diameter) is included in the model.

4.4.4. Determination of optimal model coefficients

The optimal values of the model coefficients (c_1, c_2, c_3, c_4, c_5), which enable the characterisation of the bond stress-slip expression and the subsequent evaluation of the transmission length, could be derived, for instance, from push-in tests. In principle, experimental tests would be able to capture the influence of the different primary variables on the interface bond stress. Alternatively, in the present case the calibration process has been accomplished based on the same experimental dataset of transmission length values considered for the previous TWC model (section 4.3.4.). In particular, the optimised coefficients of the governing parameters are found so as to minimise the differences between the transmission lengths measured in the literature and those predicted by the f_{bpt} - δ model for the various test setup. It is recalled that the serviceable database used for calibration of the TWC model comprises a total number of 130 small-scale specimens, where the average values between the transmission length measured at the "cut end" and at the "dead end" are taken. However, it was decided to

randomly consider only the 75% of the whole dataset in this calibration phase, so that to allocate the remaining 25% of the collected data for the model validation.

In order to implement the described approach for model calibration, the following *performance function* (*f*), representing the overall deviation between theoretical and experimental values, should be minimised:

$$f(c_1,c_2,c_3,c_4,c_5) = \frac{\sum_{i=1}^{n_{tot}} (L_{t\,exp,i} - L_{t\,theor,i})^2}{\sum_{i=1}^{n_{tot}} {L_{t\,exp,i}}^2} \tag{4-55}$$

where $L_{t\,exp,i}$ is the experimental value of the transmission length, $L_{t\,theor,i}$ is the value of the transmission length predicted by the present model and n_{tot} is the total number of data points considered for the calibration (i.e. 98 data points, corresponding to 75% of the whole dataset).

Many iterative algorithms of different complexity and accuracy can actually be adopted to minimise the performance function $f(c_1,c_2,c_3,c_4,c_5)$ in Eq. 4-55. In the context of this work, the solution of the problem is achieved by using the Quasi-Newton method, which involves using the first derivatives of the performance function. It should be noted that the described minimisation problem can be written as follows:

$$df(c_1,c_2,c_3,c_4,c_5) = \frac{\partial f}{\partial c_1} + \frac{\partial f}{\partial c_2} + \frac{\partial f}{\partial c_3} + \frac{\partial f}{\partial c_4} + \frac{\partial f}{\partial c_5} = 0 \tag{4-56}$$

which can be reasonably assumed to be equivalent to the following writing (Eq. 4-57):

$$\begin{cases} \frac{\partial f}{\partial c_1} = F_1(c_1,c_2,c_3,c_4,c_5) = 0 \\ \frac{\partial f}{\partial c_2} = F_2(c_1,c_2,c_3,c_4,c_5) = 0 \\ \frac{\partial f}{\partial c_3} = F_3(c_1,c_2,c_3,c_4,c_5) = 0 \\ \frac{\partial f}{\partial c_4} = F_4(c_1,c_2,c_3,c_4,c_5) = 0 \\ \frac{\partial f}{\partial c_5} = F_5(c_1,c_2,c_3,c_4,c_5) = 0 \end{cases} \tag{4-57}$$

or, in compact form:

$$\boldsymbol{F}(c_1,c_2,c_3,c_4,c_5) = \boldsymbol{0} \tag{4-58}$$

The Quasi-Newton method is a numerical method that uses a sequence of appropriate matrixes to approximate the Jacobian matrix at each iteration, which might be very expensive to be calculated exactly. Particularly, the Broyden's approach is considered in the following, approximating the Jacobian with the matrix described in Eq. 4-59 (where *k* plays the role of an iteration counter):

$$\boldsymbol{J}_{k+1} = \boldsymbol{J}_k + \frac{(\boldsymbol{y}_{k+1} - \boldsymbol{J}_k \boldsymbol{s}_k)\, \boldsymbol{s}_k^T}{\boldsymbol{s}_k^T \boldsymbol{s}_k} \tag{4-59}$$

where $\boldsymbol{J}$ describes the Broyden's matrix, $\boldsymbol{s}$ is the difference between the values of model coefficients at different iterations and $\boldsymbol{y}$ is the difference between the first derivatives of the function to be minimised at different iterations (see the following expressions):

$$\boldsymbol{y}_{k+1} = \boldsymbol{F}_{k+1}(c_1, c_2, c_3, c_4, c_5) - \boldsymbol{F}_k(c_1, c_2, c_3, c_4, c_5) \tag{4-60}$$

$$\boldsymbol{s}_k = \boldsymbol{C}_{k+1} - \boldsymbol{C}_k \tag{4-61}$$

being $\boldsymbol{C} = (c_1, c_2, c_3, c_4, c_5)^T$. Thus, starting from proper initial values of the model coefficients (i.e. an appropriate $\boldsymbol{C}_1$) and a suitable Broyden's matrix (i.e. $\boldsymbol{J}_1$), the whole Quasi-Newton algorithm incorporating the Broyden's approach can be outlined as follows:

$$\boldsymbol{J}_k \boldsymbol{s}_k = -\boldsymbol{F}_k(c_1, c_2, c_3, c_4, c_5) \tag{4-62}$$

$$\boldsymbol{C}_{k+1} = \boldsymbol{C}_k + \boldsymbol{s}_k \tag{4-63}$$

$$\boldsymbol{y}_{k+1} = \boldsymbol{F}_{k+1}(c_1, c_2, c_3, c_4, c_5) - \boldsymbol{F}_k(c_1, c_2, c_3, c_4, c_5) \tag{4-64}$$

$$\boldsymbol{J}_{k+1} = \boldsymbol{J}_k + \frac{(\boldsymbol{y}_{k+1} - \boldsymbol{J}_k \boldsymbol{s}_k)\, \boldsymbol{s}_k^T}{\boldsymbol{s}_k^T \boldsymbol{s}_k} \tag{4-65}$$

Such iterative algorithm has been implemented with Matlab® and repeated until convergence, i.e. until the difference between the values of the model coefficients at the *k+1* iteration and at the *k* iteration was small enough. The Broyden's matrix for the first step was selected as the identity matrix ($\boldsymbol{J}_1 = \boldsymbol{I}$). Instead, the initial values of the model coefficients were selected on the basis of the dependence relationships between the transmission length and its primary variables highlighted in section 4.3.5. Specifically, the vector $\boldsymbol{C} = (0.2, 0.2, 0.5, 0.4, 0.4)^T$ has been considered as input.

In this way, after a suitable number of steps, the optimised coefficients of the bond stress-slip model reported in Table 4-5 have been determined from the application of the Broyden's algorithm. The main statistical indicators (AVE, COV, RMSE) of the calibrated model are also listed in Table 4-5.

Table 4-5: Optimised values of the bond stress-slip model coefficients.

c_1	c_2	c_3	c_4	c_5	AVE	COV	RMSE
0.191	0.122	0.689	0.582	0.380	1.05	0.21	145.35

AVE = average ratio between theoretical and experimental values;
COV = coefficient of variation; RMSE = root mean square error

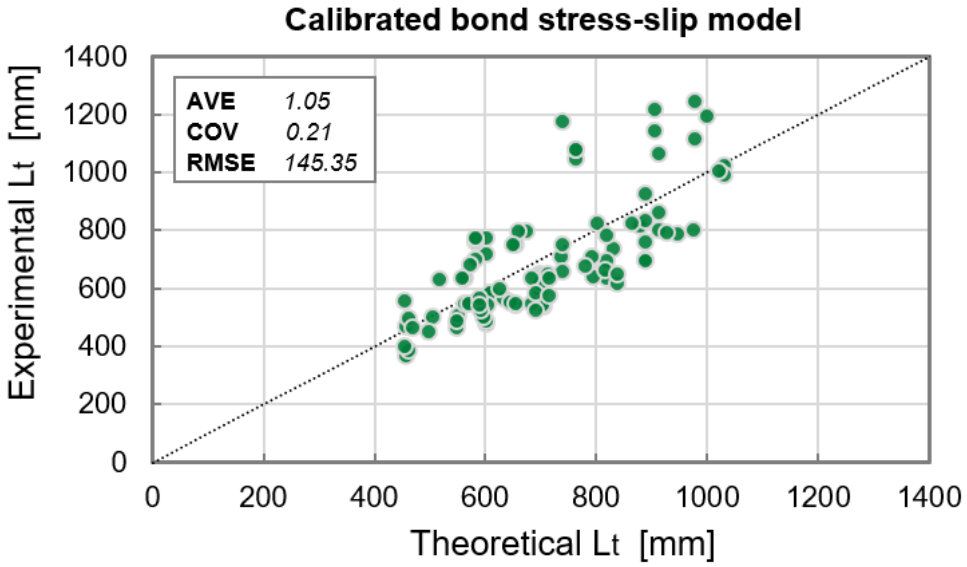

Figure 4-21: Comparison between experimental and theoretical transmission length values after calibration of the bond stress-slip model.

4.4.5. Model validation and results discussion

After calibration of the coefficients c_1, c_2, c_3, c_4, c_5 governing the bond stress-slip relationship, the whole model has been validated using the 25% of the data not considered within the optimisation procedure, i.e. the remaining 32 small-scale specimens. Again, the accuracy of the calibrated f_{bpt} - δ model has been assessed by correlating the theoretical transmission length values, predicted for the various specimen configuration, with the corresponding experimental results.

In Figure 4-22, the performance of the developed bond stress-slip model (in the top left) is presented in comparison with that of the TWC model (in the top right). The evaluation of the formulations provided by *fib* MC2010 (with α_{p2} = 0.75), Eurocode 2 (with respect to the basic value l_{pt}) and ACI 318-14 is also illustrated for comparison purposes when considering the same data points. In this case, average properties of the materials are taken. The accuracy of the different models is also described through the use of statistical indicators, as summarised in Table 4-6.

Table 4-6: Statistical indicators describing the performance of the developed analytical models, in comparison with the principal design recommendations.

Reference formulation	AVE	COV	RMSE
Calibrated bond stress-slip model	1.13	0.23	131.43
TWC model; $\mu = 0.6$	1.11	0.20	122.42
fib MC2010 (2013); $\alpha_{p2} = 0.75$ average material properties	0.92	0.25	147.86
Eurocode 2 (2004); l_{pt} average material properties	0.89	0.27	156.41
ACI 318 (2014)	1.24	0.34	195.40

AVE = average ratio between theoretical and experimental values;
COV = coefficient of variation; RMSE = root mean square error

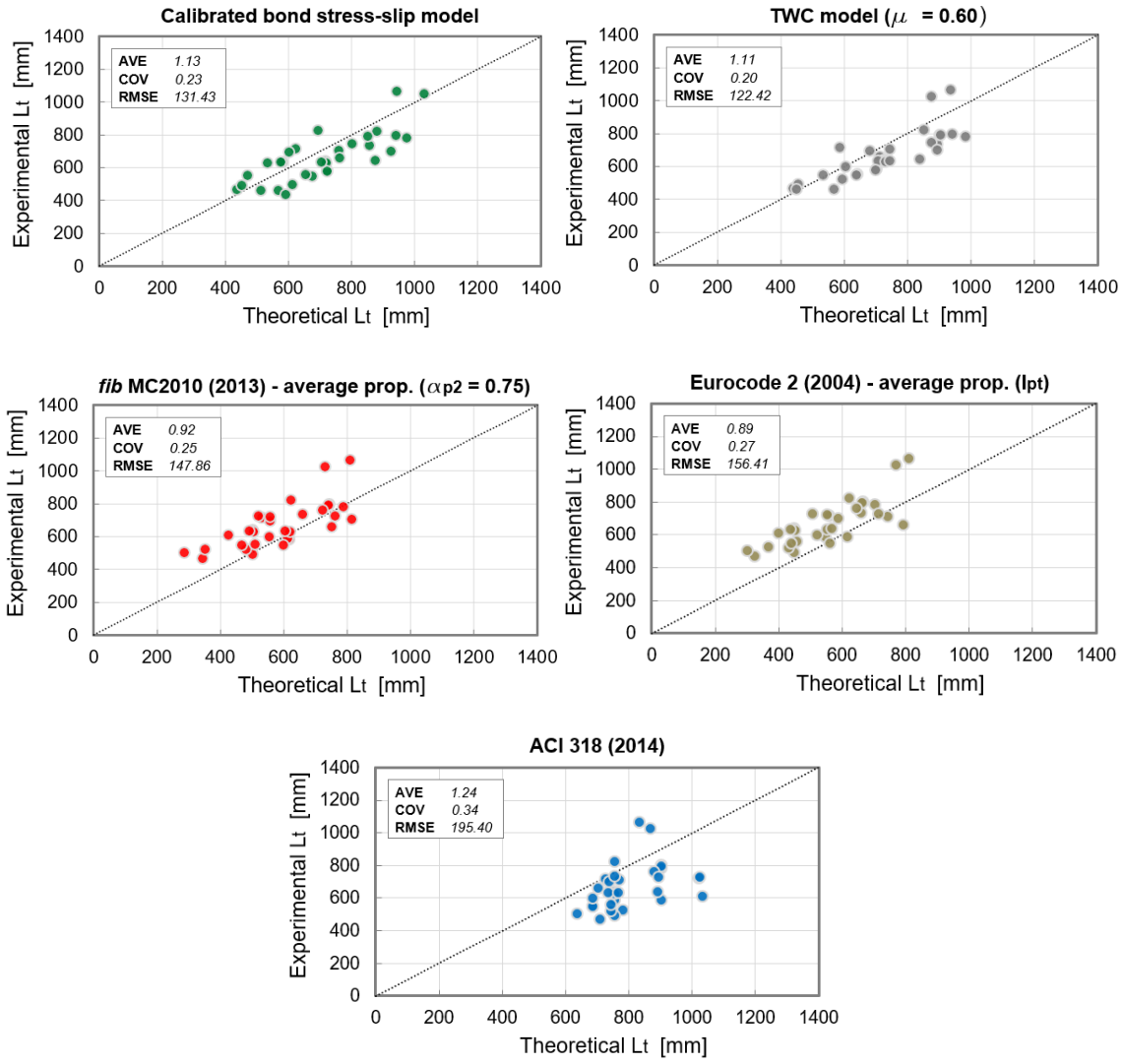

Figure 4-22: Graphical comparison of the results of the developed theoretical models and main design code provisions.

It can be noted that the overall performance of the calibrated bond stress-slip model is comparable with that of the previous bond stress-radial expansion model (i.e. the TWC model). In both cases, the estimated transmission lengths are generally in good agreement with the values measured in the literature, being the data points in the vicinity of the diagonal ideal line. The root mean square errors in the two situations are similar (RMSE = 131.43 for the bond stress-slip model and RMSE = 122.42 for the TWC model, that actually remains slightly better), as well as the good values of AVE and COV. On the other hand, the current design code formulations prove to be less effective in predicting the real transmission length values of the considered PC member configurations. *fib* MC2010 and Eurocode 2, presenting similar performance, show a point cloud where most of the data points are above the ideal line, and in fact the RMSEs are higher (147.86 and 156.41, respectively). An even weaker formulation is described by ACI 318-14, which is associated to the worst values of AVE, COV and RMSE. In this case, the data points are quite far from the "experimental vs predicted" L_t line, demonstrating the poor fit of the predicted transmission lengths with the collected experimental data.

The effectiveness of the calibrated bond stress-slip model is also shown in Figure 4-23, where the concrete strain buildup curve resulting for the 12.7 mm mono-strand test specimen "M12-H-C4-1" from Oh and Kim [4-19] is depicted in green. In the same picture, the concrete strain profiles arising from both the TWC model (μ = 0.6) and the experimental measurements are also reported (see also 4.3.4.1.).

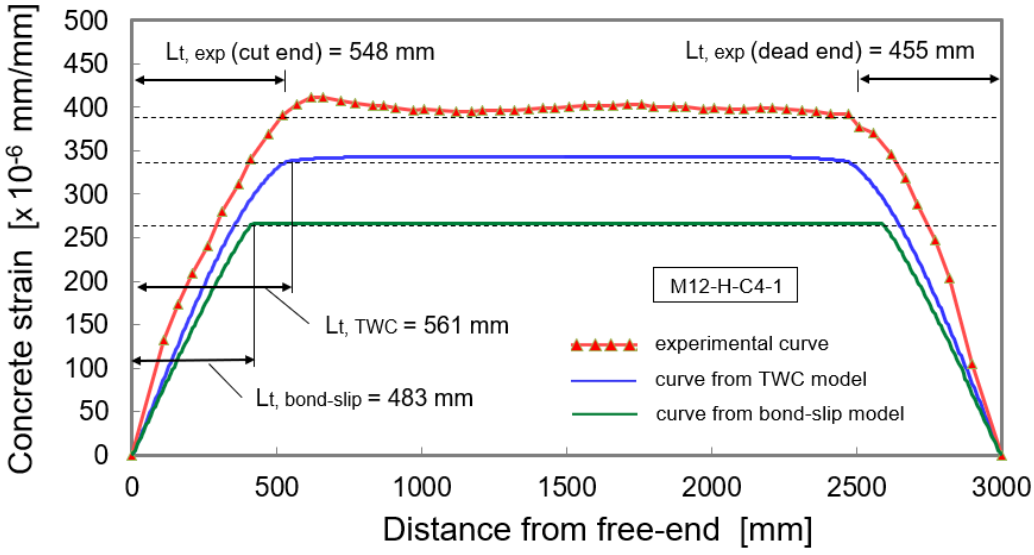

Figure 4-23: Concrete strain profiles obtained from both the developed analytical models and experimental measurements for specimen M12-H-C4-1 from [4-19].

It can be seen that concrete strain values predicted by the f_{bpt} - δ model are lower than those described by the other two curves, especially with reference to the experimental profile. Particularly, the difference in the maximum strain (at mid-span) is evident, being equal to about 270x10^6 mm/mm in the case of the bond stress-slip model and nearly 400x10^6 mm/mm in the case of the experimental curve, respectively. Such discrepancy between concrete strain values can be attributed to several causes, which may have influence on the whole model. For instance, it should be noted that the experimental database of transmission lengths considered for calibration and validation of the model encompasses only 45 multi-strand specimens out of 130 (see Annex C), i.e. it provides limited information about the tendon spacing. This can lead to approximate estimation of the optimal values of the model coefficients, especially with regard to the parameter c_5 associated to the tendon spacing. Also, the role of the different primary variables on the interface bond stress might be studied through specific push-in tests, which can improve the calibration process and thus the bond stress-slip expression. However, the general shape of the concrete strain distribution along the PC specimen depicted in Figure 4-23 is adequately described and the transmission length is in accordance with the measured value. In fact, the transmission length evaluated with the bond stress-slip model is equal to 483 mm, while the experimental reference value results to be 502 mm, as arising from the average between the "cut" and the "dead" end transmission length.

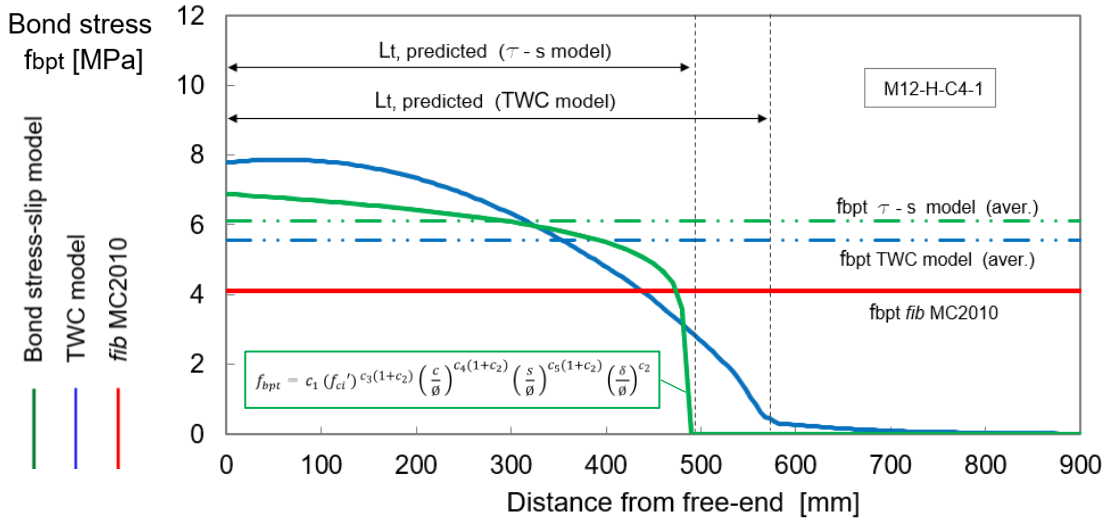

Figure 4-24: Evolution of bond stresses along the transmission length of specimen M12-H-C4-1 [4-19], arising from the analytical models and fib MC2010.

In Figure 4-24, the development of the bond stresses along the transmission zone is illustrated for the same specimen "M12-H-C4-1" [4-19]. Here, the distribution arising

from the bond stress-slip model is similar to that predicted with the TWC model. In both cases, the maximum bond strength at the interface surface is registered near the free-end of the PC member, and the values are comparable. Nevertheless, a slightly different internal behaviour is described by the bond stress-slip model in that the bond stress distribution presents an almost horizontal branch, suddenly dropping just before the transmission length is reached (L_t = 483 mm). However, the average bond strength values are also very similar for the two situations, being equal to 6.11 MPa (for the bond stress-slip model) and 5.55 MPa (for the TWC model), respectively.

In any case, both the resulting bond stress distributions are completely different from the uniform bond strength suggested by *fib* MC2010, in this case equal to 4.12 MPa (see Eq. 4-30). Such value is less than the average bond stresses computed with the bond stress-slip model (6.11 MPa) and the TWC model (5.55 MPa), thus resulting in a longer transmission length for specimen "M12-H-C4-1".

4.5. Conclusions

In the present chapter, the analytical modelling of the transmission length in PC members has been addressed, aimed at investigating the development of bond strength at the interface between the tendon and the concrete. For this purpose, two different theoretical models have been introduced. A first elastic approach is presented according to the pioneering study of Janney (1954) on steel wires. However, large radial pressures are exerted on the concrete as a result of the tendon expansion at the prestressing-force release. Thus, in order to take into account possible radial cracking of the concrete around the tendon, a more refined theory has been considered, incorporating the softening behaviour of concrete in tension. Such model, based on the Thick-Walled Cylinders (TWC) theory, considers the steel tendon as an internal solid cylinder and the surrounding concrete section as an external hollow cylinder. In this way, the interface pressure - and hence the bond stress - is derived from the equilibrium of the cracked concrete section, through the use of a proper friction coefficient. The model calibration has shown that a coefficient of friction of 0.6 gives the best fit with experimental results.

Then, a second analytical investigation has been carried out by describing the correlation between the bond stress and the longitudinal slip of tendon on concrete. In this respect, a generic power function has been introduced and calibrated so as to minimize the discrepancy between predicted and experimental transmission lengths, on

the basis of a comprehensive database collected from the literature. The major advantage of this generalized approach is that the bond stress-slip relationship can be derived incorporating the effect of as many influencing parameters as wanted. In the present case, tendon diameter, tendon spacing, concrete strength and concrete cover have been considered as primary variables.

Comparison with experimental evidences has shown the capability of the developed analytical models to adequately simulate the bond behaviour during transmission of the prestressing-force to the concrete. The following main findings have been highlighted:

- The transmission lengths predicted by the calibrated models are generally in good agreement with the measured values collected from the literature, where the typical concrete strain development along the PC member is well described. The overall performance of the theoretical models is comparable, and seems to be better than that of the formulations suggested by the existing design codes. It is thought that consideration of such analytical models could provide a sound and improved design of PC members detailing;
- Both calibrated models suggest that the prestressing-force is transferred to the concrete by a non-linear distribution of the interface bond strength along the transmission length. For the analysed case, a maximum value of the bond stress has been found in the proximity of the free-end of the member, and a non-linear decrease is registered as the transmission length is approached. This situation is in contrast to the uniform distribution assumed by all current design codes, which seems to under-estimate the effective bond strength at the interface steel-concrete, thus resulting in longer transmission length values.

References

[4-1] Pellegrino, C., Faleschini, F., Fabris, N. and Zanini, M.A. (2018). "Bond of prestressing tendons". Internal report, Submitted to: *fib Bulletin on "Advances on Bond in Concrete"*, University of Padova, Italy.

[4-2] Mohandoss, P., Pillai, R.G. and Sengupta, A.K. (2018). "Transmission length of pretensioned concrete systems - comparison of codes and test data". *Magazine of Concrete Research*, vol. 71(17), 1-13.

[4-3] Janney, J.R. (1954). "Nature of bond in pretensioned prestressed concrete". *ACI Journal*, vol. 50(9), 717-736.

[4-4] Oh, B.H., Kim, E.S. and Choi, Y.C. (2006). "Theoretical analysis of transfer lengths in pretensioned prestressed concrete members". *Journal of Engineering Mechanics,* vol. 132(10), 1057-1066.

[4-5] den Uijl, J. (1995). "Transfer length of prestressing strand in HPC". *Progress in Concrete Research*, vol. 4, 75-90.

[4-6] Han, S. J., Lee, D. H., Cho, S. H., Ka, S. B. and Kim, K. S. (2016). "Estimation of transfer lengths in precast pretensioned concrete members based on a modified thick-walled cylinder model". *Structural Concrete*, vol. 17(1), 52-62.

[4-7] Russell, B.W. and Burns, N.H. (1996). "Measured transfer lengths of 0.5 and 0.6 in. Strands in pretensioned concrete". *Journal of Structural Engineering*, vol. 123(5), 44-65.

[4-8] Tepfers, R. (1979). "Cracking of concrete cover along anchored deformed reinforcing bars". *Magazine of Concrete Research*, vol. 31(106), 3-12.

[4-9] den Uijl, J. (1998). "Bond modelling of prestressing strand". *ACI Special Publication 180*, 145-169.

[4-10] Abdelatif, A. O., Owen, J. S. and Hussein, M. F. (2015). "Modelling the prestress transfer in pre-tensioned concrete elements". *Finite Elements in Analysis and Design*, vol. 94, 47-63.

[4-11] Han, S. J., Lee, D. H., Kim, K. S., Seo, S.Y., Moon, J. and Monteiro, P.J. (2014). "Degradation of flexural strength in reinforced concrete members caused by steel corrosion". *Construction and Building Materials*, vol. 54(1), 572-583.

[4-12] Martins, J.A.C. and Oden, J.T. (1985). "Interface models, variational principles and numerical solutions for dynamic friction problems". *Mechanics of Material Interfaces - Proceedings of ASCE/ASME Mechanics Conference*, June 23-26, Albuquerque, NM, United States.

[4-13] Baltay, P. and Gjelsvik, A. (1990). "Coefficient of friction for steel on concrete at high normal stress". *Journal of Materials in Civil Engineering*, vol. 2(1), 46-49.

[4-14] Olofsson, U. and Holmgren, M. (1992). "Friction measurement at low sliding speed using a servo-hydraulic tension-torsion machine". Report SP AR 1992:51, Swedish National Testing Institute - Building Structures Section, Stockholm, Sweden.

[4-15] Arab, A.A., Badie, S.S. and Manzari, A. (2011). "A methodological approach for finite element modelling of pretensioned concrete members at the release of pretensioning". *Engineering Structures*, vol. 33(6), 1918-1929.

[4-16] Cousins, T.E., Johnston, D.W. and Zia, P. (1990). "Transfer length of epoxy-coated prestressing strand". *ACI Materials Journal,* vol. 87(3), 193-203.

[4-17] Mitchell, D., Cook, W.D., Kahn, A.A. and Tham, T. (1993). "Influence of High-Strength concrete on transfer and development length of pretensioning strand". *PCI Journal*, vol. 38(3), 52-66.

[4-18] Russell, B.W. and Burns, N.H. (1997). "Measurement of transfer lengths on pretensioned concrete elements". *PCI Journal,* vol. 41(5), 541-549.

[4-19] Oh, B.H. and Kim, E.S. (2000). "Realistic evaluation of transfer lengths in pretensioned prestressed concrete members". *ACI Structural Journal*, vol. 97(6), 821-830.

[4-20] Martì-Vargas, J.R., Arbeláez, C.A., Serna-Ros, P. and Castro-Bugallo, C. (2007). "Reliability of transfer length estimation from strand end slip". *ACI Structural Journal,* vol. 104(4), 487-494.

[4-21] Dang, C.N., Hale, W.M. and Martì-Vargas, J.R. (2017). "Assessment of transmission length of prestressing strands according to *fib* Model Code 2010". *Engineering Structures,* vol. 147, 425-433.

[4-22] Thorsen, N. (1956). "Use of large tendons in pretensioned concrete". *ACI Journal,* vol. 53(6), 649-659.

[4-23] Guyon, Y. (1953). "Pretensioned concrete: theoretical and experimental study". Paris, France, 711 pp.

[4-24] FIP (1982). "Report on prestressing steel: 7. Test for the determination of tendon transfer length under static conditions". Fédération Internationale de la Précontrainte (FIP), London, UK.

[4-25] FIP (1978). "Report on prestressing steel: 2. Anchorage and application of pretensioned 7-wire strands". Fédération Internationale de la Précontrainte (FIP), London, UK.

[4-26] Olesniewicz, A. (1975). "Statistical evaluation of transfer length of strand". Research report, Research and Design Centre for Industrial Building (BISTYP), Warsaw, Poland.

[4-27] Balàzs, G. (1993). "Transfer length of prestressing strand as a function of draw-in and initial prestress". *PCI Journal,* vol. 38(2), 86-93.

[4-28] Jonsson, E. (1992). "Anchorage of strands in prestressed extruded hollow-core slabs". *Proceedings of the International Symposium of Bond in Concrete: From Research to Practise,* Riga, Latvia.

[4-29] Balogh, T. (1992). "Statistical distribution of draw-in of seven-wire strands". *Proceedings of the International Symposium of Bond in Concrete: From Research to Practise,* Riga, Latvia.

[4-30] Brooks, M.D., Gerstle, K.H. and Logan, D.R. (1988). "Effect of initial strand slip on the strength of hollow-core slabs". *PCI Journal,* vol. 33(1), 90-111.

[4-31] Logan, D.R. (1997). "Acceptance criteria for bond quality of strand for pretensioned prestressed concrete applications". *PCI Journal,* vol. 42(2), 52-90.

[4-32] Rose, D.R. and Russell, B.W. (1997). "Investigation of standardised tests to measure the bond performance of prestressing strand". *PCI Journal,* vol. 42(4), 56-80.

[4-33] Steinberg, E., Beier, J.T. and Sargand, S. (2001). "Effects of sudden prestress force transfer in pretensioned concrete beams". *PCI Journal,* vol. 46(1), 64-75.

[4-34] Wan, B., Harries, K.A. and Petrou, M.F. (2002). "Transfer length of strands in prestressed concrete piles". *ACI Structural Journal,* vol. 99(5), 577-585.

[4-35] *fib* (2000). "Bond of reinforcement in concrete: state-of-art report". International Federation for Structural Concrete (*fib*), Bulletin d'Information, no. 10, Lausanne, Switzerland.

[4-36] Lopes, S.M. and do Carmo, R.N. (2002). “Bond of prestressed strands to concrete: transfer rate and relationship between transfer length and tendon draw-in”. *Structural Concrete,* vol. 3(3), 117-126.

[4-37] Deng, Y., Morcous, G. and Ma, Z.J. (2016). “Strand bond stress-slip relationship for prestressed concrete members at prestress release”. *Materials and Structures,* vol. 49(3), 889-903.

[4-38] Balàzs, G.L. (1992). “Transfer control of prestressing strands”. *PCI Journal,* vol. 37(6), 60-71.

[4-39] Dang, C.N., Floyd, R.W., Murray, C.D., Hale, W.M. and Martì-Vargas, J.R. (2015). “Bond stress-slip model for 0.6 in. (15.2 mm) diameter strand”. *ACI Structural Journal,* vol. 112(5), 625-634.

5. CONCLUSIONS

The extensive use of pretensioned, prestressed-concrete (PC) in the modern structural applications makes in the foreground the need for a correct bond development between the prestressing tendons and the surrounding concrete. Bond in PC members acts fundamentally in two situations. During production, it is responsible for the transmission of the prestressing-force to the concrete at the release operation. Then, during the service life of the beam, bond is crucial for anchoring the tendon stress to the concrete due to application of external loads. The correct determination of the transmission length and anchorage length of prestressing tendons is a key point for achieving a good detailing, especially in the end regions of the element. In the last decades, the study of pre-tensioning anchorage has been addressed in many research projects. However, the current knowledge is ambiguous and the topic seems to be open and still under discussion, especially within *fib* Task Group 2.5 on "Bond and Material Models", in which the author is involved.

This contribution aimed to investigate both practical and theoretical aspects on the pre-tensioning anchorage. Particular attention was paid to the evaluation of the existing design formulations and the development of analytical models describing the complex bond mechanisms governing the force transmission between steel and concrete. In the first part of the thesis, the state of the art on pre-tensioning anchorage was provided. The essential terminology was introduced and the nature of bond in the transmission and anchorage length of prestressing tendons was accurately described. Subsequently, an exhaustive overview of the commonly used experimental tests to evaluate both transmission and anchorage length was presented and discussed. Then, the existing code provisions were illustrated and compared.

The second part of the thesis was devoted to the general assessment of the current design formulations on prestressing tendons. Here, disagreeing predictions of the fundamental lengths were observed when the main standard codes are applied to the same structural configuration, due to discrepancies in the considered influencing parameters. Thus, the accuracy of the suggested relationships was investigated in detail by applying them to a comprehensive experimental database of transmission length and anchorage length values, collected from the literature. A total number of 742 data points from 21 scientific studies was included, spanning over a great variety of primary variables. Results highlighted how the evaluation of both transmission length and,

especially, anchorage length of PC members is not always acceptable, as the theoretical predictions do not always fit well the experimental evidences. This is because the calculation provided by some guidelines (such as ACI 318-14 or AASHTO) is based on a small number of influencing factors. In other models (such as *fib* MC2010 or Eurocode 2), although a larger set of variables is included in the formulation, the effect of some of them seems not completely understood yet. For this reason, the role of the major parameters affecting the transmission length was studied based on the analysis of the collected database. Particularly, tendon diameter, concrete strength, initial prestress level, tendon surface condition and release type were found to have a significant effect on the transmission length. According to such evaluation, a proposal of modification of current *fib* MC2010 was advanced in view of a possible revision of the design formulations on pre-tensioning anchorage in the 2020 version.

For practical purpose, simplified bond stress distributions at the steel-concrete interface after release are assumed by all common design codes, even though they do not reflect the real internal behaviour of PC members. Therefore, in the third part of the work, the analytical modelling of the transmission length was addressed, on the basis of some pioneering studies carried out on this topic. In this context, two different theoretical models were introduced. A first elastic approach to study the introduction of the prestressing-force to the concrete was presented according to the Thick-Walled Cylinders (TWC) theory. In this case, the interface bond stress was derived as a function of the radial pressure given by the tendon expansion at release, through the use of a proper friction coefficient. However, in order to take into account possible cracking of the concrete around the tendon, a more refined anisotropic theory was developed, incorporating the softening behaviour of concrete in tension. The calibration of the model showed that a coefficient of friction of 0.6 gives the best fit with experimental results. Then, a second analytical investigation was carried out by describing the correlation between the bond stress and the longitudinal slip of tendon on concrete. To characterize the bond stress-slip relationship, a generic power function was introduced and calibrated so as to minimize the discrepancy between predicted and experimental transmission lengths. In this way, the effect of tendon diameter, tendon spacing, concrete strength and concrete cover was considered in the formulation. Comparison with experimental evidences demonstrated the capability of both the developed analytical models to adequately simulate the bond behaviour at the steel-concrete interface during force transmission. Specifically, a non-linear evolution of the bond stresses was highlighted along the transmission length. It is thought that consideration

of such models can provide a sound and better design of PC members detailing. Furthermore, they might also be employed as validation tools in view of a possible revision of the existing design code formulations.

6. FUTURE DEVELOPMENTS

On the basis of the research findings presented in this thesis, a number of additional investigations in the area of pre-tensioning anchorage could be carried out in future works, to further improve the quality of the design of prestressed-concrete members.

First of all, an experimental campaign aiming at evaluating the separated effect of each single influencing parameter on the bond properties at the steel-concrete interface is worth considering, thus expanding the collected dataset of transmission and anchorage length. In this framework, new methods involving smart tendons with embedded fiber optic sensors could be adopted to increase the accuracy of the strain measurement along the member. Particularly, the results of the tests might be used for a different calibration of the theoretical models developed within this work. For instance, the coefficients governing the whole bond stress-slip model could be optimised through the development of specific push-in tests, able to characterize the relationships between the bond stress and the primary variables. This could enable a more accurate representation of the strain field in the concrete.

Furthermore, it might be considered the possibility to include in the proposed analytical models the contribution of additional variables which may affect the behavior of PC members in the transmission zone. Among these, the effect of corrosion on both linear and nonlinear properties of concrete can be investigated, with the aim of evaluating the bond degradation within existing elements, such as bridge girders, located in aggressive environments. Also, the study of the time-dependent effects on the concrete strength development might be of relevance for taking into account the variation of bond resistance along the tendon over time, due to the inelastic behavior of the surrounding concrete.

Another issue of significant importance for the design of PC members concerns the bond behavior of prestressing tendons under cycling loading. It should be noted that there is currently a lack of knowledge about fatigue-related effects on the quality of bond, where very few studies are reported in the literature. In this context, the analytical modelling of the anchorage length of beams also subject to cycling loading could be addressed, on the basis of the theoretical investigation already performed in this thesis for the transmission length. The deterioration of the flexural bond with the number of load cycles, as well as the interaction with the prestress transfer bond in the end regions of the member, is thought to be a relevant topic to be studied in future works.

ANNEX A

TRANSMISSION LENGTH DATABASE

Author	Specimen ID	Φ [mm]	f_{su} [MPa]	f_{si} [MPa]	f_{se} [MPa]	f_c' [MPa]	f_{ci}' [MPa]	b [mm]	h [mm]	c [mm]	s [mm]	Surface condition	Epoxy coating	Release type	L_t [mm]
Over and Au (1965)	1	12.7	1862.0	1172.2	1031.5	51.9	37.9	76.2	76.2	38.1	-	S	UN	G	889.0
Over and Au (1965)	2	9.5	1862.0	1103.2	970.8	39.5	28.8	76.2	76.2	38.1	-	S	UN	G	762.0
Over and Au (1965)	3	6.4	1862.0	1130.8	995.1	46.3	33.8	76.2	76.2	38.1	-	S	UN	G	508.0
Over and Au (1965)	4	6.4	1862.0	1323.8	1165.0	44.6	32.5	76.2	76.2	38.1	-	S	UN	G	736.6
Cousins et al. (1990)	T3UN-A	9.5	1862.0	1400.3	1263.1	34.5	27.6	88.9	88.9	44.5	-	S	UN	G	660.4
Cousins et al. (1990)	T3UN-B	9.5	1862.0	1400.3	1263.1	34.5	27.6	88.9	88.9	44.5	-	S	UN	G	896.6
Cousins et al. (1990)	T3UN-C	9.5	1862.0	1400.3	1263.1	34.5	27.6	88.9	88.9	44.5	-	S	UN	G	914.4
Cousins et al. (1990)	T3UN-D	9.5	1862.0	1400.3	1263.1	34.5	27.6	88.9	88.9	44.5	-	S	UN	G	1066.8
Cousins et al. (1990)	S3UN-A	9.5	1862.0	1400.3	1263.1	34.5	27.6	101.6	152.4	50.8	-	S	UN	S	863.6
Cousins et al. (1990)	S3UN-B	9.5	1862.0	1400.3	1263.1	34.5	27.6	101.6	152.4	50.8	-	S	UN	S	863.6
Cousins et al. (1990)	S3UN-C	9.5	1862.0	1400.3	1263.1	34.5	27.6	101.6	152.4	50.8	-	S	UN	S	965.2
Cousins et al. (1990)	S3UN-D	9.5	1862.0	1400.3	1263.1	34.5	27.6	101.6	152.4	50.8	-	S	UN	S	965.2
Cousins et al. (1990)	S3UN-E	9.5	1862.0	1400.3	1263.1	34.5	27.6	101.6	152.4	50.8	-	S	UN	S	914.4
Cousins et al. (1990)	S3UN-F	9.5	1862.0	1400.3	1263.1	34.5	27.6	101.6	152.4	50.8	-	S	UN	S	965.2
Cousins et al. (1990)	S3UN-G	9.5	1862.0	1400.3	1263.1	34.5	27.6	101.6	152.4	50.8	-	S	UN	S	965.2
Cousins et al. (1990)	S3UN-H	9.5	1862.0	1400.3	1263.1	34.5	27.6	101.6	152.4	50.8	-	S	UN	S	965.2
Cousins et al. (1990)	F3UN-A	9.5	1862.0	1400.3	1263.1	34.5	27.6	101.6	152.4	50.8	-	S	UN	S	762.0
Cousins et al. (1990)	F3UN-B	9.5	1862.0	1400.3	1263.1	34.5	27.6	101.6	152.4	50.8	-	S	UN	S	762.0
Cousins et al. (1990)	F3UN-C	9.5	1862.0	1400.3	1263.1	34.5	27.6	101.6	152.4	50.8	-	S	UN	S	660.4
Cousins et al. (1990)	F3UN-D	9.5	1862.0	1400.3	1263.1	34.5	27.6	101.6	152.4	50.8	-	S	UN	S	660.4
Cousins et al. (1990)	T3CM-A	9.5	1862.0	1400.3	1276.9	34.5	27.6	88.9	88.9	44.5	-	S	CM	G	330.2
Cousins et al. (1990)	T3CM-B	9.5	1862.0	1400.3	1276.9	34.5	27.6	88.9	88.9	44.5	-	S	CM	G	279.4
Cousins et al. (1990)	T3CM-C	9.5	1862.0	1400.3	1276.9	34.5	27.6	88.9	88.9	44.5	-	S	CM	G	381.0
Cousins et al. (1990)	T3CM-D	9.5	1862.0	1400.3	1276.9	34.5	27.6	88.9	88.9	44.5	-	S	CM	G	330.2
Cousins et al. (1990)	S3CM-A	9.5	1862.0	1400.3	1276.9	34.5	27.6	101.6	152.4	50.8	-	S	CM	S	406.4
Cousins et al. (1990)	S3CM-B	9.5	1862.0	1400.3	1276.9	34.5	27.6	101.6	152.4	50.8	-	S	CM	S	406.4
Cousins et al. (1990)	S3CM-C	9.5	1862.0	1400.3	1276.9	34.5	27.6	101.6	152.4	50.8	-	S	CM	S	355.6

Author	Specimen ID	Φ [mm]	f_{su} [MPa]	f_{si} [MPa]	f_{se} [MPa]	f_c' [MPa]	f_{ci}' [MPa]	b [mm]	h [mm]	c [mm]	s [mm]	Surface condition	Epoxy coating	Release type	L_t [mm]
Cousins et al. (1990)	S3CM-D	9.5	1862.0	1400.3	1276.9	34.5	27.6	101.6	152.4	50.8	-	S	CM	S	406.4
Cousins et al. (1990)	F3CM-A	9.5	1862.0	1400.3	1276.9	34.5	27.6	101.6	152.4	50.8	-	S	CM	S	304.8
Cousins et al. (1990)	F3CM-B	9.5	1862.0	1400.3	1276.9	34.5	27.6	101.6	152.4	50.8	-	S	CM	S	406.4
Cousins et al. (1990)	F3CM-C	9.5	1862.0	1400.3	1276.9	34.5	27.6	101.6	152.4	50.8	-	S	CM	S	254.0
Cousins et al. (1990)	F3CM-D	9.5	1862.0	1400.3	1276.9	34.5	27.6	101.6	152.4	50.8	-	S	CM	S	457.2
Cousins et al. (1990)	T5UN-E	12.7	1862.0	1410.7	1248.6	34.5	27.6	101.6	101.6	50.8	-	S	UN	S	1879.6
Cousins et al. (1990)	T5UN-F	12.7	1862.0	1410.7	1248.6	34.5	27.6	101.6	101.6	50.8	-	S	UN	S	1371.6
Cousins et al. (1990)	T5UN-G	12.7	1862.0	1410.7	1248.6	34.5	27.6	101.6	101.6	50.8	-	S	UN	S	1625.6
Cousins et al. (1990)	T5UN-H	12.7	1862.0	1410.7	1248.6	34.5	27.6	101.6	101.6	50.8	-	S	UN	S	1473.2
Cousins et al. (1990)	S5UN-A	12.7	1862.0	1410.7	1248.6	34.5	27.6	127.0	203.2	63.5	-	S	UN	S	1244.6
Cousins et al. (1990)	S5UN-B	12.7	1862.0	1410.7	1248.6	34.5	27.6	127.0	203.2	63.5	-	S	UN	S	1193.8
Cousins et al. (1990)	S5UN-C	12.7	1862.0	1410.7	1248.6	34.5	27.6	127.0	203.2	63.5	-	S	UN	S	1447.8
Cousins et al. (1990)	S5UN-D	12.7	1862.0	1410.7	1248.6	34.5	27.6	127.0	203.2	63.5	-	S	UN	S	1498.6
Cousins et al. (1990)	S5UN-E	12.7	1862.0	1410.7	1248.6	34.5	27.6	127.0	203.2	63.5	-	S	UN	S	1244.6
Cousins et al. (1990)	S5UN-F	12.7	1862.0	1410.7	1248.6	34.5	27.6	127.0	203.2	63.5	-	S	UN	S	1600.2
Cousins et al. (1990)	S5UN-G	12.7	1862.0	1410.7	1248.6	34.5	27.6	127.0	203.2	63.5	-	S	UN	S	1244.6
Cousins et al. (1990)	S5UN-H	12.7	1862.0	1410.7	1248.6	34.5	27.6	127.0	203.2	63.5	-	S	UN	S	1143.0
Cousins et al. (1990)	S5UN-I	12.7	1862.0	1410.7	1248.6	34.5	27.6	127.0	203.2	63.5	-	S	UN	S	1168.4
Cousins et al. (1990)	S5UN-J	12.7	1862.0	1410.7	1248.6	34.5	27.6	127.0	203.2	63.5	-	S	UN	S	1117.6
Cousins et al. (1990)	F5UN-A	12.7	1862.0	1410.7	1248.6	34.5	27.6	127.0	203.2	63.5	-	S	UN	S	965.2
Cousins et al. (1990)	F5UN-B	12.7	1862.0	1410.7	1248.6	34.5	27.6	127.0	203.2	63.5	-	S	UN	S	965.2
Cousins et al. (1990)	F5UN-C	12.7	1862.0	1410.7	1248.6	34.5	27.6	127.0	203.2	63.5	-	S	UN	S	812.8
Cousins et al. (1990)	F5UN-D	12.7	1862.0	1410.7	1248.6	34.5	27.6	127.0	203.2	63.5	-	S	UN	S	1117.6
Cousins et al. (1990)	F5UN-E	12.7	1862.0	1410.7	1248.6	34.5	27.6	127.0	203.2	63.5	-	S	UN	S	1295.4
Cousins et al. (1990)	F5UN-F	12.7	1862.0	1410.7	1248.6	34.5	27.6	127.0	203.2	63.5	-	S	UN	S	838.2
Cousins et al. (1990)	T5CL-A	12.7	1862.0	1356.9	1219.7	34.5	27.6	101.6	101.6	50.8	-	S	CL	G	584.2
Cousins et al. (1990)	T5CL-B	12.7	1862.0	1356.9	1219.7	34.5	27.6	101.6	101.6	50.8	-	S	CL	G	825.5

Author	Specimen ID	Φ [mm]	f_{su} [MPa]	f_{si} [MPa]	f_{se} [MPa]	f_c' [MPa]	f_{ci}' [MPa]	b [mm]	h [mm]	c [mm]	s [mm]	Surface condition	Epoxy coating	Release type	L_t [mm]
Cousins et al. (1990)	T5CL-C	12.7	1862.0	1356.9	1219.7	34.5	27.6	101.6	101.6	50.8	-	S	CL	G	685.8
Cousins et al. (1990)	T5CL-D	12.7	1862.0	1356.9	1219.7	34.5	27.6	101.6	101.6	50.8	-	S	CL	G	533.4
Cousins et al. (1990)	S5CL-A	12.7	1862.0	1356.9	1219.7	34.5	27.6	127.0	203.2	63.5	-	S	CL	S	762.0
Cousins et al. (1990)	S5CL-B	12.7	1862.0	1356.9	1219.7	34.5	27.6	127.0	203.2	63.5	-	S	CL	S	787.4
Cousins et al. (1990)	S5CL-C	12.7	1862.0	1356.9	1219.7	34.5	27.6	127.0	203.2	63.5	-	S	CL	S	990.6
Cousins et al. (1990)	S5CL-D	12.7	1862.0	1356.9	1219.7	34.5	27.6	127.0	203.2	63.5	-	S	CL	S	533.4
Cousins et al. (1990)	T5CM-A	12.7	1862.0	1436.2	1275.5	34.5	27.6	101.6	101.6	50.8	-	S	CM	G	431.8
Cousins et al. (1990)	T5CM-B	12.7	1862.0	1436.2	1275.5	34.5	27.6	101.6	101.6	50.8	-	S	CM	G	381.0
Cousins et al. (1990)	S5CM-A	12.7	1862.0	1436.2	1275.5	34.5	27.6	127.0	203.2	63.5	-	S	CM	S	584.2
Cousins et al. (1990)	S5CM-B	12.7	1862.0	1436.2	1275.5	34.5	27.6	127.0	203.2	63.5	-	S	CM	S	482.6
Cousins et al. (1990)	S5CM-C	12.7	1862.0	1436.2	1275.5	34.5	27.6	127.0	203.2	63.5	-	S	CM	S	482.6
Cousins et al. (1990)	S5CM-D	12.7	1862.0	1436.2	1275.5	34.5	27.6	127.0	203.2	63.5	-	S	CM	S	584.2
Cousins et al. (1990)	S5CM-E	12.7	1862.0	1436.2	1275.5	34.5	27.6	127.0	203.2	63.5	-	S	CM	S	431.8
Cousins et al. (1990)	S5CM-F	12.7	1862.0	1436.2	1275.5	34.5	27.6	127.0	203.2	63.5	-	S	CM	S	330.2
Cousins et al. (1990)	S5CM-G	12.7	1862.0	1436.2	1275.5	34.5	27.6	127.0	203.2	63.5	-	S	CM	S	355.6
Cousins et al. (1990)	S5CM-H	12.7	1862.0	1436.2	1275.5	34.5	27.6	127.0	203.2	63.5	-	S	CM	S	558.8
Cousins et al. (1990)	S5CM-I	12.7	1862.0	1436.2	1275.5	34.5	27.6	127.0	203.2	63.5	-	S	CM	S	685.8
Cousins et al. (1990)	S5CM-J	12.7	1862.0	1436.2	1275.5	34.5	27.6	127.0	203.2	63.5	-	S	CM	S	635.0
Cousins et al. (1990)	F5CM-A	12.7	1862.0	1436.2	1275.5	34.5	27.6	127.0	203.2	63.5	-	S	CM	S	482.6
Cousins et al. (1990)	F5CM-B	12.7	1862.0	1436.2	1275.5	34.5	27.6	127.0	203.2	63.5	-	S	CM	S	431.8
Cousins et al. (1990)	F5CM-C	12.7	1862.0	1436.2	1275.5	34.5	27.6	127.0	203.2	63.5	-	S	CM	S	355.6
Cousins et al. (1990)	F5CM-D	12.7	1862.0	1436.2	1275.5	34.5	27.6	127.0	203.2	63.5	-	S	CM	S	457.2
Cousins et al. (1990)	T5CH-A	12.7	1862.0	1356.9	1214.2	34.5	27.6	101.6	101.6	50.8	-	S	CH	G	330.2
Cousins et al. (1990)	T5CH-B	12.7	1862.0	1356.9	1214.2	34.5	27.6	101.6	101.6	50.8	-	S	CH	G	330.2
Cousins et al. (1990)	T5CH-C	12.7	1862.0	1356.9	1214.2	34.5	27.6	101.6	101.6	50.8	-	S	CH	G	482.6
Cousins et al. (1990)	T5CH-D	12.7	1862.0	1356.9	1214.2	34.5	27.6	101.6	101.6	50.8	-	S	CH	G	495.3
Cousins et al. (1990)	S5CH-A	12.7	1862.0	1356.9	1214.2	34.5	27.6	127.0	203.2	63.5	-	S	CH	S	482.6

Author	Specimen ID	Φ [mm]	f_{su} [MPa]	f_{si} [MPa]	f_{se} [MPa]	f_c' [MPa]	f_{ci}' [MPa]	b [mm]	h [mm]	c [mm]	s [mm]	Surface condition	Epoxy coating	Release type	L_t [mm]
Cousins et al. (1990)	S5CH-B	12.7	1862.0	1356.9	1214.2	34.5	27.6	127.0	203.2	63.5	-	S	CH	S	482.6
Cousins et al. (1990)	S5CH-C	12.7	1862.0	1356.9	1214.2	34.5	27.6	127.0	203.2	63.5	-	S	CH	S	431.8
Cousins et al. (1990)	S5CH-D	12.7	1862.0	1356.9	1214.2	34.5	27.6	127.0	203.2	63.5	-	S	CH	S	482.6
Cousins et al. (1990)	S6UN-A	15.2	1862.0	1424.4	1228.9	34.5	27.6	152.4	254.0	76.2	-	S	UN	S	1117.6
Cousins et al. (1990)	S6UN-B	15.2	1862.0	1424.4	1228.9	34.5	27.6	152.4	254.0	76.2	-	S	UN	S	1270.0
Cousins et al. (1990)	S6UN-C	15.2	1862.0	1424.4	1228.9	34.5	27.6	152.4	254.0	76.2	-	S	UN	S	1422.4
Cousins et al. (1990)	S6UN-D	15.2	1862.0	1424.4	1228.9	34.5	27.6	152.4	254.0	76.2	-	S	UN	S	1117.6
Cousins et al. (1990)	S6UN-E	15.2	1862.0	1424.4	1228.9	34.5	27.6	152.4	254.0	76.2	-	S	UN	S	1574.8
Cousins et al. (1990)	S6UN-F	15.2	1862.0	1424.4	1228.9	34.5	27.6	152.4	254.0	76.2	-	S	UN	S	1727.2
Cousins et al. (1990)	F6UN-A	15.2	1862.0	1424.4	1228.9	34.5	27.6	152.4	254.0	76.2	-	S	UN	S	1549.4
Cousins et al. (1990)	F6UN-B	15.2	1862.0	1424.4	1228.9	34.5	27.6	152.4	254.0	76.2	-	S	UN	S	1524.0
Cousins et al. (1990)	F6UN-C	15.2	1862.0	1424.4	1228.9	34.5	27.6	152.4	254.0	76.2	-	S	UN	S	1524.0
Cousins et al. (1990)	F6UN-D	15.2	1862.0	1424.4	1228.9	34.5	27.6	152.4	254.0	76.2	-	S	UN	S	1524.0
Cousins et al. (1990)	T6CM-A	15.2	1862.0	1400.3	1234.2	34.5	27.6	127.0	127.0	63.5	-	S	CM	G	952.5
Cousins et al. (1990)	T6CM-B	15.2	1862.0	1400.3	1234.2	34.5	27.6	127.0	127.0	63.5	-	S	CM	G	685.8
Cousins et al. (1990)	T6CM-C	15.2	1862.0	1400.3	1234.2	34.5	27.6	127.0	127.0	63.5	-	S	CM	G	977.9
Cousins et al. (1990)	T6CM-D	15.2	1862.0	1400.3	1234.2	34.5	27.6	127.0	127.0	63.5	-	S	CM	G	952.5
Cousins et al. (1990)	S6CM-A	15.2	1862.0	1400.3	1234.2	34.5	27.6	152.4	254.0	76.2	-	S	CM	S	558.8
Cousins et al. (1990)	S6CM-B	15.2	1862.0	1400.3	1234.2	34.5	27.6	152.4	254.0	76.2	-	S	CM	S	660.4
Cousins et al. (1990)	S6CM-C	15.2	1862.0	1400.3	1234.2	34.5	27.6	152.4	254.0	76.2	-	S	CM	S	762.0
Cousins et al. (1990)	S6CM-D	15.2	1862.0	1400.3	1234.2	34.5	27.6	152.4	254.0	76.2	-	S	CM	S	812.8
Cousins et al. (1990)	F6CM-A	15.2	1862.0	1400.3	1234.2	34.5	27.6	152.4	254.0	76.2	-	S	CM	S	660.4
Cousins et al. (1990)	F6CM-B	15.2	1862.0	1400.3	1234.2	34.5	27.6	152.4	254.0	76.2	-	S	CM	S	812.8
Cousins et al. (1990)	F6CM-C	15.2	1862.0	1400.3	1234.2	34.5	27.6	152.4	254.0	76.2	-	S	CM	S	965.2
Cousins et al. (1990)	F6CM-D	15.2	1862.0	1400.3	1234.2	34.5	27.6	152.4	254.0	76.2	-	S	CM	S	965.2
Mitchell et al. (1993)	9,5/31-1200a	9.5	1813.0	1219.0	1085.0	31.0	21.0	100.0	200.0	50.0	-	R	UN	G	506.0
Mitchell et al. (1993)	9,5/43-1350a	9.5	1813.0	1240.0	1095.0	43.0	27.0	100.0	200.0	50.0	-	R	UN	G	482.0

Author	Specimen ID	Φ [mm]	f_{su} [MPa]	f_{si} [MPa]	f_{se} [MPa]	f_c' [MPa]	f_{ci}' [MPa]	b [mm]	h [mm]	c [mm]	s [mm]	Surface condition	Epoxy coating	Release type	L_t [mm]
Mitchell et al. (1993)	9,5/43-1350b	9.5	1813.0	1240.0	1095.0	43.0	27.0	100.0	200.0	50.0	-	R	UN	G	584.0
Mitchell et al. (1993)	9,5/43-1000a	9.5	1813.0	1240.0	1095.0	43.0	27.0	100.0	200.0	50.0	-	R	UN	G	482.0
Mitchell et al. (1993)	9,5/43-1000b	9.5	1813.0	1240.0	1095.0	43.0	27.0	100.0	200.0	50.0	-	R	UN	G	381.0
Mitchell et al. (1993)	9,5/65-800a	9.5	1813.0	1192.0	1117.0	65.0	48.0	100.0	200.0	50.0	-	R	UN	G	303.0
Mitchell et al. (1993)	9,5/75-950a	9.5	1813.0	1230.0	1204.0	75.0	50.0	100.0	200.0	50.0	-	R	UN	G	304.0
Mitchell et al. (1993)	9,5/75-950b	9.5	1813.0	1230.0	1204.0	75.0	50.0	100.0	200.0	50.0	-	R	UN	G	406.0
Mitchell et al. (1993)	9,5/75-700a	9.5	1813.0	1230.0	1136.0	75.0	50.0	100.0	200.0	50.0	-	R	UN	G	406.0
Mitchell et al. (1993)	9,5/75-700b	9.5	1813.0	1230.0	1136.0	75.0	50.0	100.0	200.0	50.0	-	R	UN	G	304.0
Mitchell et al. (1993)	9,5/89-825a	9.5	1813.0	1234.0	1175.0	89.0	50.0	100.0	200.0	50.0	-	R	UN	G	415.0
Mitchell et al. (1993)	9,5/89-825b	9.5	1813.0	1234.0	1175.0	89.0	50.0	100.0	200.0	50.0	-	R	UN	G	313.0
Mitchell et al. (1993)	9,5/89-575a	9.5	1813.0	1234.0	1177.0	89.0	50.0	100.0	200.0	50.0	-	R	UN	G	419.0
Mitchell et al. (1993)	9,5/89-575b	9.5	1813.0	1234.0	1177.0	89.0	50.0	100.0	200.0	50.0	-	R	UN	G	317.0
Mitchell et al. (1993)	13/31-1200a	12.7	1903.0	1374.0	1254.0	31.0	21.0	150.0	225.0	50.0	-	S	UN	G	710.0
Mitchell et al. (1993)	13/43-1600a	12.7	1903.0	1217.0	1044.0	43.0	27.0	100.0	200.0	50.0	-	S	UN	G	584.0
Mitchell et al. (1993)	13/43-1600b	12.7	1903.0	1217.0	1044.0	43.0	27.0	100.0	200.0	50.0	-	S	UN	G	584.0
Mitchell et al. (1993)	13/43-1250a	12.7	1903.0	1217.0	1028.0	43.0	27.0	100.0	200.0	50.0	-	S	UN	G	584.0
Mitchell et al. (1993)	13/43-1250b	12.7	1903.0	1217.0	1028.0	43.0	27.0	100.0	200.0	50.0	-	S	UN	G	584.0
Mitchell et al. (1993)	13/65-850a	12.7	1903.0	1315.0	1254.0	65.0	48.0	150.0	225.0	50.0	-	S	UN	G	506.0
Mitchell et al. (1993)	13/75-1100a	12.7	1903.0	1303.0	1153.0	75.0	50.0	100.0	200.0	50.0	-	S	UN	G	507.0
Mitchell et al. (1993)	13/75-1100b	12.7	1903.0	1303.0	1153.0	75.0	50.0	100.0	200.0	50.0	-	S	UN	G	432.0
Mitchell et al. (1993)	13/75-950a	12.7	1903.0	1303.0	1167.0	75.0	50.0	100.0	200.0	50.0	-	S	UN	G	330.0
Mitchell et al. (1993)	13/75-950b	12.7	1903.0	1303.0	1167.0	75.0	50.0	100.0	200.0	50.0	-	S	UN	G	405.0
Mitchell et al. (1993)	13/89-950a	12.7	1903.0	1329.0	1278.0	89.0	50.0	125.0	175.0	50.0	-	S	UN	G	387.0
Mitchell et al. (1993)	13/89-950b	12.7	1903.0	1329.0	1278.0	89.0	50.0	125.0	175.0	50.0	-	S	UN	G	387.0
Mitchell et al. (1993)	13/89-650a	12.7	1903.0	1329.0	1272.0	89.0	50.0	125.0	175.0	50.0	-	S	UN	G	495.0
Mitchell et al. (1993)	13/89-650b	12.7	1903.0	1329.0	1272.0	89.0	50.0	125.0	175.0	50.0	-	S	UN	G	495.0
Mitchell et al. (1993)	16/31-1865a	15.7	1793.0	1220.0	1026.0	31.0	21.0	200.0	250.0	50.0	-	S	UN	G	735.0

Author	Specimen ID	Φ [mm]	f_{su} [MPa]	f_{si} [MPa]	f_{se} [MPa]	f_c' [MPa]	f_{ci}' [MPa]	b [mm]	h [mm]	c [mm]	s [mm]	Surface condition	Epoxy coating	Release type	L_t [mm]
Mitchell et al. (1993)	16/31-1865b	15.7	1793.0	1220.0	1026.0	31.0	21.0	200.0	250.0	50.0	-	S	UN	G	872.0
Mitchell et al. (1993)	16/31-1500a	15.7	1793.0	1220.0	1086.0	31.0	21.0	200.0	250.0	50.0	-	S	UN	G	709.0
Mitchell et al. (1993)	16/31-1500b	15.7	1793.0	1220.0	1086.0	31.0	21.0	200.0	250.0	50.0	-	S	UN	G	768.0
Mitchell et al. (1993)	16/65-1150a	15.7	1793.0	1176.0	1098.0	65.0	48.0	200.0	250.0	50.0	-	S	UN	G	528.0
Mitchell et al. (1993)	16/65-1150b	15.7	1793.0	1176.0	1098.0	65.0	48.0	200.0	250.0	50.0	-	S	UN	G	427.0
Mitchell et al. (1993)	16/65-725a	15.7	1793.0	1176.0	1096.0	65.0	48.0	200.0	250.0	50.0	-	S	UN	G	536.0
Mitchell et al. (1993)	16/65-725b	15.7	1793.0	1176.0	1096.0	65.0	48.0	200.0	250.0	50.0	-	S	UN	G	435.0
Mitchell et al. (1993)	16/89-975a	15.7	1793.0	871.0	832.0	89.0	50.0	125.0	175.0	50.0	-	S	UN	G	306.0
Mitchell et al. (1993)	16/89-975b	15.7	1793.0	871.0	832.0	89.0	50.0	125.0	175.0	50.0	-	S	UN	G	306.0
Mitchell et al. (1993)	16/89-675a	15.7	1793.0	871.0	838.0	89.0	50.0	125.0	175.0	50.0	-	S	UN	G	465.0
Mitchell et al. (1993)	16/89-675b	15.7	1793.0	871.0	838.0	89.0	50.0	125.0	175.0	50.0	-	S	UN	G	465.0
Cousins et al. (1994)	1(1,NS)-A	12.7	1862.0	1372.1	1054.9	43.5	36.6	177.8	558.8	44.5	31.8	S	UN	S	1473.2
Cousins et al. (1994)	1(1,NS)-B	12.7	1862.0	1372.1	1054.9	43.5	36.6	177.8	558.8	44.5	31.8	S	UN	S	1473.2
Cousins et al. (1994)	2(1,NS)-A	12.7	1862.0	1372.1	1054.9	43.5	36.6	177.8	558.8	44.5	31.8	S	UN	S	1727.2
Cousins et al. (1994)	2(1,NS)-B	12.7	1862.0	1372.1	1054.9	43.5	36.6	177.8	558.8	44.5	31.8	S	UN	S	1727.2
Cousins et al. (1994)	3(2,NS)-A	12.7	1862.0	1399.7	1103.2	44.5	36.9	177.8	558.8	44.5	31.8	S	UN	S	1041.4
Cousins et al. (1994)	3(2,NS)-B	12.7	1862.0	1399.7	1103.2	51.2	36.9	177.8	558.8	44.5	31.8	S	UN	S	1143.0
Cousins et al. (1994)	4(3,HS)-A	12.7	1862.0	1406.6	1137.7	75.8	56.7	177.8	558.8	44.5	31.8	S	UN	S	939.8
Cousins et al. (1994)	4(3,HS)-B	12.7	1862.0	1406.6	1137.7	75.8	56.7	177.8	558.8	44.5	31.8	S	UN	S	812.8
Cousins et al. (1994)	5(4,HS)-A	12.7	1862.0	1420.4	1144.6	69.4	53.0	177.8	558.8	44.5	31.8	S	UN	S	1244.6
Cousins et al. (1994)	6(5,NS)-A	12.7	1862.0	1427.3	1130.8	55.2	52.8	177.8	558.8	44.5	31.8	S	UN	S	1016.0
Cousins et al. (1994)	6(5,NS)-B	12.7	1862.0	1427.3	1130.8	54.7	52.8	177.8	558.8	44.5	31.8	S	UN	S	939.8
Cousins et al. (1994)	7(1,NS)-A	12.7	1862.0	1379.0	1068.7	43.5	36.6	190.5	558.8	44.5	38.1	S	UN	S	1625.6
Cousins et al. (1994)	7(1,NS)-B	12.7	1862.0	1379.0	1068.7	43.5	36.6	190.5	558.8	44.5	38.1	S	UN	S	1219.2
Cousins et al. (1994)	8(1,NS)-A	12.7	1862.0	1379.0	1068.7	43.5	36.6	190.5	558.8	44.5	38.1	S	UN	S	1625.6
Cousins et al. (1994)	8(1,NS)-B	12.7	1862.0	1379.0	1068.7	43.5	36.6	190.5	558.8	44.5	38.1	S	UN	S	1371.6
Cousins et al. (1994)	9(2,NS)-A	12.7	1862.0	1413.5	1123.9	44.5	36.9	190.5	558.8	44.5	38.1	S	UN	S	1320.8

Author	Specimen ID	Φ [mm]	f_{su} [MPa]	f_{si} [MPa]	f_{se} [MPa]	f_c' [MPa]	f_{ci}' [MPa]	b [mm]	h [mm]	c [mm]	s [mm]	Surface condition	Epoxy coating	Release type	L_t [mm]
Cousins et al. (1994)	9(2,NS)-B	12.7	1862.0	1413.5	1123.9	51.2	36.9	190.5	558.8	44.5	38.1	S	UN	S	1371.6
Cousins et al. (1994)	10(3,HS)-A	12.7	1862.0	1427.3	1158.4	80.1	56.7	190.5	558.8	44.5	38.1	S	UN	S	660.4
Cousins et al. (1994)	10(3,HS)-B	12.7	1862.0	1427.3	1158.4	75.8	56.7	190.5	558.8	44.5	38.1	S	UN	S	863.6
Cousins et al. (1994)	11(4,HS)-A	12.7	1862.0	1413.5	1144.6	72.3	53.0	190.5	558.8	44.5	38.1	S	UN	S	1041.4
Cousins et al. (1994)	11(4,HS)-B	12.7	1862.0	1413.5	1144.6	69.4	53.0	190.5	558.8	44.5	38.1	S	UN	S	1092.2
Cousins et al. (1994)	12(5,NS)-A	12.7	1862.0	1427.3	1137.7	54.7	52.8	190.5	558.8	44.5	38.1	S	UN	S	1041.4
Cousins et al. (1994)	12(5,NS)-B	12.7	1862.0	1427.3	1137.7	55.2	52.8	190.5	558.8	44.5	38.1	S	UN	S	685.8
Deatherage et al. (1994)	5-1-EXT	12.7	1862.0	1400.0	1282.5	37.8	26.1	406.4	711.2	50.8	38.1	S	UN	S	914.4
Deatherage et al. (1994)	5-1-INT	12.7	1862.0	1400.0	1289.4	37.8	26.1	406.4	711.2	50.8	38.1	S	UN	S	762.0
Deatherage et al. (1994)	5-2-EXT	12.7	1862.0	1400.0	1296.3	46.5	28.8	406.4	711.2	50.8	38.1	S	UN	S	889.0
Deatherage et al. (1994)	5-2-INT	12.7	1862.0	1400.0	1296.3	46.5	28.8	406.4	711.2	50.8	38.1	S	UN	S	736.6
Deatherage et al. (1994)	5-3-EXT	12.7	1862.0	1400.0	1310.1	47.3	32.9	406.4	711.2	50.8	38.1	R	UN	S	584.2
Deatherage et al. (1994)	5-3-INT	12.7	1862.0	1400.0	1316.9	47.3	32.9	406.4	711.2	50.8	38.1	R	UN	S	558.8
Deatherage et al. (1994)	5-4-EXT	12.7	1862.0	1400.0	1323.8	52.4	36.1	406.4	711.2	50.8	38.1	R	UN	S	558.8
Deatherage et al. (1994)	5-4-INT	12.7	1862.0	1400.0	1323.8	52.4	36.1	406.4	711.2	50.8	38.1	R	UN	S	660.4
Deatherage et al. (1994)	5-SWAI-E	12.7	1862.0	1400.0	1330.7	38.3	35.4	406.4	711.2	50.8	31.8	R	UN	S	508.0
Deatherage et al. (1994)	5-SWAI-W	12.7	1862.0	1400.0	1330.7	38.3	35.4	406.4	711.2	50.8	31.8	R	UN	S	533.4
Deatherage et al. (1994)	5-UWR-E	12.7	1862.0	1400.0	1337.6	41.3	38.3	406.4	711.2	50.8	31.8	R	UN	S	533.4
Deatherage et al. (1994)	5-UWR-W	12.7	1862.0	1400.0	1337.6	41.3	38.3	406.4	711.2	50.8	31.8	R	UN	S	482.6
Deatherage et al. (1994)	5-FWC-E	12.7	1862.0	1400.0	1323.8	36.8	32.9	406.4	711.2	50.8	31.8	R	UN	S	457.2
Deatherage et al. (1994)	5-FWC-W	12.7	1862.0	1400.0	1316.9	36.8	32.9	406.4	711.2	50.8	31.8	R	UN	S	457.2
Deatherage et al. (1994)	5-ASW-E	12.7	1862.0	1400.0	1330.7	37.2	35.5	406.4	711.2	50.8	31.8	R	UN	S	533.4
Deatherage et al. (1994)	5-ASW-W	12.7	1862.0	1400.0	1323.8	37.2	35.5	406.4	711.2	50.8	31.8	R	UN	S	457.2
Deatherage et al. (1994)	5S-1-EXT	13.3	1862.0	1400.0	1310.1	45.7	36.8	406.4	711.2	50.8	37.5	S	UN	S	838.2
Deatherage et al. (1994)	5S-1-INT	13.3	1862.0	1400.0	1316.9	45.7	36.8	406.4	711.2	50.8	37.5	S	UN	S	838.2
Deatherage et al. (1994)	5S-2-EXT	13.3	1862.0	1400.0	1316.9	46.9	34.1	406.4	711.2	50.8	37.5	S	UN	S	863.6
Deatherage et al. (1994)	5S-2-INT	13.3	1862.0	1400.0	1316.9	46.9	34.1	406.4	711.2	50.8	37.5	S	UN	S	762.0

Author	Specimen ID	Φ [mm]	f_{su} [MPa]	f_{si} [MPa]	f_{se} [MPa]	f_c' [MPa]	f_{ci}' [MPa]	b [mm]	h [mm]	c [mm]	s [mm]	Surface condition	Epoxy coating	Release type	L_t [mm]
Deatherage et al. (1994)	5S-3-EXT	13.3	1862.0	1400.0	1316.9	41.1	37.3	406.4	711.2	50.8	37.5	R	UN	S	787.4
Deatherage et al. (1994)	5S-3-INT	13.3	1862.0	1400.0	1310.1	41.1	37.3	406.4	711.2	50.8	37.5	R	UN	S	914.4
Deatherage et al. (1994)	5S-4-EXT	13.3	1862.0	1400.0	1310.1	42.6	36.5	406.4	711.2	50.8	37.5	R	UN	S	889.0
Deatherage et al. (1994)	5S-4-INT	13.3	1862.0	1400.0	1310.1	42.6	36.5	406.4	711.2	50.8	37.5	R	UN	S	558.8
Deatherage et al. (1994)	916-1-EXT	14.3	1862.0	1400.0	1261.8	38.2	23.2	406.4	711.2	50.8	36.5	S	UN	S	1066.8
Deatherage et al. (1994)	916-1-INT	14.3	1862.0	1400.0	1268.7	38.2	23.2	406.4	711.2	50.8	36.5	S	UN	S	812.8
Deatherage et al. (1994)	916-2-EXT	14.3	1862.0	1400.0	1282.5	40.8	25.9	406.4	711.2	50.8	36.5	S	UN	S	914.4
Deatherage et al. (1994)	916-2-INT	14.3	1862.0	1400.0	1282.5	40.8	25.9	406.4	711.2	50.8	36.5	S	UN	S	711.2
Deatherage et al. (1994)	916-3-EXT	14.3	1862.0	1400.0	1316.9	42.2	34.9	406.4	711.2	50.8	36.5	R	UN	S	762.0
Deatherage et al. (1994)	916-3-INT	14.3	1862.0	1400.0	1316.9	42.2	34.9	406.4	711.2	50.8	36.5	R	UN	S	584.2
Deatherage et al. (1994)	916-4-EXT	14.3	1862.0	1400.0	1316.9	43.0	34.1	406.4	711.2	50.8	36.5	R	UN	S	762.0
Deatherage et al. (1994)	916-4-INT	14.3	1862.0	1400.0	1316.9	43.0	34.1	406.4	711.2	50.8	36.5	R	UN	S	685.8
Deatherage et al. (1994)	6-1-EXT	15.2	1862.0	1400.0	1310.1	35.3	28.3	406.4	711.2	63.5	48.3	S	UN	S	635.0
Deatherage et al. (1994)	6-1-INT	15.2	1862.0	1400.0	1310.1	35.3	28.3	406.4	711.2	63.5	48.3	S	UN	S	685.8
Deatherage et al. (1994)	6-2-EXT	15.2	1862.0	1400.0	1303.2	36.4	29.5	406.4	711.2	63.5	48.3	S	UN	S	762.0
Deatherage et al. (1994)	6-2-INT	15.2	1862.0	1400.0	1303.2	36.4	29.5	406.4	711.2	63.5	48.3	S	UN	S	609.6
Deatherage et al. (1994)	6-3-EXT	15.2	1862.0	1400.0	1316.9	51.5	36.1	406.4	711.2	63.5	48.3	S	UN	S	584.2
Deatherage et al. (1994)	6-3-INT	15.2	1862.0	1400.0	1316.9	51.5	36.1	406.4	711.2	63.5	48.3	S	UN	S	533.4
Deatherage et al. (1994)	6-4-EXT	15.2	1862.0	1400.0	1310.1	55.0	37.6	406.4	711.2	63.5	48.3	S	UN	S	558.8
Deatherage et al. (1994)	6-4-INT	15.2	1862.0	1400.0	1316.9	55.0	37.6	406.4	711.2	63.5	48.3	S	UN	S	584.2
Russell and Burns (1996)	FC150-11-N	12.7	1862.0	1344.5	1183.2	46.3	30.9	101.6	127.0	50.8	-	S	UN	G	685.8
Russell and Burns (1996)	FC150-11-S	12.7	1862.0	1344.5	1183.2	46.3	30.9	101.6	127.0	50.8	-	S	UN	G	863.6
Russell and Burns (1996)	FC150-12-N	12.7	1862.0	1344.5	1183.2	46.3	30.9	101.6	127.0	50.8	-	S	UN	G	723.9
Russell and Burns (1996)	FC150-12-S	12.7	1862.0	1344.5	1183.2	46.3	30.9	101.6	127.0	50.8	-	S	UN	G	711.2
Russell and Burns (1996)	FC350-1-N	12.7	1862.0	1365.2	1201.4	45.7	29.8	127.0	228.6	63.5	38.1	S	UN	G	825.5
Russell and Burns (1996)	FC350-1-S	12.7	1862.0	1365.2	1201.4	45.7	29.8	127.0	228.6	63.5	38.1	S	UN	G	698.5
Russell and Burns (1996)	FC350-2-N	12.7	1862.0	1365.2	1201.4	45.7	29.8	127.0	228.6	63.5	38.1	S	UN	G	698.5

Author	Specimen ID	Φ [mm]	f_{su} [MPa]	f_{si} [MPa]	f_{se} [MPa]	f_c' [MPa]	f_{ci}' [MPa]	b [mm]	h [mm]	c [mm]	s [mm]	Surface condition	Epoxy coating	Release type	L_t [mm]
Russell and Burns (1996)	FC350-2-S	12.7	1862.0	1365.2	1201.4	45.7	29.8	127.0	228.6	63.5	38.1	S	UN	G	698.5
Russell and Burns (1996)	FCT350-3-N	12.7	1862.0	1365.2	1201.4	45.7	29.8	127.0	228.6	63.5	38.1	S	UN	G	774.7
Russell and Burns (1996)	FCT350-3-S	12.7	1862.0	1365.2	1201.4	45.7	29.8	127.0	228.6	63.5	38.1	S	UN	G	762.0
Russell and Burns (1996)	FCT350-4-N	12.7	1862.0	1365.2	1201.4	45.7	29.8	127.0	228.6	63.5	38.1	S	UN	G	736.6
Russell and Burns (1996)	FCT350-4-S	12.7	1862.0	1365.2	1201.4	45.7	29.8	127.0	228.6	63.5	38.1	S	UN	G	812.8
Russell and Burns (1996)	DC350-5-N	12.7	1862.0	1344.5	1183.2	43.1	29.0	127.0	228.6	63.5	38.1	S	UN	G	673.1
Russell and Burns (1996)	DC350-5-S	12.7	1862.0	1344.5	1183.2	43.1	29.0	127.0	228.6	63.5	38.1	S	UN	G	711.2
Russell and Burns (1996)	DC350-6-N	12.7	1862.0	1344.5	1183.2	43.1	29.0	127.0	228.6	63.5	38.1	S	UN	G	723.9
Russell and Burns (1996)	DC350-6-S	12.7	1862.0	1344.5	1183.2	43.1	29.0	127.0	228.6	63.5	38.1	S	UN	G	774.7
Russell and Burns (1996)	FC550-1-N	12.7	1862.0	1344.5	1183.2	37.2	26.5	127.0	330.2	63.5	38.1	S	UN	G	1003.3
Russell and Burns (1996)	FC550-1-S	12.7	1862.0	1344.5	1183.2	37.2	26.5	127.0	330.2	63.5	38.1	S	UN	G	927.1
Russell and Burns (1996)	FCT550-2-N	12.7	1862.0	1344.5	1183.2	37.2	26.5	127.0	330.2	63.5	38.1	S	UN	G	914.4
Russell and Burns (1996)	FCT550-2-S	12.7	1862.0	1344.5	1183.2	37.2	26.5	127.0	330.2	63.5	38.1	S	UN	G	1003.3
Russell and Burns (1996)	FC550-3-N	12.7	1862.0	1344.5	1183.2	37.2	26.5	127.0	330.2	63.5	38.1	S	UN	G	838.2
Russell and Burns (1996)	FC550-3-S	12.7	1862.0	1344.5	1183.2	37.2	26.5	127.0	330.2	63.5	38.1	S	UN	G	1117.6
Russell and Burns (1996)	FC160-12-N	15.2	1862.0	1344.5	1183.2	37.2	26.5	101.6	127.0	50.8	-	S	UN	G	1219.2
Russell and Burns (1996)	FC160-12-S	15.2	1862.0	1344.5	1183.2	37.2	26.5	101.6	127.0	50.8	-	S	UN	G	1168.4
Russell and Burns (1996)	FC360-1-N	15.2	1862.0	1344.5	1183.2	43.1	29.0	127.0	228.6	63.5	35.6	S	UN	G	1066.8
Russell and Burns (1996)	FC360-1-S	15.2	1862.0	1344.5	1183.2	43.1	29.0	127.0	228.6	63.5	35.6	S	UN	G	1028.7
Russell and Burns (1996)	FC360-2-N	15.2	1862.0	1344.5	1183.2	43.1	29.0	127.0	228.6	63.5	35.6	S	UN	G	939.8
Russell and Burns (1996)	FC360-2-S	15.2	1862.0	1344.5	1183.2	43.1	29.0	127.0	228.6	63.5	35.6	S	UN	G	1219.2
Russell and Burns (1996)	FCT360-3-N	15.2	1862.0	1344.5	1183.2	43.1	29.0	127.0	228.6	63.5	35.6	S	UN	G	1003.3
Russell and Burns (1996)	FCT360-3-S	15.2	1862.0	1344.5	1183.2	43.1	29.0	127.0	228.6	63.5	35.6	S	UN	G	1155.7
Russell and Burns (1996)	FCT360-4-N	15.2	1862.0	1330.7	1171.0	50.3	33.0	127.0	228.6	63.5	35.6	S	UN	G	1282.7
Russell and Burns (1996)	FCT360-4-S	15.2	1862.0	1330.7	1171.0	50.3	33.0	127.0	228.6	63.5	35.6	S	UN	G	1066.8
Russell and Burns (1996)	DC360-5-N	15.2	1862.0	1351.4	1189.2	50.3	33.0	127.0	228.6	63.5	35.6	S	UN	G	1066.8
Russell and Burns (1996)	DC360-5-S	15.2	1862.0	1351.4	1189.2	50.3	33.0	127.0	228.6	63.5	35.6	S	UN	G	914.4

Author	Specimen ID	Φ [mm]	f_{su} [MPa]	f_{si} [MPa]	f_{se} [MPa]	f_c' [MPa]	f_{ci}' [MPa]	b [mm]	h [mm]	c [mm]	s [mm]	Surface condition	Epoxy coating	Release type	L_t [mm]
Russell and Burns (1996)	DC360-6-N	15.2	1862.0	1351.4	1189.2	50.3	33.0	127.0	228.6	63.5	35.6	S	UN	G	876.3
Russell and Burns (1996)	DC360-6-S	15.2	1862.0	1351.4	1189.2	50.3	33.0	127.0	228.6	63.5	35.6	S	UN	G	1041.4
Russell and Burns (1996)	DCT360-7-N	15.2	1862.0	1330.7	1171.0	50.3	33.0	127.0	228.6	63.5	35.6	S	UN	G	1028.7
Russell and Burns (1996)	DCT360-7-S	15.2	1862.0	1330.7	1171.0	50.3	33.0	127.0	228.6	63.5	35.6	S	UN	G	876.3
Russell and Burns (1996)	FC362-11-N	15.2	1862.0	1254.9	1104.3	51.9	32.8	127.0	241.3	63.5	42.0	S	UN	G	1168.4
Russell and Burns (1996)	FC362-11-S	15.2	1862.0	1254.9	1104.3	51.9	32.8	127.0	241.3	63.5	42.0	S	UN	G	1117.6
Russell and Burns (1996)	FCT362-12-N	15.2	1862.0	1254.9	1104.3	51.9	32.8	127.0	241.3	63.5	42.0	S	UN	G	1117.6
Russell and Burns (1996)	FCT362-12-S	15.2	1862.0	1254.9	1104.3	51.9	32.8	127.0	241.3	63.5	42.0	S	UN	G	1066.8
Russell and Burns (1996)	FC362-13-N	15.2	1862.0	1254.9	1104.3	51.9	32.8	127.0	241.3	63.5	42.0	S	UN	G	1117.6
Russell and Burns (1996)	FC362-13-S	15.2	1862.0	1254.9	1104.3	51.9	32.8	127.0	241.3	63.5	42.0	S	UN	G	1016.0
Russell and Burns (1996)	FC560-1-N	15.2	1862.0	1344.5	1183.2	45.5	30.9	127.0	330.2	63.5	35.6	S	UN	G	1155.7
Russell and Burns (1996)	FC560-1-S	15.2	1862.0	1344.5	1183.2	45.5	30.9	127.0	330.2	63.5	35.6	S	UN	G	1193.8
Russell and Burns (1996)	FCT560-2-N	15.2	1862.0	1344.5	1183.2	45.5	30.9	127.0	330.2	63.5	35.6	S	UN	G	1219.2
Russell and Burns (1996)	FCT560-2-S	15.2	1862.0	1344.5	1183.2	45.5	30.9	127.0	330.2	63.5	35.6	S	UN	G	1308.1
Russell and Burns (1996)	FC560-3-N	15.2	1862.0	1344.5	1183.2	45.5	30.9	127.0	330.2	63.5	35.6	S	UN	G	1219.2
Russell and Burns (1996)	FC560-3-S	15.2	1862.0	1344.5	1183.2	45.5	30.9	127.0	330.2	63.5	35.6	S	UN	G	1219.2
Russell and Burns (1996)	FA550-1N	12.7	1862.0	1351.4	1189.2	35.2	32.0	228.6	558.8	63.5	38.1	S	UN	S	457.2
Russell and Burns (1996)	FA550-1S	12.7	1862.0	1351.4	1189.2	35.2	32.0	228.6	558.8	63.5	38.1	S	UN	S	406.4
Russell and Burns (1996)	FA550-2N	12.7	1862.0	1351.4	1189.2	35.2	32.0	228.6	558.8	63.5	38.1	S	UN	S	520.7
Russell and Burns (1996)	FA550-2S	12.7	1862.0	1351.4	1189.2	35.2	32.0	228.6	558.8	63.5	38.1	S	UN	S	533.4
Russell and Burns (1996)	FA550-3N	12.7	1862.0	1351.4	1189.2	36.4	27.9	228.6	558.8	63.5	38.1	S	UN	S	546.1
Russell and Burns (1996)	FA550-3S	12.7	1862.0	1351.4	1189.2	36.4	27.9	228.6	558.8	63.5	38.1	S	UN	S	558.8
Russell and Burns (1996)	FA550-4N	12.7	1862.0	1351.4	1189.2	36.4	27.9	228.6	558.8	63.5	38.1	S	UN	S	533.4
Russell and Burns (1996)	FA550-4S	12.7	1862.0	1351.4	1189.2	36.4	27.9	228.6	558.8	63.5	38.1	S	UN	S	533.4
Russell and Burns (1996)	DB850-5N	12.7	1862.0	1351.4	1189.2	49.8	38.5	228.6	596.9	50.8	38.1	S	UN	S	774.7
Russell and Burns (1996)	DB850-5S	12.7	1862.0	1351.4	1189.2	49.8	38.5	228.6	596.9	50.8	38.1	S	UN	S	1117.6
Russell and Burns (1996)	DB850-6N	12.7	1862.0	1351.4	1189.2	47.4	35.5	228.6	596.9	50.8	38.1	S	UN	S	927.1

Author	Specimen ID	Φ [mm]	f_{su} [MPa]	f_{si} [MPa]	f_{se} [MPa]	f_c' [MPa]	f_{ci}' [MPa]	b [mm]	h [mm]	c [mm]	s [mm]	Surface condition	Epoxy coating	Release type	L_t [mm]
Russell and Burns (1996)	DB850-6S	12.7	1862.0	1351.4	1189.2	47.4	35.5	228.6	596.9	50.8	38.1	S	UN	S	850.9
Russell and Burns (1996)	FA460-1N	15.2	1862.0	1344.5	1183.2	43.9	33.6	228.6	558.8	63.5	35.6	S	UN	S	749.3
Russell and Burns (1996)	FA460-1S	15.2	1862.0	1344.5	1183.2	43.9	33.6	228.6	558.8	63.5	35.6	S	UN	S	939.8
Russell and Burns (1996)	FA460-2N	15.2	1862.0	1365.2	1201.4	45.3	30.8	228.6	558.8	63.5	35.6	S	UN	S	863.6
Russell and Burns (1996)	FA460-2S	15.2	1862.0	1365.2	1201.4	45.3	30.8	228.6	558.8	63.5	35.6	S	UN	S	939.8
Russell and Burns (1996)	FA460-3N	15.2	1862.0	1365.2	1201.4	45.3	30.8	228.6	558.8	63.5	35.6	S	UN	S	838.2
Russell and Burns (1996)	FA460-3S	15.2	1862.0	1365.2	1201.4	45.3	30.8	228.6	558.8	63.5	35.6	S	UN	S	825.5
Russell and Burns (1996)	FA460-4N	15.2	1862.0	1372.1	1207.4	44.5	33.4	228.6	558.8	63.5	35.6	S	UN	S	698.5
Russell and Burns (1996)	FA460-4S	15.2	1862.0	1372.1	1207.4	44.5	33.4	228.6	558.8	63.5	35.6	S	UN	S	723.9
Russell and Burns (1996)	FA460-5N	15.2	1862.0	1427.2	1255.9	48.4	32.1	228.6	558.8	63.5	35.6	S	UN	S	800.1
Russell and Burns (1996)	FA460-5S	15.2	1862.0	1427.2	1255.9	48.4	32.1	228.6	558.8	63.5	35.6	S	UN	S	787.4
Russell and Burns (1996)	FA460-6N	15.2	1862.0	1427.2	1255.9	51.3	32.1	228.6	558.8	63.5	35.6	S	UN	S	800.1
Russell and Burns (1996)	FA460-6S	15.2	1862.0	1427.2	1255.9	51.3	32.1	228.6	558.8	63.5	35.6	S	UN	S	787.4
Russell and Burns (1997)	SS150-1a	12.7	1862.0	1406.0	1237.3	34.9	19.2	102.0	127.0	51.0	-	S	UN	S	1422.0
Russell and Burns (1997)	SS150-1b	12.7	1862.0	1406.0	1237.3	34.9	19.2	102.0	127.0	51.0	-	S	UN	S	1422.0
Russell and Burns (1997)	SS150-2a	12.7	1862.0	1406.0	1237.3	34.9	19.2	102.0	127.0	51.0	-	S	UN	S	1524.0
Russell and Burns (1997)	SS150-2b	12.7	1862.0	1406.0	1237.3	34.9	19.2	102.0	127.0	51.0	-	S	UN	S	1397.0
Russell and Burns (1997)	SS150-3a	12.7	1862.0	1299.0	1143.1	40.1	26.0	102.0	127.0	51.0	-	S	UN	S	813.0
Russell and Burns (1997)	SS150-3b	12.7	1862.0	1299.0	1143.1	40.1	26.0	102.0	127.0	51.0	-	S	UN	S	686.0
Russell and Burns (1997)	SS150-4a	12.7	1862.0	1299.0	1143.1	40.1	26.0	102.0	127.0	51.0	-	S	UN	S	737.0
Russell and Burns (1997)	SS150-4b	12.7	1862.0	1299.0	1143.1	40.1	26.0	102.0	127.0	51.0	-	S	UN	S	584.0
Russell and Burns (1997)	SS160-1a	15.2	1862.0	1239.0	1090.3	48.2	24.3	102.0	127.0	51.0	-	S	UN	S	1245.0
Russell and Burns (1997)	SS160-2b	15.2	1862.0	1239.0	1090.3	48.2	24.3	102.0	127.0	51.0	-	S	UN	S	1118.0
Russell and Burns (1997)	SS160-3b	15.2	1862.0	1311.0	1153.7	45.0	30.2	102.0	127.0	51.0	-	S	UN	S	1219.0
Russell and Burns (1997)	SS160-4a	15.2	1862.0	1311.0	1153.7	45.0	30.2	102.0	127.0	51.0	-	S	UN	S	1143.0
Russell and Burns (1997)	SS160-4b	15.2	1862.0	1311.0	1153.7	45.0	30.2	102.0	127.0	51.0	-	S	UN	S	1143.0
Russell and Burns (1997)	SS160-5a	15.2	1862.0	1287.0	1132.6	46.9	28.9	102.0	127.0	51.0	-	S	UN	S	1321.0

Author	Specimen ID	Φ [mm]	f_{su} [MPa]	f_{si} [MPa]	f_{se} [MPa]	f_c' [MPa]	f_{ci}' [MPa]	b [mm]	h [mm]	c [mm]	s [mm]	Surface condition	Epoxy coating	Release type	L_t [mm]
Russell and Burns (1997)	SS160-5b	15.2	1862.0	1287.0	1132.6	46.9	28.9	102.0	127.0	51.0	-	S	UN	S	813.0
Russell and Burns (1997)	SS160-6a	15.2	1862.0	1287.0	1132.6	46.9	28.9	102.0	127.0	51.0	-	S	UN	S	762.0
Russell and Burns (1997)	SS160-6b	15.2	1862.0	1287.0	1132.6	46.9	28.9	102.0	127.0	51.0	-	S	UN	S	965.0
Russell and Burns (1997)	SS160-7a	15.2	1862.0	1239.0	1090.3	46.9	28.9	102.0	127.0	51.0	-	S	UN	S	940.0
Russell and Burns (1997)	SS160-7b	15.2	1862.0	1239.0	1090.3	46.9	28.9	102.0	127.0	51.0	-	S	UN	S	914.0
Russell and Burns (1997)	SS160-8a	15.2	1862.0	1239.0	1090.3	46.9	28.9	102.0	127.0	51.0	-	S	UN	S	711.0
Russell and Burns (1997)	SS160-8b	15.2	1862.0	1239.0	1090.3	46.9	28.9	102.0	127.0	51.0	-	S	UN	S	813.0
Russell and Burns (1997)	DC150-1a	12.7	1862.0	1311.0	1153.7	40.1	26.0	102.0	127.0	51.0	-	S	UN	S	533.0
Russell and Burns (1997)	DC150-1b	12.7	1862.0	1311.0	1153.7	40.1	26.0	102.0	127.0	51.0	-	S	UN	S	432.0
Russell and Burns (1997)	DC150-2a	12.7	1862.0	1311.0	1153.7	40.1	26.0	102.0	127.0	51.0	-	S	UN	S	457.0
Russell and Burns (1997)	DC150-2b	12.7	1862.0	1311.0	1153.7	40.1	26.0	102.0	127.0	51.0	-	S	UN	S	457.0
Russell and Burns (1997)	DC160-1b	15.2	1862.0	1168.0	1027.8	45.0	30.2	102.0	127.0	51.0	-	S	UN	S	1118.0
Oh and Kim (2000)	M12-N-C3-1a	12.7	1862.0	1396.5	1228.9	48.2	34.7	112.7	200.0	36.4	-	S	UN	S	898.0
Oh and Kim (2000)	M12-N-C3-1b	12.7	1862.0	1396.5	1228.9	48.2	34.7	112.7	200.0	36.4	-	S	UN	S	753.0
Oh and Kim (2000)	M12-N-C3-2a	12.7	1862.0	1396.5	1228.9	47.6	32.5	112.7	200.0	36.4	-	S	UN	S	803.0
Oh and Kim (2000)	M12-N-C3-2b	12.7	1862.0	1396.5	1228.9	47.6	32.5	112.7	200.0	36.4	-	S	UN	S	671.0
Oh and Kim (2000)	M12-N-C4-1a	12.7	1862.0	1396.5	1228.9	50.3	35.0	112.7	200.0	46.4	-	S	UN	S	640.0
Oh and Kim (2000)	M12-N-C4-1b	12.7	1862.0	1396.5	1228.9	50.3	35.0	112.7	200.0	46.4	-	S	UN	S	535.0
Oh and Kim (2000)	M12-N-C4-2a	12.7	1862.0	1396.5	1228.9	48.8	35.0	112.7	200.0	46.4	-	S	UN	S	697.0
Oh and Kim (2000)	M12-N-C4-2b	12.7	1862.0	1396.5	1228.9	48.8	35.0	112.7	200.0	46.4	-	S	UN	S	602.0
Oh and Kim (2000)	M12-N-C5-1a	12.7	1862.0	1396.5	1228.9	48.2	34.7	112.7	200.0	56.4	-	S	UN	S	617.0
Oh and Kim (2000)	M12-N-C5-1b	12.7	1862.0	1396.5	1228.9	48.2	34.7	112.7	200.0	56.4	-	S	UN	S	512.0
Oh and Kim (2000)	M12-N-C5-2a	12.7	1862.0	1396.5	1228.9	47.6	32.5	112.7	200.0	56.4	-	S	UN	S	561.0
Oh and Kim (2000)	M12-N-C5-2b	12.7	1862.0	1396.5	1228.9	47.6	32.5	112.7	200.0	56.4	-	S	UN	S	527.0
Oh and Kim (2000)	M12-H-C3-1a	12.7	1862.0	1396.5	1228.9	57.8	44.9	112.7	200.0	36.4	-	S	UN	S	725.0
Oh and Kim (2000)	M12-H-C3-1b	12.7	1862.0	1396.5	1228.9	57.8	44.9	112.7	200.0	36.4	-	S	UN	S	557.0
Oh and Kim (2000)	M12-H-C3-2a	12.7	1862.0	1396.5	1228.9	59.6	44.5	112.7	200.0	36.4	-	S	UN	S	658.0

Author	Specimen ID	Φ [mm]	f_{su} [MPa]	f_{si} [MPa]	f_{se} [MPa]	f_c' [MPa]	f_{ci}' [MPa]	b [mm]	h [mm]	c [mm]	s [mm]	Surface condition	Epoxy coating	Release type	L_t [mm]
Oh and Kim (2000)	M12-H-C3-2b	12.7	1862.0	1396.5	1228.9	59.6	44.5	112.7	200.0	36.4	-	S	UN	S	602.0
Oh and Kim (2000)	M12-H-C4-1a	12.7	1862.0	1396.5	1228.9	61.2	46.7	112.7	200.0	46.4	-	S	UN	S	548.0
Oh and Kim (2000)	M12-H-C4-1b	12.7	1862.0	1396.5	1228.9	61.2	46.7	112.7	200.0	46.4	-	S	UN	S	455.0
Oh and Kim (2000)	M12-H-C4-2a	12.7	1862.0	1396.5	1228.9	57.0	45.8	112.7	200.0	46.4	-	S	UN	S	587.0
Oh and Kim (2000)	M12-H-C4-2b	12.7	1862.0	1396.5	1228.9	57.0	45.8	112.7	200.0	46.4	-	S	UN	S	501.0
Oh and Kim (2000)	M12-H-C5-1a	12.7	1862.0	1396.5	1228.9	57.8	44.9	112.7	200.0	56.4	-	S	UN	S	492.0
Oh and Kim (2000)	M12-H-C5-1b	12.7	1862.0	1396.5	1228.9	57.8	44.9	112.7	200.0	56.4	-	S	UN	S	434.0
Oh and Kim (2000)	M12-H-C5-2a	12.7	1862.0	1396.5	1228.9	59.6	44.5	112.7	200.0	56.4	-	S	UN	S	533.0
Oh and Kim (2000)	M12-H-C5-2b	12.7	1862.0	1396.5	1228.9	59.6	44.5	112.7	200.0	56.4	-	S	UN	S	483.0
Oh and Kim (2000)	M15-N-C3-1a	15.2	1862.0	1396.5	1228.9	50.3	35.0	115.2	200.0	37.6	-	S	UN	S	1073.0
Oh and Kim (2000)	M15-N-C3-1b	15.2	1862.0	1396.5	1228.9	50.3	35.0	115.2	200.0	37.6	-	S	UN	S	971.0
Oh and Kim (2000)	M15-N-C3-2a	15.2	1862.0	1396.5	1228.9	48.8	35.0	115.2	200.0	37.6	-	S	UN	S	1094.0
Oh and Kim (2000)	M15-N-C3-2b	15.2	1862.0	1396.5	1228.9	48.8	35.0	115.2	200.0	37.6	-	S	UN	S	887.0
Oh and Kim (2000)	M15-N-C4-1a	15.2	1862.0	1396.5	1228.9	48.2	34.7	115.2	200.0	47.6	-	S	UN	S	868.0
Oh and Kim (2000)	M15-N-C4-1b	15.2	1862.0	1396.5	1228.9	48.2	34.7	115.2	200.0	47.6	-	S	UN	S	732.0
Oh and Kim (2000)	M15-N-C4-2a	15.2	1862.0	1396.5	1228.9	47.6	32.5	115.2	200.0	47.6	-	S	UN	S	809.0
Oh and Kim (2000)	M15-N-C4-2b	15.2	1862.0	1396.5	1228.9	47.6	32.5	115.2	200.0	47.6	-	S	UN	S	764.0
Oh and Kim (2000)	M15-N-C5-1a	15.2	1862.0	1396.5	1228.9	50.3	35.0	115.2	200.0	57.6	-	S	UN	S	727.0
Oh and Kim (2000)	M15-N-C5-1b	15.2	1862.0	1396.5	1228.9	50.3	35.0	115.2	200.0	57.6	-	S	UN	S	660.0
Oh and Kim (2000)	M15-N-C5-2a	15.2	1862.0	1396.5	1228.9	48.8	35.0	115.2	200.0	57.6	-	S	UN	S	669.0
Oh and Kim (2000)	M15-N-C5-2b	15.2	1862.0	1396.5	1228.9	48.8	35.0	115.2	200.0	57.6	-	S	UN	S	604.0
Oh and Kim (2000)	M15-H-C3-1a	15.2	1862.0	1396.5	1228.9	61.2	46.7	115.2	200.0	37.6	-	S	UN	S	904.0
Oh and Kim (2000)	M15-H-C3-1b	15.2	1862.0	1396.5	1228.9	61.2	46.7	115.2	200.0	37.6	-	S	UN	S	725.0
Oh and Kim (2000)	M15-H-C3-2a	15.2	1862.0	1396.5	1228.9	57.0	45.8	115.2	200.0	37.6	-	S	UN	S	872.0
Oh and Kim (2000)	M15-H-C3-2b	15.2	1862.0	1396.5	1228.9	57.0	45.8	115.2	200.0	37.6	-	S	UN	S	799.0
Oh and Kim (2000)	M15-H-C4-1a	15.2	1862.0	1396.5	1228.9	57.8	44.9	115.2	200.0	47.6	-	S	UN	S	762.0
Oh and Kim (2000)	M15-H-C4-1b	15.2	1862.0	1396.5	1228.9	57.8	44.9	115.2	200.0	47.6	-	S	UN	S	660.0

Author	Specimen ID	Φ [mm]	f_{su} [MPa]	f_{si} [MPa]	f_{se} [MPa]	f_c' [MPa]	f_{ci}' [MPa]	b [mm]	h [mm]	c [mm]	s [mm]	Surface condition	Epoxy coating	Release type	L_t [mm]
Oh and Kim (2000)	M15-H-C4-2a	15.2	1862.0	1396.5	1228.9	59.6	44.5	115.2	200.0	47.6	-	S	UN	S	682.0
Oh and Kim (2000)	M15-H-C4-2b	15.2	1862.0	1396.5	1228.9	59.6	44.5	115.2	200.0	47.6	-	S	UN	S	596.0
Oh and Kim (2000)	M15-H-C5-1a	15.2	1862.0	1396.5	1228.9	61.2	46.7	115.2	200.0	57.6	-	S	UN	S	557.0
Oh and Kim (2000)	M15-H-C5-1b	15.2	1862.0	1396.5	1228.9	61.2	46.7	115.2	200.0	57.6	-	S	UN	S	540.0
Oh and Kim (2000)	M15-H-C5-2a	15.2	1862.0	1396.5	1228.9	57.0	45.8	115.2	200.0	57.6	-	S	UN	S	591.0
Oh and Kim (2000)	M15-H-C5-2b	15.2	1862.0	1396.5	1228.9	57.0	45.8	115.2	200.0	57.6	-	S	UN	S	486.0
Oh and Kim (2000)	T12-N-S3a	12.7	1862.0	1396.5	1228.9	47.8	34.0	150.8	200.0	56.4	25.4	S	UN	S	808.0
Oh and Kim (2000)	T12-N-S3b	12.7	1862.0	1396.5	1228.9	47.8	34.0	150.8	200.0	56.4	25.4	S	UN	S	708.0
Oh and Kim (2000)	T12-N-S4a	12.7	1862.0	1396.5	1228.9	47.6	35.5	163.5	200.0	56.4	38.1	S	UN	S	674.0
Oh and Kim (2000)	T12-N-S4b	12.7	1862.0	1396.5	1228.9	47.6	35.5	163.5	200.0	56.4	38.1	S	UN	S	591.0
Oh and Kim (2000)	T12-N-S5a	12.7	1862.0	1396.5	1228.9	50.7	37.3	176.2	200.0	56.4	50.8	S	UN	S	632.0
Oh and Kim (2000)	T12-N-S5b	12.7	1862.0	1396.5	1228.9	50.7	37.3	176.2	200.0	56.4	50.8	S	UN	S	554.0
Oh and Kim (2000)	T12-H-S3a	12.7	1862.0	1396.5	1228.9	57.6	44.2	150.8	200.0	56.4	25.4	S	UN	S	695.0
Oh and Kim (2000)	T12-H-S3b	12.7	1862.0	1396.5	1228.9	57.6	44.2	150.8	200.0	56.4	25.4	S	UN	S	591.0
Oh and Kim (2000)	T12-H-S4a	12.7	1862.0	1396.5	1228.9	58.1	43.2	163.5	200.0	56.4	38.1	S	UN	S	595.0
Oh and Kim (2000)	T12-H-S4b	12.7	1862.0	1396.5	1228.9	58.1	43.2	163.5	200.0	56.4	38.1	S	UN	S	522.0
Oh and Kim (2000)	T12-H-S5a	12.7	1862.0	1396.5	1228.9	60.3	46.3	176.2	200.0	56.4	50.8	S	UN	S	558.0
Oh and Kim (2000)	T12-H-S5b	12.7	1862.0	1396.5	1228.9	60.3	46.3	176.2	200.0	56.4	50.8	S	UN	S	503.0
Oh and Kim (2000)	T15-N-S3a	15.2	1862.0	1396.5	1228.9	49.1	37.6	160.8	200.0	57.6	30.4	S	UN	S	997.0
Oh and Kim (2000)	T15-N-S3b	15.2	1862.0	1396.5	1228.9	49.1	37.6	160.8	200.0	57.6	30.4	S	UN	S	872.0
Oh and Kim (2000)	T15-N-S4a	15.2	1862.0	1396.5	1228.9	48.8	34.8	176.0	200.0	57.6	45.6	S	UN	S	840.0
Oh and Kim (2000)	T15-N-S4b	15.2	1862.0	1396.5	1228.9	48.8	34.8	176.0	200.0	57.6	45.6	S	UN	S	750.0
Oh and Kim (2000)	T15-N-S5a	15.2	1862.0	1396.5	1228.9	47.4	33.4	191.2	200.0	57.6	60.8	S	UN	S	782.0
Oh and Kim (2000)	T15-N-S5b	15.2	1862.0	1396.5	1228.9	47.4	33.4	191.2	200.0	57.6	60.8	S	UN	S	718.0
Oh and Kim (2000)	T15-H-S3a	15.2	1862.0	1396.5	1228.9	58.9	47.2	160.8	200.0	57.6	30.4	S	UN	S	889.0
Oh and Kim (2000)	T15-H-S3b	15.2	1862.0	1396.5	1228.9	58.9	47.2	160.8	200.0	57.6	30.4	S	UN	S	780.0
Oh and Kim (2000)	T15-H-S4a	15.2	1862.0	1396.5	1228.9	61.2	46.9	176.0	200.0	57.6	45.6	S	UN	S	725.0

Author	Specimen ID	Φ [mm]	f_{su} [MPa]	f_{si} [MPa]	f_{se} [MPa]	f_c' [MPa]	f_{ci}' [MPa]	b [mm]	h [mm]	c [mm]	s [mm]	Surface condition	Epoxy coating	Release type	L_t [mm]
Oh and Kim (2000)	T15-H-S4b	15.2	1862.0	1396.5	1228.9	61.2	46.9	176.0	200.0	57.6	45.6	S	UN	S	635.0
Oh and Kim (2000)	T15-H-S5a	15.2	1862.0	1396.5	1228.9	57.1	43.9	191.2	200.0	57.6	60.8	S	UN	S	662.0
Oh and Kim (2000)	T15-H-S5b	15.2	1862.0	1396.5	1228.9	57.1	43.9	191.2	200.0	57.6	60.8	S	UN	S	612.0
Kahn et al. (2002)	G2AN	15.2	1862.0	1314.0	1156.3	70.0	51.1	459.0	914.0	50.8	35.6	S	UN	S	406.0
Kahn et al. (2002)	G2AS	15.2	1862.0	1314.0	1156.3	70.0	51.1	459.0	914.0	50.8	35.6	S	UN	S	432.0
Kahn et al. (2002)	G2BN	15.2	1862.0	1314.0	1156.3	70.0	51.1	459.0	914.0	50.8	35.6	S	UN	S	406.0
Kahn et al. (2002)	G2BS	15.2	1862.0	1314.0	1156.3	70.0	51.1	459.0	914.0	50.8	35.6	S	UN	S	406.0
Kahn et al. (2002)	G4AN	15.2	1862.0	1314.0	1156.3	100.0	73.0	459.0	914.0	50.8	35.6	S	UN	S	330.0
Kahn et al. (2002)	G4AS	15.2	1862.0	1314.0	1156.3	100.0	73.0	459.0	914.0	50.8	35.6	S	UN	S	368.0
Kahn et al. (2002)	G4BN	15.2	1862.0	1314.0	1156.3	100.0	73.0	459.0	914.0	50.8	35.6	S	UN	S	381.0
Kahn et al. (2002)	G4BS	15.2	1862.0	1314.0	1156.3	100.0	73.0	459.0	914.0	50.8	35.6	S	UN	S	318.0
Barnes et al. (2003)	L0BA	15.2	1862.0	1395.0	1170.0	41.4	29.2	406.4	711.2	50.8	35.6	S	UN	S	584.2
Barnes et al. (2003)	L0BB	15.2	1862.0	1395.0	1170.0	41.4	29.2	406.4	711.2	50.8	35.6	S	UN	S	482.6
Barnes et al. (2003)	L0BC	15.2	1862.0	1395.0	1170.0	41.4	29.2	406.4	711.2	50.8	35.6	S	UN	S	635.0
Barnes et al. (2003)	L0BD	15.2	1862.0	1395.0	1170.0	41.4	29.2	406.4	711.2	50.8	35.6	S	UN	S	533.4
Barnes et al. (2003)	L4BA-1	15.2	1862.0	1395.0	1170.0	39.2	31.0	406.4	711.2	50.8	35.6	S	UN	S	355.6
Barnes et al. (2003)	L4BB-1	15.2	1862.0	1395.0	1170.0	39.2	31.0	406.4	711.2	50.8	35.6	S	UN	S	558.8
Barnes et al. (2003)	L4BC-1	15.2	1862.0	1395.0	1170.0	39.2	31.0	406.4	711.2	50.8	35.6	S	UN	S	381.0
Barnes et al. (2003)	L6BA-1	15.2	1862.0	1395.0	1170.0	47.3	32.5	406.4	711.2	50.8	35.6	S	UN	S	533.4
Barnes et al. (2003)	L6BB-1	15.2	1862.0	1395.0	1170.0	47.3	32.5	406.4	711.2	50.8	35.6	S	UN	S	431.8
Barnes et al. (2003)	L6BC-1	15.2	1862.0	1395.0	1170.0	47.3	32.5	406.4	711.2	50.8	35.6	S	UN	S	609.6
Barnes et al. (2003)	L6BD-1	15.2	1862.0	1395.0	1170.0	47.3	32.5	406.4	711.2	50.8	35.6	S	UN	S	482.6
Barnes et al. (2003)	M0BA	15.2	1862.0	1395.0	1170.0	73.9	45.6	406.4	711.2	50.8	35.6	S	UN	S	431.8
Barnes et al. (2003)	M0BB	15.2	1862.0	1395.0	1170.0	73.9	45.6	406.4	711.2	50.8	35.6	S	UN	S	457.2
Barnes et al. (2003)	M0BC	15.2	1862.0	1395.0	1170.0	73.9	45.6	406.4	711.2	50.8	35.6	S	UN	S	406.4
Barnes et al. (2003)	M0BD	15.2	1862.0	1395.0	1170.0	73.9	45.6	406.4	711.2	50.8	35.6	S	UN	S	381.0
Barnes et al. (2003)	M4BA-1	15.2	1862.0	1395.0	1170.0	74.0	47.6	406.4	711.2	50.8	35.6	S	UN	S	254.0

Author	Specimen ID	Φ [mm]	f_{su} [MPa]	f_{si} [MPa]	f_{se} [MPa]	f_c' [MPa]	f_{ci}' [MPa]	b [mm]	h [mm]	c [mm]	s [mm]	Surface condition	Epoxy coating	Release type	L_t [mm]
Barnes et al. (2003)	M4BB-1	15.2	1862.0	1395.0	1170.0	74.0	47.6	406.4	711.2	50.8	35.6	S	UN	S	279.4
Barnes et al. (2003)	M4BC-1	15.2	1862.0	1395.0	1170.0	74.0	47.6	406.4	711.2	50.8	35.6	S	UN	S	304.8
Barnes et al. (2003)	M4BD-1	15.2	1862.0	1395.0	1170.0	74.0	47.6	406.4	711.2	50.8	35.6	S	UN	S	279.4
Barnes et al. (2003)	M9BA-1	15.2	1862.0	1395.0	1170.0	88.8	54.4	406.4	711.2	50.8	35.6	S	UN	S	558.8
Barnes et al. (2003)	M9BB-1	15.2	1862.0	1395.0	1170.0	88.8	54.4	406.4	711.2	50.8	35.6	S	UN	S	279.4
Barnes et al. (2003)	M9BC-1	15.2	1862.0	1395.0	1170.0	88.8	54.4	406.4	711.2	50.8	35.6	S	UN	S	457.2
Barnes et al. (2003)	M9BD-1	15.2	1862.0	1395.0	1170.0	88.8	54.4	406.4	711.2	50.8	35.6	S	UN	S	533.4
Barnes et al. (2003)	H0BA	15.2	1862.0	1395.0	1170.0	86.9	76.1	406.4	711.2	50.8	35.6	S	UN	S	406.4
Barnes et al. (2003)	H0BB	15.2	1862.0	1395.0	1170.0	86.9	76.1	406.4	711.2	50.8	35.6	S	UN	S	355.6
Barnes et al. (2003)	H0BC	15.2	1862.0	1395.0	1170.0	87.5	76.1	406.4	711.2	50.8	35.6	S	UN	S	330.2
Barnes et al. (2003)	H0BD	15.2	1862.0	1395.0	1170.0	87.5	76.1	406.4	711.2	50.8	35.6	S	UN	S	406.4
Barnes et al. (2003)	H4BA-1	15.2	1862.0	1395.0	1170.0	77.5	66.6	406.4	711.2	50.8	35.6	S	UN	S	304.8
Barnes et al. (2003)	H4BB-1	15.2	1862.0	1395.0	1170.0	77.5	66.6	406.4	711.2	50.8	35.6	S	UN	S	254.0
Barnes et al. (2003)	H4BC-1	15.2	1862.0	1395.0	1170.0	77.5	66.6	406.4	711.2	50.8	35.6	S	UN	S	254.0
Barnes et al. (2003)	H4BD-1	15.2	1862.0	1395.0	1170.0	77.5	66.6	406.4	711.2	50.8	35.6	S	UN	S	330.2
Barnes et al. (2003)	H9BA-1	15.2	1862.0	1395.0	1170.0	95.4	64.1	406.4	711.2	50.8	35.6	S	UN	S	355.6
Barnes et al. (2003)	H9BB-1	15.2	1862.0	1395.0	1170.0	95.4	64.1	406.4	711.2	50.8	35.6	S	UN	S	330.2
Barnes et al. (2003)	H9BC-1	15.2	1862.0	1395.0	1170.0	95.4	64.1	406.4	711.2	50.8	35.6	S	UN	S	381.0
Barnes et al. (2003)	H9BD-1	15.2	1862.0	1395.0	1170.0	95.4	64.1	406.4	711.2	50.8	35.6	S	UN	S	381.0
Barnes et al. (2003)	LORA	15.2	1862.0	1395.0	1170.0	42.9	31.3	406.4	711.2	50.8	35.6	R	UN	S	406.4
Barnes et al. (2003)	LORB	15.2	1862.0	1395.0	1170.0	42.9	31.3	406.4	711.2	50.8	35.6	R	UN	S	381.0
Barnes et al. (2003)	LORC	15.2	1862.0	1395.0	1170.0	42.9	31.3	406.4	711.2	50.8	35.6	R	UN	S	355.6
Barnes et al. (2003)	LORD	15.2	1862.0	1395.0	1170.0	42.9	31.3	406.4	711.2	50.8	35.6	R	UN	S	406.4
Barnes et al. (2003)	L4RA-1	15.2	1862.0	1395.0	1170.0	37.5	27.4	406.4	711.2	50.8	35.6	R	UN	S	355.6
Barnes et al. (2003)	L4RB-1	15.2	1862.0	1395.0	1170.0	37.5	27.4	406.4	711.2	50.8	35.6	R	UN	S	304.8
Barnes et al. (2003)	L4RC-1	15.2	1862.0	1395.0	1170.0	37.5	27.4	406.4	711.2	50.8	35.6	R	UN	S	406.4
Barnes et al. (2003)	L4RD-1	15.2	1862.0	1395.0	1170.0	37.5	27.4	406.4	711.2	50.8	35.6	R	UN	S	304.8

Author	Specimen ID	Φ [mm]	f_{su} [MPa]	f_{si} [MPa]	f_{se} [MPa]	f_c' [MPa]	f_{ci}' [MPa]	b [mm]	h [mm]	c [mm]	s [mm]	Surface condition	Epoxy coating	Release type	L_t [mm]
Barnes et al. (2003)	L6RA-1	15.2	1862.0	1395.0	1170.0	43.7	31.9	406.4	711.2	50.8	35.6	R	UN	S	406.4
Barnes et al. (2003)	L6RB-1	15.2	1862.0	1395.0	1170.0	43.7	31.9	406.4	711.2	50.8	35.6	R	UN	S	330.2
Barnes et al. (2003)	L6RC-1	15.2	1862.0	1395.0	1170.0	43.7	31.9	406.4	711.2	50.8	35.6	R	UN	S	254.0
Barnes et al. (2003)	L6RD-1	15.2	1862.0	1395.0	1170.0	43.7	31.9	406.4	711.2	50.8	35.6	R	UN	S	355.6
Barnes et al. (2003)	MORA	15.2	1862.0	1395.0	1170.0	81.0	50.3	406.4	711.2	50.8	35.6	R	UN	S	381.0
Barnes et al. (2003)	MORB	15.2	1862.0	1395.0	1170.0	81.0	50.3	406.4	711.2	50.8	35.6	R	UN	S	558.8
Barnes et al. (2003)	MORC	15.2	1862.0	1395.0	1170.0	81.0	50.3	406.4	711.2	50.8	35.6	R	UN	S	609.6
Barnes et al. (2003)	MORD	15.2	1862.0	1395.0	1170.0	81.0	50.3	406.4	711.2	50.8	35.6	R	UN	S	482.6
Barnes et al. (2003)	M4RA-1	15.2	1862.0	1395.0	1170.0	76.2	54.8	406.4	711.2	50.8	35.6	R	UN	S	254.0
Barnes et al. (2003)	M4RB-1	15.2	1862.0	1395.0	1170.0	76.2	54.8	406.4	711.2	50.8	35.6	R	UN	S	330.2
Barnes et al. (2003)	M4RC-1	15.2	1862.0	1395.0	1170.0	76.2	54.8	406.4	711.2	50.8	35.6	R	UN	S	431.8
Barnes et al. (2003)	M4RD-1	15.2	1862.0	1395.0	1170.0	76.2	54.8	406.4	711.2	50.8	35.6	R	UN	S	254.0
Barnes et al. (2003)	M9RA-1	15.2	1862.0	1395.0	1170.0	85.6	52.6	406.4	711.2	50.8	35.6	R	UN	S	431.8
Barnes et al. (2003)	M9RB-1	15.2	1862.0	1395.0	1170.0	85.6	52.6	406.4	711.2	50.8	35.6	R	UN	S	330.2
Barnes et al. (2003)	M9RC-1	15.2	1862.0	1395.0	1170.0	85.6	52.6	406.4	711.2	50.8	35.6	R	UN	S	228.6
Barnes et al. (2003)	M9RD-1	15.2	1862.0	1395.0	1170.0	85.6	52.6	406.4	711.2	50.8	35.6	R	UN	S	279.4
Barnes et al. (2003)	H0RA	15.2	1862.0	1395.0	1170.0	97.7	62.2	406.4	711.2	50.8	35.6	R	UN	S	482.6
Barnes et al. (2003)	H0RB	15.2	1862.0	1395.0	1170.0	97.7	62.2	406.4	711.2	50.8	35.6	R	UN	S	482.6
Barnes et al. (2003)	H0RC	15.2	1862.0	1395.0	1170.0	97.7	62.2	406.4	711.2	50.8	35.6	R	UN	S	609.6
Barnes et al. (2003)	H0RD	15.2	1862.0	1395.0	1170.0	97.7	62.2	406.4	711.2	50.8	35.6	R	UN	S	381.0
Barnes et al. (2003)	H4RA-1	15.2	1862.0	1395.0	1170.0	93.1	75.2	406.4	711.2	50.8	35.6	R	UN	S	228.6
Barnes et al. (2003)	H4RB-1	15.2	1862.0	1395.0	1170.0	93.1	75.2	406.4	711.2	50.8	35.6	R	UN	S	228.6
Barnes et al. (2003)	H4RC-1	15.2	1862.0	1395.0	1170.0	93.1	75.2	406.4	711.2	50.8	35.6	R	UN	S	203.2
Barnes et al. (2003)	H4RD-1	15.2	1862.0	1395.0	1170.0	93.1	75.2	406.4	711.2	50.8	35.6	R	UN	S	254.0
Barnes et al. (2003)	H9RA-1	15.2	1862.0	1395.0	1170.0	85.3	54.2	406.4	711.2	50.8	35.6	R	UN	S	330.2
Barnes et al. (2003)	H9RB-1	15.2	1862.0	1395.0	1170.0	85.3	54.2	406.4	711.2	50.8	35.6	R	UN	S	355.6
Barnes et al. (2003)	H9RC-1	15.2	1862.0	1395.0	1170.0	102.0	63.9	406.4	711.2	50.8	35.6	R	UN	S	330.2

Author	Specimen ID	Φ [mm]	f_{su} [MPa]	f_{si} [MPa]	f_{se} [MPa]	f_c' [MPa]	f_{ci}' [MPa]	b [mm]	h [mm]	c [mm]	s [mm]	Surface condition	Epoxy coating	Release type	L_t [mm]
Barnes et al. (2003)	H9RD-1	15.2	1862.0	1395.0	1170.0	102.0	63.9	406.4	711.2	50.8	35.6	R	UN	S	228.6
Kose and Burkett (2005)	L0R0-1	15.2	1862.0	1396.5	1228.9	37.5	31.3	421.6	711.2	50.8	35.6	R	UN	S	406.4
Kose and Burkett (2005)	L0R0-2	15.2	1862.0	1396.5	1228.9	37.5	31.3	421.6	711.2	50.8	35.6	R	UN	S	457.2
Kose and Burkett (2005)	L0R1-3	15.2	1862.0	1396.5	1228.9	37.5	31.3	421.6	711.2	50.8	35.6	R	UN	S	419.1
Kose and Burkett (2005)	L0R1-4	15.2	1862.0	1396.5	1228.9	37.5	31.3	421.6	711.2	50.8	35.6	R	UN	S	393.7
Kose and Burkett (2005)	L4R0-1	15.2	1862.0	1396.5	1228.9	34.8	26.1	421.6	711.2	50.8	35.6	R	UN	S	368.3
Kose and Burkett (2005)	L4R0-2	15.2	1862.0	1396.5	1228.9	34.8	26.1	421.6	711.2	50.8	35.6	R	UN	S	698.5
Kose and Burkett (2005)	L4R1-3	15.2	1862.0	1396.5	1228.9	34.8	26.1	421.6	711.2	50.8	35.6	R	UN	S	774.7
Kose and Burkett (2005)	L6R0-1	15.2	1862.0	1396.5	1228.9	51.6	31.9	421.6	711.2	50.8	35.6	R	UN	S	495.3
Kose and Burkett (2005)	L6R0-2	15.2	1862.0	1396.5	1228.9	51.6	31.9	421.6	711.2	50.8	35.6	R	UN	S	406.4
Kose and Burkett (2005)	L6R1-3	15.2	1862.0	1396.5	1228.9	51.6	31.9	421.6	711.2	50.8	35.6	R	UN	S	368.3
Kose and Burkett (2005)	L6R1-4	15.2	1862.0	1396.5	1228.9	51.6	31.9	421.6	711.2	50.8	35.6	R	UN	S	508.0
Oh et al. (2006)	M12-N-C3-a	12.7	1862.0	1402.1	1233.8	47.9	33.6	112.7	200.0	36.4	-	S	UN	S	851.0
Oh et al. (2006)	M12-N-C3-b	12.7	1862.0	1402.1	1233.8	47.9	33.6	112.7	200.0	36.4	-	S	UN	S	712.0
Oh et al. (2006)	M12-N-C4-a	12.7	1862.0	1391.9	1224.9	49.6	35.0	112.7	200.0	46.4	-	S	UN	S	669.0
Oh et al. (2006)	M12-N-C4-b	12.7	1862.0	1391.9	1224.9	49.6	35.0	112.7	200.0	46.4	-	S	UN	S	569.0
Oh et al. (2006)	M12-N-C5-a	12.7	1862.0	1402.7	1234.4	47.9	33.6	112.7	200.0	56.4	-	S	UN	S	589.0
Oh et al. (2006)	M12-N-C5-b	12.7	1862.0	1402.7	1234.4	47.9	33.6	112.7	200.0	56.4	-	S	UN	S	520.0
Oh et al. (2006)	M12-H-C3-a	12.7	1862.0	1359.3	1196.2	58.7	44.7	112.7	200.0	36.4	-	S	UN	S	692.0
Oh et al. (2006)	M12-H-C3-b	12.7	1862.0	1359.3	1196.2	58.7	44.7	112.7	200.0	36.4	-	S	UN	S	580.0
Oh et al. (2006)	M12-H-C4-a	12.7	1862.0	1375.1	1210.1	59.1	46.3	112.7	200.0	46.4	-	S	UN	S	568.0
Oh et al. (2006)	M12-H-C4-b	12.7	1862.0	1375.1	1210.1	59.1	46.3	112.7	200.0	46.4	-	S	UN	S	478.0
Oh et al. (2006)	M12-H-C5-a	12.7	1862.0	1394.7	1227.3	58.7	44.7	112.7	200.0	56.4	-	S	UN	S	513.0
Oh et al. (2006)	M12-H-C5-b	12.7	1862.0	1394.7	1227.3	58.7	44.7	112.7	200.0	56.4	-	S	UN	S	459.0
Oh et al. (2006)	M15-N-C3-a	15.2	1862.0	1377.1	1211.8	49.6	35.0	115.2	200.0	37.6	-	S	UN	S	1084.0
Oh et al. (2006)	M15-N-C3-b	15.2	1862.0	1377.1	1211.8	49.6	35.0	115.2	200.0	37.6	-	S	UN	S	929.0
Oh et al. (2006)	M15-N-C4-a	15.2	1862.0	1392.5	1225.4	47.9	33.6	115.2	200.0	47.6	-	S	UN	S	839.0

Author	Specimen ID	Φ [mm]	f_{su} [MPa]	f_{si} [MPa]	f_{se} [MPa]	f_c' [MPa]	f_{ci}' [MPa]	b [mm]	h [mm]	c [mm]	s [mm]	Surface condition	Epoxy coating	Release type	L_t [mm]
Oh et al. (2006)	M15-N-C4-b	15.2	1862.0	1392.5	1225.4	47.9	33.6	115.2	200.0	47.6	-	S	UN	S	748.0
Oh et al. (2006)	M15-N-C5-a	15.2	1862.0	1393.2	1226.0	49.6	35.0	115.2	200.0	57.6	-	S	UN	S	698.0
Oh et al. (2006)	M15-N-C5-b	15.2	1862.0	1393.2	1226.0	49.6	35.0	115.2	200.0	57.6	-	S	UN	S	632.0
Oh et al. (2006)	M15-H-C3-a	15.2	1862.0	1357.5	1194.6	59.1	46.4	115.2	200.0	37.6	-	S	UN	S	888.0
Oh et al. (2006)	M15-H-C3-b	15.2	1862.0	1357.5	1194.6	59.1	46.4	115.2	200.0	37.6	-	S	UN	S	762.0
Oh et al. (2006)	M15-H-C4-a	15.2	1862.0	1364.9	1201.1	58.7	44.7	115.2	200.0	47.6	-	S	UN	S	722.0
Oh et al. (2006)	M15-H-C4-b	15.2	1862.0	1364.9	1201.1	58.7	44.7	115.2	200.0	47.6	-	S	UN	S	628.0
Oh et al. (2006)	M15-H-C5-a	15.2	1862.0	1384.4	1218.3	59.1	45.6	115.2	200.0	57.6	-	S	UN	S	574.0
Oh et al. (2006)	M15-H-C5-b	15.2	1862.0	1384.4	1218.3	59.1	45.6	115.2	200.0	57.6	-	S	UN	S	513.0
Oh et al. (2006)	T12-N-S3a	12.7	1862.0	1398.4	1230.6	47.8	34.0	163.5	200.0	56.4	25.4	S	UN	S	808.0
Oh et al. (2006)	T12-N-S3b	12.7	1862.0	1398.4	1230.6	47.8	34.0	163.5	200.0	56.4	25.4	S	UN	S	708.0
Oh et al. (2006)	T12-N-S4a	12.7	1862.0	1418.0	1247.8	47.6	35.5	176.2	200.0	56.4	38.1	S	UN	S	674.0
Oh et al. (2006)	T12-N-S4b	12.7	1862.0	1418.0	1247.8	47.6	35.5	176.2	200.0	56.4	38.1	S	UN	S	591.0
Oh et al. (2006)	T12-N-S5a	12.7	1862.0	1389.1	1222.4	50.7	37.3	188.9	200.0	56.4	50.8	S	UN	S	632.0
Oh et al. (2006)	T12-N-S5b	12.7	1862.0	1389.1	1222.4	50.7	37.3	188.9	200.0	56.4	50.8	S	UN	S	554.0
Oh et al. (2006)	T12-H-S3a	12.7	1862.0	1374.2	1209.3	57.6	44.2	163.5	200.0	56.4	25.4	S	UN	S	695.0
Oh et al. (2006)	T12-H-S3b	12.7	1862.0	1374.2	1209.3	57.6	44.2	163.5	200.0	56.4	25.4	S	UN	S	591.0
Oh et al. (2006)	T12-H-S4a	12.7	1862.0	1377.9	1212.6	58.1	43.2	176.2	200.0	56.4	38.1	S	UN	S	595.0
Oh et al. (2006)	T12-H-S4b	12.7	1862.0	1377.9	1212.6	58.1	43.2	176.2	200.0	56.4	38.1	S	UN	S	522.0
Oh et al. (2006)	T12-H-S5a	12.7	1862.0	1392.8	1225.7	60.3	46.3	188.9	200.0	56.4	50.8	S	UN	S	558.0
Oh et al. (2006)	T12-H-S5b	12.7	1862.0	1392.8	1225.7	60.3	46.3	188.9	200.0	56.4	50.8	S	UN	S	503.0
Oh et al. (2006)	T15-N-S3a	15.2	1862.0	1357.4	1194.5	49.1	37.6	160.8	200.0	57.6	30.4	S	UN	S	997.0
Oh et al. (2006)	T15-N-S3b	15.2	1862.0	1357.4	1194.5	49.1	37.6	160.8	200.0	57.6	30.4	S	UN	S	872.0
Oh et al. (2006)	T15-N-S4a	15.2	1862.0	1361.1	1197.8	48.8	34.8	176.0	200.0	57.6	45.6	S	UN	S	840.0
Oh et al. (2006)	T15-N-S4b	15.2	1862.0	1361.1	1197.8	48.8	34.8	176.0	200.0	57.6	45.6	S	UN	S	750.0
Oh et al. (2006)	T15-N-S5a	15.2	1862.0	1381.6	1215.8	47.4	33.4	191.2	200.0	57.6	60.8	S	UN	S	782.0
Oh et al. (2006)	T15-N-S5b	15.2	1862.0	1381.6	1215.8	47.4	33.4	191.2	200.0	57.6	60.8	S	UN	S	718.0

Author	Specimen ID	Φ [mm]	f_{su} [MPa]	f_{si} [MPa]	f_{se} [MPa]	f_c' [MPa]	f_{ci}' [MPa]	b [mm]	h [mm]	c [mm]	s [mm]	Surface condition	Epoxy coating	Release type	L_t [mm]
Oh et al. (2006)	T15-H-S3a	15.2	1862.0	1376.0	1210.9	58.9	47.2	160.8	200.0	57.6	30.4	S	UN	S	889.0
Oh et al. (2006)	T15-H-S3b	15.2	1862.0	1376.0	1210.9	58.9	47.2	160.8	200.0	57.6	30.4	S	UN	S	780.0
Oh et al. (2006)	T15-H-S4a	15.2	1862.0	1400.2	1232.2	61.2	46.9	176.0	200.0	57.6	45.6	S	UN	S	725.0
Oh et al. (2006)	T15-H-S4b	15.2	1862.0	1400.2	1232.2	61.2	46.9	176.0	200.0	57.6	45.6	S	UN	S	635.0
Oh et al. (2006)	T15-H-S5a	15.2	1862.0	1377.9	1212.6	57.1	43.9	191.2	200.0	57.6	60.8	S	UN	S	662.0
Oh et al. (2006)	T15-H-S5b	15.2	1862.0	1377.9	1212.6	57.1	43.9	191.2	200.0	57.6	60.8	S	UN	S	612.0
Martì-Vargas et al. (2007)	M-350-0.50	12.7	1862.0	1396.5	1117.2	35.8	26.1	100.0	100.0	50.0	-	S	UN	G	550.0
Martì-Vargas et al. (2007)	M-350-0.45	12.7	1862.0	1396.5	1117.2	51.1	37.3	100.0	100.0	50.0	-	S	UN	G	550.0
Martì-Vargas et al. (2007)	M-350-0.40	12.7	1862.0	1396.5	1117.2	64.0	46.7	100.0	100.0	50.0	-	S	UN	G	550.0
Martì-Vargas et al. (2007)	M-400-0.50	12.7	1862.0	1396.5	1117.2	33.2	24.2	100.0	100.0	50.0	-	S	UN	G	650.0
Martì-Vargas et al. (2007)	M-400-0.45	12.7	1862.0	1396.5	1117.2	38.7	28.3	100.0	100.0	50.0	-	S	UN	G	550.0
Martì-Vargas et al. (2007)	M-400-0.40	12.7	1862.0	1396.5	1117.2	56.7	41.4	100.0	100.0	50.0	-	S	UN	G	550.0
Martì-Vargas et al. (2007)	M-400-0.35	12.7	1862.0	1396.5	1117.2	62.1	45.3	100.0	100.0	50.0	-	S	UN	G	500.0
Martì-Vargas et al. (2007)	M-450-0.40	12.7	1862.0	1396.5	1117.2	49.7	36.3	100.0	100.0	50.0	-	S	UN	G	550.0
Martì-Vargas et al. (2007)	M-450-0.35	12.7	1862.0	1396.5	1117.2	63.8	46.6	100.0	100.0	50.0	-	S	UN	G	500.0
Martì-Vargas et al. (2007)	M-500-0.40	12.7	1862.0	1396.5	1117.2	42.2	30.8	100.0	100.0	50.0	-	S	UN	G	600.0
Martì-Vargas et al. (2007)	M-500-0.35	12.7	1862.0	1396.5	1117.2	63.8	46.6	100.0	100.0	50.0	-	S	UN	G	450.0
Martì-Vargas et al. (2007)	M-500-0.30	12.7	1862.0	1396.5	1117.2	75.1	54.8	100.0	100.0	50.0	-	S	UN	G	400.0
Dang et al. (2017)	M1-S1-1a	18.0	1862.0	1335.6	1175.3	64.1	40.9	165.0	305.0	50.0	-	S	UN	G	685.0
Dang et al. (2017)	M1-S1-1b	18.0	1862.0	1335.6	1175.3	64.1	40.9	165.0	305.0	50.0	-	S	UN	G	720.0
Dang et al. (2017)	M1-S1-2a	18.0	1862.0	1335.6	1175.3	64.1	40.9	165.0	305.0	50.0	-	S	UN	G	700.0
Dang et al. (2017)	M1-S1-2b	18.0	1862.0	1335.6	1175.3	64.1	40.9	165.0	305.0	50.0	-	S	UN	G	690.0
Dang et al. (2017)	M1-S1-3a	18.0	1862.0	1338.3	1177.7	66.9	45.6	165.0	305.0	50.0	-	S	UN	G	640.0
Dang et al. (2017)	M1-S1-3b	18.0	1862.0	1338.3	1177.7	66.9	45.6	165.0	305.0	50.0	-	S	UN	G	590.0
Dang et al. (2017)	M1-S1-4a	18.0	1862.0	1338.3	1177.7	66.9	45.6	165.0	305.0	50.0	-	S	UN	G	660.0
Dang et al. (2017)	M1-S1-4b	18.0	1862.0	1338.3	1177.7	66.9	45.6	165.0	305.0	50.0	-	S	UN	G	635.0
Dang et al. (2017)	M2-S1-1a	18.0	1862.0	1348.0	1186.2	94.5	65.4	165.0	305.0	50.0	-	S	UN	G	590.0

Author	Specimen ID	Φ [mm]	f_{su} [MPa]	f_{si} [MPa]	f_{se} [MPa]	f_c' [MPa]	f_{ci}' [MPa]	b [mm]	b [mm]	c [mm]	s [mm]	Surface condition	Epoxy coating	Release type	L_t [mm]
Dang et al. (2017)	M2-S1-1b	18.0	1862.0	1348.0	1186.2	94.5	65.4	165.0	305.0	50.0	-	S	UN	G	575.0
Dang et al. (2017)	M2-S1-2a	18.0	1862.0	1348.0	1186.2	94.5	65.4	165.0	305.0	50.0	-	S	UN	G	520.0
Dang et al. (2017)	M2-S1-2b	18.0	1862.0	1348.0	1186.2	94.5	65.4	165.0	305.0	50.0	-	S	UN	G	530.0
Dang et al. (2017)	M2-S1-3a	18.0	1862.0	1345.9	1184.4	91.0	61.3	165.0	305.0	50.0	-	S	UN	G	615.0
Dang et al. (2017)	M2-S1-3b	18.0	1862.0	1345.9	1184.4	91.0	61.3	165.0	305.0	50.0	-	S	UN	G	655.0
Dang et al. (2017)	M2-S1-4a	18.0	1862.0	1345.9	1184.4	91.0	61.3	165.0	305.0	50.0	-	S	UN	G	625.0
Dang et al. (2017)	M2-S1-4b	18.0	1862.0	1345.9	1184.4	91.0	61.3	165.0	305.0	50.0	-	S	UN	G	525.0
Dang et al. (2017)	M2-S2-1a	18.0	1862.0	1298.3	1142.5	84.8	66.8	165.0	305.0	50.0	32.0	S	UN	G	585.0
Dang et al. (2017)	M2-S2-1b	18.0	1862.0	1298.3	1142.5	84.8	66.8	165.0	305.0	50.0	32.0	S	UN	G	570.0
Dang et al. (2017)	M2-S2-2a	18.0	1862.0	1298.3	1142.5	84.8	66.8	165.0	305.0	50.0	32.0	S	UN	G	670.0
Dang et al. (2017)	M2-S2-2b	18.0	1862.0	1298.3	1142.5	84.8	66.8	165.0	305.0	50.0	32.0	S	UN	G	675.0
Dang et al. (2017)	M2-S2-3a	18.0	1862.0	1299.0	1143.1	91.7	68.1	165.0	305.0	50.0	32.0	S	UN	G	585.0
Dang et al. (2017)	M2-S2-3b	18.0	1862.0	1299.0	1143.1	91.7	68.1	165.0	305.0	50.0	32.0	S	UN	G	550.0
Dang et al. (2017)	M2-S2-4a	18.0	1862.0	1299.0	1143.1	91.7	68.1	165.0	305.0	50.0	32.0	S	UN	G	585.0
Dang et al. (2017)	M2-S2-4b	18.0	1862.0	1299.0	1143.1	91.7	68.1	165.0	305.0	50.0	32.0	S	UN	G	500.0

* grey values are assumed data, derived from publications

Total: 555 data points

Nomenclature:

Φ = tendon diameter (all experimental tests involve 7-wire strands)
f_{su} = ultimate tensile strength of the tendon
f_{si} = jacking stress of the tendon at release
f_{se} = tendon stress after allowance of all prestress losses
f_c' = concrete compressive strength at 28 days
f_{ci}' = concrete compressive strength at release
b = width of the concrete section
h = height of the concrete section
c = concrete cover thickness
s = tendon clear spacing
L_t = transmission length of the tendon

Surface condition: S = Smooth; R = Rusted

Epoxy coating: UN = Uncoated tendon; CL = Coated tendon with low level of grit; CM = Coated medium level; CH = Coated high level

Release type: S = Sudden; G = Gradual

ANNEX B

ANCHORAGE LENGTH DATABASE

Author	Specimen ID	Φ [mm]	f_{ps} [MPa]	f_{si} [MPa]	f_{se} [MPa]	f_c' [MPa]	f_{ci}' [MPa]	b [mm]	h [mm]	c [mm]	s [mm]	Surface condition	Epoxy coating	Release type	Failure mode	L_b [mm]
Hanson and Kaar (1959)	1_1	6.4	1503.1	1104.8	972.2	41.6	31.0	152.4	218.7	38.1	N.A.	S	UN	S	B	685.8
Hanson and Kaar (1959)	1_2	6.4	1613.4	1104.8	972.2	45.6	31.0	152.4	216.9	38.1	N.A.	S	UN	S	B	939.8
Hanson and Kaar (1959)	1_3	6.4	1613.4	1104.8	972.2	53.8	31.0	152.4	217.4	38.1	N.A.	S	UN	S	B	1066.8
Hanson and Kaar (1959)	1_4	6.4	1723.8	1104.8	972.2	41.6	31.0	152.4	222.5	38.1	N.A.	S	UN	S	F	1219.2
Hanson and Kaar (1959)	1_5	6.4	1723.8	1104.8	972.2	41.6	31.0	152.4	220.2	76.2	N.A.	S	UN	S	F	2286.0
Hanson and Kaar (1959)	1_6	6.4	1723.8	1104.8	972.2	41.2	31.0	152.4	220.5	76.2	N.A.	S	UN	S	F	4419.6
Hanson and Kaar (1959)	1_7	9.5	1289.4	1016.2	894.3	39.5	31.0	152.4	217.4	76.2	N.A.	S	UN	S	B	685.8
Hanson and Kaar (1959)	1_8	9.5	1454.8	1016.2	894.3	39.5	31.0	152.4	219.2	76.2	N.A.	S	UN	S	B	1219.2
Hanson and Kaar (1959)	1_9	9.5	1703.1	1016.2	894.3	39.5	31.0	152.4	219.7	76.2	N.A.	S	UN	S	F	2286.0
Hanson and Kaar (1959)	1_10	9.5	1144.6	1133.0	997.0	35.4	31.0	152.4	218.4	76.2	N.A.	S	UN	S	F	4419.6
Hanson and Kaar (1959)	1_11	12.7	1144.6	1159.6	1020.5	38.2	31.0	152.4	213.4	76.2	N.A.	S	UN	S	B	838.2
Hanson and Kaar (1959)	1_12	12.7	1241.1	1034.3	910.1	38.6	31.0	154.9	215.9	77.5	N.A.	S	UN	S	B	914.4
Hanson and Kaar (1959)	1_13	12.7	1241.1	1034.3	910.1	43.4	31.0	154.9	215.9	77.5	N.A.	S	UN	S	B	1016.0
Hanson and Kaar (1959)	1_14	12.7	1323.8	1089.1	958.4	38.2	31.0	152.4	213.6	76.2	N.A.	S	UN	S	B	1371.6
Hanson and Kaar (1959)	1_15	12.7	1420.4	1034.3	910.1	38.6	31.0	154.9	214.4	77.5	N.A.	S	UN	S	B	1676.4
Hanson and Kaar (1959)	1_16	12.7	1420.4	1034.3	910.1	38.6	31.0	154.9	211.1	77.5	N.A.	S	UN	S	B	1955.8
Hanson and Kaar (1959)	1_17	12.7	1510.0	1034.3	910.1	35.1	31.0	154.9	220.7	77.5	N.A.	S	UN	S	F	2286.0
Hanson and Kaar (1959)	1_18	12.7	1510.0	1034.3	910.1	35.1	31.0	154.9	213.4	77.5	N.A.	S	UN	S	F	4419.6
Hanson and Kaar (1959)	2_1	9.5	1516.9	978.6	861.2	25.5	24.1	152.4	218.9	76.2	N.A.	S	UN	S	F	1524.0
Hanson and Kaar (1959)	2_1R	9.5	1516.9	978.6	861.2	25.5	24.1	152.4	215.1	76.2	N.A.	R	UN	S	F	1524.0
Hanson and Kaar (1959)	2_1A	9.5	1516.9	978.6	861.2	25.5	24.1	152.4	213.6	76.2	N.A.	R	UN	S	F	1524.0
Hanson and Kaar (1959)	2_2	9.5	1516.9	935.5	823.3	37.4	24.1	152.4	218.9	76.2	N.A.	S	UN	S	B	1524.0
Hanson and Kaar (1959)	2_2R	9.5	1516.9	935.5	823.3	37.4	24.1	152.4	214.4	76.2	N.A.	R	UN	S	F	1524.0
Hanson and Kaar (1959)	2_2A	9.5	1516.9	935.5	823.3	37.4	24.1	152.4	214.4	76.2	N.A.	R	UN	S	B	1524.0
Hanson and Kaar (1959)	2_3	9.5	1516.9	949.6	835.7	49.9	24.1	152.4	220.7	76.2	N.A.	S	UN	S	B	1524.0
Hanson and Kaar (1959)	2_3R	9.5	1516.9	949.6	835.7	49.9	24.1	152.4	217.4	76.2	N.A.	R	UN	S	B	1524.0
Hanson and Kaar (1959)	2_3A	9.5	1516.9	949.6	835.7	49.9	24.1	152.4	214.6	76.2	N.A.	R	UN	S	B	1524.0

Author	Specimen ID	Φ [mm]	f_{ps} [MPa]	f_{si} [MPa]	f_{se} [MPa]	f_c' [MPa]	f_{ci}' [MPa]	b [mm]	h [mm]	c [mm]	s [mm]	Surface condition	Epoxy coating	Release type	Failure mode	L_b [mm]
Hanson and Kaar (1959)	3_1	6.4	1613.4	1143.9	1006.7	34.6	31.0	101.6	144.5	50.8	N.A.	S	UN	S	B	1016.0
Hanson and Kaar (1959)	3_2	6.4	1613.4	1112.6	979.1	39.4	31.0	101.6	143.8	50.8	N.A.	S	UN	S	B	1016.0
Hanson and Kaar (1959)	3_3	6.4	1613.4	885.4	779.1	40.7	31.0	101.6	148.8	50.8	N.A.	S	UN	S	B	1016.0
Hanson and Kaar (1959)	3_4	9.5	1516.9	1049.9	923.9	36.5	31.0	152.4	214.4	76.2	N.A.	S	UN	S	B	1524.0
Hanson and Kaar (1959)	3_5	9.5	1516.9	1026.4	903.2	37.2	31.0	152.4	212.6	76.2	N.A.	S	UN	S	B	1524.0
Hanson and Kaar (1959)	3_6	9.5	1516.9	1065.6	937.7	36.5	31.0	152.4	216.7	76.2	N.A.	S	UN	S	B	1524.0
Hanson and Kaar (1959)	3_7	9.5	1516.9	932.4	820.5	40.7	31.0	152.4	216.9	76.2	N.A.	S	UN	S	B	1524.0
Hanson and Kaar (1959)	3_8	9.5	1516.9	1038.2	913.6	37.6	31.0	152.4	216.7	76.2	N.A.	S	UN	S	F	1524.0
Hanson and Kaar (1959)	3_9	9.5	1516.9	995.1	875.7	39.3	31.0	152.4	205.0	76.2	N.A.	S	UN	S	B	1524.0
Hanson and Kaar (1959)	3_10	12.7	1468.6	940.2	827.4	44.5	31.0	203.2	291.3	101.6	N.A.	S	UN	S	B	2032.0
Hanson and Kaar (1959)	3_11	12.7	1468.6	1057.8	930.8	41.7	31.0	203.2	289.6	101.6	N.A.	S	UN	S	F	2032.0
Hanson and Kaar (1959)	3_12	12.7	1468.6	1034.3	910.1	37.4	31.0	203.2	287.8	101.6	N.A.	S	UN	S	B	2032.0
Hanson and Kaar (1959)	4_1	9.5	1289.4	1002.9	882.6	39.6	31.0	101.6	141.2	50.8	-	S	UN	S	B	863.6
Hanson and Kaar (1959)	4_1R	9.5	1289.4	1002.9	882.6	39.6	31.0	101.6	141.2	50.8	-	R	UN	S	B	863.6
Hanson and Kaar (1959)	4_2	12.7	1144.6	1104.8	972.2	39.4	31.0	101.6	142.0	50.8	-	S	UN	S	B	812.8
Hanson and Kaar (1959)	4_2R	12.7	1144.6	1089.1	958.4	39.4	31.0	101.6	139.7	50.8	-	R	UN	S	B	812.8
Hanson and Kaar (1959)	4_3	12.7	1323.8	1151.8	1013.6	37.4	31.0	152.4	210.6	76.2	-	S	UN	S	B	1219.2
Hanson and Kaar (1959)	4_3R	12.7	1323.8	1104.8	972.2	37.9	31.0	152.4	213.4	76.2	-	R	UN	S	B	1219.2
Hanson and Kaar (1959)	4_4	12.7	1323.8	1112.6	979.1	36.9	31.0	152.4	212.9	76.2	N.A.	S	UN	S	B	1219.2
Hanson and Kaar (1959)	4_4R	12.7	1323.8	1151.8	1013.6	36.9	31.0	152.4	214.6	76.2	N.A.	R	UN	S	B	1219.2
Cousins et al. (1990)	S3UN-1	9.5	1758.0	1400.3	1263.1	34.5	27.6	101.6	152.4	50.8	-	S	UN	S	F	1524.0
Cousins et al. (1990)	S3UN-2	9.5	1758.0	1400.3	1263.1	34.5	27.6	101.6	152.4	50.8	-	S	UN	S	F	1498.6
Cousins et al. (1990)	S3UN-3	9.5	1758.0	1400.3	1263.1	34.5	27.6	101.6	152.4	50.8	-	S	UN	S	F	1447.8
Cousins et al. (1990)	S3UN-4	9.5	1758.0	1400.3	1263.1	34.5	27.6	101.6	152.4	50.8	-	S	UN	S	B	1371.6
Cousins et al. (1990)	S3UN-5	9.5	1758.0	1400.3	1263.1	34.5	27.6	101.6	152.4	50.8	-	S	UN	S	B	1371.6
Cousins et al. (1990)	S3UN-6	9.5	1758.0	1400.3	1263.1	34.5	27.6	101.6	152.4	50.8	-	S	UN	S	B	1219.2
Cousins et al. (1990)	S3CM-1	9.5	1500.0	1400.3	1276.9	34.5	27.6	101.6	152.4	50.8	-	S	CM	S	F	609.6

Author	Specimen ID	Φ [mm]	f_{ps} [MPa]	f_{si} [MPa]	f_{se} [MPa]	f_c' [MPa]	f_{ci}' [MPa]	b [mm]	h [mm]	c [mm]	s [mm]	Surface condition	Epoxy coating	Release type	Failure mode	L_b [mm]
Cousins et al. (1990)	S3CM-2	9.5	1500.0	1400.3	1276.9	34.5	27.6	101.6	152.4	50.8	-	S	CM	S	B	533.4
Cousins et al. (1990)	S3CM-3	9.5	1500.0	1400.3	1276.9	34.5	27.6	101.6	152.4	50.8	-	S	CM	S	S	533.4
Cousins et al. (1990)	S3CM-4	9.5	1500.0	1400.3	1276.9	34.5	27.6	101.6	152.4	50.8	-	S	CM	S	B	457.2
Cousins et al. (1990)	S5UN-1	12.7	1758.0	1410.7	1248.6	34.5	27.6	127.0	203.2	63.5	-	S	UN	S	B	3022.6
Cousins et al. (1990)	S5UN-2	12.7	1758.0	1410.7	1248.6	34.5	27.6	127.0	203.2	63.5	-	S	UN	S	B	2667.0
Cousins et al. (1990)	S5UN-3	12.7	1758.0	1410.7	1248.6	34.5	27.6	127.0	203.2	63.5	-	S	UN	S	B	2667.0
Cousins et al. (1990)	S5UN-4	12.7	1758.0	1410.7	1248.6	34.5	27.6	127.0	203.2	63.5	-	S	UN	S	B	1828.8
Cousins et al. (1990)	S5UN-5	12.7	1758.0	1410.7	1248.6	34.5	27.6	127.0	203.2	63.5	-	S	UN	S	B	1828.8
Cousins et al. (1990)	S5UN-6	12.7	1758.0	1410.7	1248.6	34.5	27.6	127.0	203.2	63.5	-	S	UN	S	B	1219.2
Cousins et al. (1990)	S5CM-1	12.7	1500.0	1436.2	1275.5	34.5	27.6	127.0	203.2	63.5	-	S	CM	S	F	1219.2
Cousins et al. (1990)	S5CM-2	12.7	1500.0	1436.2	1275.5	34.5	27.6	127.0	203.2	63.5	-	S	CM	S	F	914.4
Cousins et al. (1990)	S5CM-3	12.7	1500.0	1436.2	1275.5	34.5	27.6	127.0	203.2	63.5	-	S	CM	S	F	838.2
Cousins et al. (1990)	S5CM-4	12.7	1500.0	1436.2	1275.5	34.5	27.6	127.0	203.2	63.5	-	S	CM	S	F-B	762.0
Cousins et al. (1990)	S5CM-5	12.7	1500.0	1436.2	1275.5	34.5	27.6	127.0	203.2	63.5	-	S	CM	S	B	685.8
Cousins et al. (1990)	S5CL-1	12.7	1500.0	1356.9	1219.7	34.5	27.6	127.0	203.2	63.5	-	S	CL	S	F	1625.6
Cousins et al. (1990)	S5CL-2	12.7	1500.0	1356.9	1219.7	34.5	27.6	127.0	203.2	63.5	-	S	CL	S	B	1219.2
Cousins et al. (1990)	S5CL-3	12.7	1500.0	1356.9	1219.7	34.5	27.6	127.0	203.2	63.5	-	S	CL	S	B	1066.8
Cousins et al. (1990)	S5CL-4	12.7	1500.0	1356.9	1219.7	34.5	27.6	127.0	203.2	63.5	-	S	CL	S	B	914.4
Cousins et al. (1990)	S5CH-1	12.7	1500.0	1356.9	1214.2	34.5	27.6	127.0	203.2	63.5	-	S	CH	S	F-S	838.2
Cousins et al. (1990)	S5CH-2	12.7	1500.0	1356.9	1214.2	34.5	27.6	127.0	203.2	63.5	-	S	CH	S	F	762.0
Cousins et al. (1990)	S5CH-3	12.7	1500.0	1356.9	1214.2	34.5	27.6	127.0	203.2	63.5	-	S	CH	S	S-B	685.8
Cousins et al. (1990)	S5CH-4	12.7	1500.0	1356.9	1214.2	34.5	27.6	127.0	203.2	63.5	-	S	CH	S	S	609.6
Cousins et al. (1990)	S6UN-1	15.2	1758.0	1424.4	1228.9	34.5	27.6	152.4	254.0	76.2	-	S	UN	S	F	3352.8
Cousins et al. (1990)	S6UN-2	15.2	1758.0	1424.4	1228.9	34.5	27.6	152.4	254.0	76.2	-	S	UN	S	B	3200.4
Cousins et al. (1990)	S6UN-3	15.2	1758.0	1424.4	1228.9	34.5	27.6	152.4	254.0	76.2	-	S	UN	S	B	3048.0
Cousins et al. (1990)	S6UN-4	15.2	1758.0	1424.4	1228.9	34.5	27.6	152.4	254.0	76.2	-	S	UN	S	B	2743.2
Cousins et al. (1990)	S6CM-1	15.2	1500.0	1400.3	1234.2	34.5	27.6	152.4	254.0	76.2	-	S	CM	S	F	1625.6

Author	Specimen ID	Φ [mm]	f_{ps} [MPa]	f_{si} [MPa]	f_{se} [MPa]	f_c' [MPa]	f_{ci}' [MPa]	b [mm]	h [mm]	c [mm]	s [mm]	Surface condition	Epoxy coating	Release type	Failure mode	L_b [mm]
Cousins et al. (1990)	S6CM-2	15.2	1500.0	1400.3	1234.2	34.5	27.6	152.4	254.0	76.2	-	S	CM	S	B	1219.2
Cousins et al. (1990)	S6CM-3	15.2	1500.0	1400.3	1234.2	34.5	27.6	152.4	254.0	76.2	-	S	CM	S	B	1066.8
Cousins et al. (1990)	S6CM-4	15.2	1758.0	1400.3	1234.2	34.5	27.6	152.4	254.0	76.2	-	S	CM	S	B	914.4
Mitchell et al. (1993)	9,5/31-1200	9.5	1628.0	1219.0	1085.0	31.0	21.0	100.0	200.0	50.0	-	R	UN	G	F	1200.0
Mitchell et al. (1993)	9,5/31-1100	9.5	1628.0	1219.0	1085.0	31.0	21.0	100.0	200.0	50.0	-	R	UN	G	F-B	1100.0
Mitchell et al. (1993)	9,5/43-1350	9.5	1662.0	1240.0	1095.0	43.0	27.0	100.0	200.0	50.0	-	R	UN	G	F	1350.0
Mitchell et al. (1993)	9,5/43-1000	9.5	1662.0	1240.0	1095.0	43.0	27.0	100.0	200.0	50.0	-	R	UN	G	B	1000.0
Mitchell et al. (1993)	9,5/65-800	9.5	1698.0	1192.0	1117.0	65.0	48.0	100.0	200.0	50.0	-	R	UN	G	F	800.0
Mitchell et al. (1993)	9,5/65-725	9.5	1698.0	1192.0	1117.0	65.0	48.0	100.0	200.0	50.0	-	R	UN	G	F	725.0
Mitchell et al. (1993)	9,5/75-950	9.5	1713.0	1230.0	1204.0	75.0	50.0	100.0	200.0	50.0	-	R	UN	G	F	950.0
Mitchell et al. (1993)	9,5/75-700	9.5	1713.0	1230.0	1136.0	75.0	50.0	100.0	200.0	50.0	-	R	UN	G	F-B	700.0
Mitchell et al. (1993)	9,5/89-825	9.5	1729.0	1234.0	1175.0	89.0	50.0	100.0	200.0	50.0	-	R	UN	G	F	825.0
Mitchell et al. (1993)	9,5/89-575	9.5	1729.0	1234.0	1177.0	89.0	50.0	100.0	200.0	50.0	-	R	UN	G	F	575.0
Mitchell et al. (1993)	13/31-1250	12.7	1758.0	1374.0	1254.0	31.0	21.0	150.0	225.0	50.0	-	S	UN	G	F	1250.0
Mitchell et al. (1993)	13/31-1200	12.7	1758.0	1374.0	1254.0	31.0	21.0	150.0	225.0	50.0	-	S	UN	G	B	1200.0
Mitchell et al. (1993)	13/31-1100	12.7	1758.0	1374.0	1254.0	31.0	21.0	150.0	225.0	50.0	-	S	UN	G	B	1100.0
Mitchell et al. (1993)	13/43-1600	12.7	1696.0	1217.0	1044.0	43.0	27.0	100.0	200.0	50.0	-	S	UN	G	F	1600.0
Mitchell et al. (1993)	13/43-1250	12.7	1696.0	1217.0	1028.0	43.0	27.0	100.0	200.0	50.0	-	S	UN	G	F	1250.0
Mitchell et al. (1993)	13/65-850	12.7	1814.0	1315.0	1254.0	65.0	48.0	150.0	225.0	50.0	-	S	UN	G	F	850.0
Mitchell et al. (1993)	13/65-700	12.7	1814.0	1315.0	1254.0	65.0	48.0	150.0	225.0	50.0	-	S	UN	G	F	700.0
Mitchell et al. (1993)	13/65-650	12.7	1814.0	1315.0	1254.0	65.0	48.0	150.0	225.0	50.0	-	S	UN	G	F-B	650.0
Mitchell et al. (1993)	13/75-1100	12.7	1767.0	1303.0	1153.0	75.0	50.0	100.0	200.0	50.0	-	S	UN	G	F	1100.0
Mitchell et al. (1993)	13/75-950	12.7	1767.0	1303.0	1167.0	75.0	50.0	100.0	200.0	50.0	-	S	UN	G	F	950.0
Mitchell et al. (1993)	13/89-950	12.7	1794.0	1329.0	1278.0	89.0	50.0	125.0	175.0	50.0	-	S	UN	G	F	950.0
Mitchell et al. (1993)	13/89-650	12.7	1794.0	1329.0	1272.0	89.0	50.0	125.0	175.0	50.0	-	S	UN	G	B	650.0
Mitchell et al. (1993)	16/31-1865	15.2	1667.0	1220.0	1026.0	31.0	21.0	200.0	250.0	50.0	-	S	UN	G	F-B	1865.0
Mitchell et al. (1993)	16/31-1800	15.2	1667.0	1220.0	1056.0	31.0	21.0	200.0	250.0	50.0	-	S	UN	G	B	1800.0

Author	Specimen ID	Φ [mm]	f_{ps} [MPa]	f_{si} [MPa]	f_{se} [MPa]	f_c' [MPa]	f_{ci}' [MPa]	b [mm]	h [mm]	c [mm]	s [mm]	Surface condition	Epoxy coating	Release type	Failure mode	L_b [mm]
Mitchell et al. (1993)	16/31-1650	15.2	1667.0	1220.0	1056.0	31.0	21.0	200.0	250.0	50.0	-	S	UN	G	B	1650.0
Mitchell et al. (1993)	16/31-1500	15.2	1667.0	1220.0	1086.0	31.0	21.0	200.0	250.0	50.0	-	S	UN	G	B	1500.0
Mitchell et al. (1993)	16/65-1150	15.2	1716.0	1176.0	1098.0	65.0	48.0	200.0	250.0	50.0	-	S	UN	G	F	1150.0
Mitchell et al. (1993)	16/65-1050	15.2	1716.0	1176.0	1097.0	65.0	48.0	200.0	250.0	50.0	-	S	UN	G	F	1050.0
Mitchell et al. (1993)	16/65-950	15.2	1716.0	1176.0	1097.0	65.0	48.0	200.0	250.0	50.0	-	S	UN	G	F	950.0
Mitchell et al. (1993)	16/65-800	15.2	1716.0	1176.0	1097.0	65.0	48.0	200.0	250.0	50.0	-	S	UN	G	F	800.0
Mitchell et al. (1993)	16/65-700	15.2	1716.0	1176.0	1096.0	65.0	48.0	200.0	250.0	50.0	-	S	UN	G	F-B	700.0
Mitchell et al. (1993)	16/65-725	15.2	1716.0	1176.0	1096.0	65.0	48.0	200.0	250.0	50.0	-	S	UN	G	B	725.0
Mitchell et al. (1993)	16/89-975	15.2	1647.0	871.0	832.0	89.0	50.0	125.0	175.0	50.0	-	S	UN	G	B	975.0
Mitchell et al. (1993)	16/89-675	15.2	1647.0	871.0	838.0	89.0	50.0	125.0	175.0	50.0	-	S	UN	G	B	675.0
Deatherage et al. (1994)	5-1-EXT	12.7	1827.2	1400.0	1316.9	37.8	26.1	406.4	711.2	50.8	38.1	S	UN	S	F-B	2336.8
Deatherage et al. (1994)	5-1-INT	12.7	1654.8	1400.0	1316.9	37.8	26.1	406.4	711.2	50.8	38.1	S	UN	S	S-B	1767.8
Deatherage et al. (1994)	5-2-EXT	12.7	1785.8	1400.0	1316.9	46.5	28.8	406.4	711.2	50.8	38.1	S	UN	S	S-B	1966.0
Deatherage et al. (1994)	5-2-INT	12.7	1668.6	1400.0	1316.9	46.5	28.8	406.4	711.2	50.8	38.1	S	UN	S	F-B	2159.0
Deatherage et al. (1994)	5-3-INT	12.7	1827.2	1400.0	1316.9	47.3	32.9	406.4	711.2	50.8	38.1	R	UN	S	F-B	1966.0
Deatherage et al. (1994)	5-4-EXT	12.7	1792.7	1400.0	1316.9	52.4	36.1	406.4	711.2	50.8	38.1	R	UN	S	F	2063.8
Deatherage et al. (1994)	5-SWAI-E	12.7	1854.8	1400.0	1379.0	38.3	35.4	406.4	711.2	50.8	31.8	R	UN	S	F	2057.4
Deatherage et al. (1994)	5-SWAI-W	12.7	1861.7	1400.0	1379.0	38.3	35.4	406.4	711.2	50.8	31.8	R	UN	S	F-B	1767.8
Deatherage et al. (1994)	5S-1-EXT	13.3	1599.6	1400.0	1372.1	45.7	36.8	406.4	711.2	50.8	37.5	S	UN	S	S-B	1752.6
Deatherage et al. (1994)	5S-1-INT	13.3	1496.2	1400.0	1372.1	45.7	36.8	406.4	711.2	50.8	37.5	S	UN	S	F-B	2057.4
Deatherage et al. (1994)	5S-2-INT	13.3	1792.7	1400.0	1372.1	46.9	34.1	406.4	711.2	50.8	37.5	S	UN	S	F-B	2095.5
Deatherage et al. (1994)	5S-3-EXT	13.3	1744.4	1400.0	1379.0	41.1	37.3	406.4	711.2	50.8	37.5	R	UN	S	F-B	2057.4
Deatherage et al. (1994)	5S-3-INT	13.3	1689.3	1400.0	1379.0	41.1	37.3	406.4	711.2	50.8	37.5	R	UN	S	S-B	1905.0
Deatherage et al. (1994)	5S-4-EXT	13.3	1675.5	1400.0	1379.0	42.6	36.5	406.4	711.2	50.8	37.5	R	UN	S	S-B	1727.2
Deatherage et al. (1994)	5S-4-INT	13.3	1758.2	1400.0	1379.0	42.6	36.5	406.4	711.2	50.8	37.5	R	UN	S	F-B	1828.8
Deatherage et al. (1994)	916-1-EXT	14.3	1654.8	1400.0	1275.6	38.2	23.2	406.4	711.2	50.8	36.5	S	UN	S	F-B	2692.4
Deatherage et al. (1994)	916-1-INT	14.3	1668.6	1400.0	1275.6	38.2	23.2	406.4	711.2	50.8	36.5	S	UN	S	F-B	2209.8

Author	Specimen ID	Φ [mm]	f_{ps} [MPa]	f_{si} [MPa]	f_{se} [MPa]	f_c' [MPa]	f_{ci}' [MPa]	b [mm]	h [mm]	c [mm]	s [mm]	Surface condition	Epoxy coating	Release type	Failure mode	L_b [mm]
Deatherage et al. (1994)	916-2-INT	14.3	1399.7	1400.0	1275.6	40.8	25.9	406.4	711.2	50.8	36.5	S	UN	S	F-B	2209.8
Deatherage et al. (1994)	916-3-EXT	14.3	1503.1	1400.0	1289.4	42.2	34.9	406.4	711.2	50.8	36.5	R	UN	S	F-B	2425.7
Deatherage et al. (1994)	916-4-EXT	14.3	1696.2	1400.0	1289.4	43.0	34.1	406.4	711.2	50.8	36.5	R	UN	S	F-B	2651.8
Deatherage et al. (1994)	916-4-INT	14.3	1730.6	1400.0	1289.4	43.0	34.1	406.4	711.2	50.8	36.5	R	UN	S	F	2743.2
Deatherage et al. (1994)	6-2-INT	15.2	1682.4	1400.0	1268.7	36.4	29.5	406.4	711.2	63.5	48.3	S	UN	S	F-B	1889.8
Deatherage et al. (1994)	6-3-INT	15.2	1847.9	1400.0	1316.9	51.5	36.1	406.4	711.2	63.5	48.3	S	UN	S	F	2239.3
Deatherage et al. (1994)	6-4-EXT	15.2	1806.5	1400.0	1316.9	55.0	37.6	406.4	711.2	63.5	48.3	S	UN	S	F	2180.3
Deatherage et al. (1994)	6-4-INT	15.2	1827.2	1400.0	1316.9	55.0	37.6	406.4	711.2	63.5	48.3	S	UN	S	F	2180.3
Shahawy (2001)	A0-0-R-N	12.7	1758.0	1396.2	1087.0	35.0	28.0	457.2	914.4	76.2	38.1	S	UN	S	S-B	2159.0
Shahawy (2001)	A0-0-R-S	12.7	1758.0	1396.2	1086.6	35.0	28.0	457.2	914.4	76.2	38.1	S	UN	S	S	2159.0
Shahawy (2001)	A0-0-RD-N	12.7	1758.0	1396.2	1086.6	35.0	28.0	457.2	914.4	76.2	38.1	S	UN	S	S-B	1879.6
Shahawy (2001)	A0-0-RD-S	12.7	1758.0	1396.2	1086.6	35.0	28.0	457.2	914.4	76.2	38.1	S	UN	S	S-B	2159.0
Shahawy (2001)	A1-0-R-N	12.7	1758.0	1396.2	1086.6	35.0	28.0	457.2	914.4	76.2	38.1	S	UN	S	S-B	2590.8
Shahawy (2001)	A1-0-R-S	12.7	1758.0	1396.2	1086.6	35.0	28.0	457.2	914.4	76.2	38.1	S	UN	S	F-B	3149.6
Shahawy (2001)	A1-0-RD-N	12.7	1758.0	1396.2	1086.6	35.0	28.0	457.2	914.4	76.2	38.1	S	UN	S	S-B	2590.8
Shahawy (2001)	A1-0-RD-S	12.7	1758.0	1396.2	1086.6	35.0	28.0	457.2	914.4	76.2	38.1	S	UN	S	S-B	3149.6
Shahawy (2001)	A3-0-RA-N	12.7	1758.0	1396.2	1086.6	35.0	28.0	457.2	914.4	76.2	38.1	S	UN	S	S-B	2590.8
Shahawy (2001)	A3-0-RA-S	12.7	1758.0	1396.2	1086.6	35.0	28.0	457.2	914.4	76.2	38.1	S	UN	S	S-B	3149.6
Shahawy (2001)	A3-0-RB-N	12.7	1758.0	1396.2	1086.6	35.0	28.0	457.2	914.4	76.2	38.1	S	UN	S	F-B	2159.0
Shahawy (2001)	A3-0-RB-S	12.7	1758.0	1396.2	1086.6	35.0	28.0	457.2	914.4	76.2	38.1	S	UN	S	S-B	2159.0
Shahawy (2001)	B0-0-R-N	12.7	1758.0	1396.2	1086.6	35.0	28.0	457.2	914.4	76.2	38.1	S	UN	S	F-B	2590.8
Shahawy (2001)	B0-0-R-S	12.7	1758.0	1396.2	1086.6	35.0	28.0	457.2	914.4	76.2	38.1	S	UN	S	F-S	3149.6
Shahawy (2001)	B1-0-R-N	12.7	1758.0	1396.2	1086.6	35.0	28.0	457.2	914.4	76.2	38.1	S	UN	S	S-B	1524.0
Shahawy (2001)	B1-0-R-S	12.7	1758.0	1396.2	1086.6	35.0	28.0	457.2	914.4	76.2	38.1	S	UN	S	S-B	1371.6
Shahawy (2001)	C0-0-R-N	15.2	1758.0	1396.2	1086.6	35.0	28.0	457.2	914.4	76.2	35.6	S	UN	S	F	3606.8
Shahawy (2001)	C0-0-R-S	15.2	1758.0	1396.2	1086.6	35.0	28.0	457.2	914.4	76.2	35.6	S	UN	S	F	3352.8
Shahawy (2001)	C0-0-RD-N	15.2	1758.0	1396.2	1086.6	35.0	28.0	457.2	914.4	76.2	35.6	S	UN	S	S-B	1524.0

Author	Specimen ID	Φ [mm]	f_{ps} [MPa]	f_{si} [MPa]	f_{se} [MPa]	f_c' [MPa]	f_{ci}' [MPa]	b [mm]	h [mm]	c [mm]	s [mm]	Surface condition	Epoxy coating	Release type	Failure mode	L_b [mm]
Shahawy (2001)	C0-0-RD-S	15.2	1758.0	1396.2	1086.6	35.0	28.0	457.2	914.4	76.2	35.6	S	UN	S	F-S	3759.2
Shahawy (2001)	C1-0-R-N	15.2	1758.0	1396.2	1086.6	35.0	28.0	457.2	914.4	76.2	35.6	S	UN	S	F	3606.8
Shahawy (2001)	C1-0-R-S	15.2	1758.0	1396.2	1086.6	35.0	28.0	457.2	914.4	76.2	35.6	S	UN	S	F	3352.8
Shahawy (2001)	C1-0-RD-N	15.2	1758.0	1396.2	1086.6	35.0	28.0	457.2	914.4	76.2	35.6	S	UN	S	F	3784.6
Shahawy (2001)	C1-0-RD-S	15.2	1758.0	1396.2	1086.6	35.0	28.0	457.2	914.4	76.2	35.6	S	UN	S	F	3784.6
Kahn et al. (2002)	G2AN	15.2	1875.0	1314.0	1156.3	70.0	51.1	406.4	914.0	50.8	35.6	S	UN	S	F	3048.0
Kahn et al. (2002)	G2AS	15.2	1889.0	1314.0	1156.3	70.0	51.1	406.4	914.0	50.8	35.6	S	UN	S	F	2032.0
Kahn et al. (2002)	G2BN	15.2	1893.0	1314.0	1156.3	70.0	51.1	406.4	914.0	50.8	35.6	S	UN	S	F	2235.0
Kahn et al. (2002)	G2BS	15.2	1863.0	1314.0	1156.3	70.0	51.1	406.4	914.0	50.8	35.6	S	UN	S	B	1905.0
Kahn et al. (2002)	G4AN	15.2	1931.0	1314.0	1156.3	100.0	73.0	406.4	914.0	50.8	35.6	S	UN	S	F	2667.0
Kahn et al. (2002)	G4AS	15.2	1846.0	1314.0	1156.3	100.0	73.0	406.4	914.0	50.8	35.6	S	UN	S	B	2032.0
Kahn et al. (2002)	G4BN	15.2	1926.0	1314.0	1156.3	100.0	73.0	406.4	914.0	50.8	35.6	S	UN	S	F	2362.0
Kahn et al. (2002)	G4BS	15.2	1852.0	1314.0	1156.3	100.0	73.0	406.4	914.0	50.8	35.6	S	UN	S	B	1651.0
Kose and Burkett (2005)	L0R0-1	15.2	1793.0	1396.5	1228.9	37.5	31.3	421.6	711.2	50.8	35.6	R	UN	S	F	1372.0
Kose and Burkett (2005)	L0R0-2	15.2	1793.0	1396.5	1228.9	37.5	31.3	421.6	711.2	50.8	35.6	R	UN	S	F	1372.0
Kose and Burkett (2005)	L0R1-3	15.2	1793.0	1396.5	1228.9	37.5	31.3	421.6	711.2	50.8	35.6	R	UN	S	F	1372.0
Kose and Burkett (2005)	L0R1-4	15.2	1793.0	1396.5	1228.9	37.5	31.3	421.6	711.2	50.8	35.6	R	UN	S	F	1372.0
Kose and Burkett (2005)	L4R0-1	15.2	1793.0	1396.5	1228.9	34.8	26.1	421.6	711.2	50.8	35.6	R	UN	S	F	2438.0
Kose and Burkett (2005)	L4R0-2	15.2	1793.0	1396.5	1228.9	34.8	26.1	421.6	711.2	50.8	35.6	R	UN	S	B	2438.0
Kose and Burkett (2005)	L4R1-3	15.2	1793.0	1396.5	1228.9	34.8	26.1	421.6	711.2	50.8	35.6	R	UN	S	F	2438.0
Kose and Burkett (2005)	L4R1-4	15.2	1793.0	1396.5	1228.9	34.8	26.1	421.6	711.2	50.8	35.6	R	UN	S	F	2438.0
Kose and Burkett (2005)	L6R0-1	15.2	1793.0	1396.5	1228.9	51.6	31.9	421.6	711.2	50.8	35.6	R	UN	S	F	2896.0
Kose and Burkett (2005)	L6R0-2	15.2	1793.0	1396.5	1228.9	51.6	31.9	421.6	711.2	50.8	35.6	R	UN	S	F-B	2896.0
Kose and Burkett (2005)	L6R1-3	15.2	1793.0	1396.5	1228.9	51.6	31.9	421.6	711.2	50.8	35.6	R	UN	S	F-B	2896.0
Kose and Burkett (2005)	L6R1-4	15.2	1793.0	1396.5	1228.9	51.6	31.9	421.6	711.2	50.8	35.6	R	UN	S	F-B	2896.0

* grey values are assumed data, derived from publications

Total: 187 data points

Nomenclature:

Φ = tendon diameter (all experimental tests involve 7-wire strands)
f_{ps} = tendon stress at nominal strength
f_{si} = jacking stress of the tendon at release
f_{se} = tendon stress after allowance of all prestress losses
f_c' = concrete compressive strength at 28 day
f_{ci}' = concrete compressive strength at release

b = width of the concrete section
h = height of the concrete section
c = concrete cover thickness
s = tendon clear spacing
L_b = anchorage length of the tendon

Surface condition: S = Smooth; R = Rusted
Epoxy coating: UN = Uncoated tendon; CL = Coated tendon with low level of grit; CM = Coated medium level; CH = Coated high level
Release type: S = Sudden; G = Gradual
Failure mode: F = Flexure; S = Shear; B = Bond; F-S = Combined flexure/shear; F-B = Combined flexure/bond; S-B = Combined shear/bond

N.A. = not available data

ANNEX C

TRANSMISSION LENGTH DATABASE FOR TWC MODEL CALIBRATION

Author	Specimen ID	Φ [mm]	f_{si} [MPa]	f_{se} [MPa]	f_c' [MPa]	f_{ci}' [MPa]	b [mm]	h [mm]	c [mm]	s [mm]	Release type	$L_{t,exp}$ [mm]	$L_{t,TWC}$ [mm]	$L_{t,ACI}$ [mm]	$L_{t,MC10}$ [mm]	$L_{t,EC2}$ [mm]
Mitchell et al. (1993)	13/31-1200a	12.7	1374.0	1254.0	31.0	21.0	150.0	225.0	50.0	-	G	710.0	793.0	769.4	913.2	892.4
Mitchell et al. (1993)	13/43-1600a	12.7	1217.0	1044.0	43.0	27.0	100.0	200.0	50.0	-	G	584.0	588.0	640.5	628.1	613.7
Mitchell et al. (1993)	13/43-1250a	12.7	1217.0	1028.0	43.0	27.0	100.0	200.0	50.0	-	G	584.0	588.0	630.7	628.1	613.7
Mitchell et al. (1993)	13/65-850a	12.7	1315.0	1254.0	65.0	48.0	150.0	225.0	50.0	-	G	506.0	463.0	769.4	413.2	403.7
Mitchell et al. (1993)	13/75-1100a	12.7	1303.0	1153.0	75.0	50.0	100.0	200.0	50.0	-	G	469.5	438.0	707.4	396.3	387.2
Mitchell et al. (1993)	13/75-950a	12.7	1303.0	1167.0	75.0	50.0	100.0	200.0	50.0	-	G	367.5	438.0	716.0	396.3	387.2
Mitchell et al. (1993)	13/89-950a	12.7	1329.0	1278.0	89.0	50.0	125.0	175.0	50.0	-	G	387.0	453.0	784.1	404.2	395.0
Mitchell et al. (1993)	13/89-650a	12.7	1329.0	1272.0	89.0	50.0	125.0	175.0	50.0	-	G	495.0	453.0	780.4	404.2	395.0
Mitchell et al. (1993)	16/31-1865a	15.7	1220.0	1026.0	31.0	21.0	200.0	250.0	50.0	-	G	803.5	1033.0	780.6	1005.5	982.5
Mitchell et al. (1993)	16/31-1500a	15.7	1220.0	1086.0	31.0	21.0	200.0	250.0	50.0	-	G	738.5	1033.0	826.2	1005.5	982.5
Mitchell et al. (1993)	16/65-1150a	15.7	1176.0	1098.0	65.0	48.0	200.0	250.0	50.0	-	G	477.5	583.0	835.3	458.2	447.7
Mitchell et al. (1993)	16/65-725a	15.7	1176.0	1096.0	65.0	48.0	200.0	250.0	50.0	-	G	485.5	583.0	833.8	458.2	447.7
Mitchell et al. (1993)	16/89-975a	15.7	871.0	832.0	89.0	50.0	125.0	175.0	50.0	-	G	306.0	448.0	633.0	328.5	321.0
Mitchell et al. (1993)	16/89-675a	15.7	871.0	838.0	89.0	50.0	125.0	175.0	50.0	-	G	465.0	448.0	637.5	328.5	321.0
Russell and Burns (1996)	FC150-11-N	12.7	1344.5	1183.2	46.3	30.9	101.6	127.0	50.8	-	G	774.7	583.0	725.9	612.9	598.9
Russell and Burns (1996)	FC150-12-N	12.7	1344.5	1183.2	46.3	30.9	101.6	127.0	50.8	-	G	717.6	583.0	725.9	612.9	598.9
Russell and Burns (1996)	FC350-1-N	12.7	1365.2	1201.4	45.7	29.8	127.0	228.6	63.5	38.1	G	762.0	678.0	737.1	643.1	628.4
Russell and Burns (1996)	FC350-2-N	12.7	1365.2	1201.4	45.7	29.8	127.0	228.6	63.5	38.1	G	698.5	678.0	737.1	643.1	628.4
Russell and Burns (1996)	FCT350-3-N	12.7	1365.2	1201.4	45.7	29.8	127.0	228.6	63.5	38.1	G	768.4	678.0	737.1	643.1	628.4
Russell and Burns (1996)	FCT350-4-N	12.7	1365.2	1201.4	45.7	29.8	127.0	228.6	63.5	38.1	G	774.7	678.0	737.1	643.1	628.4
Russell and Burns (1996)	FC550-1-N	12.7	1344.5	1183.2	37.2	26.5	127.0	330.2	63.5	38.1	G	965.2	788.0	725.9	705.2	689.1
Russell and Burns (1996)	FCT550-2-N	12.7	1344.5	1183.2	37.2	26.5	127.0	330.2	63.5	38.1	G	958.9	788.0	725.9	705.2	689.1
Russell and Burns (1996)	FC550-3-N	12.7	1344.5	1183.2	37.2	26.5	127.0	330.2	63.5	38.1	G	977.9	788.0	725.9	705.2	689.1
Russell and Burns (1996)	FC160-12-N	15.2	1344.5	1183.2	37.2	26.5	101.6	127.0	50.8	-	G	1193.8	873.0	868.8	844.0	824.7
Russell and Burns (1996)	FC360-1-N	15.2	1344.5	1183.2	43.1	29.0	127.0	228.6	63.5	35.6	G	1047.8	943.0	868.8	777.9	760.1
Russell and Burns (1996)	FC360-2-N	15.2	1344.5	1183.2	43.1	29.0	127.0	228.6	63.5	35.6	G	1079.5	943.0	868.8	777.9	760.1
Russell and Burns (1996)	FCT360-3-N	15.2	1344.5	1183.2	43.1	29.0	127.0	228.6	63.5	35.6	G	1079.5	943.0	868.8	777.9	760.1

Author	Specimen ID	Φ [mm]	f_{si} [MPa]	f_{se} [MPa]	f_c' [MPa]	f_{ci}' [MPa]	b [mm]	h [mm]	c [mm]	s [mm]	Release type	$L_{t,exp}$ [mm]	$L_{t,TWC}$ [mm]	$L_{t,ACI}$ [mm]	$L_{t,MC10}$ [mm]	$L_{t,EC2}$ [mm]
Russell and Burns (1996)	FCT360-4-N	15.2	1330.7	1171.0	50.3	33.0	127.0	228.6	63.5	35.6	G	1174.8	858.0	859.9	684.1	668.4
Russell and Burns (1996)	FC362-11-N	15.2	1254.9	1104.3	51.9	32.8	127.0	241.3	63.5	42.0	G	1143.0	773.0	810.9	648.6	633.8
Russell and Burns (1996)	FCT362-12-N	15.2	1254.9	1104.3	51.9	32.8	127.0	241.3	63.5	42.0	G	1092.2	773.0	810.9	648.6	633.8
Russell and Burns (1996)	FC362-13-N	15.2	1254.9	1104.3	51.9	32.8	127.0	241.3	63.5	42.0	G	1066.8	773.0	810.9	648.6	633.8
Russell and Burns (1996)	FC560-1-N	15.2	1344.5	1183.2	45.5	30.9	127.0	330.2	63.5	35.6	G	1174.8	998.0	868.8	733.5	716.8
Russell and Burns (1996)	FCT560-2-N	15.2	1344.5	1183.2	45.5	30.9	127.0	330.2	63.5	35.6	G	1263.7	998.0	868.8	733.5	716.8
Russell and Burns (1996)	FC560-3-N	15.2	1344.5	1183.2	45.5	30.9	127.0	330.2	63.5	35.6	G	1219.2	998.0	868.8	733.5	716.8
Russell and Burns (1997)	SS150-1a	12.7	1406.0	1237.3	34.9	19.2	102.0	127.0	51.0	-	S	1422.0	1029.0	759.1	902.4	882.5
Russell and Burns (1997)	SS150-2a	12.7	1406.0	1237.3	34.9	19.2	102.0	127.0	51.0	-	S	1460.5	1029.0	759.1	902.4	882.5
Russell and Burns (1997)	SS150-3a	12.7	1299.0	1143.1	40.1	26.0	102.0	127.0	51.0	-	S	749.5	759.0	701.3	868.8	848.9
Russell and Burns (1997)	SS150-4a	12.7	1299.0	1143.1	40.1	26.0	102.0	127.0	51.0	-	S	660.5	759.0	701.3	868.8	848.9
Russell and Burns (1997)	SS160-1a	15.2	1239.0	1090.3	48.2	24.3	102.0	127.0	51.0	-	S	1245.0	1029.0	802.7	1062.3	1038.1
Russell and Burns (1997)	SS160-2b	15.2	1239.0	1090.3	48.2	24.3	102.0	127.0	51.0	-	S	1118.0	1029.0	802.7	1062.3	1038.1
Russell and Burns (1997)	SS160-3b	15.2	1311.0	1153.7	45.0	30.2	102.0	127.0	51.0	-	S	1219.0	921.0	849.4	914.9	894.0
Russell and Burns (1997)	SS160-4a	15.2	1311.0	1153.7	45.0	30.2	102.0	127.0	51.0	-	S	1143.0	921.0	849.4	914.9	894.0
Russell and Burns (1997)	SS160-5a	15.2	1287.0	1132.6	46.9	28.9	102.0	127.0	51.0	-	S	1067.0	933.0	833.8	935.0	913.6
Russell and Burns (1997)	SS160-6a	15.2	1287.0	1132.6	46.9	28.9	102.0	127.0	51.0	-	S	863.5	933.0	833.8	935.0	913.6
Russell and Burns (1997)	SS160-7a	15.2	1239.0	1090.3	46.9	28.9	102.0	127.0	51.0	-	S	927.0	903.0	802.7	900.1	879.5
Russell and Burns (1997)	SS160-8a	15.2	1239.0	1090.3	46.9	28.9	102.0	127.0	51.0	-	S	762.0	903.0	802.7	900.1	879.5
Oh and Kim (2000)	M12-N-C3-1	12.7	1396.5	1228.9	48.2	34.7	112.7	200.0	36.4	-	S	825.5	807.0	754.0	718.1	701.7
Oh and Kim (2000)	M12-N-C3-2	12.7	1396.5	1228.9	47.6	32.5	112.7	200.0	36.4	-	S	737.0	846.0	754.0	760.4	743.1
Oh and Kim (2000)	M12-N-C4-1	12.7	1396.5	1228.9	50.3	35.0	112.7	200.0	46.4	-	S	587.5	664.0	754.0	712.8	696.5
Oh and Kim (2000)	M12-N-C4-2	12.7	1396.5	1228.9	50.3	35.0	112.7	200.0	46.4	-	S	649.5	664.0	754.0	712.8	696.5
Oh and Kim (2000)	M12-N-C5-1	12.7	1396.5	1228.9	48.2	34.7	112.7	200.0	56.4	-	S	564.5	618.0	754.0	718.1	701.7
Oh and Kim (2000)	M12-N-C5-2	12.7	1396.5	1228.9	47.6	32.5	112.7	200.0	56.4	-	S	544.0	641.0	754.0	760.4	743.1
Oh and Kim (2000)	M12-H-C3-1	12.7	1396.5	1228.9	57.8	44.9	112.7	200.0	36.4	-	S	641.0	687.0	754.0	578.8	565.5
Oh and Kim (2000)	M12-H-C3-2	12.7	1396.5	1228.9	59.6	44.5	112.7	200.0	36.4	-	S	630.0	687.0	754.0	583.0	569.7

Author	Specimen ID	Φ [mm]	f_{si} [MPa]	f_{se} [MPa]	f_c' [MPa]	f_{ci}' [MPa]	b [mm]	h [mm]	c [mm]	s [mm]	Release type	$L_{t,exp}$ [mm]	$L_{t,TWC}$ [mm]	$L_{t,ACI}$ [mm]	$L_{t,MC10}$ [mm]	$L_{t,EC2}$ [mm]
Oh and Kim (2000)	M12-H-C4-1	12.7	1396.5	1228.9	61.2	46.7	112.7	200.0	46.4	-	S	501.5	561.0	754.0	560.7	547.9
Oh and Kim (2000)	M12-H-C4-2	12.7	1396.5	1228.9	57.0	45.8	112.7	200.0	46.4	-	S	544.0	567.0	754.0	569.5	556.5
Oh and Kim (2000)	M12-H-C5-1	12.7	1396.5	1228.9	57.8	44.9	112.7	200.0	56.4	-	S	463.0	539.0	754.0	578.8	565.5
Oh and Kim (2000)	M12-H-C5-2	12.7	1396.5	1228.9	59.6	44.5	112.7	200.0	56.4	-	S	508.0	539.0	754.0	583.0	569.7
Oh and Kim (2000)	M15-N-C3-1	15.2	1396.5	1228.9	50.3	35.0	115.2	200.0	37.6	-	S	1022.0	1109.0	902.4	853.1	833.6
Oh and Kim (2000)	M15-N-C3-2	15.2	1396.5	1228.9	48.8	35.0	115.2	200.0	37.6	-	S	990.5	1109.0	902.4	853.1	833.6
Oh and Kim (2000)	M15-N-C4-1	15.2	1396.5	1228.9	48.2	34.7	115.2	200.0	47.6	-	S	800.0	892.0	902.4	859.4	839.8
Oh and Kim (2000)	M15-N-C4-2	15.2	1396.5	1228.9	47.6	32.5	115.2	200.0	47.6	-	S	786.5	932.0	902.4	910.1	889.3
Oh and Kim (2000)	M15-N-C5-1	15.2	1396.5	1228.9	50.3	35.0	115.2	200.0	57.6	-	S	693.5	767.0	902.4	853.1	833.6
Oh and Kim (2000)	M15-N-C5-2	15.2	1396.5	1228.9	48.8	35.0	115.2	200.0	57.6	-	S	636.5	767.0	902.4	853.1	833.6
Oh and Kim (2000)	M15-H-C3-1	15.2	1396.5	1228.9	61.2	46.7	115.2	200.0	37.6	-	S	814.5	909.0	902.4	671.0	655.7
Oh and Kim (2000)	M15-H-C3-2	15.2	1396.5	1228.9	57.0	45.8	115.2	200.0	37.6	-	S	835.5	921.0	902.4	681.6	666.1
Oh and Kim (2000)	M15-H-C4-1	15.2	1396.5	1228.9	57.8	44.9	115.2	200.0	47.6	-	S	711.0	750.0	902.4	692.7	676.9
Oh and Kim (2000)	M15-H-C4-2	15.2	1396.5	1228.9	59.6	44.5	115.2	200.0	47.6	-	S	639.0	750.0	902.4	697.7	681.8
Oh and Kim (2000)	M15-H-C5-1	15.2	1396.5	1228.9	61.2	46.7	115.2	200.0	57.6	-	S	548.5	653.0	902.4	671.0	655.7
Oh and Kim (2000)	M15-H-C5-2	15.2	1396.5	1228.9	57.0	45.8	115.2	200.0	57.6	-	S	538.5	664.0	902.4	681.6	666.1
Oh and Kim (2000)	T12-N-S3	12.7	1396.5	1228.9	47.8	34.0	150.8	200.0	56.4	25.4	S	758.0	761.0	754.0	730.9	714.2
Oh and Kim (2000)	T12-N-S4	12.7	1396.5	1228.9	47.6	35.5	163.5	200.0	56.4	38.1	S	632.5	681.0	754.0	704.1	688.0
Oh and Kim (2000)	T12-N-S5	12.7	1396.5	1228.9	50.7	37.3	176.2	200.0	56.4	50.8	S	593.0	636.0	754.0	674.9	659.5
Oh and Kim (2000)	T12-H-S3	12.7	1396.5	1228.9	57.6	44.2	150.8	200.0	56.4	25.4	S	643.0	641.0	754.0	586.2	572.8
Oh and Kim (2000)	T12-H-S4	12.7	1396.5	1228.9	58.1	43.2	163.5	200.0	56.4	38.1	S	558.5	607.0	754.0	597.2	583.6
Oh and Kim (2000)	T12-H-S5	12.7	1396.5	1228.9	60.3	46.3	176.2	200.0	56.4	50.8	S	530.5	561.0	754.0	564.6	551.7
Oh and Kim (2000)	T15-N-S3	15.2	1396.5	1228.9	49.1	37.6	160.8	200.0	57.6	30.4	S	934.5	926.0	902.4	802.3	784.0
Oh and Kim (2000)	T15-N-S4	15.2	1396.5	1228.9	48.8	34.8	176.0	200.0	57.6	45.6	S	795.0	881.0	902.4	857.3	837.7
Oh and Kim (2000)	T15-N-S5	15.2	1396.5	1228.9	47.4	33.4	191.2	200.0	57.6	60.8	S	750.0	835.0	902.4	888.5	868.2
Oh and Kim (2000)	T15-H-S3	15.2	1396.5	1228.9	58.9	47.2	160.8	200.0	57.6	30.4	S	834.5	801.0	902.4	665.3	650.1
Oh and Kim (2000)	T15-H-S4	15.2	1396.5	1228.9	61.2	46.9	176.0	200.0	57.6	45.6	S	680.0	727.0	902.4	668.7	653.5

Author	Specimen ID	Φ [mm]	f_{si} [MPa]	f_{se} [MPa]	f_c' [MPa]	f_{ci}' [MPa]	b [mm]	h [mm]	c [mm]	s [mm]	Release type	$L_{t,exp}$ [mm]	$L_{t,TWC}$ [mm]	$L_{t,ACI}$ [mm]	$L_{t,MC10}$ [mm]	$L_{t,EC2}$ [mm]
Oh and Kim (2000)	T15-H-S5	15.2	1396.5	1228.9	57.1	43.9	191.2	200.0	57.6	60.8	S	637.0	710.0	902.4	705.5	689.4
Oh et al. (2006)	M12-N-C3	12.7	1402.1	1233.8	47.9	33.6	112.7	200.0	36.4	-	S	781.5	829.0	757.0	741.5	724.5
Oh et al. (2006)	M12-N-C4	12.7	1391.9	1224.9	49.6	35.0	112.7	200.0	46.4	-	S	619.0	658.0	751.5	710.4	694.2
Oh et al. (2006)	M12-N-C5	12.7	1402.7	1234.4	47.9	33.6	112.7	200.0	56.4	-	S	554.5	630.0	757.3	741.8	724.8
Oh et al. (2006)	M12-H-C3	12.7	1359.3	1196.2	58.7	44.7	112.7	200.0	36.4	-	S	636.0	670.0	733.9	565.4	552.5
Oh et al. (2006)	M12-H-C4	12.7	1375.1	1210.1	59.1	46.3	112.7	200.0	46.4	-	S	523.0	561.0	742.4	555.9	543.2
Oh et al. (2006)	M12-H-C5	12.7	1394.7	1227.3	58.7	44.7	112.7	200.0	56.4	-	S	486.0	539.0	753.0	580.1	566.9
Oh et al. (2006)	M15-N-C3	15.2	1377.1	1211.8	49.6	35.0	115.2	200.0	37.6	-	S	1006.5	1092.0	889.9	841.2	822.0
Oh et al. (2006)	M15-N-C4	15.2	1392.5	1225.4	47.9	33.6	115.2	200.0	47.6	-	S	793.5	909.0	899.8	881.4	861.2
Oh et al. (2006)	M15-N-C5	15.2	1393.2	1226.0	49.6	35.0	115.2	200.0	57.6	-	S	665.0	767.0	900.3	851.0	831.6
Oh et al. (2006)	M15-H-C3	15.2	1357.5	1194.6	59.1	46.4	115.2	200.0	37.6	-	S	825.0	886.0	877.2	655.7	640.7
Oh et al. (2006)	M15-H-C4	15.2	1364.9	1201.1	58.7	44.7	115.2	200.0	47.6	-	S	675.0	732.0	882.0	679.5	663.9
Oh et al. (2006)	M15-H-C5	15.2	1384.4	1218.3	59.1	45.6	115.2	200.0	57.6	-	S	543.5	658.0	894.6	678.1	662.6
Oh et al. (2006)	T12-N-S3	12.7	1398.4	1230.6	47.8	34.0	163.5	200.0	56.4	25.4	S	758.0	767.0	755.0	731.9	715.2
Oh et al. (2006)	T12-N-S4	12.7	1418.0	1247.8	47.6	35.5	176.2	200.0	56.4	38.1	S	632.5	693.0	765.6	714.9	698.6
Oh et al. (2006)	T12-N-S5	12.7	1389.1	1222.4	50.7	37.3	188.9	200.0	56.4	50.8	S	593.0	636.0	750.0	671.4	656.0
Oh et al. (2006)	T12-H-S3	12.7	1374.2	1209.3	57.6	44.2	163.5	200.0	56.4	25.4	S	643.0	636.0	741.9	576.8	563.6
Oh et al. (2006)	T12-H-S4	12.7	1377.9	1212.6	58.1	43.2	176.2	200.0	56.4	38.1	S	558.5	607.0	743.9	589.3	575.8
Oh et al. (2006)	T12-H-S5	12.7	1392.8	1225.7	60.3	46.3	188.9	200.0	56.4	50.8	S	530.5	561.0	752.0	563.1	550.2
Oh et al. (2006)	T15-N-S3	15.2	1357.4	1194.5	49.1	37.6	160.8	200.0	57.6	30.4	S	934.5	903.0	877.1	779.9	762.1
Oh et al. (2006)	T15-N-S4	15.2	1361.1	1197.8	48.8	34.8	176.0	200.0	57.6	45.6	S	795.0	858.0	879.5	835.6	816.5
Oh et al. (2006)	T15-N-S5	15.2	1381.6	1215.8	47.4	33.4	191.2	200.0	57.6	60.8	S	750.0	829.0	892.8	879.0	858.9
Oh et al. (2006)	T15-H-S3	15.2	1376.0	1210.9	58.9	47.2	160.8	200.0	57.6	30.4	S	834.5	795.0	889.1	655.6	640.6
Oh et al. (2006)	T15-H-S4	15.2	1400.2	1232.2	61.2	46.9	176.0	200.0	57.6	45.6	S	680.0	732.0	904.8	670.5	655.2
Oh et al. (2006)	T15-H-S5	15.2	1377.9	1212.6	57.1	43.9	191.2	200.0	57.6	60.8	S	637.0	704.0	890.4	696.1	680.2
Martì-Vargas et al. (2007)	M-350-0.50	12.7	1396.5	1117.2	35.8	26.1	100.0	100.0	50.0	-	G	550.0	673.0	685.4	744.4	727.4
Martì-Vargas et al. (2007)	M-350-0.45	12.7	1396.5	1117.2	51.1	37.3	100.0	100.0	50.0	-	G	550.0	533.0	685.4	540.0	527.6

Author	Specimen ID	Φ [mm]	f_{si} [MPa]	f_{se} [MPa]	f_c' [MPa]	f_{ci}' [MPa]	b [mm]	h [mm]	c [mm]	s [mm]	Release type	$L_{t,exp}$ [mm]	$L_{t,TWC}$ [mm]	$L_{t,ACI}$ [mm]	$L_{t,MC10}$ [mm]	$L_{t,EC2}$ [mm]
Martì-Vargas et al. (2007)	M-350-0.40	12.7	1396.5	1117.2	64.0	46.7	100.0	100.0	50.0	-	G	550.0	473.0	685.4	448.5	438.3
Martì-Vargas et al. (2007)	M-400-0.50	12.7	1396.5	1117.2	33.2	24.2	100.0	100.0	50.0	-	G	650.0	713.0	685.4	801.5	783.2
Martì-Vargas et al. (2007)	M-400-0.45	12.7	1396.5	1117.2	38.7	28.3	100.0	100.0	50.0	-	G	550.0	638.0	685.4	690.3	674.5
Martì-Vargas et al. (2007)	M-400-0.40	12.7	1396.5	1117.2	56.7	41.4	100.0	100.0	50.0	-	G	550.0	503.0	685.4	495.1	483.8
Martì-Vargas et al. (2007)	M-400-0.35	12.7	1396.5	1117.2	62.1	45.3	100.0	100.0	50.0	-	G	500.0	478.0	685.4	459.7	449.2
Martì-Vargas et al. (2007)	M-450-0.40	12.7	1396.5	1117.2	49.7	36.3	100.0	100.0	50.0	-	G	550.0	538.0	685.4	552.6	540.0
Martì-Vargas et al. (2007)	M-450-0.35	12.7	1396.5	1117.2	63.8	46.6	100.0	100.0	50.0	-	G	500.0	473.0	685.4	449.3	439.0
Martì-Vargas et al. (2007)	M-500-0.40	12.7	1396.5	1117.2	42.2	30.8	100.0	100.0	50.0	-	G	600.0	603.0	685.4	638.2	623.6
Martì-Vargas et al. (2007)	M-500-0.35	12.7	1396.5	1117.2	63.8	46.6	100.0	100.0	50.0	-	G	450.0	473.0	685.4	449.3	439.0
Martì-Vargas et al. (2007)	M-500-0.30	12.7	1396.5	1117.2	75.1	54.8	100.0	100.0	50.0	-	G	400.0	433.0	685.4	395.2	386.1
Dang et al. (2017)	M1-S1-1a	18.0	1335.6	1175.3	64.1	40.9	165.0	305.0	50.0	-	G	702.5	893.0	1022.0	677.5	662.0
Dang et al. (2017)	M1-S1-2a	18.0	1335.6	1175.3	64.1	40.9	165.0	305.0	50.0	-	G	695.0	893.0	1022.0	677.5	662.0
Dang et al. (2017)	M1-S1-3a	18.0	1338.3	1177.7	66.9	45.6	165.0	305.0	50.0	-	G	615.0	838.0	1024.1	621.1	606.9
Dang et al. (2017)	M1-S1-4a	18.0	1338.3	1177.7	66.9	45.6	165.0	305.0	50.0	-	G	647.5	838.0	1024.1	621.1	606.9
Dang et al. (2017)	M2-S1-1a	18.0	1348.0	1186.2	94.5	65.4	165.0	305.0	50.0	-	G	582.5	698.0	1031.5	491.8	480.5
Dang et al. (2017)	M2-S1-2a	18.0	1348.0	1186.2	94.5	65.4	165.0	305.0	50.0	-	G	525.0	698.0	1031.5	491.8	480.5
Dang et al. (2017)	M2-S1-3a	18.0	1345.9	1184.4	91.0	61.3	165.0	305.0	50.0	-	G	635.0	713.0	1029.9	505.0	493.5
Dang et al. (2017)	M2-S1-4a	18.0	1345.9	1184.4	91.0	61.3	165.0	305.0	50.0	-	G	575.0	713.0	1029.9	505.0	493.5
Dang et al. (2017)	M2-S2-1a	18.0	1298.3	1142.5	84.8	66.8	165.0	305.0	50.0	32.0	G	577.5	803.0	993.5	469.4	458.6
Dang et al. (2017)	M2-S2-2a	18.0	1298.3	1142.5	84.8	66.8	165.0	305.0	50.0	32.0	G	672.5	803.0	993.5	469.4	458.6
Dang et al. (2017)	M2-S2-3a	18.0	1299.0	1143.1	91.7	68.1	165.0	305.0	50.0	32.0	G	567.5	798.0	994.0	465.8	455.1
Dang et al. (2017)	M2-S2-4a	18.0	1299.0	1143.1	91.7	68.1	165.0	305.0	50.0	32.0	G	542.5	798.0	994.0	465.8	455.1

* grey values are assumed data, derived from publications

Total: 130 data points

Nomenclature:

Φ = tendon diameter (all experimental tests involve 7-wire strands)
f_{si} = jacking stress of the tendon at release
f_{se} = tendon stress after allowance of all prestress
f_c' = concrete compressive strength at 28 day
f_{ci}' = concrete compressive strength at release
b = width of the concrete section
h = height of the concrete section
c = concrete cover thickness
s = tendon clear spacing
$L_{t,exp}$ = experimental transmission length (average between "cut" and "dead" end values)
$L_{t,TWC}$ = transmission length predicted by the TWC model (with μ = 0.6)
$L_{t,ACI}$ = transmission length predicted by ACI 318-14
$L_{t,MC10}$ = transmission length predicted by *fib* MC2010 (with α_{p2} = 0.75)
$L_{t,EC2}$ = transmission length predicted by Eurocode 2 (l_{pt})
Release type: S = Sudden; G = Gradual

All prestressing tendons are smooth and uncoated